LA-1100

ORNL-4953

The Use of Supernovae Light Curves for Testing the Expansion Hypothesis and Other Cosmological Relations

B. W. Rust

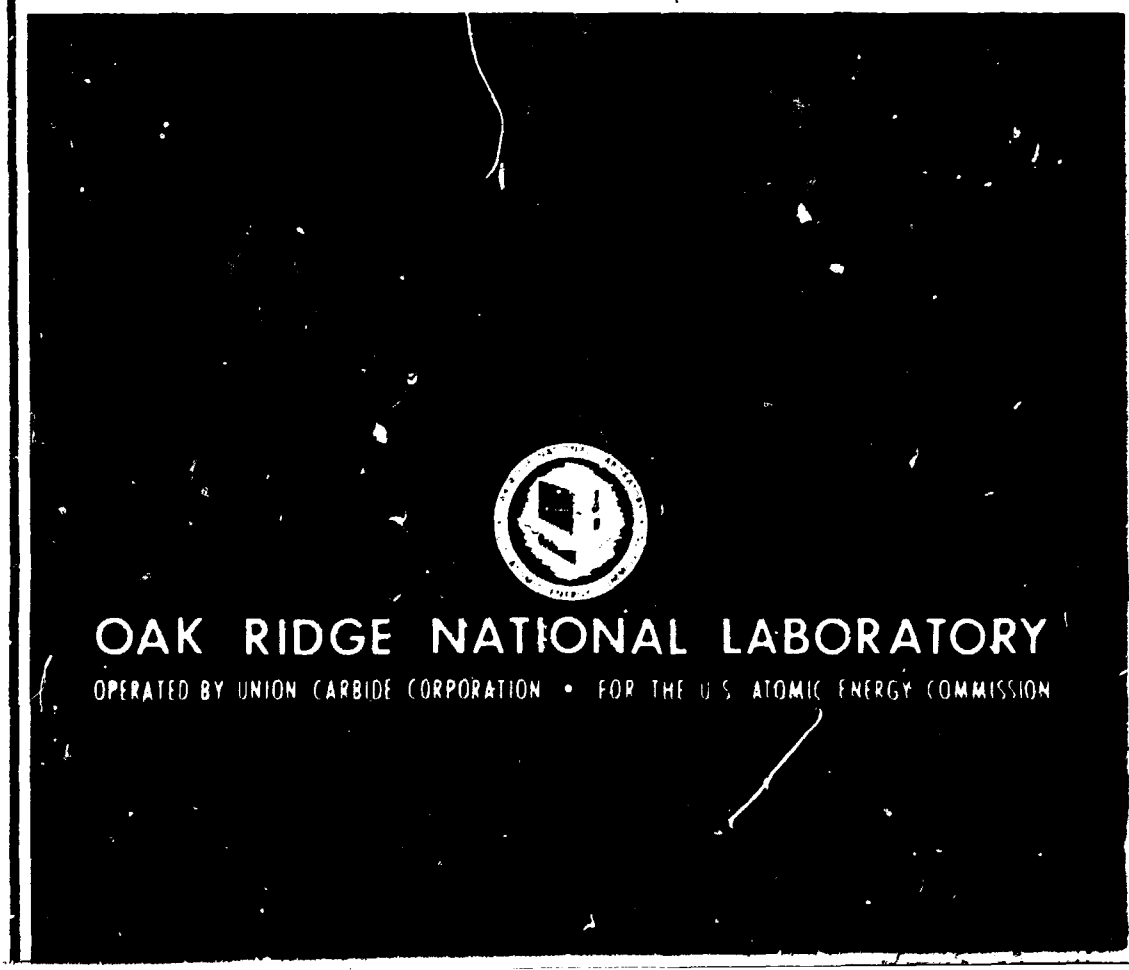

BLANK PAGE

Printed in the United States of America. Available from
National Technical Information Service
U.S. Department of Commerce
5285 Port Royal Road, Springfield, Virginia 22161
Price: Printed Copy $10.60; Microfiche $2.25

ORNL-4953
UC-34b
Physics — Cosmic and Terrestrial

Contract No. W-7405-eng-26

COMPUTER SCIENCES DIVISION

THE USE OF SUPERNOVAE LIGHT CURVES FOR TESTING THE EXPANSION HYPOTHESIS AND OTHER COSMOLOGICAL RELATIONS

(Dissertation)

B. W. Rust

This report has been adopted from a dissertation presented to the University of Illinois in partial fulfillment of the requirements for the degree of Doctor of Philosophy in Astronomy by Bert Woodard Rust

DECEMBER 1974

OAK RIDGE NATIONAL LABORATORY
Oak Ridge, Tennessee 37830
operated by
UNION CARBIDE CORPORATION
for the
U.S. ATOMIC ENERGY COMMISSION

ACKNOWLEDGMENTS

The author acknowledges the Computer Sciences Division, located at Oak Ridge National Laboratory, operated by Union Carbide Corporation, Nuclear Division, for the U.S. Atomic Energy Commission.

The author would like to thank Professor E. C. Olson for good and encouraging advice during the preparation of this thesis and Professor S. P. Wyatt and Professor L. M. Foss, as well, for their penetrating criticisms and suggested revisions which led to this final version. Special appreciation is offered to Ms. Karen T. Barry and Ms. Janice K. Varner for their careful editing and typing of the manuscript. The author would also like to thank Professor Konrad Rudnicki for providing him with a copy of the Preliminary Catalogue of Supernovae. Finally, and most importantly, the author would like to acknowledge the many astronomers who made the observations upon which this thesis is based.

TABLE OF CONTENTS

Page

APPENDICES

LIST OF FIGURES

LIST OF TABLES

BLANK PAGE

ABSTRACT

This thesis is primarily concerned with a test of the expansion hypothesis based on the relation $\Delta t_{obs} = (1 + V_r/c)\Delta t_{int}$ where Δt_{int} is the time lapse characterizing some phenomenon in a distant galaxy, Δt_{obs} is the observed time lapse and V_r is the symbolic velocity of recession. If the red shift is a Doppler effect, the observed time lapse should be lengthened by the same factor as the wave length of the light. Many authors have suggested type I supernovae for such a test because of their great luminosity and the uniformity of their light curves, but apparently the test has heretofore never actually been performed. Thirty-six light curves were gathered from the literature and one (SN1971i) was measured. All of the light curves were reduced to a common (m_{pg}) photometric system. The comparison time lapse, Δt_c, was taken to be the time required for the brightness to fall from $0^m.5$ below peak to $2^m.5$ below peak. The straight line regression of Δt_c on V_r gives a correlation coefficient significant at the 93% level, and the simple static Euclidean hypothesis is rejected at that level. The regression line also deviates from the prediction of the classical expansion hypothesis. Better agreement was obtained using the chronogeometric theory of I. E. Segal (1972 Astron. and Astrophys. 18, 143), but the scatter in the present data makes it impossible to distinguish between these alternate hypotheses at the 95% confidence level. The question of how many additional light curves would be needed to give definitive tests is addressed. It is shown that at the present rate of supernova discoveries, only a few more years would be required to obtain the necessary data if light curves are systematically measured for the more distant supernovae.

Peak absolute magnitudes M_o were calculated and a plot of M_o against Δt_c gave two well separated bands with a high degree of correlation (significant at the 99.5% level) within each band. These bands almost surely represent two distinct populations of Type I supernovae, each having a characteristic linear relation between the rate of decline in brightness, Δt_c, and the maximum luminosity M_o. The slopes of these relations are not sensitive to errors in estimating the M_o so if an independent method is used to recalibrate the zero points, then they can be used for estimating extragalactic distances by a method analagous to the use of Cepheid variable period-luminosity relations. Also they can be combined with the corresponding relations between log (V_r) and peak apparent magnitude m_o to obtain a new method for estimating the Hubble constant H, assuming that the velocity distance law is truly linear. Supernovae are ideal candidates for testing the linearity of that relation because they are point sources and hence do not require aperture corrections. The regression of m_o on log (V_r) for the present sample gave a slope intermediate between the predictions of a linear and a quadratic relation. Both of those predictions are rejected at the 95% level, but the present sample is dominated by relatively nearby galaxies. The M_o - Δt_c relations were recalibrated using six supernovae in the Virgo cluster together with de Vaucouleurs' [IAU Symposium No. 44 (1972) 353-366] best estimate of its distance modulus. These relations were used to construct a velocity-distance plot for the supernovae with distances less than 50 Mpc. The resulting plot gave extremely good agreement with the quadratic relation found by de Vaucouleurs for nearby groups and clusters. Combining

the recalibrated $M_o - \Delta t_c$ relations with the best fitting linee ·locity distance relations for the entire sample gave H = 32/km/sec/M_{pc} for the Hubble constant.

CHAPTER 1

INTRODUCTION

The aim of this thesis is to put the expanding universe hypothesis to an observational test. The test, which is based on supernova light curves, has been suggested many times, but, to the author's knowledge, has never actually been applied.

Few of the hypotheses of modern science enjoy an acceptance so universal as that of the expanding universe. The evidence supporting this hypothesis is compelling but it is all of one kind - namely, measurements of the red shifts of lines in the spectra of distant galaxies. These measurements and their interpretation as Doppler velocity effects constitute the only observational evidence directly supporting the hypothesis. In spite of this the idea is widely accepted, perhaps in part because of other considerations. These other considerations include: (1) the expansion hypothesis has not led to any obvious contradictions with other cosmological data; (2) no one has been able to find a better or more attractive interpretation of the red-shift measurements; and (3) an expanding universe resolves many of the theoretical difficulties and paradoxes which plagued 19th century cosmologists.

Most of the cosmological thought of the last century was dominated by the view that the universe is infinite, Euclidean, uniform, static and governed by the Newtonian gravitational theory. One of the severe problems generated by this world-view was Olbers' paradox, which pointed

BLANK PAGE

out that the sky in such a world should be everywhere as bright as the disk of the sun. Moreover, in such a universe the gravitational potential at any point becomes infinite. Charlier's hierarchic model was an attempt to avoid these difficulties. Other attempts to deal with the gravitational problem consisted in the ad hoc addition to Poisson's equation of modifying factors which had very little effect over small distances but which over large distances produced repulsions stronger than the gravitational forces. It was not until the early twentieth century that cosmologists realized that these problems could be avoided more easily by dropping the assumption that the universe is static.

In 1917 de Sitter introduced a cosmology which, although it was based on a static metric, was on the verge of being a non-static model. It predicted a systematic lowering of the frequency of light from distant sources, the so-called "de Sitter effect," which was attributed to a slowing down of time at large distances from the observer. In 1922 Lanczos and Friedmann introduced cosmologies with actual time-dependent metrics. It is this work - especially that of Friedmann - that is often cited by present-day theoreticians to support the claim that the expansion was predicted theoretically before it was actually observed. Actually, these claims are not completely justified for, although Friedmann's model did have a variable radius, Friedmann himself did not relate his results to the extragalactic red-shift measurements which were known at the time. Furthermore his work was not given much attention by other theoreticians until almost ten years later when the systematic red-shift effect was well established by observations.

The first successful measurement of a spectral shift of another galaxy was made in 1912 by Slipher, who obtained a radial velocity for M31 whose spectrum is blue-shifted. By 1925 some 45 such radial velocities had been measured, almost all by Slipher. After only a few such measurements had been made, observers began to try to use them in order to derive the solar motion relative to the extragalactic nebulae. In 1918 Wirtz pointed out that the measured nebular velocities could not be explained without allowing for a systematic velocity effect in addition to the solar velocity. He proposed the addition of the "K-term" which was taken to be a constant velocity that must be subtracted from the nebular velocities before the solar motion is evaluated. The most astonishing thing about the "K-term" was its value - approximately 800 km/sec. In 1922 Wirtz suggested that the "K-term" might represent a systematic recession of the other galaxies from ours and further that the "K-term" might not be constant but rather a function of distance. He actually found a rough correlation between increasing red shifts and decreasing angular diameters of the galaxies. The latter quantity was the only available nebular distance indicator at that time. This work of Wirtz, like that of Friedmann, was for the most part overlooked by the then practicing theorists, some of whom were at the same time working on the "de Sitter effect" without making a connection between the spectral shifts and the kinematics of the source galaxies. Eddington was one of the first theorists to speak of radial velocities of the galaxies and of the expansion of the universe. In his book, The Mathematical Theory of Relativity, published in 1922, he acknowledged the assistance

of Slipher, who had provided for him a complete list of the "radial velocities" that had been measured up to that time.

Part of the reason that the Doppler-velocity hypothesis was somewhat slow in gaining general acceptance, in spite of the significant number of measured red shifts, was that it was not yet definitely established that the other galaxies lay outside the Milky Way. This latter feat was accomplished in 1924 by Hubble, who determined the distance to M31 by Cepheid variable measurements. He also measured distances to other nearby galaxies, out to about 10,000,000 light years, using Cepheids and supergiant stars as distance indicators. By 1929 he knew the relative distances to 18 galaxies and to the Virgo cluster. Using these distances together with Slipher's radial velocity measurements, he was able to obtain his famous linear "velocity-distance relation", which can be written

$$V_r = Hr, \qquad (1\text{-}1)$$

where V_r is radial velocity, r is distance, and H is the Hubble constant. According to North (1), Hubble was not acquainted with the work of Friedmann, but he did believe that his relation might represent the de Sitter effect.

The value initially obtained by Hubble for the recession constant H was 500 km/sec per Mpc. Between 1928 and 1936 Humason extended the work of Slipher and Hubble. Using the Mount Wilson 100-inch reflector, he was able to measure radial velocities as high as 42,000 km/sec. During the 1930's there were several small revisions of the work on Cepheid variable light curves, leading to a new estimate of 550 km/sec

per Mpc for the value of H, but no really significant change was proposed until 1952, when Baade demonstrated the existence of two different populations of the Cepheids. He was able to show that a Type I Cepheid was about 1.5 magnitudes brighter than a Type II Cepheid with the same period. Since the Cepheids that had been observed in other galaxies were Type I, whereas the ones in the Milky Way which had been used to calibrate the distance scale were Type II, it followed that extragalactic distances had been systematically underestimated. When these considerations were taken into account, the estimate of H was revised downward to 180 km/sec per Mpc. More recent estimates of H give values between 53 and 115 km/sec per Mpc with the most often quoted value being 100 km/sec per Mpc. This latter value is the one that will be adopted for use in this thesis.

Although Hubble's work convinced most astronomers that the universe is expanding, there were a few who felt that the systematic red-shift effect is caused not by systematic nebular recessions but rather by a progressive reddening of the light while it is traveling from the source to the observer. Zwicky proposed a gravitational analogue of the Compton effect in which the photons transfer momentum and energy to any gravitating matter which they encounter on their journeys. Although Zwicky's idea found some observational support, the evidence was not compelling enough to convince many other astronomers. Other suggested alternatives included a proposal by J. Q. Stewart that light quanta become fatigued during their journeys, and a proposal by P. I. Wold that the red shifts

are caused by a secular change in the velocity of light as a function of time. Neither of the proposals attracted a significant following in the astronomical community.

One property that Doppler red shifts must possess is a constancy of the relative shift $\Delta\lambda/\lambda$ for all values of λ. McVittie (2) has described measurements by Minkowski and Wilson (3, 4) on the spectra of the galaxies Cygnus A and NGC 4151 which reveal no significant variation in the value of $\Delta\lambda/\lambda$ between the violet and red ends of the visual spectra. These measurements established the constancy of $\Delta\lambda/\lambda$ over the wavelength range of 3400 to 6600 Angstroms. Even more convincing evidence for the constancy of $\Delta\lambda/\lambda$ comes from the 21-cm radial velocities measured by radio astronomers. The first successful 21-cm measurements of external galaxies were accomplished in 1954 by Kerr, Hindman, and Robinson (5), who observed the Magellanic Clouds, and in 1956 by van de Hulst, Raimond, and van Woerden (6), who obtained a central radial velocity and a rotation curve for M31. Since that time, 21-cm velocities have been measured for about 130 galaxies ranging between -343 km/sec and +2620 km/sec. These measurements indicate that the optical and radio measurements of $\Delta\lambda/\lambda$ agree to within one percent. For the few cases where there were significant discrepancies, the optical velocities were recently remeasured by Ford, Rubin, and Roberts (7), with the result that the new optical values give much better agreement with the radio measurements than do the old ones.

The agreement between the optical and radio measurements establishes a constancy of the relative red shifts over a wavelength ratio

of 5×10^5 to 1. Although this constancy of [illegible] is impressive, it should be regarded as evidence for the Doppler hypothesis only in the sense that it does not contradict the hypothesis. It is possible to construct models for other red-shifting mechanisms which also display this same constancy. One such model, which is attributed to Sistero, has recently been described by H. C. Arp (3). It involves the forward scattering of the photons from the source by relativistic electrons moving in essentially the same direction. Another model involving inelastic photon interactions has recently been proposed by Pecker, et al. (41). This model has the advantage that it can apparently be tested fairly readily in the laboratory. Other models which attribute the red shift to the space-time geometry of the universe are discussed in Chapter 10 of this thesis.

Chapters 2 and 3 review a few of the recent observations which seem to suggest that at least part of the extragalactic red shifts may be caused by some effect other than recessional velocity. These chapters make no attempt to give an exhaustive review of the very considerable work in this area. They are meant to suggest that the question of the nature of the red shift is still an open one and to underscore the need for an independent test of the expansion hypothesis.

Chapter 4 gives a brief description of the test that is performed in this thesis. This test seeks a correlation between the rate of fall of the light curves of Type I supernovae and the symbolic velocities of recession of their parent galaxies. Type I supernovae are the ideal candidates for this kind of test because of their great luminosity and the uniformity of their light curves.

Chapter 5 describes the observational data used for the test. These data include 37 light curves, one of which was measured by the present author and his colleagues at Prairie Observatory. The other light curves were gathered from the literature.

Chapter 6 describes the reduction of the light curves to a common photometric system (the international m_{pg} system) and the estimation of the peak brightness and date of peak brightness for each curve. It was necessary to reduce all of the curves to a common system because the rate of decline in brightness may be different in different systems. The parameters of the brightness peak were needed for making many of the photometric conversions and for fitting a model to the observed light curves.

Chapter 7 describes the model that was fitted to the light curves and the fitting procedure. It also describes the choice of the comparison parameter used for the test. The model and the comparison parameter were chosen to give a consistent measure of the rate of decline of the light curves even for fragmentary light curves. The model that was chosen was the light-echo model of Morrison and Sartori, and the fitting procedure was non-linear least squares.

Chapter 3 gives the results of the fits. The intrinsic distribution of the comparison parameter was estimated using only the 21 supernovae in the study with measured symbolic velocities less than 2000 km/sec. The average value for this subsample was used to estimate the prediction of the expansion hypothesis for the slope of the relation between the comparison parameter and the symbolic velocity of recession. The regression of comparison parameter on velocity of recession was performed

using the entire sample, and in spite of the wide scatter in the data, the correlation was found to be significant at the 95% level. The slope of the regression line was more than five times greater than that predicted by the expansion hypothesis. Extensive tests were performed to determine whether this larger than expected slope could have resulted from systematic errors in the data reduction and fitting procedures. No systematic errors were found.

Chapter 9 is concerned with estimating the absolute magnitudes of the supernovae in this sample. Although these estimates are interesting in themselves, the main reason for computing them was to check for luminosity selection effects in the sample. No selection effects were detected, but an apparent division of the sample into two distinct luminosity subgroups was found. The discussion of these subgroups was deferred to Chapter 11.

Chapter 10 reviews some of the theories that have been proposed as alternatives to the expansion hypothesis and compares the observed relation between the comparison parameter and the symbolic velocity of recession with the relations predicted by the various theories. Most of the theories predict the same relation as either the classical expansion or the static Euclidean hypothesis. One of the theories that was reviewed is the covariant chronogeometry proposed recently by the mathematician I. E. Segal. The derivation that is given for the predicted relation is based on the present author's interpretation of the theory. That prediction gives much better agreement with the observed regression line than does the prediction of the expansion hypothesis, but the scatter in the data is too great to reject the expansion hypothesis

or the static Euclidean hypothesis at the traditionally accepted 95% level of significance (the former was rejected at the 91% and the latter at the 93% level). Since seven of the supernovae in the study did not have measured red shifts, it was necessary to calculate estimates for their symbolic velocities. These estimates depend on the value adopted for the Hubble constant. Therefore, a sensitivity study was performed in order to determine the effect of changes in the adopted value on the regression line obtained from the observed data. The results of this study, which are reported at the end of Chapter 10, indicate that reasonable changes in the Hubble constant do not produce very large changes in the regression line, which agrees best with Segal's theory in all cases.

Chapter 11 returns to the question of the two distinct luminosity groups in the sample. These groups, which were first noted in Chapter 9, appear as two well separated bands in the graph of the relation between the comparison parameter (rate of fall of the light curve) and the estimated peak absolute magnitude. In each of the bands, the correlation between these two parameters is significant at a level exceeding 99.5%. Extensive tests were performed in order to determine whether or not this division resulted from systematic errors in the estimates of the peak apperent or peak absolute magnitudes. No systematic effects were found, so it was concluded that the two groups probably do represent two distinct populations of type I supernovae. The chapter ends with a comparison of these two groups with previous schemes that have been proposed for dividing the parent population into subpopulations.

Chapter 12 discusses further refinements and future prospects for the comparison parameter-symbolic velocity test which take the two luminosity populations into account. It is necessary to consider the effect of the two groups because they not only have different average luminosities but also different average values of the comparison parameter. Since the slopes of the relations between these quantities are so similar for the two groups, it was possible to reconcile the two so that together they simulated a single sample with less scatter in the comparison parameter than the unreconciled sample. The regression of comparison parameter on symbolic velocity gave results very similar to those obtained from the unreconciled sample, with Segal's theory giving the best agreement with the regression line. The scatter in the reconciled sample was used to estimate the number of additional light curves that must be obtained for various limiting symbolic velocities in order to discriminate at the 95% level of significance among the various alternative theories.

Chapter 13 discusses the red shift-apparent magnitude relation defined by the supernovae in the present sample. The slope of this relation is a very important parameter because its value determines the form of the velocity-distance relation. Observations of galaxies cannot be used to give an independent estimate of this parameter because the necessary aperture corrections require an assumption about the form of the relation. Supernovae are the ideal candidates for this analysis because they are extremely bright point sources with reasonably small scatter in intrinsic luminosities. Previous studies using supernovae have assumed that the Hubble law is valid and held the slope fixed during

the regression. In the present study, the peak apparent magnitude was regressed on $\log(V_r)$ with both the slope and the intercept free to vary. The slope of the resulting regression line was less than the value predicted by a linear velocity-distance relation but greater than the value predicted by a quadratic one. Both of these possibilities were rejected at significance levels greater than 95%. The results are qualitatively the same if the two luminosity groups are analyzed separately, but the sample is dominated by low red-shift objects. Therefore, the results may be more indicative of a local anomaly in the relation than of a true rejection of the linear Hubble law (or of the quadratic law). If the linear law is accepted, then the regressions for the two separate luminosity groups can be combined with the two corresponding regression relations between the comparison parameter and the absolute magnitude to give a new method for estimating the Hubble constant. This method is described in the last part of Chapter 13. When the method was applied to the present sample, the resulting estimate was H = 92 km/sec/Mpc.

Chapter 14 describes a new method for estimating distances to supernovae using the relations between the comparison parameter and the peak absolute magnitude in a manner analogous to the use of Cepheid variable period-luminosity relations for estimating distances. It was shown in Chapter 13 that the errors in estimating the absolute magnitudes did not produce an error in the slope of the relation between comparison parameter and absolute magnitude, and any zero-point error that might have been introduced was hopefully removed by recalibrating the intercept using the six supernovae which occurred in the Virgo cluster. It is this

recalibrated relation that should be used for distance estimation. The method was applied to the supernovae in the sample whose distances are less than 30 Mpc, and the resulting distance estimates were used to construct a graph of the local velocity-distance relation. This plot was compared to the one given recently by de Vaucouleurs which was based on average distances to nearby clusters. The agreement between the two was extremely good, with the supernova data adding confirmatory evidence to de Vaucouleurs' hypothesis that the local velocity-distance relation is quadratic rather than linear.

Chapter 15 gives a brief summary of the results obtained in the chapters that precede it.

CHAPTER 2

QUASARS AND THE POSSIBILITY OF NON-DOPPLER RED SHIFTS

After the work of Hubble became generally known in the astronomical community, the possibility that extragalactic red shifts could be due to some cause other than the Doppler effect was scarcely ever considered until the discovery of quasi-stellar objects in the early 1960's. The first QSO red shift was measured in 1963 by Schmidt (10). Since then more than 200 QSO red shifts have been measured. Most of these red shifts are extremely large in comparison to the red shifts of galaxies. Although some astronomers, probably the majority of them, accepted a Doppler interpretation of these red shifts, a significant number sought a non-Doppler explanation. In particular, a number of them worked on the mechanism of gravitational red shift until it was shown to be an untenable hypothesis for a number of reasons. Not the least of these reasons was that the densities required to produce the red shifts would preclude the appearance in the spectra of certain emission lines that are actually observed.

The Doppler school was at first divided into two branches - one that held that the QSO's are actually at the cosmological distances indicated by combining their measured red shifts with a Hubble-type velocity distance relationship and one that held that the QSO's were local objects which had relativistic velocities because they originated in tremendous explosions in our own and/or other nearby galaxies. The local origin theory was hard pressed to explain the absence of blue-

BLANK PAGE

shifted quasars and was virtually completely abandoned after the failure by Jeffreys (11) and by Luyten and Smith (12) to find any significant proper motions for quasars.

The cosmological-Doppler partisans soon ran into difficulties also. One of the first things they attempted to do, as soon as enough data became available, was to use the QSO's to extend the Hubble relationship. However, in 1966, Hoyle and Burbidge (13) demonstrated that there is almost no correlation between the apparent magnitudes and red shifts of the QSO's and that what little correlation exists is lost in a scatter that is nearly as large as the span of the relation. Even worse scatter was found in the relation between red shift and radio flux density measurements. This scatter was generally interpreted as evidence that QSO's have widely varying optical and radio luminosities, a circumstance which does not contradict their being at cosmological distances, but which does render them unsuitable for extending the Hubble relationship. But Hoyle and Burbidge also plotted a log N-log S relationship for the 38 QSO's which, at that time, had known red shifts. The result was a straight-line relationship with a slope very close to -1.5, which corresponds to Euclidean space. When these same QSO's were plotted as a relation between red shift and radio apparent magnitude, the result was a complete scatter diagram. This means that if one assumes the usual distance-volume interpretation of the log N-log S relation, then it is necessary to conclude that the QSO red shifts have nothing to do with their distances. Conversely, if the red shifts are assumed to be cosmological distance indicators, then it is necessary to abandon the geometrical interpretation of the log N-log S relation.

Another difficulty with the cosmological hypothesis is the apparent lack of correlation between the locations on the celestial sphere of QSO's with low red shifts and the location of clusters of galaxies with the same red shifts. According to Arp (8), none of the nine QSO's known in 1969 to have red shifts $z \leq 0.2$ fall in one of the 2712 clusters listed in Abell's catalogue (14) of the richest clusters containing galaxies brighter than a limiting magnitude corresponding to $z = 0.2$. In fact, a study by Bahcall (15) showed that even if the Abell cluster diameters are doubled, the resulting regions on the celestial sphere do not contain any of the 9 QSO's with $z \leq 0.2$. Since well over 50 percent of all galaxies are known to lie in clusters, it is very difficult to explain why QSO's should systematically avoid these basic mass concentrations if they are truly at the distances indicated by their red shifts. This objection to a cosmological distance scale for QSO's loses some of its force, perhaps, when a recent discovery by Gunn (16) is taken into account. Gunn has found that the QSO PKS 2251+11, which has a red shift $z = 0.323$, is superposed on a small cluster of galaxies. One of the galaxies has a measured red shift of $z = 0.33$. The red shifts of both the QSO and the galaxy as well as that of another galaxy in the cluster have recently been remeasured by Robinson and Wampler (17). These measurements, made with greater resolution, confirmed Gunn's earlier conclusions about the agreement of the red shifts.

Although it seems fairly certain that Gunn has indeed found a QSO superposed on a cluster of galaxies with the same red shift, this one case does not definitely establish that QSO red shifts are cosmological.

There remains the possibility that PKS 2251-11 is a relatively nearby object between us and the cluster. This question would be immediately resolved if other QSO-cluster coincidences are discovered. Two previous such "discoveries" have recently been shown to involve objects that were not really QSO's (18). Thus after several years of work on the problem, only one such coincidence has been found.

Recent observations, on the other hand, seem to indicate that at least some of the QSO's are associated with nearby galaxies. The galaxy NGC 520, which is galaxy number 157 in Arp's Atlas of Peculiar Galaxies (19), is a very bright and very disrupted galaxy which has been shown (20, 21) to have lines of radio sources emanating from it. Four of these radio sources are QSO's which fall along a straight line that terminates on the galaxy (8). The total angular extent of the system is about 3 degrees. The red shifts of the four QSO's are z = 0.67, 0.72, 0.77, and 2.11. The red shift of the galaxy is z = 0.007. The radio properties of the QSO's vary in a systematic way along the line. Flux densities decrease and spectral indices flatten with increasing distance from the galaxy. It seems rather unlikely that such a configuration could occur as a result of chance projection effects.

At the present time two QSO's have been observed to be connected to galaxies with differing red shifts by luminous filaments. The first to be observed was the QSO Markarian 205, which has a red shift of 0.070 and has been shown by Arp (22) to be connected by a luminous tube (faintly visible in Hα) to the galaxy NGC 4319, whose red shift is 0.006. The second QSO shown to be connected to a nearby galaxy was discovered by

Burbidge, et al. (23) on the National Geographic Society - Palomar Observatory Sky Survey prints. The radio quiet QSO PHL 1226, which has red shift z = 0.404, is shown on the Sky Survey prints to be connected by a luminous bridge to the Sb galaxy IC 1746, which has red shift z = 0.026. The bridge is clearer on the red print than on the blue. A later plate taken by Arp with the 200-inch Hale telescope on 103a-J emulsion does not reveal the bridge but does show a nonstellar compact object exactly between the QSO and the galaxy. This compact object is not visible on the Sky Survey prints.

Burbidge, et al. (23) also made a statistical comparison of the distribution of the 47 known QSO's in the 3C and 3CR catalogues with the galaxies in the Reference Catalogue of Bright Galaxies. They found four QSO's much closer to bright galaxies than would be expected if the 47 were distributed randomly on the celestial sphere. The four galaxy QSO pairs are listed in Table 2-1.

Table 2-1

QSO's With Small Angular Separations From Bright Galaxies

QSO	Galaxy	Separation	z (QSO)	z (Galaxy)
3C 232	NGC 3067	1'.9	0.534	0.0050
3C 268.4	NGC 4138	2'.9	1.400	0.0036
3C 275.1	NGC 4651	3'.5	0.557	0.0025
3C 309.1	NGC 5832	6'.2	0.904	0.0020

In each case the red shift of the QSO is very much larger than that of the galaxy. Burbidge, et al. estimated the probability of 4 such close pairings occurring by chance to be less than 0.005.

The evidence for close associations between QSO's and nearby galaxies is further strengthened by the recent discovery by Arp, et al. (24) that the radio source 3C 455 is a QSO which is situated 23" northeast of the galaxy NGC 7413. The radio source had originally been identified with the galaxy, but more accurate measurements of its radio position by R. L. Adgie revealed that the source was actually associated with the faint ($m_v \approx 19$) blue stellar object northeast of the galaxy. Optical studies by Arp, et al. revealed the object to be a QSO with red shift $z = 0.543$. The red shift of the galaxy was measured to be $z = 0.03321$.

As more associations between QSO's of high red shift and nearby galaxies are discovered, it becomes more nearly certain that at least some of the QSO's are relatively local objects. Furthermore, since none of them have been observed to have blue shifts, it becomes more apparent that at least part of the red shifts are due to something other than velocity effects.

CHAPTER 3

GALAXIES WITH RED-SHIFT ANOMALIES

Although most galaxies that have been observed appear to obey the Hubble law, there are a few exceptions which seem to have discrepant red shifts. One such example is the galaxy IC 3483, which is a member of a triple system composed of IC 3481, an anonymous galaxy (which shall be called Anon. in the following text), and IC 3483. A detailed description of this system has been given by Zwicky (25). The radial velocities deduced from the measured red shifts of the three galaxies are: V_r (IC 3481) = 7304 km/sec, V_r (Anon.) = 7276 km/sec, and V_r (IC 3483) = 108 km/sec. The three are connected in a chain by two faintly luminous bridges which are apparently composed of stars rather than fluorescent gases. The presence of these bridges rules out the possibility that IC 3483 is a nearby foreground galaxy which projects into the chain by chance. If all three red shifts are pure velocity shifts, then the velocity of IC 3483 relative to the other is much larger than the typical velocity dispersion observed in large clusters (~ 2000 km/sec).

Another example of a chain of galaxies in which one member has a discrepant red shift is the chain VV 172, which has been described by Sargent (26). Four of the galaxies in this chain of five have red shifts corresponding to velocities of about 16,000 km/sec, but the fifth has an apparent velocity of 36,880 km/sec. Sargent gave statistical arguments to counter the possibility that the discrepant galaxy is really a background galaxy which projects into the chain by chance. He concluded

that the probability of such an occurrence is only about 1 in 5000. If the galaxy is at the same distance as the others, and if all the red shifts are strictly velocity effects, then the time-scale for the discrepant galaxy to cross the system is ~ 3×10^6 years and its kinetic energy is $10^{60} - 10^{62}$ ergs.

Another group with a discrepant member is Stephan's Quintet, which has recently been investigated by Burbidge and Burbidge (27). This is a group of disturbed galaxies containing the spiral NGC 7320, which has a red shift velocity of +1073 km/sec. The other four members of the group have an average velocity of +6695. Burbidge and Burbidge argued statistically that the probability that NGC 7320 is a foreground galaxy projecting into the group is less than 1 in 1000. Furthermore, they were able to obtain an estimate of its mass from its rotation curve. They concluded from this estimate that if it is a foreground galaxy at the indicated red-shift distance, then it is extremely dwarfish and denser by about two orders of magnitude than normal spiral galaxies. If NGC 7320 is really a member of the group, and if its red shift is a true velocity indicator, then it is in a state of explosive expansion out of the system toward us. Burbidge and Burbidge calculate that the kinetic energy involved would be $\sim 7 \times 10^{61}$ ergs.

The three examples that have just been given involve groups in which all of the galaxies are more or less the same size. Recent work by H. C. Arp on galaxies with smaller companion galaxies has raised the possibility that such companions sometimes have excess red shifts. One example is the disturbed spiral galaxy NGC 772 which, according to Arp (28),

has several smaller companions connected to it by luminous filaments. From the seven observed companions, Arp picked the three brightest for spectral observations. Following his notation the three will be called (in order of brightness) G 1, G 2, and G 3. A summary of his red-shift measurements is given in the following table.

Table 3-1

Red Shifts of the Galaxies Apparently Associated with NGC 772

Galaxy	Red Shift (km/sec)
NGC 772	2,437
G 1	2,454
G 2	20,174
G 3	19,680

Arp argued inconclusively on the basis of the Hubble red shift - apparent magnitude relationship and the observed properties of G 2 and G 3 that they could not be background galaxies. His direct photographic evidence was, however, more conclusive. He observed that G 2 is on the end of a double spiral arm from NGC 772 and that G 3 is on a luminous protuberance of an isophote of NGC 772.

Another example of a galaxy with an excess red shift companion is NGC 7603, which has recently been studied by Arp (29). It has a red-shift velocity of 8,800 km/sec while the companion, which is connected to it by a luminous filament, has a velocity of 16,900 km/sec. Actually, there are two filaments connecting the galaxies, one of them being a

spiral arm of NGC 7603 and the other outside the spiral arm, curving more sharply into the companion. NGC 7603 is very disturbed and the companion is peculiar, having a core of high surface brightness and a halo of low surface brightness. The halo has a slightly deformed bright rim at the point where the spiral arm enters it. Thus there is virtually no doubt that the two galaxies are at the same distance and are interacting with each other.

In all of the examples given so far, the discrepant red shifts might be explained by an explosive expansion of the discrepant member or members out of the group. This is a very attractive possibility for Stephan's Quintet, in which the four non-discrepant members appear to be very disturbed. The chain VV 172, on the other hand, does not appear to be disturbed, and the galaxies in the triplet IC 3481, Anon., IC 3483 are connected by luminous bridges of apparently stellar matter. Furthermore, the energies demanded by such explosive events are extremely high, although perhaps not unreasonable for objects as big as galaxies. The times required for the discrepant members to cross their respective groups are of the order of 10^6 years, so that such explosions would have to be fairly frequent events if many groups are to be observed with the discrepant member still in the group. Also, it seems reasonable to expect that the stars in such a discrepant member should all be young, having formed after the explosion.

Both of the galaxies NGC 772 and NGC 7603 are highly disturbed so that it is tempting to interpret the excess red shifts of the smaller companions as a true velocity effect with the higher velocities of the

companions being attributed to their being explosively ejected from the larger galaxy. Probably the most effective argument against this interpretation is the one given by Arp (29) in connection with NGC 7603 and its companion. According to Arp, if the red shift difference is indicative of a true velocity difference, then the two galaxies are separating too fast for gravitational interaction to have formed a connecting bridge between them. Thus he is led to the conclusion that at least part of the red shift difference is caused by some non-velocity effect.

Another reason for discarding the differential velocity interpretation for discrepant red shifts of companion galaxies is that most of the discrepancies are excess red shifts and only a few excess blue shifts are observed. Thus, unless one is willing to accept the proposition that parent galaxies preferentially eject their companions in directions away from us, one is forced to admit a non-velocity component of the red shifts of the companions. Of course the examples given so far, namely NGC 772 with its two companions of excess red shift and NGC 7603 with its companion, do not constitute a very large sample, but a study involving a larger sample has recently been made by Arp (30). He picked for the study three groups of galaxies in which one galaxy is unquestionably the dominant member and in which the others are unquestionably companions. These groups were M 31 and its four companions, M 81 and its five companions, and NGC 5128 and its four companions. Of the 13 companions he found that 11 had higher red shifts than the primary. He took the measured red shifts from the de Vaucouleurs Reference Catalogue

of Bright Galaxies so that most of them were the means of two or more optical determinations which usually did not differ by more than 20 km/sec. Five of them had radio determinations which agreed to about the same accuracy. To the above described sample, he also added six spiral galaxies which have companions on the ends of spiral arms. Of this total sample of 19 companions he found that 16 had excess red shifts and only three had excess blue shifts. The distribution of the residual red shifts, z (companion) - z (dominant), shows a pronounced asymmetry toward positive values and is strongly peaked at about 75 km/sec. Ten of the companions in the sample have residual red shifts in the range 50 - 100 km/sec, and five more of them have even greater residual red shifts.

According to Arp, his sample of 19 companions contains essentially all the small companions with known red shifts and known with certainty to belong to a group obviously dominated by a larger galaxy. He has been criticized in his choice of sample by B. M. Lewis (31). Lewis maintained that a better sample is obtained by including groups regardless of whether they have obviously dominant members, as long as a working rule for choosing a dominant member is consistently followed. Using such a sample containing 186 galaxies, he obtained a residual red shift distribution containing 103 excess red shifts and 83 blue shifts and with a mean of about +40-50 km/sec. He claimed, however, that this slight asymmetry toward excess red shifts is not significant and is probably the result of observational errors, one of them being the mistaken identification of foreground galaxies as dominant members of

faster moving groups in the background. He also studied the residual red shifts of galaxies which are members of pairs. For his sample he chose the pairs from two studies by Page (42, 43) and found no significant asymmetry in the residual red shifts.

Arp's reply (32) to Lewis' criticism was short and direct. He argued that Lewis' rule for picking the dominant members of groups was very speculative and that the data for Page's pairs were completely inapplicable since they were originally chosen to be more or less equal pairs. He pointed out that Lewis did find an asymmetry, even using questionable data, and then tried to explain it away by the very projection effect that he (Arp) had sought to avoid by limiting his sample to groups whose memberships were certain. Arp's final assessment of Lewis' criticisms is eloquent enough to bear repeating:

> In summary, then, Lewis has tested with lower weight and inapplicable data. In spite of this he confirms the original result. He then postulates that this confirmation is due to ". . . the mistaken adoption of foreground and relatively low velocity galaxies as dominant members of groups." But it was this very objection that I was trying to avoid by excluding the lower-weight data in the first place.

Even more recent evidence for non-velocity red shifts in galaxies has been published by Jaakkola (33). He made a study of red shifts of galaxies in clusters, groups and pairs using the dimensionless parameter $u = \Delta V/\sigma_V$ where ΔV = V(galaxy) - V(system) is the residual red shift of the galaxy (expressed as a velocity) and σ_V is the red shift dispersion of the system. This particular parameter was chosen so that systems of differing sizes and velocity dispersions could be analyzed together.

He found that in almost all the different kinds of systems studied, E, SO, and Sa galaxies show an excess of residual blue shifts while Sb and Sc spirals show an excess of residual red shifts. His values for $\overline{\Delta V}$ (average ΔV), σ_V, and $\bar{u}$ (average u) are given in Table 3-2. Within the different types he also found significant correlations between red shifts

Table 3-2

Residual Red Shifts of the Galaxies in Jaakkola's Study

Type	Number in Study	$\overline{\Delta V}$ (km/sec)	σ_V km/sec)	$\bar{u}$
E	131	-39	645	-0.07
SO	114	-28	433	-0.05
Sa	73	-124	463	-0.18
Sb	84	+56	406	+0.13
Sc	51	+131	517	+0.20

and various other parameters such as absolute magnitude. The implications of his results are perhaps best expressed in his own words: "The result means that in some part even for normal galaxies, of late Hubble types, with small color indices and small inclinations, part of the red shift cannot be explained by systematic velocity".

CHAPTER 4

AN OBSERVATIONAL TEST OF THE EXPANSION HYPOTHESIS

The apparent discoveries of non-velocity red shifts in nearby QSO's and ordinary galaxies lends a special urgency to the search for an independent test of the expansion hypothesis. Even if the recent discoveries had not been made, such a test would still have been highly desirable, since any scientific hypothesis which is based on only one bit of evidence must be regarded as provisional at best. Even though the expanding universe idea has dominated twentieth century cosmology, quite a number of workers have worried about testing the reality of the expansion. In 1935 W. H. McCrea published a paper (34) entitled "Observable Relations in Relativistic Cosmology" in which he pointed out that, if the expansion is indeed real, then any periodic phenomenon in another galaxy must be subject to the same Doppler effect as the radiation from that galaxy. In particular he suggested that the periods of Cepheid variable stars in a distant galaxy should be lengthened in the same proportion as the wavelength of the radiation from the galaxy.

A variation of the same idea appeared again in 1939 in a paper by O. C. Wilson (35), who pointed out that if the red shift is a Doppler effect, then two events occurring in a distant galaxy with observed red shift V/c would appear to us to have a longer time separation than to an observer in that galaxy. If Δt_o is the time lapse measured by the distant observer, then, according to Wilson, the time lapse measured by us would be

$$\Delta t = \Delta t_o(1 + \frac{V}{c}). \qquad (4\text{-}1)$$

Of course this formula is good only for galaxies which are not far enough away to have apparent velocities large enough to require a relativistic treatment. Wilson was impressed by the then recent determinations by Baade and Zwicky of the light curves of three supernovae in other galaxies. Because of the good agreement of the shapes of the three curves, he suggested that such light curves would provide a good test of the expansion hypothesis. For a supernova in a distant galaxy with velocity V, he argued: "Hence, the light curve of a supernova occurring in such a nebula should appear to be expanded along the axis in the ratio $(1 + V/c):1$ with respect to the 'standard' light curve given by relatively nearby objects."

The same idea appeared again in 1955 in a paper by S. N. Milford (36), who was familiar with McCrea's earlier paper but not with Wilson's. Milford pointed out that Cepheids could not be used for a test because they are not intrinsically luminous enough to be observed in any but the very nearest galaxies. He suggested that Type I supernovae are the only objects which are known to be luminous enough to be seen at very great distances and which possess the necessary degree of similarity in their intrinsic light curves.

The declining portion of the light curve of a Type I supernovae consists of two parts: an initial rapid decline to about three magnitudes below peak brightness, occurring in about 35 - 40 days, followed by a slower, very nearly linear decline which continues until the supernova becomes too faint to be observed. The light curves of the three supernovae which so impressed Wilson are shown in Fig. 4-1 in order to

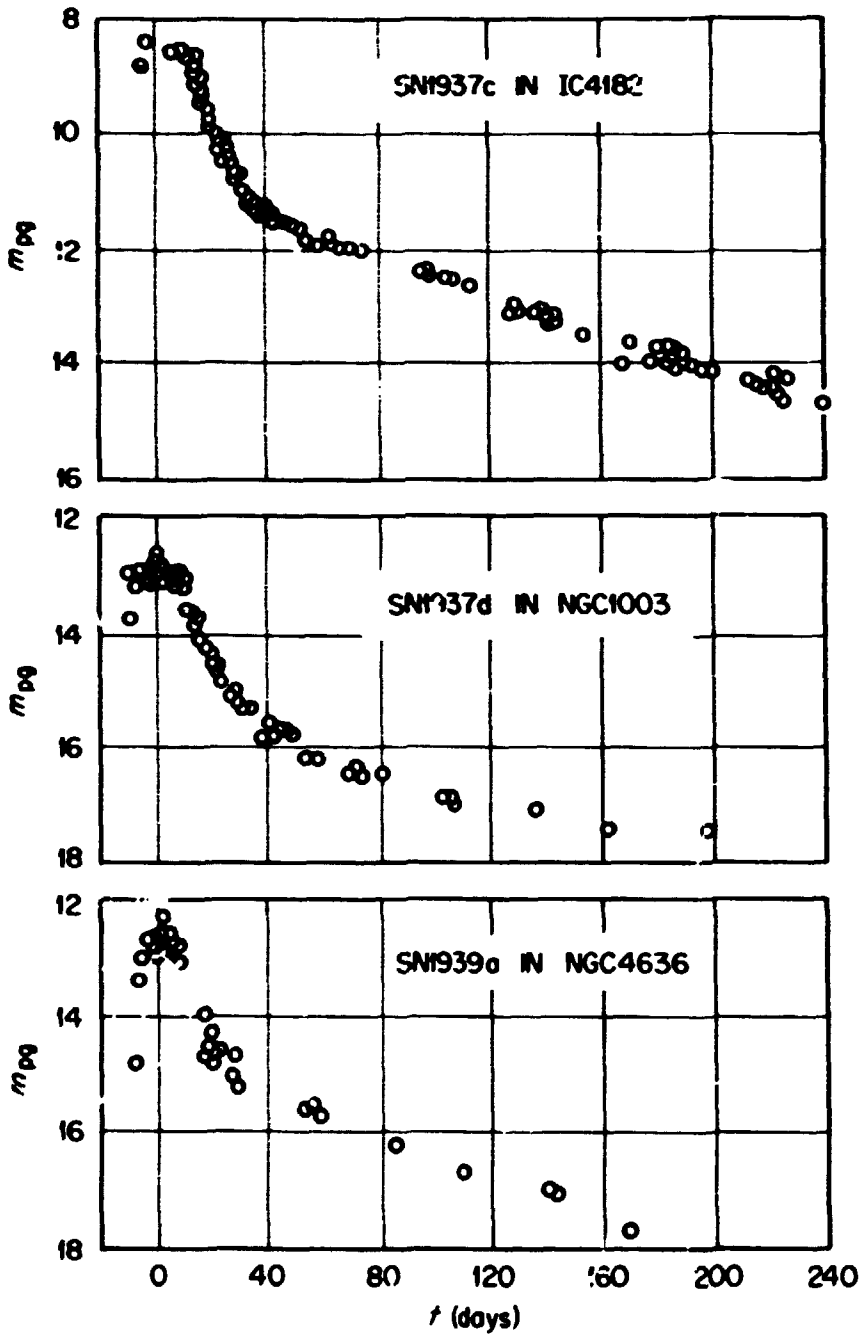

Figure 4-1. The Light Curves of Supernovae SN1937c, SN1937d, and SN1939a.

illustrate the form of th Type I light curve and the basic uniformi'y of the phenomenon.

Milford suggested that the test of the expansion hypothesis should be based on the linear decline portion of the light curve. Using a very general homogeneous, isotropic, general relativistic cosmological model he was able to show that the observed rate of decline, expressed in terms of photographic magnitude m_p, is related to the intrinsic rate by

$$\left(\frac{dm_p}{dt}\right)_{obs} = \frac{1}{1+z}\left(\frac{dm_p}{dt}\right)_{int} \qquad (4\text{-}2)$$

where z is the observed red shift. He noted that this result is identical to one that he had obtained earlier (37) using special relativity. He stated that the same test could also be derived for cosmological models even more general than the one he used. He noted that only differences in magnitude need be measured along with the corresponding time lapses, thus avoiding the problem of determining an absolute zero point for the magnitude scale.

Milford pointed out that the greatest disadvantage of his proposed test was that it applied to the linear decline portion of the light curve, which starts three magnitudes below the maximum brightness. In spite of this disadvantage, he concluded that the test was still practically possible with existing equipment. This same problem was discussed again in 1961 by Finzi (38), who proposed the same time lapse test that Wilson had previously proposed. Finzi pointed out that the initial decline portion of the light curve offered the best opportunity

for applying the test because this brighter portion can be seen for supernovae at greater distances, but he concluded that using this portion would require several observations and statistical methods because ". . . the decay of the luminosity of a supernova during the first 100 days is not a very regular phenomenon." He was evidently under the impression that the linear decline portion of the curve, if it were bright enough, would not require statistical methods in the application of the test. In actual fact, there is as much variation from one supernova to another in this later part of the light curve as in the earlier more rapidly falling part. But at the time Finzi was writing his paper a large number of astronomers believed that all Type I supernovae had almost identical light curves after the initial bright part, with the luminosity decaying according to an exponential law with a half-life of 55 days. It had been pointed out by Burbidge, et al. (39) that this is the same as the half-life of the transuranic element ^{254}Cf, and it was widely believed that the linear decline portion of the light curve could be explained by the radioactive decay of this and other heavy isotopes. More recently Mihalas has shown (40) that many supernovae exhibit considerable deviations from a 55-day half-life decline, and the radioactive decay theory has been abandoned by most astronomers.

Thus, regardless of which section of the light curve is used, it is necessary to obtain as many light curves as possible in order to reduce statistically the fluctuations caused by the intrinsic variations from one supernova to another. The chief task of this thesis will be to apply Wilson's test to the bright part of Type I supernova light curves.

CHAPTER 5

THE OBSERVATIONAL DATA

The first observed extragalactic supernova was the 1885 outburst in the Andromeda galaxy, which was at first thought to be a common nova. This mistaken identification led to a drastic underestimate of the distance to M 31, thus causing great difficulties for those astronomers who were trying to prove that the spiral "nebulae" were truly extragalactic objects. This difficulty lingered until 1917, when the work of Ritchey and Curtis revealed the distinction between ordinary novae and supernovae.

In the years between 1885 and 1936 a total of 15 supernovae was discovered by various observers. The first systematic search for supernovae was carried out between 1936 and 1941 by Zwicky and Johnson with the 18-inch Schmidt telescope at Mount Palomar. This patrol yielded a total of 19 new discoveries. In the years between 1941 and 1956 discoveries by various observers brought the total number of discoveries up to 54. A summary of these discoveries was reported by Zwicky in the Handbuch der Physik (44). In 1956 an international cooperative search was organized by Zwicky. Observatories participating in this effort included Palomar and Mount Wilson, Steward, Tonantzintla, Meudon, Asiago, Berne, Crimea, and Cordoba. Preliminary results of this search were reported by Zwicky in 1965 (45). Since that time a number of other observatories have joined in the search for supernovae, and at present on the average about 15 new discoveries are made each year. Karpowicz and Rudnicki have published a complete catalogue of all the

BLANK PAGE

supernovae discovered up to 1967 (46). A summary list of all the discoveries through May, 1971, has been published by Kowal and Sargent (47); it includes 300 supernovae.

Observations of the light curves and spectra of supernovae have revealed that there are at least two very different types of supernovae. Zwicky and many of his colleagues believe that they have found five different types, which they call type I, II, III, IV, and V, but only a few of the latter three types have ever been identified. Of the 300 supernovae in Kowal and Sargent's list, 83 have been classified according to type. Of these 83, 51 are type I, 26 are type II, 2 are type III, 1 is type IV, and 3 are type V.

A description of the properties of the various types of supernovae can be found in recent survey articles by Zwicky (45) and Minkowski (48). Type I supernovae are remarkable in having uniform light curves and high intrinsic luminosities. The light curves for type I were described in Chapter 4. The light curves for type II supernovae are generally flatter and have much wider intrinsic variations than those of type I. The peak luminosities of the various types of supernovae have been the subject of recent studies by Kowal (49) and Pskovskii (50, 51), who find that type I supernovae are on the average about two magnitudes brighter than type II. Because of their lower luminosities and the irregularities in their light curves, type II supernovae are not suitable for testing the expansion hypothesis.

Not every one of the 51 identified type I supernovae in Kowal and Sargent's list is a suitable candidate for the test proposed in

this thesis. Some were observed only sporadically so it is possible to obtain only very fragmentary light curves for them. The ones for which good light curves do exist have been measured in many different magnitude systems, ranging from the visual observations for the 1885 Andromeda outburst to modern narrow band photoelectric photometer measurements. Because the light curves may decay at different rates in different wavelength bands, it is necessary to reduce all of the light curves to a common magnitude system. These reductions to a common photometric system are the subject of the next chapter.

Although most of the data used in this thesis were gathered from the existing literature, one of the light curves was actually measured by the author and other members of the University of Illinois Astronomy Department. These observations have been reported by Deming, Rust, and Olson in a paper for the Publications of the Astronomical Society of the Pacific (52). The results of a preliminary reduction of the data will also be given in this thesis in order to illustrate how the various kinds of photometric data are reduced to a common system. The supernova in question is the 1971 outburst in the galaxy NGC 5055 (M 63), which was discovered by G. Jolly on May 24, 1971 (53). It was observed at the University of Illinois Prairie Observatory using the four-inch Ross camera and the 40-inch reflector. The Ross camera observations were made on IIa-O plates without a filter so that the resulting photometric system was very nearly the standard international photographic magnitude system, denoted in this thesis by the symbol m_{pg}. The 40-inch reflector observations include photoelectric B and V observations and photographic B, V, and m_{pg} observations.

The observed data were reduced using a sequence of comparison stars whose B and V magnitudes were measured photoelectrically and whose m_{pg} magnitudes were then synthesized according to the standard conversion formula

$$m_{pg} = B - 0.29 + 0.18(B - V). \qquad (5\text{-}1)$$

The details of the reduction and the final resulting magnitudes are given in (52). Table 5-1 gives the results of a preliminary reduction.

Although equation (5-1) was originally derived for transforming the magnitudes of main sequence stars, it works quite well for transforming supernova magnitudes. For example, when it is applied to the B and V magnitudes measured on 6/22/71 and on 7/16/71, it gives m_{pg} magnitudes of 14.65 and 15.21. The corresponding measured m_{pg} magnitudes on these dates were 14.60 and 15.25. When all of the measured B and V magnitudes are converted to m_{pg} by Eq. (5.1), the result is the light curve shown in Fig. 5-1, which also shows a measurement made on May 20, 1971, by van Herk and Schoenmaker (54, 55) and one made on May 25, 1971, by K. Ishida (56). These last two measurements are shown as open circles while the Prairie Observatory measurements are shown in closed circles. The measurement by van Herk and Schoenmaker was made originally in the m_{pg} system, while that of Ishida was made in the UBV system and converted to m_{pg} by Eq. (5.1).

A thorough search of the literature revealed 36 other type I supernovae with light curves complete enough to be used in this study. Some of these light curves were extremely well defined by the observations, while others were somewhat fragmentary although still usable.

Table 5-1

Prairie Observatory Measurement of the Light Curve of SN 1971i

Date	Telescope	Recorder	B	V	m_{pg}
5/30/71	Ross	Photograph.			12.1
5/30/71	40 inch	Photoelec.	12.45	12.10	
5/31/71	Ross	Photograph.			11.8
5/31/71	40 inch	Photoelec.	12.29	11.98	
6/1/71	Ross	Photograph.			11.7
6/1/71	40 inch	Photoelec.	11.94	11.51	
6/3/71	Ross	Photograph.			12.3
6/9/71	40 inch	Photograph.	13.12	12.20	
6/10/71	40 inch	Photograph.	13.45	12.30	
6/14/71	40 inch	Photograph.	13.95	12.70	
6/16/71	40 inch	Photograph.	13.95	12.75	
6/17/71	Ross	Photograph.			14.10
6/22/71	40 inch	Photograph.	14.70	13.35	14.60
6/23/71	40 inch	Photoelec.	14.58	13.39	
6/29/71	40 inch	Photoelec.	15.06	13.83	
7/3/71	40 inch	Photoelec.	14.83	13.97	
7/14/71	40 inch	Photoelec.	15.25	14.05	
7/16/71	40 inch	Photograph.	15.35	14.50	15.25
7/29/71	40 inch	Photograph.	15.45	14.90	
7/31/71	40 inch	Photograph.	15.50	15.00	
8/2/71	40 inch	Photograph.	15.50	14.90	
8/3/71	40 inch	Photograph.	15.30	15.05	
8/14/71	40 inch	Photograph.	15.8		

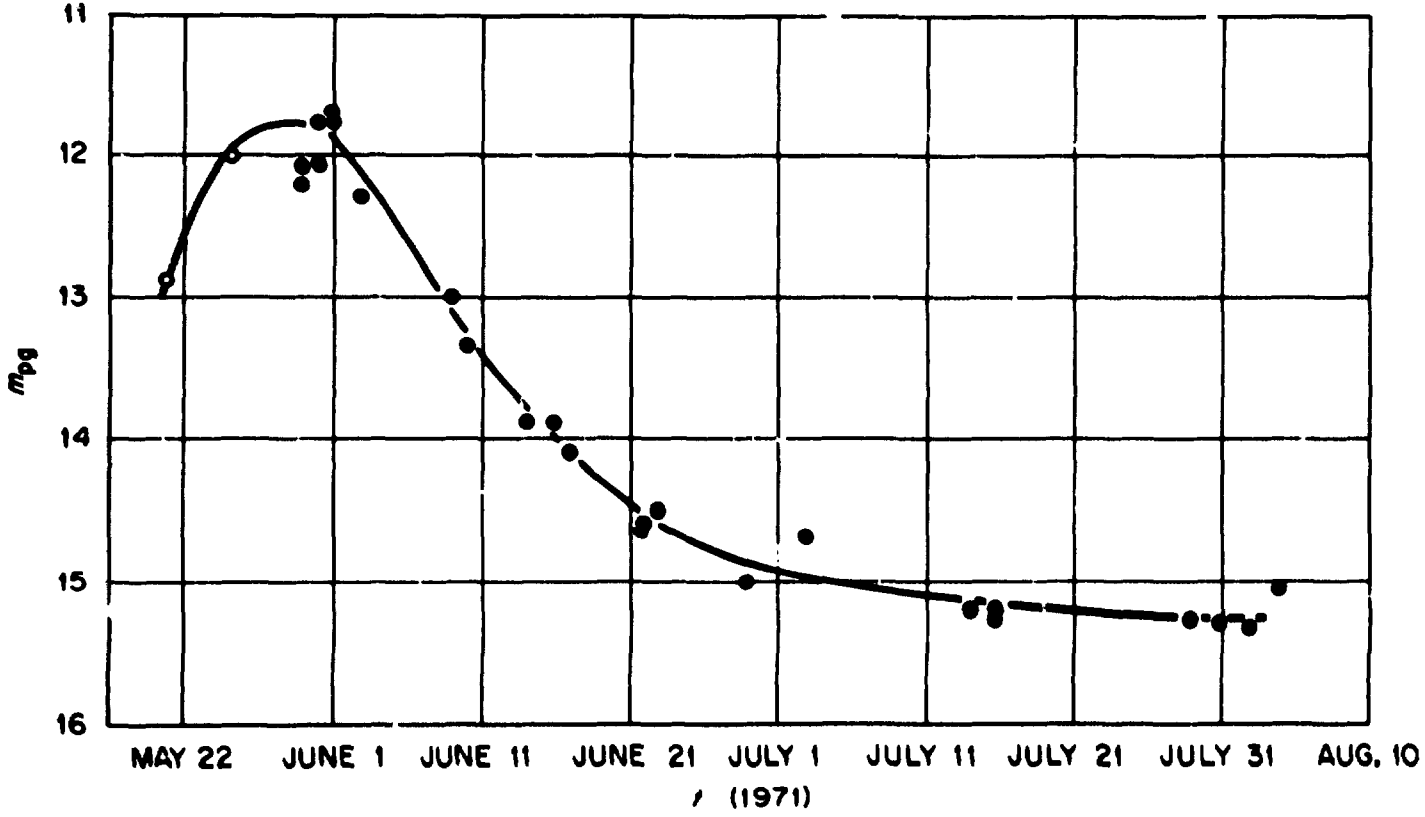

Figure 5-1. The Light Curve Measured at Prairie Observatory for SN1973i.

Table 5-2 lists all the supernovae used and gives for each of them, the observers, the magnitude systems in which the measurements were made, and the observational references. It also lists some of the relevant data about the parent galaxies in which the supernovae occurred.

Column 1 gives the supernova designation, which consists of the year of occurrence followed by a letter designating the order of occurrence within that year.

Column 2 gives the discovery number of the supernova. It is a continuation of a numbering system first used by Zwicky, and since adopted by others, in which the supernovae are numbered consecutively in the order of their discovery.

Column 3 contains the name of the parent galaxy in which the outburst occurred.

Column 4 gives the right ascension (epoch 1950.0) of the parent galaxy.

Column 5 gives the declination (epoch 1950.0) of the parent galaxy.

Column 6 contains the Hubble type of the parent galaxy.

Column 7 gives the symbolic velocity of recession of the parent galaxy expressed in km/sec. Entries in this column which are not enclosed in parentheses are based on measured red shifts, taken for the most part, from the Reference Catalogue of de Vancouleurs and de Vancouleurs (117) and from a paper by Humason, Mayall, and Sandage (118). In a few cases the given red shifts were measured by the supernova observers. In the cases where no red shifts have been measured for

the galaxies, the symbolic velocities were computed from the velocity-distance relationship with the Hubble constant equal to 100 km/sec/Mpc, using distance estimates obtained by comparing the apparent magnitudes of the galaxies with the absolute magnitudes derived from various luminosity functions for galaxies. More details on these calculations will be given in Chapter 9. Symbolic velocities calculated in this fashion are the ones enclosed by parentheses.

Column 8 contains the apparent photographic magnitudes of the parent galaxies. Many of these magnitudes are averages of measurements taken by more than one observer. The preferred sources were Holmberg (120), Pettit (121), and Humason, Mayall, and Sandage (118). Other sources included Bigay (122), de Vancouleurs and de Vancouleurs (117), and Zwicky, et al. (123, 124). The magnitudes listed here have not been corrected for absorption within our own galaxy.

Column 9 lists, for each supernova, all the observers whose measurements were used in the final light curves given in this thesis. For some objects additional observations exist, but were not used because they were either (a) measured in a magnitude system which could not be converted to the standard m_{pg} system, or (b) measured in some magnitude system other than m_{pg} but were largely redundant because many m_{pg} measurements existed for that supernova, or (c) measured only at times several months after the peak so that they were outside the time range of interest. Although they were not used for composing the final light curves, some of these discarded magnitudes were, nonetheless, used to derive color excesses in order to estimate internal absorptions within

the parent galaxies. These estimates are described in Chapter 9, and the references to the data used are given there.

Column 10 gives, for each observer, the magnitude system or systems in which the measurements were made. The symbols used in this column are:

m_{vis} = visual magnitude measured by eye,

m_{pg} = international standard photographic magnitude,

m_{pv} = photovisual magnitude,

B = blue magnitude in UBV system,

V = yellow magnitude in UBV system (same as m_{pv}),

m_K = blue magnitude in system of Kaho (98, 108),

b = blue magnitude in system of Marx and Pfau (111).

Column 11 gives, for each observer, the reference to the article where the data were published.

Column 12 is used for additional comments about the supernova or one of the sets of measurements. These comments are listed as footnotes at the end of the table.

Tables listing all the magnitude data used in this thesis are given in Appendix 1. All of the magnitudes were reduced to the standard m_{pg} system for consistency. These reductions are described in the next chapter. Appendix 1 gives both the unreduced and the reduced data.

Table 5-2

General Information About the Supernovae Included in This Study

SN	No.	Galaxy	α(1950)	δ(1950)	Type	V_r	m_{pg}	Observers	Mag. System	Ref.	Notes
1885a	1	M 31	$00^h\ 40^m.0$	41°00'	Sb	-299	4.33	Hartwig & Others	m_{vis}	(57, 58)	
1921c	16	NGC 3184	$10^h\ 15^m.3$	41°40'	Sc	418	10.24	Shapley	m_{pg}	(59)	*
1937c	25	IC 4182	$13^h\ 03^m.5$	37°52'	Sc	50C	13.5	Baade & Zwicky	m_{pg}	(60)	
								Deutsch	m_{pg}	(61)	
								Parenago	m_{pg}	(57)	
1937d	26	NGC 1003	$02^h\ 36^m.1$	40°40'	Sc	58?	12.0	Baade & Zwicky	m_{pg}	(60)	
								Parenago	m_{pg}	(57)	
1939a	30	NGC 4636	$12^h\ 40^m.3$	2°38'	E0	883	10.6	Baade	m_{pg}	(48)	*
								Giuliano	m_{pg}	(62)	
								Hoffleit	m_{pg}	(63)	
1939b	31	NGC 4621	$12^h\ 39^m.5$			414	11.0	Shapley	m_{pg}	(64)	
								Baade	m_{pg}	(48)	*
1954a	30	NGC 4214	$12^h\ 13^m.1$	36°37'	Irr	290	10.16	Wild	m_{pg}	(65)	
								Pietra	m_{pg}	(65, 66)	*
								Hoffmeister	m_{pg}	(66)	
1954b	31	NGC 5668	$14^h\ 30^m.9$	4°40'	Sc	1,737	12.2	Wild	m_{pg}	(65)	
								Pietra	m_{pg}	(65, 66)	*

Table 5-2 (Continued)

SN	No.	Galaxy	α(1950)	δ(1950)	Type	V_r	m_{pg}	Observers	Mag. System	Ref.	Notes
1955-	53	Anon.	$1^h\ 05^m.0$	-13°30'	SBa	16,024	15.7	Zwicky	m_{pg}	(67)	*
1956a	54	NGC 3992	$11^h\ 55^m.0$	53°39'	SBb	1,059	10.56	Zwicky & Karpowicz	m_{pg}, m_{pv}	(68)	
1957a	55	NGC 2841	$09^h\ 18^m.5$	51°12'	Sb	631	10.05	Zwicky & Karpowicz	m_{pg}, m_{pv}	(69)	*
								Bertola	m_{pg}	(70)	
								Wenzel	m_{pg}	(71)	
1957b	56	NGC 4374	$12^h\ 22^m.5$	13°10'	E1	954	10.35	Bertola	m_{pg}	(70)	
								Gotz	m_{pg}	(72)	
								Romano	m_{pg}	(75)	
								Li Tzin	m_{pg}	(73)	
1959c	62	Anon.	$13^h\ 08^m.8$	3°40'	SBc	2,990	15.8	Mihalas	m_{pg}, B, V	(74)	
1960f	69	NGC 4496	$12^h\ 29^m.1$	4°13'	SBc	1,773	11.9	Bertola	m_{pg}	(70)	
								Huth	m_{pg}	(76)	
								Kulikov	m_{pg}	(77)	
								Tempesti	m_{pg}	(78)	
								Mannino	m_{pg}	(79)	
1960r	86	NGC 4382	$12^h\ 22^m.9$	18°28'	S0	773	10.05	Bertola	m_{pg}	(70)	
								Zaitseva	m_{pg}	(80)	
								Gates	B, V	(81)	
1961d	87	Anon.	$12^h\ 48^m.3$	28°06'	E0	7,700	15.0	Zwicky	m_{pv}, m_{pg}	(82)	

Table 5-2 (Continued)

SN	No.	Galaxy	α(1950)	δ(1950)	Type	V_r	m_{pg}	Observers	Mag. System	Ref.	Notes
1961h	92	NGC 4564	$12^h\ 33^m.9$	11°43'	E6	941	12.2	Romano	m_{pg}	(83)	*
1961p	100	Anon.	$2^h\ 32^m.5$	37°25'	Sc	3,665	13.2	Bertola	m_{pg}	(70)	
1962m	106	Anon.	$13^h\ 04^m.3$	28°08'	S0	6,137	16.0	Zwicky & Barbon	m_{pv}, m_{pg}	(84)	
1962e	111	Anon.	$11^h\ 12^m.5$	26°10'	E0, E3	14,190	15.5	Rudnicki & Zwicky	m_{pv}, m_{pg}	(85)	*
1962j	117	NGC 6835	$19^h\ 51^m.8$	-12°42'	SBa	(2,500)	13.0	Bertola	m_{pg}	(86)	
1962i	119	NGC 1073	$2^h\ 41^m.1$	1°10'	SBc	1,874	11.6	Bertola	B, V	(87)	
								Rosino	m_{pg}	(88)	
1962p	145	NGC 1654	$4^h\ 43^m.3$	-2°11'	E	(3,600)	14.2	Rosino	m_{pg}	(89)	
1963d	126	NGC 4146	$12^h\ 07^m.8$	26°42'	SBa	(6,000)	13.8	Bertola	m_{pg}	(86)	
								Rosino	m_{pg}	(90)	
1963i	131	NGC 4178	$12^h\ 10^m.3$	11°08'	SBc	233	11.8	Zaitseva	m_{pg}	(91)	
								Lochel	m_{pg}	(92)	
								Bertaud	m_{pg}	(93)	
1963j	132	NGC 3913	$11^h\ 48^m.0$	55°37'	Sc	(3,200)	14.2	Zwicky	m_{pg}	(94)	
								Wild	m_{pg}	(95)	
								Chincarini & Margoni	m_{pg}	(96)	
1963p	138	NGC 1084	$2^h\ 43^m.5$	-7°47'	Sc	1,465	11.1	Bertola, et al.	B	(97)	
								Kaho	m_K	(98)	

Table 5-2 (Continued)

SN	No.	Galaxy	α(1950)	δ(1950)	Type	V_r	m_{pg}	Observers	Mag. System	Ref.	Notes
1964e	150	Anon.	11^h $56.^m6$	52°59'	SBc	(2,900)	14.5	Lovas	m_{pg}	(99)	
								Ahnert	m_{pg}	(100)	
								Chuadze	m_{pg}	(101)	
								Zaitseva	m_{pg}	(102)	
								Lochel	m_{pg}	(103)	
1964f	159	NGC 3938	11^h $50.^m2$	44°23'	Sc	874	10.8	Bertola, et al.	m_{pg}	(97)	
1965l	170	NGC 4753	12^h $49.^m8$	-0°5c'	Irr	1,364	10.7	Van Lyong & Panarin	m_{pg}	(104)	
								Ciatti & Barbon	B, V	(105)	
1966j	186	NGC 3198	10^h $16.^m9$	45°49'	SBc	649	10.8	Wild	m_{pg}	(106)	
								Chincarini & Perinotto	B	(107)	
								Kaho	m_K	(108)	
1966k	187	Anon.	11^h $15.^m6$	28°33'	SO	(5,000)	14.7	Rudnicki	m_{pg}, m_{pv}	(109)	
1966n	198	Anon.	4^h $34.^m3$	-3°08'	SB?	(9,600)	16.0	Ciatti & Barbon	m_{pg}	(105)	
1967c	192	NGC 3389	10^h $45.^m8$	12°48'	Sc	1,276	12.1	de Vancouleurs, et al.	B, V	(110)	
								Marx & Pfau	b	(111)	
								Borsov, et al.	~ B	(112)	*
								Chuadze & Barblishvili	m_{pv}	(113)	
								Kaho	m_K	(108)	

Table 5-2 (Continued)

SN	No.	Galaxy	α(1950)	δ(1950)	Type	V_r	m_{pg}	Observers	Mag. System	Ref.	Notes
1968e	211	NGC 2713	$8^h\ 54^m.7$	3°06'	Sb	3,810	12.7	Chevira	m_{pg}	(114)	
								Rusev	m_{pg}	(91)	*
								Ciatti & Barbon	B, V	(105)	
1969c	235	NGC 3811	$11^h\ 38^m.6$	47°58'	Sc	3,120	13.0	Bertola & Ciatti	B, V	(115)	
1971i	299	NGC 5055	$13^h\ 13^m.5$	42°17'	Sb	520	9.1	Deming, et al.	m_{pg}, B, V	(52)	
								Ishida	B, V	(56)	
								Van Herk & Schoenmaker	m_{pg}	(54, 55)	
								Scovil	m_{pv}	(116)	

Table 5-2 (Continued)

1921c: Karpowicz and Rudnicki (46) classify this as a type II supernova, and Kowal and Sargent (47) do not classify it. In 1968, Kowal (49) classified it as type I and estimated its absolute magnitude at peak to be -18.7 which is nearly equal to the average peak absolute magnitude that he found for type I and more than two magnitudes brighter than the average that he found for type II. The light curve, although somewhat fragmentary, is entirely consistent with the type I interpretation. Coupled with its high intrinsic luminosity, it is almost certain that SN 1921c was indeed a type I supernova.

1939a: The actual measurements of Baade have been published only in graphical form. The values used were read as accurately as possible from a graph given by Minkowski (48).

1939b: Same as note for SN 1939a

1954a: The magnitudes of Pietra were remeasured by Rosino using the same comparison stars as Wild. These "corrected" magnitudes are the ones used for deriving the light curve used in this thesis.

1954b: Same as note for SN 1954a.

1955b: This supernova has apparently never been classified as to type by anyone. The light curve is consistent with a type I interpretation, and Zwicky (67) estimated that it was intrinsically one of the brightest supernovae ever observed. Zwicky's estimate was made on the basis of Hubble's old distance scale, but an estimate based on a more modern value of the Hubble constant (H = 100 km/sec/Mpc) gives a peak absolute magnitude of -20.3 which indeed is extremely bright and virtually guarantees that it was a type I supernova.

Table 5-2 (Continued)

1957a: Bertola classified this supernova as type I, but Zwicky classified it as type II. The light curve strongly indicates type I, but estimates of its peak absolute magnitude are much lower than the average for type I and are, in fact, consistent with a type II interpretation. The spectra that were obtained do not settle the matter either way. Measurements of the color index indicate an extremely high degree of reddening and hence a large amount of absorption within the parent galaxy. This absorption correction is calculated in Chapter 9. It amounts to almost three magnitudes, and makes the peak luminosity consistent with the type I interpretation.

1961h: The light curve for this supernova was too fragmentary to be useful in the test of the expansion hypothesis, but it is useful for other calculations which are described in Chapter 9.

1962e: This supernova occurred on a luminous bridge between two elliptical galaxies. According to Rudnicki and Zwicky (85), the bridge is apparently composed of late type stars.

1967c: According to Borzov, et al., their photometric system is very close to the B system, but small systematic differences are present.

1968e: The magnitudes of Rusev were read as accurately as possible from a graph given by Pskovskii (51).

CHAPTER 6

REDUCTION OF THE DATA

Light curves of type I supernovae exhibit a high degree of uniformity, but the possibility that the rate of decline in luminosity is different in different wave length bands must be allowed for if the rate of decline is to be used to test for the Doppler effect. All the supernovae used in the test must have their light curves expressed in the same bandpass or magnitude system. A quick inspection of Table 5-2 reveals that the most commonly used system thus far has been the standard m_{pg} system. Furthermore, the spectrum of the typical type I supernova is dominated by a wide bright band centered between 4600Å and 4700Å [see, for examples, refs. (60), (86), (87), (96), (97), and (107)]. This band, which is generally interpreted as the λ4686, n=4 → n=3 transition of HeII, is completely encompassed by the bandpass of the m_{pg} system and, in fact, typically contains about one half of the total photographic intensity. Thus, the logical choice for the common magnitude system is the m_{pg} system.

In the preceding chapter, a light curve was given for SN 1971i (Fig. 5-1), in which part of the magnitudes were measured m_{pg} and part were calculated by the standard transformation equation,

$$m_{pg} = B - 0.29 + 0.18\ (B - V), \qquad (6\text{-}1)$$

using measured B and V magnitudes. There were two nights in which both B, V and m_{pg} magnitudes were measured by the same technique on the same telescope. A comparison of the measured and calculated m_{pg} magnitudes for those nights is given in Table 6-1.

Table 6-1

Comparison of Measured m_{pg} Magnitudes
With Values Computed From B, V Magnitudes

Date	Measured m_{pg}	B, V → m_{pg} by (6-1)
6/22/71	14.60	14.65
7/16/71	15.25	15.21

The agreement is quite good. In other cases where both B, V and m_{pg} magnitudes are available, Eq. (6-1) gives the same sort of result, with the average discrepancies between the calculated and the measured m_{pg} lying within the range of scatter due to measuring errors. Particular examples are SN 1962*l* and SN 1965i, whose light curves can be found in Appendix 2. Thus, Eq. (6-1), which was originally derived for converting the magnitudes of main sequence stars, apparently gives accurate conversions for supernova magnitudes also.

It is easy to use Eq. (6-1) when both B and V measurements are available, but some supernova observers have measured only B or else only V (or, what is equivalent, only m_{pv} or only m_{vis}). The work of the Russian astronomer Yu. P. Pskovskii (51, 125) on the time dependence of the colors of supernovae makes it possible to use Eq. (6-1) for converting the magnitudes even in these cases. Pskovskii has determined the relationship between the intrinsic B-V color of a supernova and the time in days after the date of maximum brightness. In

(51) he gave this relationship in the form of a graph which is shown in Figure 6-1. The ordinate $(B-V)_o$ is the intrinsic color of the supernova light, i.e., the color of the light before it is reddened by absorption in our own and the parent galaxy of the supernova. It represents the average of the color curves of six different supernovae all corrected for reddening due to absorption. These corrections were determined by shifting the various color curves vertically until all six were superimposed. The only remaining problem then was to calibrate the resulting composite color curve by determining the absolute color excess,

$$E(B - V) = (B - V) - (B - V)_o ,$$

for one or more of the component light curves. One of the supernovae used for this purpose was SN 1954a, which occurred in the irregular galaxy NGC 4214. According to Pskovskii, the amount of reddening in the parent galaxy is negligible for elliptical and irregular galaxies. Thus in the case of SN 1954a, it was only necessary to worry about the reddening in our own galaxy. Since NGC 4214 is located at galactic latitude $b^{II} = 78°.07$, this reddening was small, and Pskovskii was able to estimate it by using the Lick counts of faint galaxies in neighboring areas of the sky.

It is quite easy to convert B magnitudes to m_{pg}, using Eq. (6-1) and Figure 6-1, provided that the date of maximum brightness of the supernova is known. For each B magnitude to be converted, the value of $(B - V)_o$ for that day is read from the graph and the m_{pg} magnitude

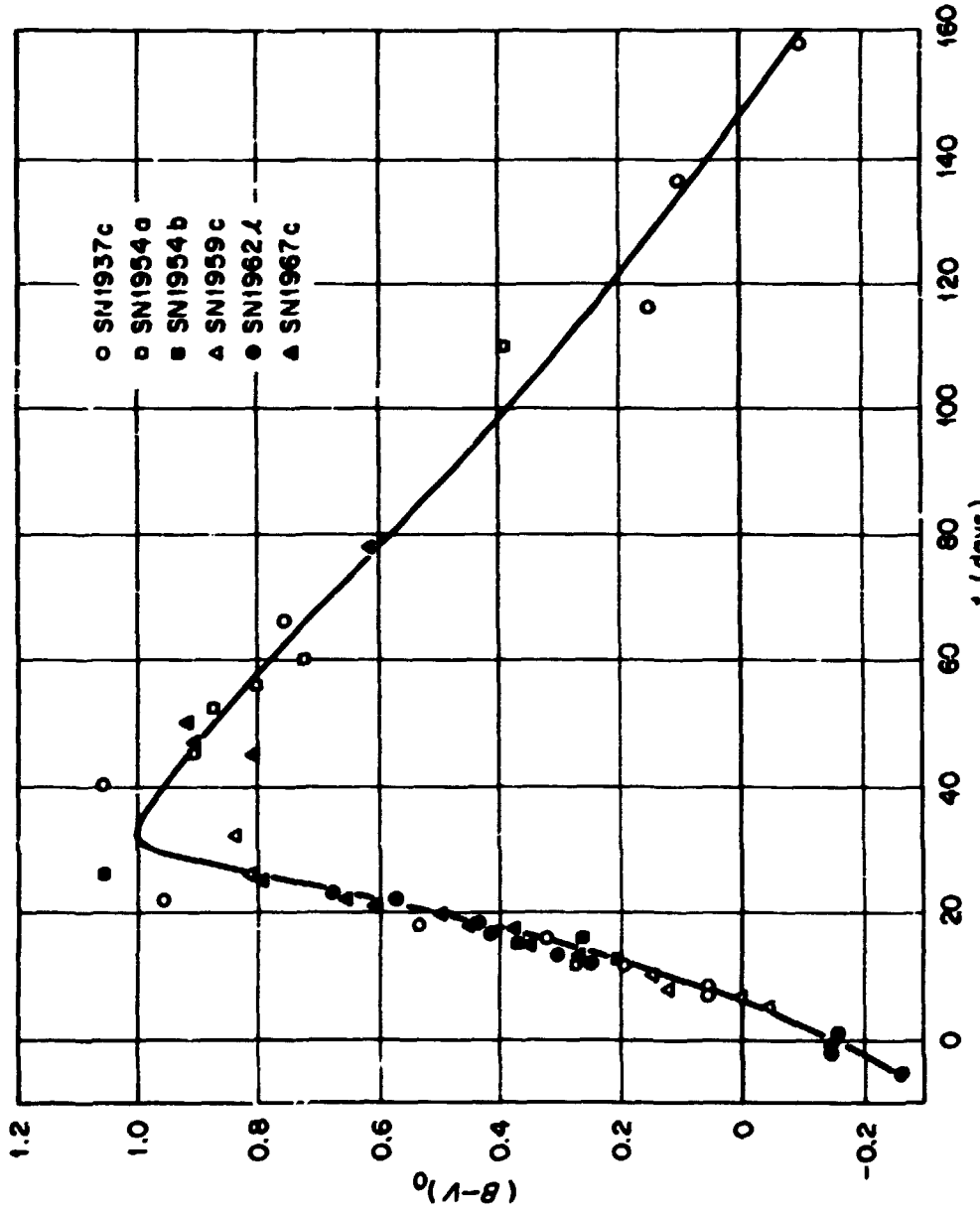

Figure 6-1. Pakovskii's $(B - V)_o$ - t Relation.

is calculated by

$$m_{pg} = B - 0.29 + 0.18\ (B - V)_o \ . \qquad (6\text{-}2)$$

Of course, there will be a zero point error in these magnitudes because of the unknown amount of reddening due to absorption. In some cases it is possible to estimate this reddening correction. One common situation is to have both B and V measurements for a few days, but B only for other days. The color excess E(B - V) can then be determined from the vertical shift needed to bring the Pskovskii color curve into coincidence with the measured values of (B - V). This color excess can then be added to values of $(B - V)_o$ read from the graph, and the resulting corrected B - V colors can then be used to convert the B magnitudes to m_{pg} by means of Eq. (6-1) rather than by (6-2).

Another situation that arises quite often is to have some measured B magnitudes and no V magnitudes and to also have some measured m_{pg} magnitudes. In these cases the B magnitudes can be converted to m_{pg} by means of Eq. (6-2) and the zero point correction can be determined from the vertical shift required to bring the light curve of the converted magnitudes into coincidence with the light curve of the measured m_{pg} magnitudes.

If only B magnitudes are available, then it is not possible to determine the zero point error in the magnitudes calculated from Eq. (6-2). But light curves obtained by this method can still be used to test the expansion hypothesis because it is the slope, or rate of decline,

of the light curve that is used for the test. Since a zero point error simply shifts the entire curve vertically by a constant amount, the rate of decline is not changed by the error.

The Pskovskii graph can also be used to convert magnitudes measured in the V system. One way to carry out this conversion is to note that if V is subtracted from both sides of Eq. (6-1), the result is

$$m_{pg} - V = B - V - 0.29 + 0.18\ (B - V),$$

which can also be written

$$m_{pg} = V - 0.29 + 1.18\ (B - V). \qquad (6\text{-}3)$$

If measured values of both B and V are available, then the V magnitudes can be converted directly to m_{pg} by means of (6-3). If only V magnitudes are available, then the corresponding values of $(B - V)_o$ can be read from the Pskovskii graph and the conversion can be accomplished by

$$m_{pg} = V - 0.29 + 1.18\ (B - V)_o. \qquad (6\text{-}4)$$

Of course, there will be a zero point error in the magnitudes determined by the latter formula, and all of the comments that were made in the preceding paragraphs with regard to the zero point errors in the conversion of B magnitudes can be rephrased to apply here also. Since the m_{pv} system is just another name for V and since it was designed to be the photographic equivalent of the m_{vis} system, Eq. (6-4) can also be written as

$$m_{pg} = m_{pv} - 0.29 + 1.18\ (B - V)_o, \qquad (6\text{-}5)$$

or as

$$m_{pg} = m_{vis} - 0.29 + 1.18\ (B - V)_o\ . \qquad (6\text{-}6)$$

There is another way by which m_{pv} or m_{vis} magnitudes can be converted to m_{pg} using the Pskovskii $(B - V)_o$ - t relationship. It is apparent from Eq. (6-5) that intrinsic $(m_{pg} - m_{pv})$ color indices [denoted by $(m_{pg} - m_{pv})_o$] can be calculated from intrinsic (B - V) colors by means of the equation

$$(m_{pg} - m_{pv})_o = 1.18\ (B - V)_o - 0.29. \qquad (6\text{-}7)$$

By this means, the Pskovskii $(B - V)_o$ - t relationship is converted to an $(m_{pg} - m_{pv})_o$ - t relation. The result of this conversion is shown graphically in Figure 6-2. Measured m_{pv} or m_{vis} magnitudes can be converted to m_{pg} by reading the corresponding $(m_{pg} - m_{pv})_o$ values from this graph and adding them to the measured magnitudes. This conversion will also contain an unknown zero point shift.

All of the magnitude conversion methods based on Pskovskii's (B - V) - t relation require a knowledge of the date t_o on which the supernova attained maximum brightness. For a well observed supernova, it is usually an easy matter to determine t_o and the peak magnitude m_o simply by inspecting the light curve. For more fragmentary light curves, this method is often not feasible, but Pskovskii (51) has developed several methods for estimating t_o and m_o in such cases. Before discussing these methods, it seems appropriate to point out that in cases where a number of B - V measurements are available, covering a time span of two weeks or more, it is possible to use the (B - V) - t relationship itself for determining t_o. This is done by shifting the graph of the

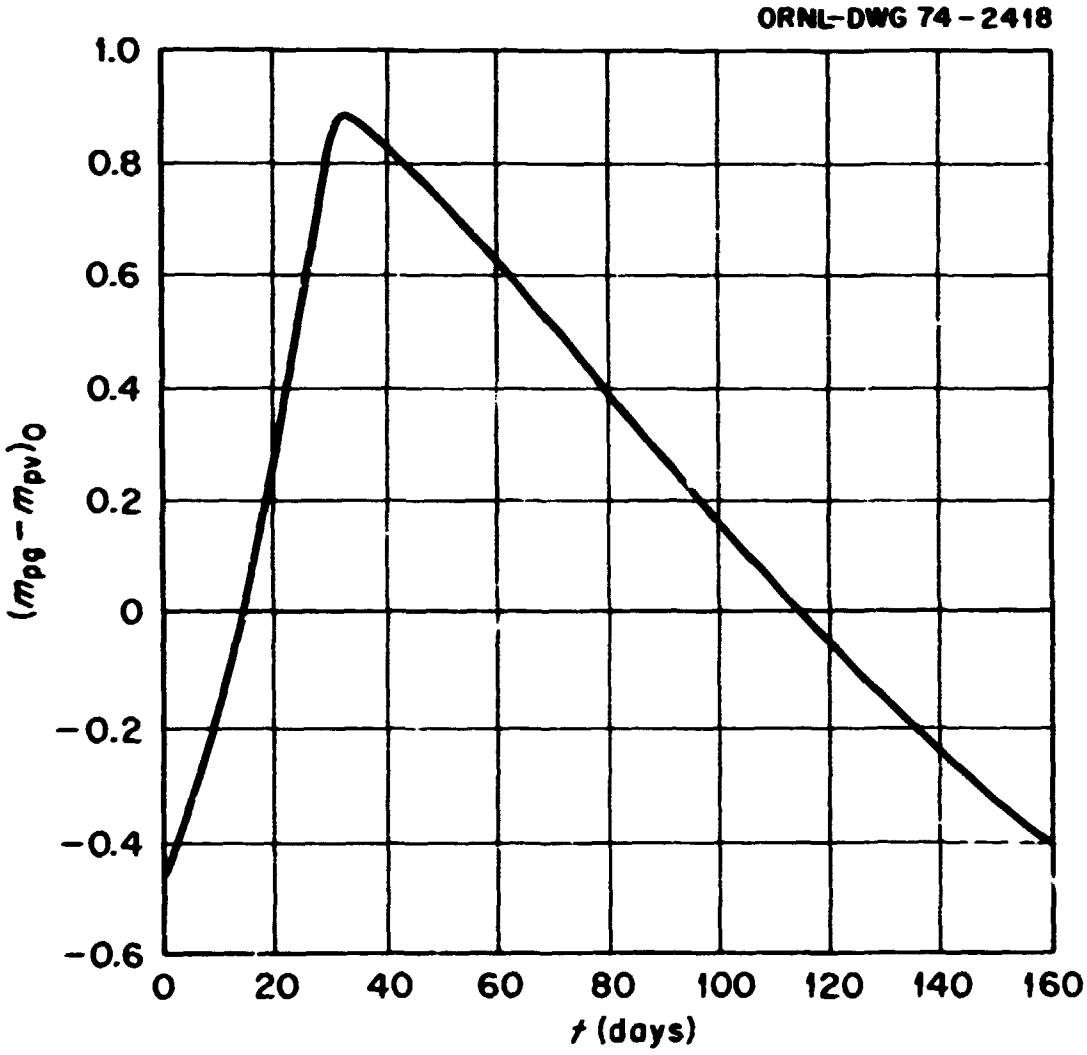

Figure 6-2. The $(m_{pg} - m_{pv})_o$ - t Relation Derived from Pskovskii's (B - V) - t Relation.

relationship horizontally until it coincides with the observed data. Of course, the horizontal shifts must be accompanied by simultaneous vertical shifts to take into account the reddening. Thus, the final "fit" of the curve to the measured data gives both the date of maximum t_o and the color excess E(B - V). The main limitation of this technique is the extent of the measured data which is required. Because the color curve is very nearly linear on both sides of the peak, which occurs at about 33 days after maximum, the measured data must span a considerable time range and should preferably span the peak in order to determine unambiguously both t_o and E(B - V). Of course, if one of these parameters can be independently determined, then the other one can be unambiguously estimated by shifting the color curve in only one direction, and this can be accomplished even with a small number of measured points covering only a short time span. This is a particularly useful technique for determining the color excess once t_o is known. Values of E(B - V) obtained in this way can then be used to determine the absorption correction for the magnitudes. Similarly, if the measured color indices are $(m_{pg} - m_{pv})$ indices, then the same technique can be used for estimating $E(m_{pg} - m_{pv})$ color excesses simply by using the converted $(m_{pg} - m_{pv})_o$ - t relation given in Figure 6-2. The use of color excesses, determined by these methods, for correcting the peak magnitudes m_o will be discussed in Chapter 9.

One method which Pskovskii and a number of other observers have used quite successfully for estimating the date t_o of maximum brightness of a supernova is based upon the time behavior of the spectrum of the

supernova. Many observers have noticed that the bands in the spectrum of a typical type I supernova shift to the red as the light curve decays. According to Pskovskii, the best band to use for estimating the phase of the light curve is the λ4686 band, which dominates the photographic region of the spectrum. He was able to establish the relationship between the phase and the position of the center of the band by using supernovae with numerous measured spectra and also well defined light curves from which he could estimate t_o. He was then able to use this relationship to estimate the date t_o for three supernovae having fragmentary light curves but with a number of good spectral observations spread over several days. The details of the method are given in (51).

The spectral method requires several good spectra taken on different nights. This constraint limits the method to supernovae which are relatively nearby so that they are bright enough for good spectra to be obtained. Furthermore, if a number of good spectra are taken, then it is quite likely that a good light curve is measured also, so that the spectrum estimate is not needed except as confirmation.

Pskovskii has also developed two other good methods for estimating m_o and t_o which use only the fragmentarily observed light curves. Both of the methods are analogous to procedures that are used for estimating the maxima of novae with incomplete light curves. One of them involves the use of a series of average light curves, and the other reconstructs the maximum from the point where the slope of the light curve changes from rapid decay to gradual decay.

Pskovskii's average light curve method grew out of his studies of the rates of decline of the light curves of the various types of supernovae (50). He found that if straight lines are fitted to the rapidly descending portions of well observed type I light curves, then the rates of fall of the resulting straight lines vary between the extremes of 1 magnitude per six days and 1 magnitude per 12 days. In (51) he denoted this rate of fall by the letter b. He selected a group of well defined light curves and separated them into four different subgroups so that all the curves in a given subgroup had approximately the same b. The four subgroups were characterized by the four values b = 6, 8, 10, and 12. He then averaged all of the light curves within each subgroup and thus obtained four average light curves corresponding to the four b values. Using these average light curves, he was then able to estimate m_o and t_o for many fragmentary light curves whose peaks were not well defined by existing observations. The method was applicable in cases where there were enough observations in the rapid decay portion to give a good straight line fit. Using the value of b defined by the straight line fit, he could choose the most appropriate average light curve. He then fitted that average light curve to the fragmentary light curve and used the fitted curve to extrapolate backwards in order to estimate m_o and t_o.

Pskovskii's point-of-slope-change method is based on his observation that the point at which the slope changes from rapid decay to gradual decay almost always occurs between 2.8 and 3.3 magnitudes below peak brightness and is equal, on the average, to 3.1 magnitudes below

peak. To estimate the peak magnitude of a fragmentary light curve by this method, Pskovskii fitted straight lines to the rapid decay portion and the gradual decay portion. He used the letter k to denote the point at which these two straight lines intersected, and denoting the corresponding magnitude by m_k, he calculated the estimate of the peak magnitude m_o by the formula

$$m_o = m_k - 3^m.1. \qquad (6\text{-}8)$$

Pskovskii also used the point k for extrapolating backwards to determine the time of maximum but this method gives generally less accurate estimates of t_o than does the average light curve method.

By applying these methods to supernovae with well determined light curves, it was possible to estimate the average errors of all the methods. He found that the accuracies of the t_o computed by the point k method ranged from 1 to 5 days whereas the accuracies of the average light curve estimates were 0.5 to 1.5 days. The spectral method gave the lowest accuracy, with errors on the order of ± 5 days. In estimating the peak magnitude, the average light curve method gave accuracies of $0^m.05$ to $0^m.2$. The accuracies of the point k estimates of m_o were comparable.

It is a natural extension of Pskovskii's work to combine his point k and average light curve methods. There are undoubtedly several ways to combine them, but one natural method, which the present author has found to be effective, is first to apply the point k method in order to obtain an estimate of m_o and of the straight line slope b of the rapidly

falling segment of the light curve, and then to fit the most closely corresponding average light curve to the measured light curve using the point k estimate of m_o as a constraint. Using the m_o constraint makes t_o the only undetermined parameter of the fit and hence removes some of the ambiguity of the fitting method since only horizontal shifts along the time axis are required. This technique is illustrated for the supernova SN 1957a in Figures 6-3 and 6-4. Figure 6-3 illustrates the point k method. The straight line fit to the rapid descent portion of the light curve intersects the straight line fit to the later portion at a point k with magnitude $m_k = 16.95$. Since this point occurs, on the average, 3.1 magnitudes below peak brightness, the best estimate for peak brightness is $m_o = 13.85$. The only remaining problem is to estimate the date of maximum t_o. Since the slope of the straight line fit to the rapid descent portion is -1 magnitude per 6 days, Pskovskii's b = 6 average light curve is used in Figure 6-4 to obtain the estimate of t_o. The solid points represent measured magnitudes and the open circles connected by the curve represent the average light curve. The latter is shifted along the time axis, with its peak always constrained to lie on the horizontal straight line corresponding to $m_o = 13.85$, until the best fit to the measured light curve is obtained. In the case of SN 1957a, this best fit appears to occur at t_o = Feb. 27, 1957.

Pskovskii's methods were designed for use on fragmentary light curves measured in the m_{pg} system. For some of the supernovae used in this study (e.g., SN 1962e and SN 1966k) the light curves were fragmentary, with most of the magnitudes measured in the m_{pv} rather than

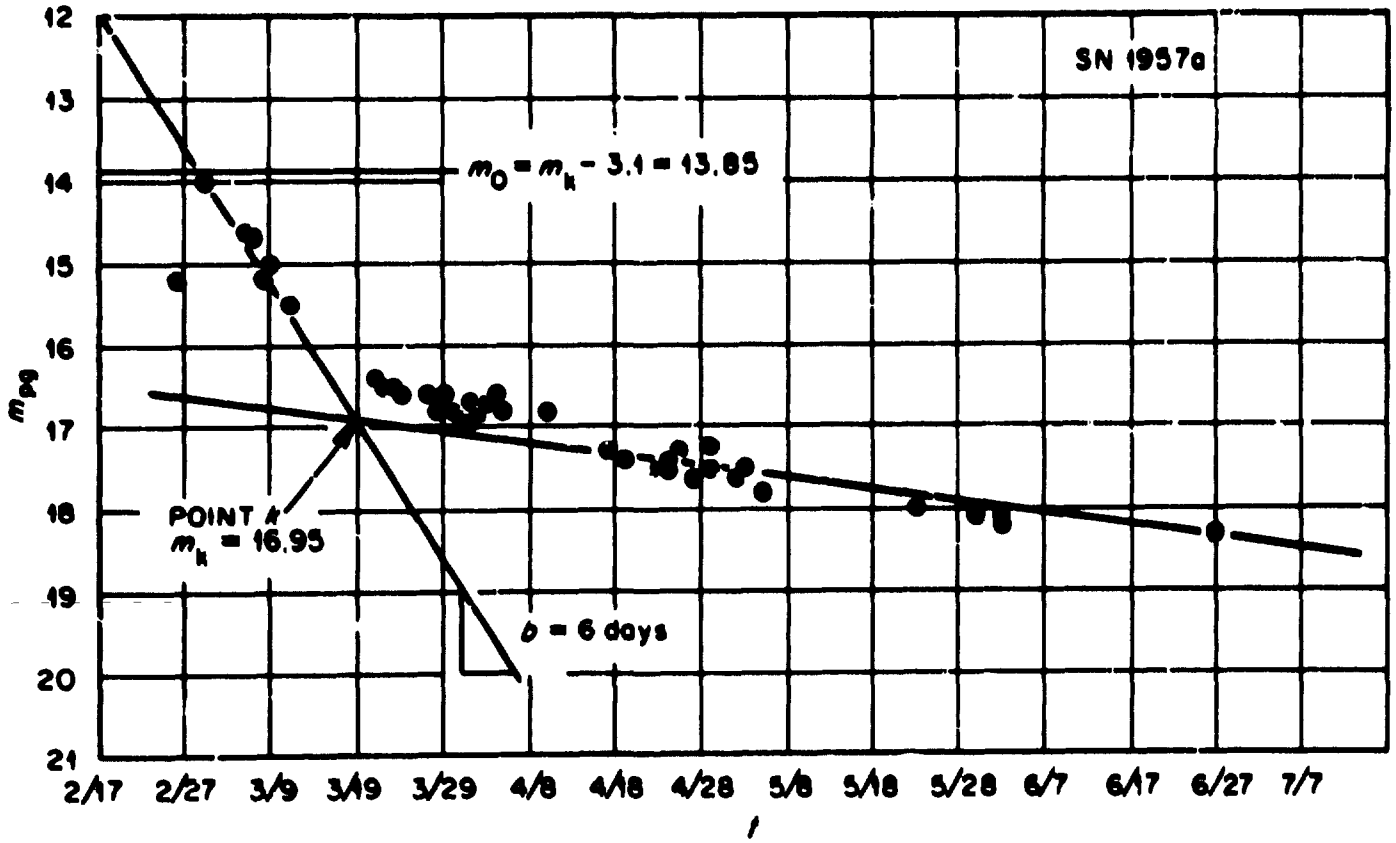

Figure 6-3. Pskovskii's Point k Method for Determining the Peak Magnitude m_o.

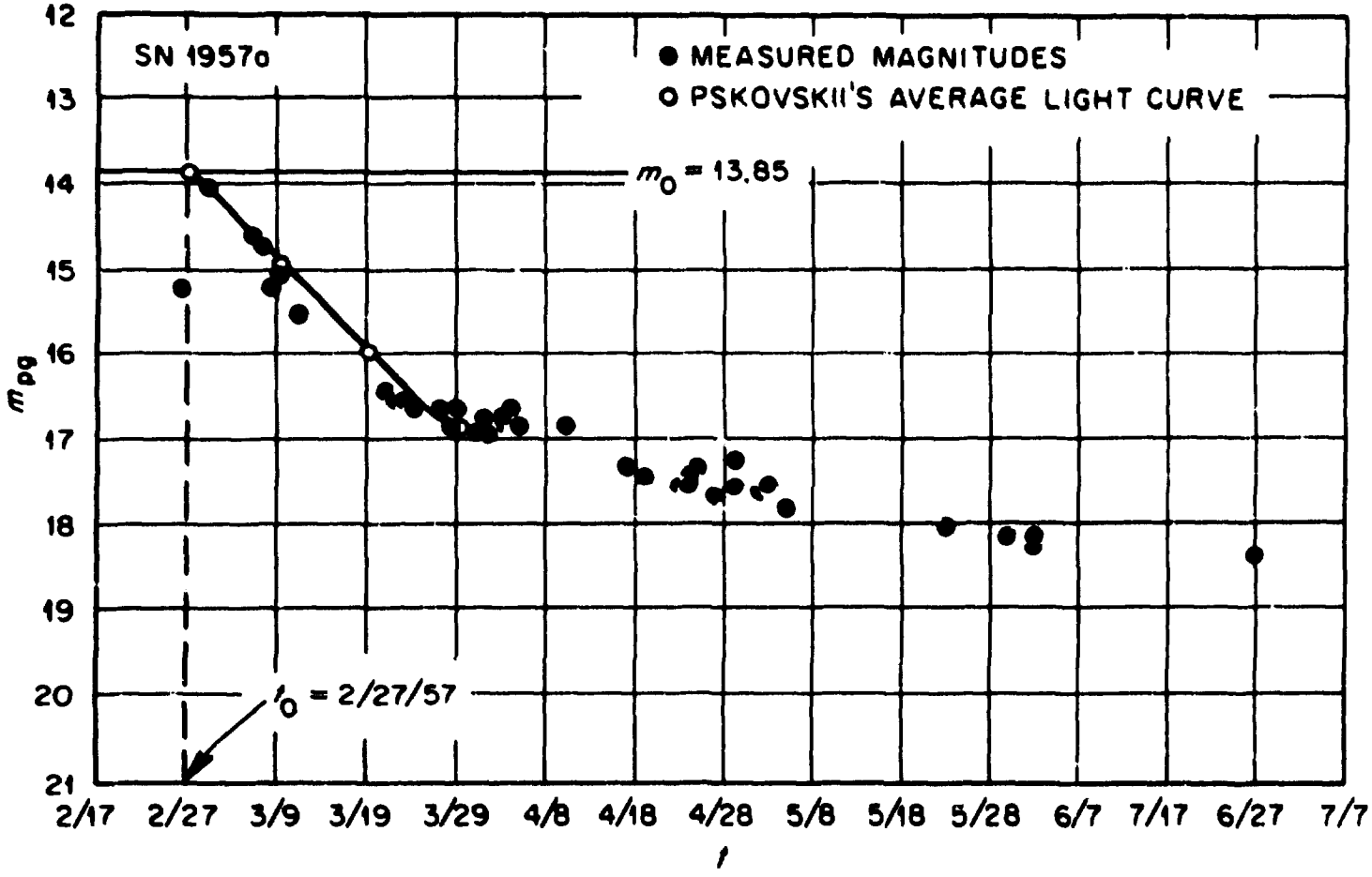

Figure 6-4. Pskovskii's Average Light Curve Method for Determining the Day t_o Peak Brightness.

the m_{pg} system. These m_{pv} magnitudes could not be converted directly to m_{pg} by means of the $(m_{pg} - m_{pv})_o$ - t relation discussed earlier because the date of maximum, t_o, was not known. On the other hand t_o could not be estimated directly from the extrapolation techniques because the magnitudes were measured in the m_{pv} system. The method adopted in such cases was an iterative one. Beginning with an initial guess for t_o, the m_{pv} magnitudes were converted to m_{pg} using the Pskovskii $(m_{pg} - m_{pv})_o$ - t relationship with the assumed t_o. A new estimate of t_o was then obtained by applying the combined point k, average light curve method described in the preceding paragraph. The whole process was then repeated until the estimates for t_o converged. This final converged value and the final converted magnitudes gave a consistent light curve which was adopted as the best estimate. In most cases there were a few measured values of m_{pg} so that it was possible also to determine the absorption correction which could then be used to eliminate the zero point error in the magnitude conversions.

Although this iterated conversion method used the Pskovskii $(m_{pg} - m_{pv})_o$ - t relation, the point k extrapolation method, and the average light curve method, it will be referred to in this thesis simply as the iterated point k method. Experiments with different starting estimates t_o revealed that a poor initial estimate would usually fail to give a converging iteration but that good estimates all gave convergence to the same final value. In some cases, poor initial estimates gave convergence also but the rate of convergence was considerably slower.

Table 6-2 gives, for the 37 supernovae used in this study, the dates of maximum, the peak magnitudes, and the methods used to obtain them in each case.

Column 1 gives the supernova designation.

Column 2 gives the discovery number in the Zwicky sequence.

Column 3 gives the name of the parent galaxy.

Column 4 gives the estimated peak magnitude of the supernova in the m_{pg} system.

Column 5 gives the method by which the peak magnitude estimate was obtained. The abbreviations in this column can be interpreted as follows: obs. l. c. means inspection of the observed light curve, pt. k means Pskovskii's point k method, av. l. c. means Pskovskii's average light curve method, and iterated pt. k means the iterated point k method.

Column 6 gives the estimated date of maximum either on the Julian day calendar or in month/day/year notation, depending for each supernova on how most of the observations were given in the literature.

Column 7 gives the method by which the estimated date of maximum was obtained. Most of the abbreviations in this column are the same as those in column 5. The two abbreviations which do not appear in column 5 are obs. color curve, which means that t_o was obtained by fitting measured color indices to one of Pskovskii's color index-time relations, and spectrum which means that t_o was estimated from one or more spectra of the supernova.

Column 8 indicates additional notes about the supernova. A single P means that the estimates m_o and t_o are both those of Pskovskii, and a single R means that both were done by the present author. The combination P, R means that the m_o estimate is that of Pskovskii and the t_o estimate was done by the present author. Similarly the combination R, P means that m_o is due to the present author and t_o is due to Pskovskii. The symbol * in this column indicates additional comments given in the notes following the table.

In addition to the standard m_{pg}, m_{pv}, B, and V systems, there were two other magnitude systems which were used by some observers of some of the light curves included in this study. One of these systems was that of Kaho (98, 108) who used Fuji FL-OII plates. According to Kaho, these plates are blue sensitive, but they do not correspond exactly to either the m_{pg} or the B system. Several of the supernovae observed by Kaho were also observed in the B system by various other observers. In almost all of these cases some of the comparison stars used by the other observers were also used as comparison stars by Kaho. By comparing the B-magnitudes of these common comparison stars with the magnitudes measured by Kaho, it was possible to establish the relationship between the two systems. This relationship is shown in Figure 6-5, where magnitudes in Kaho's system are denoted by m_K. For each of the common comparison stars, the difference $B - m_K$ is plotted against m_K. The data appear to indicate that Kaho's magnitudes have a non-linear scale error. The four supernovae with common observed comparison stars were SN 1962*l* which was also observed by Bertola (87), SN 1963*p*

Table 6-2

The Peak Magnitudes and Dates of Peak Brightness for the Supernovae in This Study

SN	No.	Galaxy	m_o	Method	t_o	Method	Notes
1885a	1	M 31	5.24	obs. l. c.	JD2409776	obs. l. c.	
1921c	16	NGC 3184	11.9	obs. l. c.	12/9/21	obs. l. c.	
1937c	25	IC 4182	8.4	obs. l. c.	JD2428768	obs. l. c.	
1937d	26	NGC 1003	12.8	obs. l. c.	JD2428792	obs. l. c.	
1939a	30	NGC 7636	12.6	obs. l. c.	JD2429290	obs. l. c.	
1939b	31	NGC 4621	11.8	obs. l. c.	JD2429385	obs. l. c.	
1954a	50	NGC 4214	9.5	av. l. c.	JD2434851	av. l. c.	P
1954b	51	NGC 5668	12.5	pt. k	JD2434866	pt. k	P
1955b	53	Anon.	15.7	pt. k	10/3/55	av. l. c.	R
1956a	54	NGC 3992	12.2	av. l. c.	3/14/56	av. l. c.	P
1957a	55	NGC 2841	13.85	pt. k	2/27/57	av. l. c.	R
1957b	56	NGC 4374	12.1	av. l. c.	5/9/57	av. l. c.	P
1959c	62	Anon.	13.55	obs. l. c.	7/1/59	obs. l. c.	
1960f	69	NGC 4496	11.6	obs. l. c.	4/16/60	obs. l. c.	
1960r	86	NGC 4382	11.5	pt. k	12/19/60	pt. k	P
1961d	87	Anon.	16.20	obs. l. c.	1/17/61	obs. color curve	R
1961h	92	NGC 4564	11.2	obs. l. c.	5/8/61	obs. l. c.	
1961p	100	Anon.	14.3	obs. l. c.	9/11/61	obs. l. c.	
1962a	106	Anon.	15.6	pt. k	1/15/62	obs. color curve	R
1962e	111	Anon.	16.4	iterated pt. k	2/19/62	iterated pt. k	R

Table 6-2 (Continued)

SN	No.	Galaxy	m_o	Method	t_o	Method	Notes
1962J	117	NGC 6835	13.65	pt. k	8/24/62	spectrum	R, P, *
1962l	119	NGC 1073	13.7	pt. k	12/5/62	obs. color curve	R
1962p	145	NGC 1654	14.2	av. l. c.	10/29/62	av. l. c.	P
1963d	126	NGC 4146	15.6	av. l. c.	1/20/63	av. l. c.	P
1963i	131	NGC 4178	12.9	av. l. c.	5/5/63	av. l. c.	P
1963J	132	NGC 3913	12.0	pt. k	5/10/63	av. l. c.	R
1963p	138	NGC 1084	13.5	av. l. c.	JD2438300	av. l. c.	P
1964e	150	Anon.	12.2	pt. k	2/27/64	av. l. c.	R
1964l	159	NGC 3938	13.1	pt. k	12/8/64	pt. k	P
1965i	170	NGC 4753	11.0	obs. l. c.	6/13/65	spectrum	*
1966J	186	NGC 3198	11.1	pt. k	11/23/66	spectrum	R, P, *
1966k	187	Anon.	16.6	iterated pt. k	JD2439489	iterated pt. k	R
1966n	198	Anon.	14.3	pt. k	10/7/66	av. l. c.	R
1967c	192	NGC 3389	12.6	pt. k	2/22/67	obs. color curve	P, R, *
1968e	211	NGC 2713	12.7	pt. k	3/15/68	pt. k	P
1969c	235	NGC 3811	13.94	obs. l. c.	1/31/69	obs color curve	*
1971i	299	NGC 5055	11.7	pt. k	5/27/71	av. l. c.	R

*Notes:

1962J - Applying Pskovskii av. l. c. technique gave t_o = 8/25/62.

1965i - Estimate of t_o is due to Ciatti and Barbon (105).

Table 6-2 (Continued)

1966J - Chincarini and Perinotto (107) estimate on basis of spectrum that t_o = 11/21/66, but Pskovskii's estimate will be used in this thesis.
1967c - Pskovskii's estimate of t_o was 2/23/67. It was based on his point k method.
1969c - Applying Pskovskii's point k and average light curve methods gave the same values for m_o and t_o.

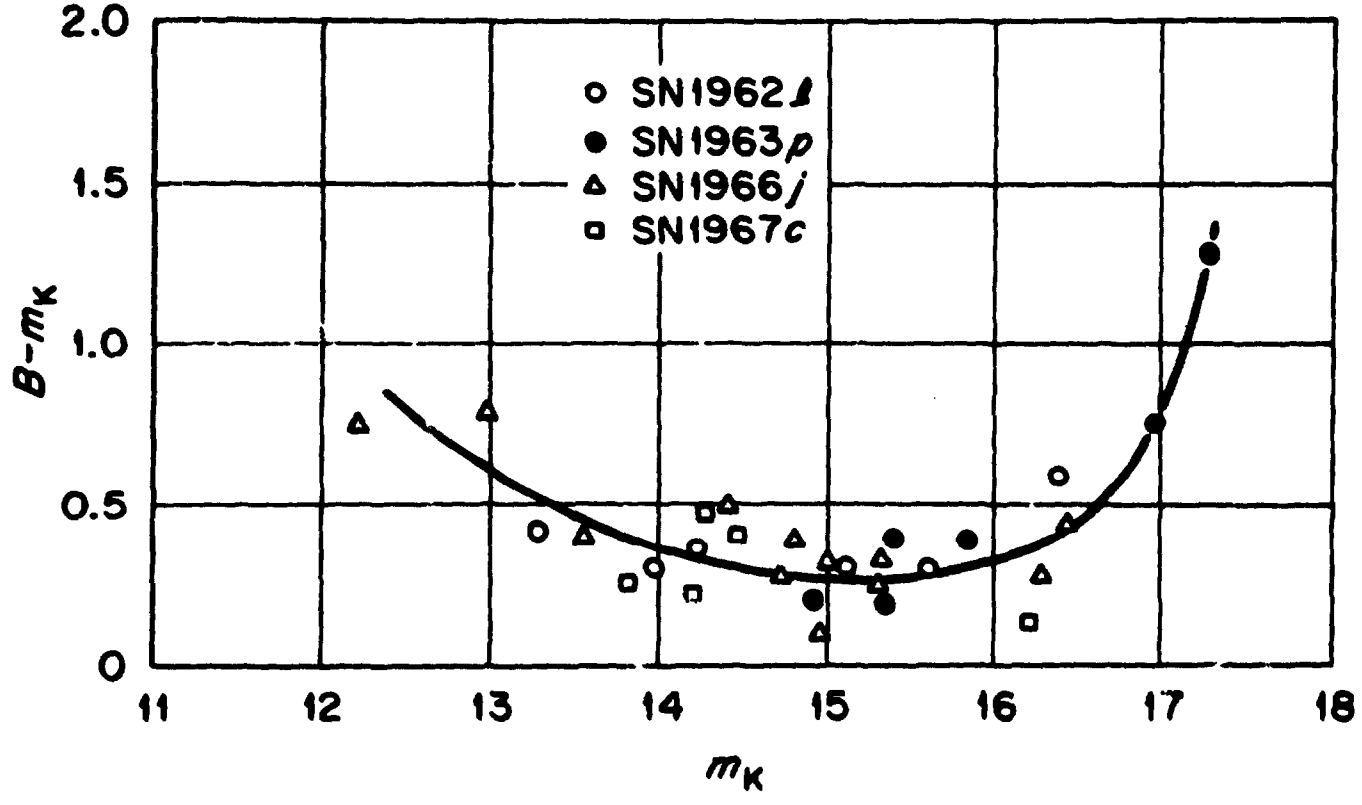

Figure 6-5. The Scale Correction for Converting Kaho's Magnitudes to the B System.

which was observed by Bertola, Mammano, and Perinotto (97), SN 1966j which was observed by Chincarini and Perinotto (107), and SN 1967c which was also observed by deVaucouleurs, Solheim, and Brown (110). The points for SN 1962*l* were arbitrarily selected as the standard and the points for the other three sets of comparison stars were shifted vertically to give the best possible agreement with those of the standard. Thus the relation shown in the figure has an indeterminate constant zero-point error which was propagated into any magnitudes converted from m_K to B by means of the relationship. The B magnitudes obtained from this relationship could then be converted to m_{pg} magnitudes either by Eq. (6-1) if the color excess E(B - V) was known or by Eq. (6-2) if it was not known. In the latter case, an additional unknown zero point error was added to the error from the m_K to B transformation. In some cases it was possible to determine the required zero-point correction by comparing the converted magnitudes to magnitudes measured in one of the other systems. In cases where it was not possible to determine the zero-point correction, the basic shape of the curve was not altered by the constant zero-point error, and so its slope could still be used for testing the expansion hypothesis.

The other non-standard magnitude system used for light curves treated in this thesis is the b magnitude system of Marx and Pfau (111). This system is related to the B system by the relation

$$B = b + 0.14\ (B - V).$$

Combining this expression with Eq. (6-1) gives

$$m_{pg} = b - 0.29 + 0.32\ (B - V). \qquad (6\text{-}9)$$

If the values of B - V are unknown, the transformation can be made by

$$m_{pg} = b - 0.29 + 0.32\ (B - V)_o\ , \qquad (6\text{-}10)$$

where $(B - V)_o$ is obtained from Pskovskii's $(B - V_o)$ - t relation. If this latter relation is used, there will, of course, be an unknown zero-point error in the converted magnitude because of the unknown color excess E(B - V) due to absorption.

Thus far, this chapter has described the various techniques that were used to reduce the light curves to the standard m_{pg} system. Many of these techniques required accurate estimates of the peak magnitude m_o and the date of its occurrence t_o, so the techniques used for obtaining those estimates have also been described. Table 6-2 gave a summary of those estimates and the method used for each of the supernovae in the study. The chief purpose of the discussion given in this chapter has been to develop the background needed in order to construct a similar table, which gives for each supernova a summary of the techniques used to reduce all of the measured magnitudes to the m_{pg} system. Before doing that, however, it is convenient to summarize the various conversion methods that were used. This is done in Table 6-3. Column 1 gives the system or systems of measurement. Column 2 briefly describes the method used for conversion to the m_{pg} system. Column 3 gives a Roman numeral code which will be used as an abbreviation for the method. Column 4 gives additional comments about the method.

In many cases it was necessary to know the color excesses of the supernovae in order to eliminate zero point errors in the conversion. In most of these cases, it was possible to derive these color excesses

Table 6-3

Summary of the Techniques Used to Convert the Magnitudes
From the Various Systems of Measurement to the Standard m_{pg} System

Measured	Conversion	Code	Comments
B and V	$m_{pg} = B - 0.29 + 0.18(B - V)$	I	
B and some V	(a) nights when both B & V measured: $m_{pg} = B - 0.29 + 0.18(B - V)$, and $C = (B - V) - (B - V)_o$ determines color excess (b) nights when B only measured: $m_{pg} = B - 0.29 + 0.18[(B - V)_o + C]$ (c) nights when V only measured: $m_{pg} = V - 0.29 + 1.18[(B - V)_o + C]$	II	The color excess C is determined by comparing the measured (B - V) values with the corresponding $(B - V)_o$ values from Pskovskii's relationship. The value of C can then be used to convert $(B - V)_o$ to (B - V) on nights when B & V were not both measured.
V and some B	"	III	"
B only	$m_{pg} = B - 0.29 + 0.18(B - V)_o$	IV	In general, there will be a zero point error because of the unknown color excess.

Table 6-3 (Continued)

Measured	Conversion	Code	Comments
V only	$m_{pg} = V - 0.29 + 1.18(B - V)_o$	V	In general, there will be a zero point error because of the unknown color excess.
m_{pv} and some m_{pg}	(a) nights when both m_{pg}, m_{pv} measured: $C = (m_{pg} - m_{pv}) - (m_{pg} - m_{pv})_o$ determines C. (b) nights when only m_{pv} measured: $m_{pg} = m_{pv} + [(m_{pg} - m_{pv})_o + C]$	VI	Color excess C is determined by comparing measured $(m_{pg} - m_{pv})$ with Pskovskii $(m_{pg} - m_{pv})_o$ on those nights when both m_{pg} and m_{pv} were measured.
m_{pv} and some m_{pg}	(a) nights when both m_{pg}, m_{pv} measured: $(B - V) = \frac{(m_{pg} - m_{pv}) + 0.29}{1.18}$, $C = (B - V) - (B - V)_o$ (b) nights when only m_{pv} measured: $m_{pg} = m_{pv} - 0.29 + 1.18[(B - V)_o + C]$.	VII	This method is similar to the immediately preceding one, but it uses the Pskovskii $(B - V)_o - t$ relation rather than $(m_{pg} - m_{pv})_o - t$.
m_{vis} or m_{pv} only	$m_{pg} = m_{pv} + (m_{pg} - m_{pv})_o$	VIII	In general, there will be a zero point error because of the unknown color excess.

Table 6-3 (Continued)

Measured	Conversion	Code	Comments
m_K (Kaho)	(1) $B = m_K + (B - m_K)$ with $(B - m_K)$ determined from the relation in Figure 6-5. (2) $m_{pg} = B - 0.29 + 0.18[(B - V)_o + C]$ if color excess C is known, or $m_{pg} = B - 0.29 + 0.18(B - V)_o$ if C is not known	IX	Step (1) will, in general, give a zero point error. Step (2) will give an additional zero point error if C is not determined by other measurements
b (Marx and Pfau)	$m_{pg} = b - 0.29 + 0.32[(B - V)_o + C]$ if color excess C is known, or $m_{pg} = b - 0.29 + 0.32(B - V)_o$ if C is not known.	X	There will be a zero point error if the color excess C is not determined by other measurements.

by comparing measured $(B-V)-t$ data with Pskovskii's $(B-V)_0-t$ relation [or in some cases comparing measured $(m_{pg}-m_{pv})-t$ data with the $(m_{pg}-m_{pv})_0-t$ relation]. In those few cases in which there were no measured color indices, the conversions preserved the shape of the curve even though they may have introduced a zero point error. Color excesses were determined for every supernova for which color indices had been measured, regardless of whether or not the excesses were needed for magnitude conversions. These color excess data will be used again in Chapter 9 for computing absorption corrections to the supernovae peak magnitudes.

Table 6-4 gives the final summary of the techniques used for reducing each of the light curves to the standard m_{pg} system. Column 1 gives the supernova designation. Column 2 gives its number in the Zwicky numbering system. Column 3 gives the name of the parent galaxy. Column 4 contains the names of the various observers. Column 5 gives, for each of the observers, the magnitude system or systems used for the observations. Column 6 gives the method used for converting the magnitudes if such a conversion was necessary. The method is indicated by a Roman numeral in the range I to X. These Roman numerals correspond to the ones given in column 3 of Table 6-3. In some cases it was necessary to make a zero point correction in the magnitudes of one or more of the observers. Column 7 gives these zero point corrections. Column 8 contains the word "yes" if there was a possible zero-point error in the conversion. Note that in many cases a conversion introduced a zero point error which could be removed by comparing the converted magnitudes to m_{pg} magnitudes measured by other observers. These corrections were included in the

conversion, so column 8 contains a "yes" only if there was no way to correct the error. Column 9 contains the E(B - V) color excess and Column 10 contains the $E(m_{pg} - m_{pv})$ color excess for those supernovae which had measured color indices. Column 11 contains an asterisk (*) for those supernovae which have additional information given in a note at the end of the table.

When all the magnitude conversions were completed for a given supernova, the resulting m_{pg} light curves from all the observers were used as input for an IBM 360 computer program, called EDIT, which combined the various light curves from different observers into a single final light curve for the supernova. The final light curves were plotted on a Calcomp plotter and an inspection of the plot immediately showed whether some of the light curves of individual observers still needed zero-point corrections. The final combined light curves were later fitted in the least squares sense by an analytic function derived from a theoretical model which is described in the next chapter. The light curves plotted out by EDIT were also very useful for determining the limits of the fit [only the rapid decline portion of the curve was fitted]. EDIT also punched out the combined light curves on IBM cards which were later used as input data cards for the fitting program.

Plots of all the combined light curves are given in Appendix 2. These plots also show the results of the fits described in the next chapter.

Table 6-4

Summary of the Photometric Data and Conversions
Used to Obtain the Light Curves for This Study

SN	No.	Galaxy	Observers	Mag. System	Conversion	Zero-pt. Correc.	Zero-pt. Error	E(B - V)	$\sigma(m_{pg} - m_{pv})$	Notes
1885a	1	M31	Hartwig and others	m_{vis}	VIII		yes			
1921c	16	NGC3184	Shapley	m_{pg}						
1937c	25	IC4182	Baade and Zwicky	m_{pg}				0.05		*
			Deutsch	m_{pg}						
			Parenago	m_{pg}						
1937d	26	NGC1003	Baade and Zwicky	m_{pg}				0.45		*
			Parenago	m_{pg}						
1939a	30	NGC4636	Baade	m_{pg}				0.43		*
			Ciclas	m_{pg}						
			Hoffleit	m_{pg}		$+0^m.5$				
1939b	31	NGC4621	Shapley	m_{pg}						
			Baade	m_{pg}						
1954a	50	NGC4214	Wild	m_{pg}				0.13	0.15	*
			Pietra	m_{pg}						*
			Hoffmeister	m_{pg}						

Table 6-4 (Continued)

SN	No.	Galaxy	Observers	Mag. System	Conversion	Zero-pt. Correc.	Zero-pt. Error	E(B - V)	$E(m_{pg} - m_{pv})$	Notes
1954b	51	NGC5668	Wild	m_{pg}				0.25		*
			Pietra	m_{I-E}						*
1955b	53	Anon.	Zwicky	m_{pg}						
1956a	54	NGC3992	Zwicky and Karpowicz	m_{pg}, m_{pv}					0.44	*
1957a	55	NGC2841	Zwicky and Karpowicz	m_{pg}, m_{pv}					0.80	*
			Bertola	m_{pg}						
			Wenzel	m_{pg}		+0.2				
1957b	56	NGC4374	Bertola	m_{pg}						
			Götz	m_{pg}						
			Rumeno	m_{pg}		+0.8				
			Li Tain	m_{pg}		+0.08				
1959c	62	Anon.	Mihalas	B,V	I	-0.29		0.10		
			Mihalas	m_{pg}						
1960f	69	NGC4496	Bertola	m_{pg}						
			Huth	m_{pg}		+0.84				
			Kulikov	m_{pg}		+0.42				
			Tempesti	m_{pg}		+0.61				
			Mannino	m_{pg}						*

Table 6-4 (Continued)

SN	No.	Galaxy	Observers	Mag. System	Conversion	Zero-pt. Correc.	Zero-pt. Error	E(B - V)	$E(m_{pg} - m_{pv})$	Notes
1960r	86	NGC4382	Bertola	m_{pg}						
			Zaitseva	m_{pg}						
			Gates	B,V	II			0.34		
1961d	87	Anon.	Zwicky	m_{pg}, m_{pv}	VII				0.05	
1961h	92	NGC4564	Romano	m_{pg}						
1961p	100	Anon.	Bertola	m_{pg}						
1962a	106	Anon.	Zwicky and Barbon	m_{pg}, m_{pv}	VI				0.10	
1962e	111	Anon.	Rudnicki and Zwicky	m_{pg}, m_{pv}	VIII				0.0	•
1962j	117	NGC6835	Bertola	m_{pg}						
1962l	119	NGC1073	Bertola	B,V	II			0.85		
			Rosino	m_{pg}						
1962p	145	NGC1654	Rosino	m_{pg}						
1963d	126	NGC4146	Bertola	m_{pg}						
			Rosino	m_{pg}						
1963i	131	NGC4178	Zaitseva	m_{pg}						
			Lochel	m_{pg}						
			Bertaud	m_{pg}						

Table 6-4 (Continued)

SN	No.	Galaxy	Observers	Mag. System	Conversion	Zero-pt. Correc.	Zero-pt. Error	E(B - V)	$E(m_{pg} - m_{pv})$	Notes
1963j	132	NGC3983	Zwicky	m_{pg}						
			Wild	m_{pg}						
			Chincarini and Margoni	m_{pg}						•
1963p	138	NGC1084	Bertola et al.	B	IV					
			Kaho	m_k	IX	-0.09	yes			
1964e	150	Anon.	Lovas	m_{pg}						
			Ahlert	m_{pg}		-0.6				
			Chunadze	m_{pg}		-0.35				
			Zaitseva	m_{pg}						
			Lochel	m_{pg}		-0.6				
1964f	159	NGC3938	Bertola, et al.	m_{pg}						
1965l	170	NGC4753	Van Lyong and Panarin	m_{pg}						
			Ciatti and Barbon	B,V	III			0.03		•
1966j	186	NGC3198	Wild	m_{pg}						•
			Chincarini and Perinotto	B	IV					
			Kaho	m_k	IX	-0.3				
1966k	187	Anon.	Rudnicki	m_{pg}, m_{pv}	VI				0.2	
1966n	198	Anon.	Ciatti and Barbon	m_{pg}						

Table 6-4 (Continued)

SN	No.	Galaxy	Observers	Mag. System	Conversion	Zero-pt. Correc.	Zero-pt. Error	E(B-V)	$E(m_{pg}-m_{pv})$	Notes
1957e	192	NGC5389	de Vaucouleurs, et al.	B,V	II			0.10		
			Marx and Pfau	b	X					
			Borsov, et al.	~b	IV					
			Chunduo and Barblishvili	m_{pv}	VIII	$-0^m.46$				
			Kaho	m_k	IX	$-0^m.15$				
1968e	211	NGC2715	Chevire	m_{pg}						
			Rusov	m_{pg}						
			Ciatti and Barbon	B,V	V	-0.27		0.25		*
1969e	295	NGC3811	Bertola and Ciatti	B,V	II			0.20		
1971i	299	NGC5055	Deming, et al.	m_{pg}						
			Deming, et al.	B,V	I			0.4		
			Ichida	B,V	I					
			Van Herk and Schoenmaker	m_{pg}						
			Seovil	m_{pv}	V					

Table 6-4 (Continued)

1957c: The value E(B - V) 0.05 was derived by Pskovskii (51) from synthetic (B - V) color indices measured from tracings of the spectra. A fairly extensive m_{vis} light curve was measured for this supernova by M. Beyer (126); and if these magnitudes are compared with the m_{pg} magnitudes of Baade and Zwicky and of Parenago, it is possible to derive a color excess of $E(m_{pg} - m_{pv}) = 0.55$, which corresponds to E(B - V) 0.50. According to Pskovskii, however, the latter color excess is in error because the m_{pg} and m_{vis} measurements were made by different observers at different observatories. The same observers also observed SN1937d; and therefore, assuming the same inconsistencies were present, the color excess computed from these observations must be corrected by an amount which is just the difference of the two values obtained above. Thus, the E(B - V) color excess calculated for SN1937d must be corrected by the amount $\Delta E(B - V) = -0.25$.

1937d: Using the m_{vis} magnitudes measured by Beyer (126) together with the measured m_{pg} magnitudes of Baade and Zwicky and of Parenago, a color excess $E(m_{pg} - m_{pv})$ 0.82 or E(B - V) 0.70 is obtained. This value must be corrected by the amount $\Delta E(B - V)$ -0.25 as explained in the note above for SN1937c.

1939a: Beyer (126) measured m_{vis} magnitudes for this supernova and when they are compared with Baade's m_{pg} magnitudes, a color excess of $E(m_{pg} - m_{pv})$ 0.80 or E(B - V) 0.68 is obtained. Assuming that Baade and Beyer had the same inconsistencies in their magnitude scales for these measurements as the ones in the measurements for SN1937c, then the color excess given above must be corrected by the amount $\Delta E(B - V)$ -0.25 as explained in the above note for SN1937c. Thus the corrected value is E(B - V) 0.43.

Table 6-4 (Continued)

1954a: Pietra's magnitudes were remeasured by Rosini, who used the same comparison stars as Wild. These remeasured values are the ones used in this thesis. An m_{pv} light curve was also measured by Beyer (127, 128), but it was not used for the light curve in this thesis. It was, however, used in conjunction with the m_{pg} magnitudes of Wild and Pietra to derive a color excess $E(m_{pg} - m_{pv}) = 0.15$. Since the m_{pg} and m_{pv} measurements were made at different observatories, this color excess value might have been in error. But it was possible to get an independent estimate in the present case because Wild (65) measured (B - V) color indices for several nights between the 44th and 109th day after maximum. Comparing these (B - V) measurements with Pskovskii's $(B - V)_0$ - t relation gave a color excess $E(B - V) = 0.15$ or, equivalently, $E(m_{pg} - m_{pv}) = 0.15$.

1958b: The magnitudes of Pietra have been corrected by Wild (65). The color excess was obtained from five (B - V) measurements by Wild (65). The measurements were made between days 6 and 27 after maximum. The color excess was obtained by comparing them with Pskovskii's (B - V) - t relation.

1956a: The m_{pv} magnitudes were not used in constructing the final light curve for this thesis. They were, however, used in deriving the color excess.

1957a: The m_{pv} magnitudes were not used in constructing the final light curve for this thesis. They were, however, used in deriving the color excess. There was a high degree of scatter in the $(m_{pg} - m_{pv})$ - t color curve for this supernova, which is apparently due to a large amount of obscuring matter between us and it. This large absorption is probably the cause of the low apparent luminosity of this supernova.

Table 6-4 (Continued)

1960f: The magnitudes of Mannino required a scale correction to make them consistent with those of Bertola. The scale correction relation was obtained from their measurements of the magnitudes of comparison stars common to both comparison sequences.

1962e: There were not enough measured values of $m_{pg} - m_{pv}$ to give the color excess directly, but the color excess can be taken to be 0 because the supernova appeared in a faint luminous bridge of presumably late type stars between two elliptical galaxies. Furthermore, the two galaxies are at a very high galactic latitude (+68°); so there was probably very little absorption or reddening of the light within our own galaxy.

1963j: The magnitude measured on 5/24/63 by Chincarini and Margoni (96) was very far out of line when compared to the other measured magnitudes. It was therefore judged to be in error and was omitted from the light curve used in this study.

1965i: The B magnitudes of Ciatti and Barbon appear to have a zero point error of $\Delta B = -0^m.17$, i.e., they must be corrected by $+0^m.17$ so that the converted m_{pg} magnitudes agree with those of Van Lyong and Panarin. The converted V magnitudes agree quite nicely with the magnitudes of Van Lyong and Panarin without any zero point correction. The B correction was also taken into account in computing the color excess E(B - V).

1966j: This supernova occurred at the extreme edge of the galaxy so there was probably not very much reddening or absorption of its light in its parent galaxy. Thus any zero-point error introduced by the magnitude conversions was probably quite small.

1968e: The B magnitudes of Ciatti and Barbon appear to have a zero point error, so they were not used in constructing the light curve for this thesis. They were used in determining the color excess E(B - V), but the zero point error was taken into account. (See also note above for SN1965i.)

CHAPTER 7

A MODEL FOR FITTING THE LIGHT CURVE DATA

Once the observed light curve data had been collected and reduced to a common photometric system, it was necessary to determine a standard parameter to be used as a measure of the rate of decline of each of the light curves. It would have been simplest just to fit straight lines to the rapid decline portion of each light curve and to use the slope of the line as the standard parameter. But many of the light curves were somewhat fragmentary, and in some cases the gaps in the data would have made the fitting of such a physically unmotivated function a rather arbitrary procedure. This was especially true in those cases in which gaps occurred at the very beginning or the very end of the rapid decline portion of the light curve. In such cases it would have been difficult, and perhaps even impossible, to determine correctly a mean straight line fit to the entire rapid decline region. A better procedure seemed to be to fit the light curves with a function which is derived from a physically motivated model. The physical theory would hopefully guarantee that the function would correctly fit through the gaps in the data, and furthermore, even in curves where there are no gaps, would give a better fit to the data than would a simple straight line. Fortunately there does exist a physically well-motivated model for the type I supernova event which gives a relatively simple functional expression for the light curve. This model is the optical reverberation theory of Morrison and Sartori.

Morrison and Sartori have described their model quite extensively in their papers (129, 130), so there is no point in giving anything more

BLANK PAGE

than a brief description of it in this thesis. Basically, the model assumes that the light from a supernova comes not from the explosion itself but rather from the response of circumstellar matter to the explosion. The explosion produces a strong ultraviolet pulse which in turn excites fluorescence in the circumstellar medium at distances out to about 1 light year. For type I supernovae this secondary radiation is thought to be excited in a helium rich envelope which was formed around the presupernova star by mass ejection. The properties of such an envelope have recently been investigated in a paper by Arnett (151). In the case of type II supernovae, no appreciable mass ejection is thought to have occurred so that the source of the fluorescence is chiefly the interstellar medium. Thus, type II supernovae are not so luminous as type I, and furthermore occur only in galaxies which are rich in gas, i.e. spirals and irregulars. In addition, the spectra of type II supernovae are dominated by the lines of hydrogen while those of type I are dominated by the $4 \rightarrow 3$ transition of He II. In both cases the spectra are characteristic of a low density gas with Doppler broadened atomic lines present from the first. The optical reverberation model also accounts quite naturally for the fact that supernova light curves never exhibit secondary maxima since the observer is seeing, even on the first day, a considerable amount of light emitted from regions several light months from the explosion. This optical echo effect produces a smoothing of the light received, which obscures any structure in the primary pulse.

The light echo phenomenon is illustrated in Figure 7-1. The supernova is at point S and observer is at point O which is at a distance L from S. The observer first detects the supernova at time $\frac{L}{c}$ after the primary explosion. If the primary explosion is a δ-function pulse, then at time t after this first detection the observer is receiving secondary radiation from the points on the ellipsoidal surface defined by

$$r + d = L + ct. \qquad (7-1)$$

If the primary explosion is not a δ-function pulse, but rather is spread over a time interval Δt, then the observer is receiving, at observer time t, light from an ellipsoidal shell whose thickness is $\frac{1}{2}c\Delta t$.

Morrison and Sartori constructed their model by considering a single line of the secondary spectrum (e.g., the 4 → 3 transition of He II) and a δ-function primary pulse. They assumed that the spectral intensity $\frac{dN}{d\nu}\left(\frac{\text{photons}}{\text{Hz}}\right)$ of the primary pulse was equal to a constant value $\left(\frac{dN}{d\nu}\right)_o$ across the absorption resonance which excites the line in question. They assumed that the secondary emitters were distributed isotropically about the supernova. If the number density, absorption optical depth, and cross-section for absorption at distance r from the supernova are denoted by n(r), $\tau_\nu(r)$, and $\sigma_\nu(r)$ respectively, and if the probability that an absorber which is excited to the proper initial state will decay by emitting the line in question is denoted by α, then the luminosity at observer time t was shown to be

$$\mathcal{L}(t) = \tfrac{1}{2}\alpha c \left(\frac{dN}{d\nu}\right)_o \int_{\frac{ct}{2}}^{\infty} dr \, \frac{n(r)}{r} \int d\nu e^{-\tau_\nu(r)} \sigma_\nu(r) \, , \qquad (7-2)$$

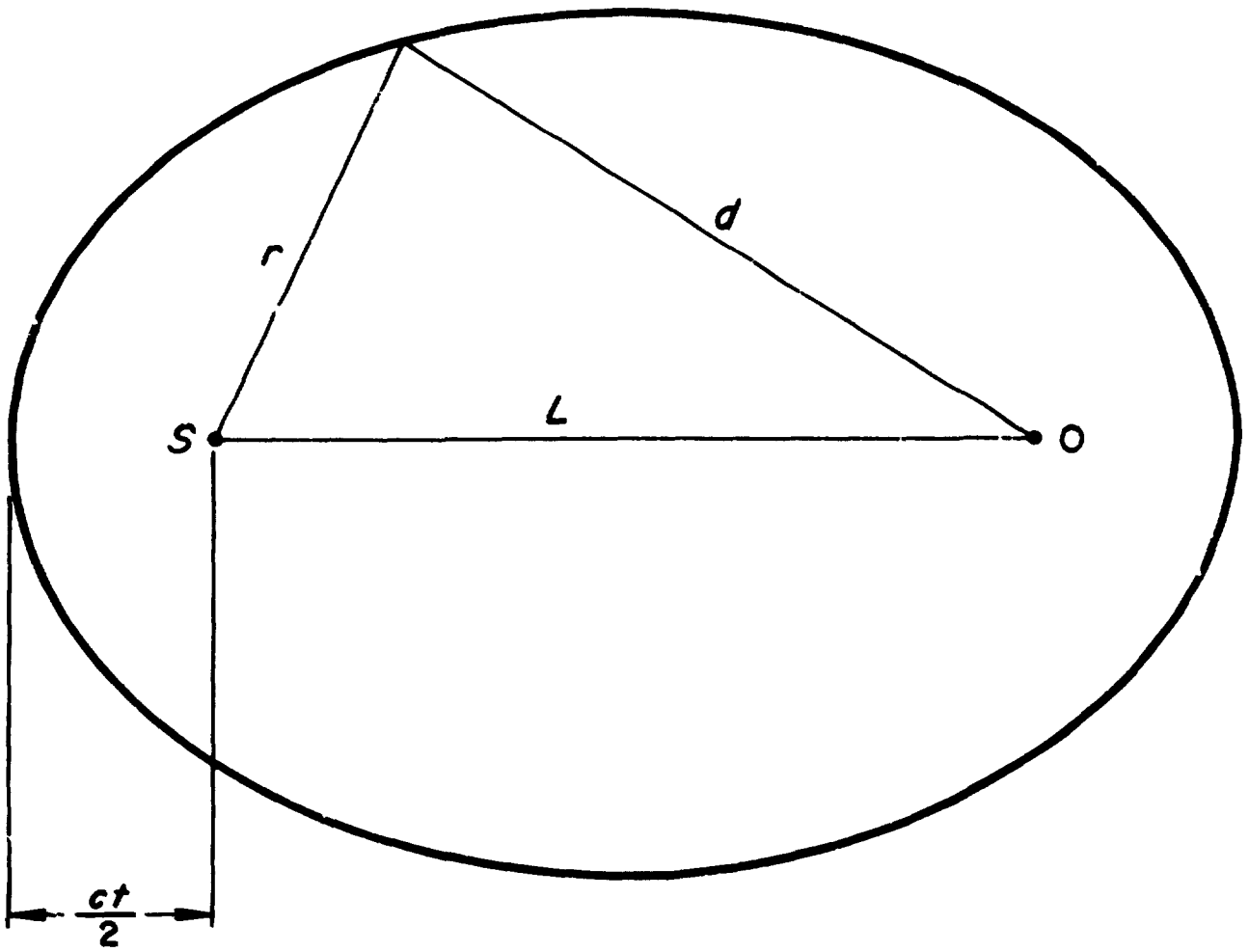

Figure 7-1. The Morrison-Sartori Light Echo Model.

where the last integral is taken across the absorption resonance. This is the basic equation of their theory. They then further simplified the model by assuming that the absorption resonance is approximated by a rectangle of width $\Delta\nu$ and further that both $\Delta\nu$ and the number density $n(r)$ are independent of r. This means that $\tau_\nu(r)$ is independent of ν within the line and is given by the equation

$$\tau_\nu(r) = \frac{r}{\Lambda} , \tag{7-3}$$

where Λ is the mean free path of the photons within the uniform envelope. They were then able to show that the luminosity is given by

$$\mathcal{L}(t) = \left(\frac{\pi e^2}{m}\right) f \left(\frac{dN}{d\nu}\right)_0 n \, E_1\left(\frac{ct}{2\Lambda}\right) \tag{7-4}$$

where e and m are the electron charge and mass, f is the oscillator strength of the transition, n is the uniform number density and $E_1\left(\frac{ct}{2\Lambda}\right)$ denotes the exponential integral function evaluated for the argument $\frac{ct}{2\Lambda}$. This latter function is defined by the expression

$$E_1(x) = \int_1^\infty \frac{e^{-xz}}{z}\, dz. \tag{7-5}$$

Morrison and Sartori called the model defined by Equation (7-4) their uniform model. One cannot expect such a simple model to fit the entire light curve, and in fact they show that for a δ-function primary pulse, the luminosity defined by Eq. (7-4) always decreases. Hence, the model is only good for the declining portion of the light curve. Like almost everyone who has worked with type I light curves, they sought to fit their model to the exponential tail of the light curve and were extremely successful in doing it. Figure (7-2) shows their fit

Figure 7-2. Morrison's and Cartori's Fit of Their Model to the Light Curve for SN1937d.

to the light curve of SN1937d (in NGC1003). The fit is very good over the range from about day 75 after maximum to the last recorded observations nearly 350 days later. Their other fits were just as good or better; they were, for example, able to fit the light curve for SN1937c (in IC4182) from about day 30 to about day 600 after maximum. The values of A for their fits range between 50 and 100 light days thus implying helium densities in the range of 1 to 4 ions cm^{-3}.

Although Morrison's and Sartori's fits to the tails of the light curves are impressive evidence for the correctness of their model, they are not of much use for analyzing the data in this thesis since it is the rapid decline portion of the light curve that is being considered here. But upon inspecting their fits, the present author concluded that the same model might be used to fit that portion of the light curve also, if the tail were simply ignored. Of course smaller values of A would be expected from such fits since the rapid decline portion originates from the echo interaction of the primary pulse with the inner layers of the circumstellar envelope. The ion densities in these inner layers would be expected to be greater than in the outer layers, and thus the mean free path of the photons would be less.

In order to perform any fits at all with the model, it is necessary to reduce Eq. (7-4) to an expression which relates observable quantities. Lumping all the constant multiplying factors on the right of (7-4) into a single constant value k gives

$$\mathcal{L}(t) = k\, E_1\left(\frac{ct}{2A}\right). \qquad (7\text{-}6)$$

In measuring a light curve, the apparent magnitude m, rather than

luminosity $\mathcal{L}$, is observed. There are at least two ways of converting Eq. (7-6) to an expression involving m(t). One way is based on the relation

$$m(t) - m_o = -2.5 \log \left[\frac{\mathcal{L}(t)}{\mathcal{L}_o}\right] \qquad (7\text{-}7)$$

where m_o and $\mathcal{L}_o$ denote the peak magnitude and peak luminosity. Substituting (7-6) into this expression and replacing the quotient $k/\mathcal{L}_o$ by a single constant C gives

$$m(t) - m_o = -2.5 \log \left[C\, E_1\left(\frac{ct}{2\Lambda}\right)\right] . \qquad (7\text{-}8)$$

This expression could then be used for fitting the observed light curve. The constants C and Λ would be the unknown parameters to be determined by the best fit.

Another way to reduce Eq. (7-6) to an expression involving magnitudes is to rewrite (7-7) in the form

$$\frac{1}{\log^{-1}\left\{0.4\left[m(t) - m_o\right]\right\}} = \frac{\mathcal{L}(t)}{\mathcal{L}_o} .$$

Substituting (7-6) into this last expression gives

$$\frac{1}{\log^{-1}\left\{0.4\left[m(t) - m_o\right]\right\}} = C\, E_1\left(\frac{ct}{2\Lambda}\right) , \qquad (7\text{-}9)$$

which involves only measured quantities and the two constants C and Λ to be determined by the fit. In order to choose which of the two expressions (7-8) and (7-9) gives the best fits, it is first necessary to specify the fitting procedure.

The usual criterion of best fit is the least squares principle and that is the one that was chosen here. Since both (7-8) and (7-9) are non-linear in the parameters to be determined, the procedure

necessarily involves non-linear least squares. The solution technique that was chosen was a simple iteration which begins with initial estimates $C^{(o)}$ and $\Lambda^{(o)}$ and calculates at each step, i, improved estimates

$$C^{(i)} = C^{(i-1)} + \Delta C^{(i)},$$
$$\Lambda^{(i)} = \Lambda^{(i-1)} + \Delta\Lambda^{(i)},$$

where the corrections $\Delta C^{(i)}$ and $\Delta\Lambda^{(i)}$ are obtained by solving a linear least squares problem. Equation (7-9) was chosen as the formulation to use because it gives a much simpler linear least squares problem at each step than does (7-8).

It is convenient to rewrite Equation (7-9) in the form

$$y(t) = C\, E_1\left(\frac{ct}{2\Lambda}\right), \tag{7-10}$$

where

$$y(t) = \frac{1}{\log^{-1}\left\{0.4\left[m(t) - m_o\right]\right\}}. \tag{7-11}$$

A light curve consists of a total of, say M, observed points $\left[t_i, m_i\right]$ from which the set of points $\left[t_i, y_i\right]$ can be computed by means of Eq. (7-11). The least squares problem that must be solved then is that of minimizing the expression

$$D = \sum_{i=1}^{M}\left[y_i - C\, E_1\left(\frac{ct_i}{2\Lambda}\right)\right]^2. \tag{7-12}$$

In order to find the minimum, it is necessary to differentiate D with respect to the two parameters C and Λ and to set these two derivatives equal to zero. Taking into account that the exponential integral,

$$E_1(z) = \int_1^\infty \frac{e^{-zx}}{x}\, dx,$$

has as its derivative

$$\frac{dE_1(z)}{dz} = -\frac{e^{-z}}{z} ,$$

one gets

$$\frac{\partial D}{\partial C} = \sum_{i=1}^{M} \left[y_i - C\, E_1\left(\frac{ct_i}{2\Lambda}\right) \right] E_1\left(\frac{ct_i}{2\Lambda}\right) = 0, \qquad (7\text{-}13)$$

$$\frac{\partial D}{\partial \Lambda} = \sum_{i=1}^{M} \left[y_i - C\, E_1\left(\frac{ct_i}{2\Lambda}\right) \right] \frac{C}{\Lambda} \exp\left[-\frac{ct_i}{2\Lambda} \right] = 0. \qquad (7\text{-}14)$$

These two equations are analogous to the normal equations which arise in connection with linear least squares problems. They are, however, non-linear in the unknown parameters C and Λ, and hence, they must be solved iteratively. The iterative technique that was chosen is based upon a Taylor series expansion in terms of C and Λ. If $C^{(o)}$ and $\Lambda^{(o)}$ are estimates of C and Λ, then for each point t_i, the fitting function can be written

$$C\, E_1\left(\frac{ct_i}{2\Lambda}\right) = C^{(o)} E_1\left(\frac{ct_i}{2\Lambda^{(o)}}\right) + \left.\frac{\partial\left[C E_1\left(\frac{ct_i}{2\Lambda}\right)\right]}{\partial C}\right|_{\substack{C=C^{(o)} \\ \Lambda=\Lambda^{(o)}}} \left(C - C^{(o)}\right)$$

$$+ \left.\frac{\partial\left[C E_1\left(\frac{ct_i}{2\Lambda}\right)\right]}{\partial \Lambda}\right|_{\substack{C=C^{(o)} \\ \Lambda=\Lambda^{(o)}}} \left(\Lambda - \Lambda^{(o)}\right) + \text{(higher order terms)},$$

where the higher order terms are products of the higher order derivatives with respect to C and Λ with higher powers of the quantities $\left(C - C^{(o)}\right)$ and $\left(\Lambda - \Lambda^{(o)}\right)$, including terms with mixed derivatives and mixed powers.

In order to obtain a manageable iterative technique, one drops the higher order terms. Defining ΔC and $\Delta\Lambda$ by

$$\Delta C = C - C^{(o)},$$

$$\Delta\Lambda = \Lambda - \Lambda^{(o)},$$

calculating the required derivatives, and ignoring the higher order terms gives

$$CE_1\left(\frac{ct_i}{2\Lambda}\right) \cong C^{(o)}E_1\left(\frac{ct_i}{2\Lambda^{(o)}}\right) + E_1\left(\frac{ct_i}{2\Lambda^{(o)}}\right)\Delta C + \frac{C^{(o)}}{\Lambda^{(o)}} \exp\left[-\frac{ct_i}{2\Lambda^{(o)}}\right]\Delta\Lambda.$$

If this expression is substituted into Equations (7-13) and (7-14), with the values $C^{(o)}$ and $\Lambda^{(o)}$ being substituted also in the multiplying factor outside the square brackets, one obtains, after considerable algebraic simplifications, the two equations

$$\left.\begin{aligned} &\left|\sum_{i=1}^{M}\left[E_1\left(\frac{ct_i}{2\Lambda^{(o)}}\right)\right]^2\right|\Delta C + \left|\sum_{i=1}^{M} E_1\left(\frac{ct_i}{2\Lambda^{(o)}}\right)\frac{C^{(o)}}{\Lambda^{(o)}}\exp\left(-\frac{ct_i}{2\Lambda^{(o)}}\right)\right|\Delta\Lambda \\ &= \sum_{i=1}^{M} E_1\left(\frac{ct_i}{2\Lambda^{(o)}}\right)\left[y_i - C^{(o)}E_1\left(\frac{ct_i}{2\Lambda^{(o)}}\right)\right], \end{aligned}\right\} \quad (7\text{-}15)$$

$$\left.\begin{aligned} &\left|\sum_{i=1}^{M}\frac{C^{(o)}}{\Lambda^{(o)}}\exp\left(-\frac{ct_i}{2\Lambda^{(o)}}\right)E_1\left(\frac{ct_i}{2\Lambda^{(o)}}\right)\right|\Delta C + \left|\sum_{i=1}^{M}\left[\frac{C^{(o)}}{\Lambda^{(o)}}\exp\left(-\frac{ct_i}{2\Lambda^{(o)}}\right)\right]^2\right|\Delta\Lambda \\ &= \sum_{i=1}^{M}\frac{C^{(o)}}{\Lambda^{(o)}}\exp\left(-\frac{ct_i}{2\Lambda^{(o)}}\right)\left[y_i - C^{(o)}E_1\left(\frac{ct_i}{2\Lambda^{(o)}}\right)\right]. \end{aligned}\right\} \quad (7\text{-}16)$$

These two equations are linear in the unknown parameters ΔC and $\Delta\Lambda$. They are, in fact, the normal equations for a linear least squares problem. If this linear least squares problem is viewed as an over-determined system of linear equations, then the system matrix is given by

$$\underline{\underline{A}}^{(o)} = \begin{bmatrix} E_1\left(\frac{ct_1}{2\Lambda^{(o)}}\right) & \frac{C^{(o)}}{\Lambda^{(o)}} \exp\left(-\frac{ct_1}{2\Lambda^{(o)}}\right) \\ E_1\left(\frac{ct_2}{2\Lambda^{(o)}}\right) & \frac{C^{(o)}}{\Lambda^{(o)}} \exp\left(-\frac{ct_2}{2\Lambda^{(o)}}\right) \\ \vdots & \vdots \\ E_1\left(\frac{ct_M}{2\Lambda^{(o)}}\right) & \frac{C^{(o)}}{\Lambda^{(o)}} \exp\left(-\frac{ct_M}{2\Lambda^{(o)}}\right) \end{bmatrix} , \qquad (7\text{-}17)$$

the right hand side vector is given by

$$\underline{b}^{(o)} = \begin{bmatrix} y_1 - C^{(o)} E_1\left(\frac{ct_1}{2\Lambda^{(o)}}\right) \\ y_2 - C^{(o)} E_1\left(\frac{ct_2}{2\Lambda^{(o)}}\right) \\ \vdots \\ y_M - C^{(o)} E_1\left(\frac{ct_M}{2\Lambda^{(o)}}\right) \end{bmatrix} , \qquad (7\text{-}18)$$

and the required solution vector is

$$\underline{x}^{(o)} = \begin{bmatrix} \Delta C^{(o)} \\ \Delta\Lambda^{(o)} \end{bmatrix} . \qquad (7\text{-}19)$$

Of course, if M > 2, then the system

$$\underline{\underline{A}}^{(o)}\underline{x} = \underline{b}^{(o)}$$

will not generally have any exact solutions. The least squares solution $\underline{x}^{(o)}$ is the best approximate solution, i.e. best in the sense that it minimizes the sum of the squares of the deviations, a quantity which can be written in vector-matrix notation as $\left(\underline{b}^{(o)} - \underline{\underline{A}}^{(o)}\underline{x}\right)^T\left(\underline{b}^{(o)} - \underline{\underline{A}}^{(o)}\underline{x}\right)$. The least squares solution is, however, the exact solution of the set of normal equations

$$\left[\underline{\underline{A}}^{(o)}\right]^T\underline{\underline{A}}^{(o)}\underline{x}^{(o)} = \left[\underline{\underline{A}}^{(o)}\right]^T\underline{b}^{(o)}. \tag{7-20}$$

This last expression is just the vector-matrix way of writing Eqs. (7-15) and (7-16) as can easily be verified by substituting Eqs. (7-17), (7-18), and (7-19) into the above expression.

Once the solution vector $\underline{x}^{(o)}$ is obtained, new, and hopefully improved, estimates of C and Λ can be calculated by

$$\left.\begin{aligned} C^{(1)} &= C^{(o)} + \Delta C^{(o)}, \\ \Lambda^{(1)} &= \Lambda^{(o)} + \Delta\Lambda^{(o)}. \end{aligned}\right\} \tag{7-21}$$

Then the whole process can be repeated, using the new estimates $C^{(1)}$ and $\Lambda^{(1)}$ to compute two new corrections $\Delta C^{(1)}$ and $\Delta\Lambda^{(1)}$, which are in turn used to compute new estimates $C^{(2)}$ and $\Lambda^{(2)}$, etc. The iterative method thus consists of solving at each step a linear least squares problem in order to obtain the next correction to the solution of the non-linear problem. The iteration is continued until the corrected solution parameters converge to a suitable number of decimal places (provided of course that the iteration does converge).

There are a number of good ways for solving the linear least square problem at each step. The classical method is to form the normal equations (7-20), or equivalently, (7-15) and (7-16), and to solve them. More modern techniques, developed mainly for use on automatic digital computers, calculate the solution directly from the matrix $\underline{A}$, Eq. (7-17), and the vector $\underline{b}$, Eq. (7-13). One of the latter methods was chosen for the program used here - mainly because of the relative ease with which it could be generalized in case a different or more complex model should be adopted in the future. In such a case it would be necessary only to change the input matrix $\underline{A}$ and the input vector $\underline{b}$ to accommodate the new model. The remainder of the computer program would not be changed.

The method that was chosen is the Householder orthogonal factorization technique which was invented by Alston S. Householder, who refers to it as factorization by elementary Hermitian matrices (132). The specific algorithm that was used has been described by Gene Golub (133). A FORTRAN program was written for the IBM System 360 computer of the University of Illinois Digital Computer Laboratory. This program was designed to accept as input: (a) the light curve data from the EDIT program described in the previous chapter, (b) the time limits for which the fit was desired (e.g. from 10 to 40 days after maximum brightness), and (c) the initial estimates $C^{(o)}$ and $\Lambda^{(o)}$. It set up the iteration and allowed it to run until either: (a) the parameters had converged to the desired accuracy (4 to 5 decimal places), (b) a pre-specified, upper-limiting number of iterations had been completed, or (c) the parameters began to diverge wildly. For solving the linear least squares

problem at each step, it called a subroutine named DLLSQ which was obtained from the IBM Scientific Subroutine Package (13-). This subroutine uses the Householder factorization technique to obtain the solution. The program also used the subroutine EXPI (13-) from the same Subroutine Package for calculating the values of the exponential integral function needed in forming the matrix $\underline{\underline{A}}$ and the vector $\underline{b}$ at each step. The program gave as output the final "converged" values of the parameters and the observed light curve together with the fitted light curve both in tabular and graphical form. An example of the graphical output is given in Figure 7-3. The height of the vertical straight line at t = 1 represents the estimate of the peak magnitude m_o. The fitted curve was obtained after 5 iterations of the non-linear least squares program. The initial estimates for the two parameters of the fit were $C^{(o)} = 1.31$ and $A^{(o)} = 6.9$. The final converged values were C = .3721 and A = 9.095.

The curve gives a very good fit of the observed data in the rapid decay section but diverges widely from the observed data in the slowly decaying tail. In fact, no attempt was made to fit the latter segment. The only data used in the fitting procedure were the observations taken between t = 4 and t = 28 days. There is no need to fit the data outside the region used for the expansion test. Furthermore, a few test runs soon revealed that the Morrison-Sartori Model is not capable of simultaneously fitting both segments of the light curve. The results of three of these test runs are illustrated in Figure 7-4. The observed light curve for SN1961p was fitted in segments using different fitting limits for each fit. The fitting limits together with the resulting

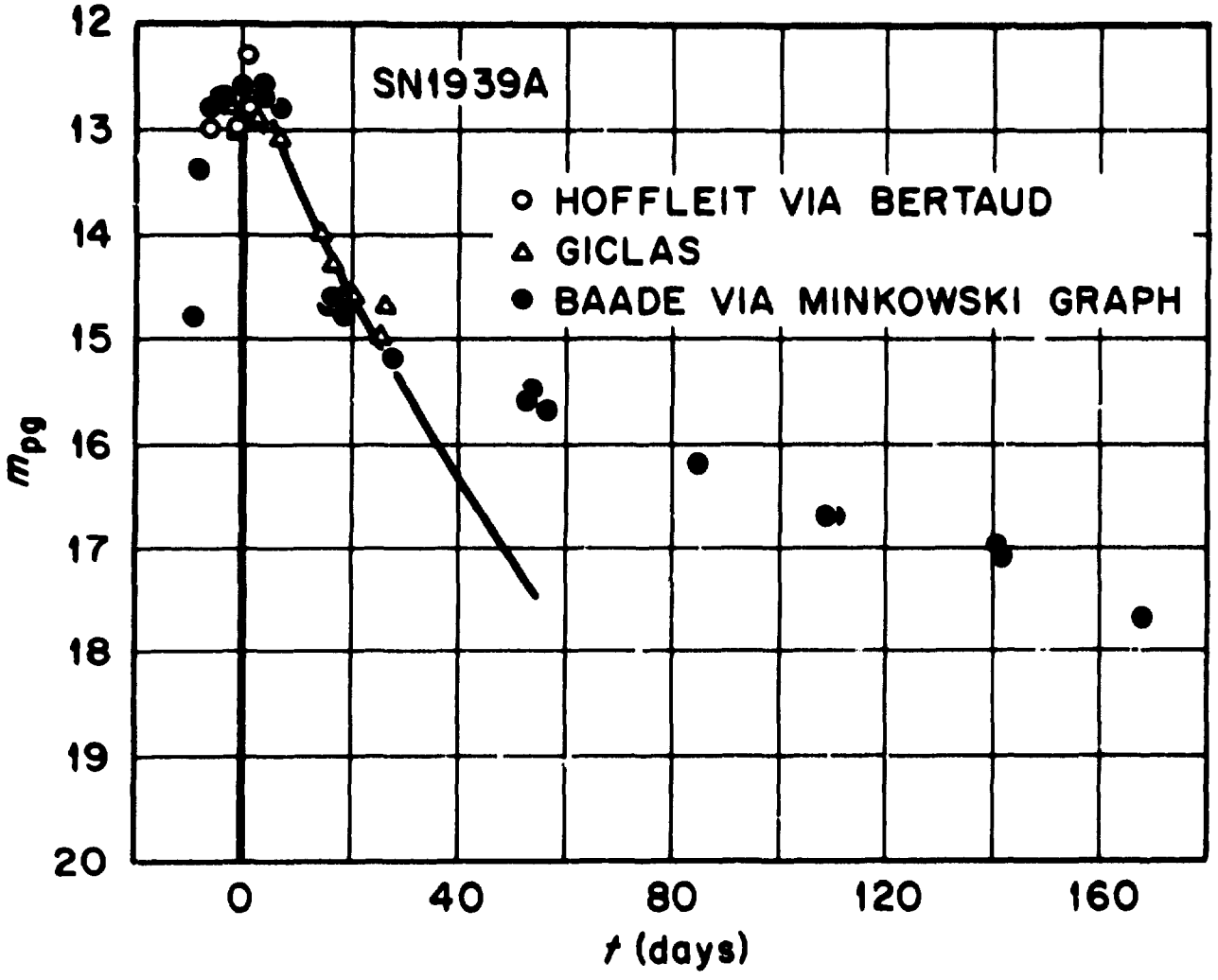

Figure 7-3. Rust's Fit of Morrison's and Sartori's Model to the Light Curve for SN1939a.

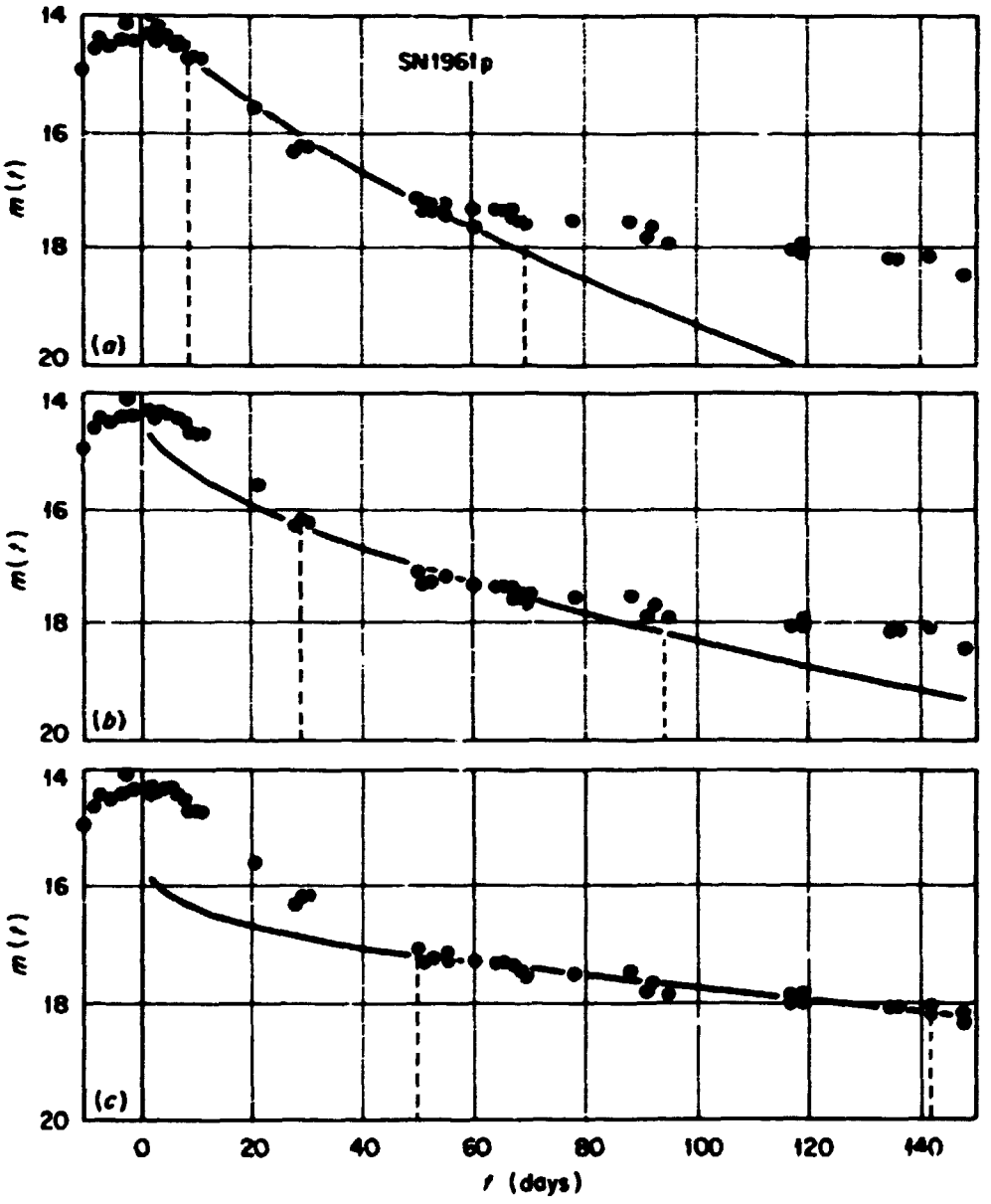

Figure 7-4. Fit of Morrison's and Sartori's Model to Three Different Regions of the Light Curve for SN1961p.

final parameter values C and A are given in Table 7-1. The fitting

Table 7-1

Results of the Fits of Morrison's and Sartori's Model to Three Different Regions of the Light Curve for SN1961p.

Fit	Fitting Limits (days after t_o)		C	A	Range in Which The Fit is Good
(a)	8.6	68.6	.715	17.0	4.5 - 55.3
(b)	28.5	94.5	.246	34.3	28.5 - 68.6
(c)	50.4	142.3	.0342	137.3	50.4 - 143.4

limits are indicated in the figure by the dashed vertical straight lines. The first curve, (a), gives a good fit to the rapid-decline part of the light curve but does not fit the observations over the entire range of the fitting limits. It diverges noticeably after day 55. On the other hand it extrapolates backward quite nicely from the lower limit and fits the observed data back to day 4.5. This backward extrapolation bonus was a very common occurrence in fitting the early parts of other light curves. Extending the range of the fitting limits to 8.6 - 94.5 gave a fit (not shown in the figure) which was very similar to (a). Its range of good fit was also 4.5 - 55.3 days. Thus including more points from the tail of the light curve within the fitting limits made almost no difference in the fit. The fit was dominated by the points in the rapid decline portion.

Skipping (b) for the moment, consider the third curve, (c), which illustrates what happens when the fitting limits include only points

from the tail of the light curve. The curve fits the observed data over the entire range of the fitting limits. The observed data for this supernova go only through 148.4 days past maximum, but Morrison and Sartori have given examples (130) in which they were able to fit the tails of some light curves over ranges of several hundred days (e.g. they were able to fit the tail of the light curve of SN1937c over a range of ~30 days to ~600 days after maximum).

Curves (a) and (c) show that the model can be used to fit either the rapid decline part or the tail of the light curve quite well. Curve (b) illustrates what happens when one attempts to fit the middle section of the light curve. It is the poorest fit of the three. The curve does not fit the data over the entire range of the fitting limits but tends to favor the earlier part. This inability to succesfully fit the middle part of the light curve was noticed in other examples also. It is as though the region where the slope changes from rapid decline to slow decline arises from a physical cause that is beyond the power of the simple uniform model to explain. On either side of this region it seems quite adequate.

It is not surprising that the simple uniform model is not adequate to fit the entire declining portion of the light curve. It assumes a constant uniform density for the envelope surrounding the star. The formation of such an envelope with a radius on the order of 100 light days is very unlikely. One would rather expect a decreasing density with increasing radius, and this is exactly what the three fits shown in Figure 7-4 predict. The values of Λ for the three fits were (a) 17.0, (b) 34.3, and (c) 137.3 light days. Since Λ is equal to the

mean free path of photons in the envelope, this increasing sequence of values represents a steady decrease in density. For the first 30 or 40 days the light curve represents the reponse of the denser inner layers of the envelope and after 50 days or so it represents the response of less dense outer layers (or perhaps of the surrounding interstellar medium). The fact that it is easy to fit either the earlier part or the later part of the light curve separately, but not to fit through the region where the slope changes, suggests that the envelope may be composed of two regions. The assumptions of the uniform model are approximately satisfied in each region. While this is an interesting speculative hypothesis, to pursue it further is outside the scope of this thesis. It suffices for the present purpose to have a model that can be used to fit the rapid-decline part of the light curve alone.

In order to test the expansion hypothesis, it is necessary to have some property or parameter of the fitted curve which can be used in a test for correlation with red shift. If a simple straight line fit had been chosen, then the natural parameter for comparison would have been the slope of the straight line. The situation is not so simple in the case of the exponential integral fit. In the case of the straight line, the slope gives an average measure of the rate of decline over the entire rapid-decline portion of the light curve. In the case of the exponential integral there is no easy way to define such an average rate. Of course one might try to use the slope at a certain "standard" point in the curve, such as 25 days after t_o, or at the point where the apparent magnitude is equal to $m_o + 2^m.0$, or some other specifically designated point that could be readily determined for each fitted light

curve. The flaw in this kind of procedure is that the slope obtained would be very sensitive to errors in the estimates of t_o and/or m_o.

Another approach would be to use some "standard" time lapse on the light curve. According to Equation (4-1), an observed time lapse Δt is related to the time lapse Δt_o which would be measured by an observer in the same galaxy with the supernova by

$$\Delta t = \Delta t_o \left(1 + \frac{V}{c}\right), \qquad (7\text{-}22)$$

where V is the red-shift velocity -- assuming that the red shift is truly a Doppler velocity effect. Thus one could pick some "standard" time interval that could easily be determined for each fitted light curve and could test this interval for correlations with the red-shift velocity V. One such time lapse would be the time required for the apparent brightness to drop by a certain amount below peak brightness, e.g. from m_o to $m_o + 3^m.0$. But this kind of time period would be sensitive to errors in the estimates of m_o and t_o. An alternative would be to choose some time interval like the time required to change in apparent brightness from $m_o + 1^m.0$ to $m_o + 3^m.0$. In calculating this kind of interval, one would hopefully subtract out most of the effects of errors in the estimates of m_o and t_o, and, in fact a series of numerical tests, which are described in the following paragraphs showed quite clearly that this is exactly what happens.

In order to test for the effects of variations in the estimate of t_o, the light curve data for SN1936a were run through the fitting program 5 times, each time with a different value of t_o. The same points were used in the fitting procedure each time, and the value of m_o was also

held constant so that the only thing that varied was the estimate of t_o. The results of these tests are summarized in Table 7-2. Column 1 gives the estimate of t_o. Column 2 gives the lower limit of the fitting range measured in days after t_o, and Column 3 gives the upper limit of the fitting range. Note that the limits of the fitting range change by exactly the same amounts as the estimates of t_o. This was done so that exactly the same data points would be used in each of the five fits. Columns 4 and 5 give the final converged values of the parameters of the fit. Columns 6, 7, and 8 give the number of days (measured from t_o) required for the fitted light curve to fall to the values $m_o + 1^m.0$, $m_o + 2^m.0$ and $m_o + 3^m.0$ respectively. Note that the changes in the entries along any one of these three columns are almost exactly the same as the changes in the estimates of t_o. Column 9 gives the number of days required for the fitted curve to fall from $m_o + 1^m.0$ to $m_o + 2^m.0$, and Column 10 gives the number of days required to fall from $m_o + 1^m.0$ to $m_o + 3^m.0$. The entries in column 9 are obtained by subtracting those in column 6 from column 7, and column 10 is obtained by subtracting column 6 from column 8. The entries in these last two columns are almost invariant. This lack of sensitivity to variations in t_o makes these two parameters much better candidates for the comparison parameter than the three quantities in columns 6, 7, and 8.

The tests for the effects of variations in the estimate of m_o were very similar to the ones just described for variations in t_o. The light curves of several supernovae were tested. One of these was SN1957b, and the results, which are summarized in Table 7-3, are quite representative. The estimate of t_o (t_o = JD2435969.0) and the fitting

Table 7-2

Effect of Changes in the Estimate of t_o on Various Comparison Parameters Δt

(1) t_o	(2) t_{lo}	(3) t_{MP}	(4) C	(5) A	(6) Δt ($\Delta m=1$)	(7) Δt ($\Delta m=2$)	(8) Δt ($\Delta m=3$)	(9) Δt ($\Delta m=2-1$)	(10) Δt ($\Delta m=3-1$)
3/10/56 00:00UT	21.1	85.2	5.7	5.62	19.7	27.2	[illegible]	7.5	1[illegible]
3/12/56 00:00UT	19.1	83.2	4.1	5.80	17.7	25.2	[illegible]	7.5	1[illegible]
3/14/56 00:00UT	17.1	81.2	2.9	6.01	15.7	23.2	[illegible]	7.5	1[illegible]
3/16/56 12:00UT	14.6	78.7	1.9	6.35	13.2	20.8	21.2	7.6	1[illegible]
3/19/56 00:00UT	12.1	76.2	1.2	6.84	10.7	18.3	[illegible]	7.6	1[illegible]

range (t_{lo} = 9.0, and t_{up} = 81.9 days after t_o) were held constant while the estimate of m_o was varied. Column 1 gives the estimate of m_o. Columns 2 and 3 give the final converged values of the fitting parameters. Columns 4, 5, and 6 give the number of days (measured from t_o) required for the fitted light curve to fall to the values $m_o + 1^m.0$, $m_o + 2^m.0$, and $m_o + 3^m.0$, respectively. Column 7 gives the number of days required for the fitted curve to fall from $m_o + 1^m.0$ to $m_o + 2^m.0$,

Table 7-3

Effect of Changes in the Estimate of m_o on Various Comparison Parameters Δt

(1) m_o	(2) C	(3) A	(4) Δt (Δm=1)	(5) Δt (Δm=2)	(6) Δt (Δm=3)	(7) Δt (Δm=2-1)	(8) Δt (Δm=3-1)
12.20	.74	11.0	11.40	22.29	35.33	10.89	23.93
12.40	.89	11.0	13.36	24.75	38.13	11.39	24.77
12.60	1.07	11.0	15.44	27.30	40.97	11.86	25.53

and Column 8 gives the number of days required to fall from $m_o + 1^m.0$ to $m_o + 3^m.0$. The effect of a $0^m.2$ variation in m_o is to produce changes of approximately 15%, 10%, and 7.5% in the parameters tabulated in columns 4, 5, and 6, respectively. The same variation in m_o produced changes of only about 4.5% and 3.2% in the parameters tabulated in columns 7 and 8. Clearly, these last two parameters are better candidates for the comparison parameter than the former three.

The comparison parameter that was finally chosen was the time, measured in days, required for the fitted curve to drop from the value $m_o + 0^m.5$ to the value $m_o + 2^m.5$. This parameter, which shall be

denoted by Δt_c, is relatively insensitive to variations in the estimates of m_o and t_o. It describes a region of the light curve which is completely contained in the rapid descent portion and furthermore covers about 60-70% of that region and is centered in the middle of it. Also, for all the supernovae in this study, the final fitted curves gave very good fits to the data in that region.

The numerical tests revealed that the goodness of the fit is not much influenced by variations in the values of m_o and t_o. The goodness of the fit is, however, affected by variations in the fitting range (i.e. the set of points used for the fit). This fact has already been discussed in connection with the light curve for SN1961p. Another series of tests was carried out using the light curve for SN1937c. In this series, the light curve data was run through the fitting program 16 times, each time with a different fitting range. The results of these tests can be summarized very succinctly. If the fitting range gives a good coverage of the rapid descent portion of the curve, then the program gives a good fit to that portion of the curve even if the fitting range extends somewhat into the flat portion of the curve. The fits are somewhat better if only points from the rapid descent portion are included in the fitting range. Therefore, for all the fits used in this study, the fitting range was chosen to cover only the rapid descent portion of the light curve.

The tests on fitting range also showed that if the fitting range is shifted away from t_o in such a way as to exclude the first part of the rapid descent portion but to include the second part together with several points from the flat portion, then the fitted curves do not

give good representations of the entire rapid descent portion. Said otherwise they do not extrapolate backwards very well. On the other hand, if the fitting range leaves out the first part (say half or less) of the rapid descent portion and includes the remainder of that portion only, with no points from the flat portion, then the resulting fits do extrapolate backwards to fit the first part of the curve very well. Similarly, if the fitting range includes only the first part (say half or more) of the rapid descent portion, then the resulting fit extrapolates forward to give a good fit to the remainder of the rapid descent portion. Thus, if the fits are carried out properly, then the model achieves one of the goals that was set for it when it was adopted for use in this study. It helps to fill in gaps in the data.

The effects of gaps in the middle of the fitting ranges were tested also. This was done by running another series of 16 different fits on the light curve data for SN1937c. The fitting range was varied and each of the 16 fits had gaps in the data which were introduced by discarding some of the points in the middle of the fitting range. The results showed clearly that if the fitting range includes only points from the rapid descent portion and that if the gap in the middle is not too long (say not more than half the length of the fitting range), then the fitted curves give a good representation of the data that was removed to create the gap. It does not make much difference whether the gap is centered in the middle of the fitting range or falls slightly earlier or slightly later in the range so long as the remaining data give a fairly adequate representation of the light curve.

The one rule that most clearly emerged from all the tests on fitting ranges and gaps in the data was that in dealing with a light curve which has gaps, it is essential to include in the fitting range only points from the rapid descent portion of the light curve. If the data for the light curve were somewhat sporadic, then it was sometimes difficult to tell exactly where the rapid descent portion left off and the flat portion began. In such cases, the fits were carried out several times for that light curve, using a different fitting range each time. The fit which appeared to give the best representation of the data was then chosen for use in this study. One trick which helped in making this decision was to superimpose the light curve in question on that of a supernova whose light curve did not have any gaps and which had the same shape as the light curve in question (i.e. the poorly measured light curve was fitted by a well measured light curve). The final fitted curve was then chosen to be the one which gave the best fit to the superimposed well-measured curve.

CHAPTER 8

THE RESULTS OF THE FITS

All of the light curves in this study were run through the fitting program described in the preceding chapter. Most of them were run several times using different fitting ranges in order to get the best possible fit. Nearly 100 fits were made in order to get the final 37 used for this study. All of the fits were completed before any attempt was made to detect a correlation between the comparison parameter Δt_c and the redshift symbolic velocity V_r. This procedure was adopted so that the final choice of fit for each light curve would be completely objective and uninfluenced by any presuppositions about the nature of the red shift. The graphical results of the final fits are given in Appendix 2. The final converged parameters of the fits are given in Table 8-1.

Columns 1 and 2 identify the supernova.

Columns 3 and 4 give the estimates of peak apparent magnitude, m_o, and date of peak, t_o.

Column 5 gives the symbolic velocity of recession, V_r, corresponding to the red shift of the parent galaxy. These velocities have not been corrected for the solar motion about the nucleus of our own galaxy. The red shifts for some of the galaxies have not yet been measured. In these cases it was necessary to estimate the symbolic velocity by using the Hubble law and various luminosity functions for galaxies. The methods used are described in more detail in the next chapter. These estimates are the values enclosed in parentheses.

Columns 6 and 7 give the lower and upper bounds of the fitting range expressed in days after peak brightness.

BLANK PAGE

Column 8 gives the number of points used in making the fit.

Columns 9 and 10 give the final converged parameters of the fit.

Column 11 gives the value of the comparison parameter Δt_c, the number of days required for the apparent magnitude to change from $m_o + 0^m.5$ to $m_o + 2^m.5$.

The main purpose of this thesis is to test whether there is a correlation between the comparison parameter Δt_c and the symbolic velocity of recession V_r. The prediction of the standard expanding universe theory is that

$$\Delta t_c = \left(1 + \frac{V_r}{c}\right)(\Delta t_c)_o \cdot \qquad (8\text{-}1)$$

where $(\Delta t_c)_o$ is the intrisic value of the comparison parameter, i.e. the value that would be determined by an observer in the same galaxy as the supernova. This formula is strictly valid only for velocities V_r which are small relative to the velocity of light c, a restriction that is completely satisfied by all the galaxies in this study.

Rewriting equation (8-1) in the form

$$\Delta t_c = (\Delta t_c)_o + \frac{(\Delta t_c)_o}{c} V_r \qquad (8\text{-}2)$$

emphasizes the linear form of the correlation that is predicted by the expanding universe hypothesis. Even though the type I supernova phenomenon is remarkably uniform, there is still a considerable amount of variation among supernovae in the rates at which their luminosities decline. Hence, it is not reasonable to expect that $(\Delta t_c)_o$ is a single constant value which applies to all supernovae. This means that the expected slope of the above linear relation must be calculated from an estimate of the mean value of $(\Delta t_c)_o$. The best way to get such an

TABLE 8-1

Summary of the Final Results of the Fits

① SN	② Galaxy	③ m_o	④ t_o	⑤ V_r	⑥ t_{lo}	⑦ t_{up}	⑧ N	⑨ C	⑩ A	⑪ Δ_c
1885a	M31	5.2	JD2409776	-299	3.0	28.0	23	.424	5.60	9.1
1921c	NGC3184	11.0	12/9/21	418	10.0	23.0	4	2.041	7.77	18.6
1937c	IC4182	8.4	JD2428768	500	10.5	26.6	58	1.942	7.14	17.0
1937d	NGC1003	12.8	JD2428792	585	7.7	32.7	40	.919	10.36	21.4
1939a	NGC4636	12.6	1/26/39	883	7.0	20.9	9	1.276	6.58	14.6
1939b	NGC4621	11.8	5/1/39	414	5.0	21.0	26	1.573	3.84	8.8
1954a	NGC4214	9.5	4/18/54	290	4.9	16.4	3	.684	7.62	14.6
1954b	NGC5668	12.5	5/3/54	1,737	8.2	25.3	15	1.103	7.70	16.6
1955b	Anon.	15.7	10/3/55	16,000	8.0	21.0	3	1.116	7.56	16.3
1956a	NGC3992	12.2	3/14/56	1,059	17.1	26.5	7	2.870	5.85	14.6
1957a	NGC2841	13.9	2/27/57	631	6.9	24.8	10	.642	8.91	16.8
1957b	NGC4374	12.1	5/9/57	954	10.0	30.9	26	1.030	8.72	18.5
1959c	Anon.	13.6	7/1/59	2,990	7.9	27.9	8	1.137	9.73	21.1
1960f	NGC4496	11.6	4/16/60	1,773	6.3	39.8	31	.953	11.09	23.1
1960r	NGC4382	11.5	12/19/60	773	24.5	26.5	2	3.422	5.62	14.3
1961d	Anon.	16.2	1/17/61	7,700	4.0	27.0	4	.574	10.61	19.3

TABLE 8-1

① SN	② Galaxy	③ m_o	④ t_o	⑤ V_r	⑥ t_{1o}	⑦ t_{up}	⑧ N	⑨ C	⑩ Λ	⑪ Δt_c
1961h	NGC4564	11.2	5/8/61	941	10.0	25.0	3	.682	15.43	29.5
1961p	Anon.	14.3	9/11/61	3,665	8.0	31.0	8	.916	13.60	28.1
1962a	Anon.	15.6	1/15/62	6,137	18.4	50.3	5	1.959	10.98	26.1
1962e	Anon.	16.4	2/19/62	14,190	11.4	37.2	4	.837	9.86	19.9
1962j	NGC6835	13.7	9/2/62	(2,500)	16.8	32.8	6	1.509	9.68	22.1
1962l	NGC1073	13.7	12/5/62	1,874	9.7	22.9	23	1.456	7.91	18.0
1962p	NGC1654	14.2	10/29/62	(3,600)	25.0	32.0	3	1.077	9.05	19.4
1963d	NGC4146	15.6	1/20/63	(6,000)	7.0	35.0	4	1.033	8.76	18.6
1963i	NGC4178	12.9	5/5/63	233	9.8	21.8	10	.850	8.96	18.2
1963j	NGC3913	12.0	5/10/63	(3,200)	8.0	22.1	7	.620	11.83	22.0
1963p	NGC1084	13.5	9/27/63	1,465	13.0	30.0	10	2.252	5.73	13.9
1964e	Anon.	12.2	2/27/64	(2,900)	10.0	24.0	13	1.304	9.61	21.4
1964l	NGC3938	13.1	12/8/64	874	15.1	34.0	13	.903	8.79	18.1
1965i	NGC4753	11.0	6/13/65	1,364	5.9	38.3	31	.5727	7.55	13.7
1966j	NGC3198	11.1	11/23/66	649	28.1	31.1	3	1.080	11.06	23.7
1966k	Anon.	16.6	JD2439489	(5,000)	16.0	17.9	2	1.531	7.60	17.4
1966n	Anon.	14.3	10/7/66	(9,600)	7.0	38.0	3	.676	13.13	25.1
1967c	NGC3389	12.6	2/22/67	1,276	9.7	25.9	32	1.426	9.30	21.0
1968e	NGC2713	12.7	3/15/68	3,810	6.0	20.0	10	.743	6.32	12.4
1969c	NGC3811	13.9	1/31/69	3,120	9.9	34.8	13	.800	12.08	24.1
1971i	NGC5055	11.7	5/27/71	520	7.0	27.0	12	1.027	7.03	14.9

estimate is to calculate the average value of (Δt_c) for some collection of light curves which is thought to be a representative sample of the basic parent distribution of light curves. It is important to make sure that no bias is introduced into the sample by the effect which is being tested for. In the present case, that means that the sample should include only light curves for which the associated values of V_r are so small that they can be neglected. The sample should include only supernovae in relatively nearby galaxies.

There are 22 supernovae in this study with values of V_r less than 2000 km/sec. All of these symbolic recession velocities are based on measured red shifts. One of them, SN1961h, has a Δt_c value which is much larger than the others. If the other 21 are taken as a sample, the resulting average value of Δt_c is

$$\overline{(\Delta t_c)_o} = 16.64 \text{ days}, \tag{8-3}$$

and the standard deviation is

$$\sigma\left[(\Delta t_c)_o\right] = 3.89 \text{ days}. \tag{8-4}$$

For SN1961h, the value of Δt_c is 29.5 days which is more than 3 standard deviations greater than the mean value. Since none of the other 21 values of Δt_c vary more than 2 standard deviations from the mean value, it is natural to suspect that SN1961h is an outlier. Therefore, a standard outlier test, which has been described by F. E. Grubbs (136), was applied to the sample. The test is based on the statistic

$$\frac{s_n^2}{s^2} = \frac{\sum_{i=1}^{n-1} (x_i - \bar{x}_n)^2}{\sum_{i=1}^{n} (x_i - \bar{x})^2}, \qquad (8\text{-}5)$$

where

$$x_1 \leq x_2 \leq x_3 \leq \ldots \leq x_n,$$

$$\bar{x}_n = \frac{1}{n-1} \sum_{i=1}^{n-1} x_i,$$

and

$$\bar{x} = \frac{1}{n} \sum_{i=1}^{n} x_i .$$

In the present context, n = 22, and the x_i are the values of Δt_c arranged in increasing order with x_n being the Δt_c for 1961h, i.e. 29.5. The value of $\bar{x}_n$ is the average of the sample when 1961h is excluded and is equal to 16.64. When 1961h is included in the sample the average $\bar{x}$ is equal to 17.23. The value of the test statistic is

$$\frac{s_n^2}{s^2} = 0.657,$$

a value which rejects the observation at the 95% level of significance. Thus the test indicates that 1961h is almost certainly a true outlier and so it will be rejected in the following for any tests involving the parameter Δt_c. It will, however, be used for some of the studies in the next chapter on the absolute magnitudes of supernovae because its light curve has a very well defined, measured peak. An inspection of that light curve (see Appendix 2) shows why 1961h is an outlier.

Although the peak is well defined by the observations, the part of the curve that is of interest for determining Δt_c is defined by only the last three observations. The observation preceding the last one appears to be inconsistent with the others, being too high. It probably represents a measuring error. It would present no problem if there were a large number other observations defining the light curve, but because of the paucity of points, it carries an inordinate weight in the fitting procedure.

When the Δt_c value for SN1961h is excluded from the sample of supernovae with measured symbolic velocities less than 2000 km/sec, the resulting average value of Δt_c is 16.64 days. Using this average as an estimate of $(\Delta t_c)_o$ gives

$$\frac{(\Delta t_c)_o}{c} = 5.55 \times 10^{-5} \ \frac{\text{days}}{\text{km/sec}} \qquad (8\text{-}6)$$

as the estimate for the slope of the linear relationship given by Equation (8-2). This is the slope which the expanding universe hypothesis predicts for the linear correlation between Δt_c and V_r (if the two are indeed linearly correlated). The obvious next step is to perform a least squares, straight line regression of Δt_c on V_r for all 36 supernovae in the sample in order to determine whether there is a correlation and, if so, what the slope of the correlation line is. Before doing that, however, it is interesting to check the distribution of Δt_c for the 21 supernovae with $V_r \leq 2000$ km/sec. This distribution is shown in Figure 8-1, where the relative frequency of occurrence of Δt_c is plotted against the deviation of Δt_c from the average value $\overline{(\Delta t_c)}_o = 16.64$. The histogram is the observed distribution and the smooth

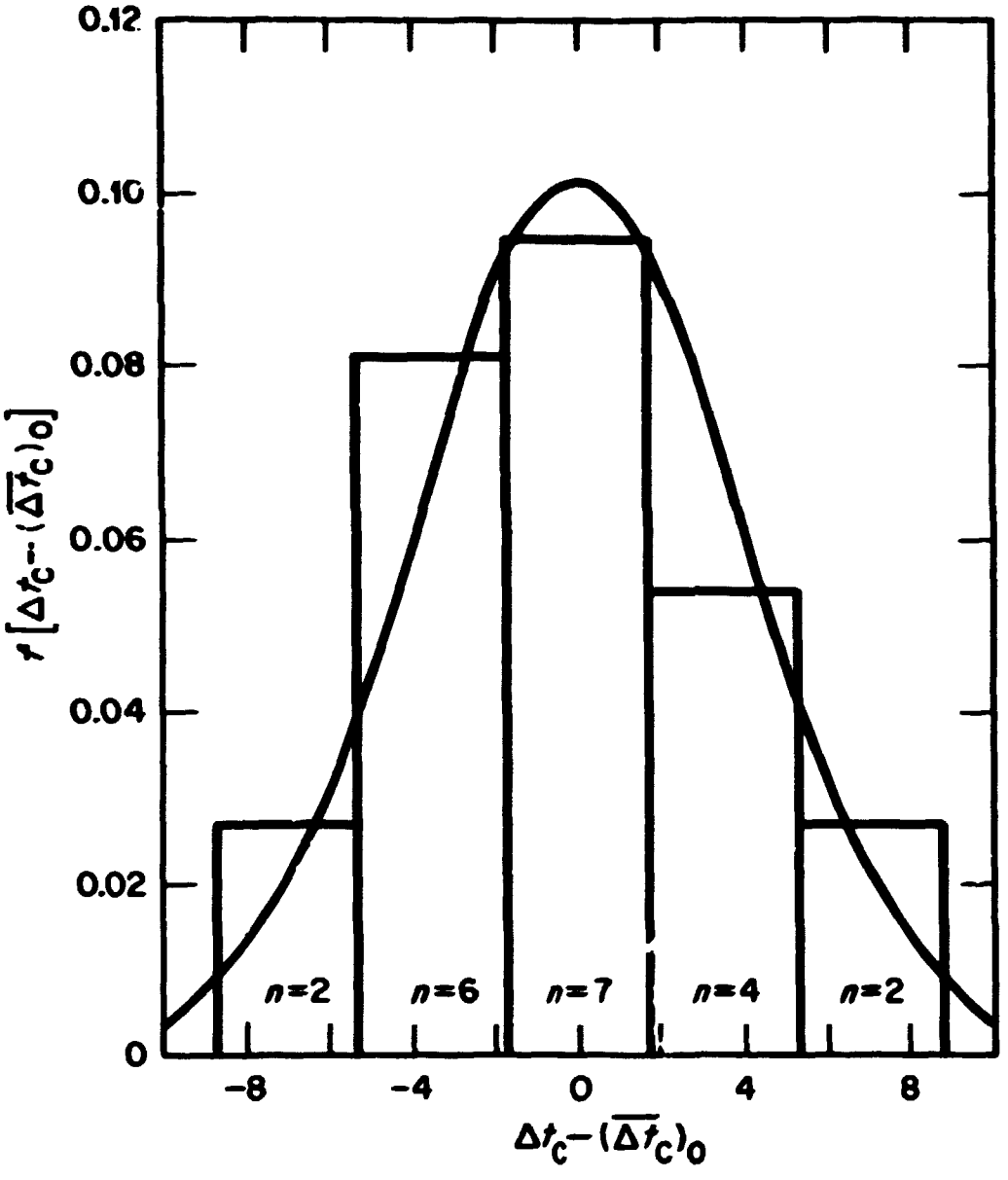

Figure 8-1. The Distribution of Δt_c for the 21 Supernovae with Measured Red Shifts 2000 km/sec.

curve is the normal distribution which best fits the observations. Each box of the histogram is 3.5 days wide and the number of sample points that fall in the box is written at the bottom. The standard deviation for the distribution is 3.89 days. There are not enough points in the total sample to apply the Chi-square goodness of fit test, but it is obvious by visual inspection that the normal distribution fits the observed distribution quite well.

Since the intrinsic distribution of $(\Delta t_c)_o$ is apparently normal, the least squares technique is appropriate for fitting a straight line relation to the sample of 36 $(V_r, \Delta t_c)$ observations. (The condition of normality is not a necessary condition to make the least squares procedure valid, but it is certainly a sufficient condition). A FORTRAN program, called LINFIT, which gives the output graphically, was written for an IBM 360 computer. The result of the fit to the 36 $(V_r, \Delta t_c)$ observations is shown in Figure 8-2. The horizontal dashed line represents the average value of Δt_c for the 36 points; that average is

$$\overline{(\Delta t_c)} = 18.41 \text{ days}. \tag{8-7}$$

The solid line is the least squares regression line,

$$\Delta t_c = 17.4 + (3.21 \times 10^{-4})\, V_r \,. \tag{8-8}$$

The standard deviations of the parameters are ± 0.93 for the intercept and ± 1.96×10^{-4} for the slope. The latter value is quite large relative to the slope itself as should be expected considering the wide scatter in the data. The correlation coefficient is 0.271, a value which at first glance seems to be so low that it would be impossible to support the hypothesis that the observations differ significantly from a random scatter diagram.

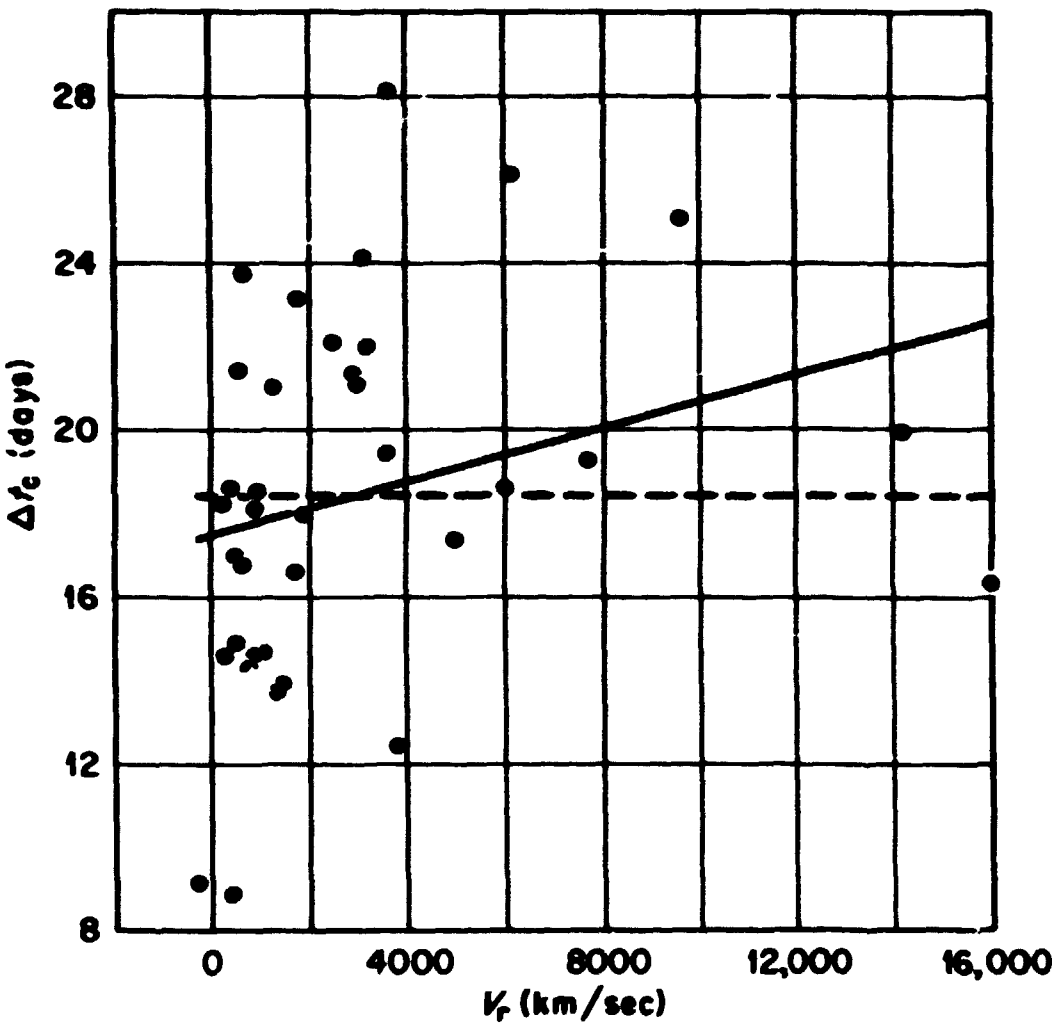

Figure 8-2. The Regression of Δt_c on Symbolic Velocity of Recession.

But the significance of the correlation coefficient depends also on the number of observations. In the present case 36 points is enough to assure that the correlation is significant. The statistic for testing the correlation is

$$t_c = \frac{r\sqrt{n-2}}{\sqrt{1-r^2}} \qquad (8\text{-}9)$$

where r is the correlation coefficient and n is the number of points in the sample. Its distribution is the t-distribution with n - 2 degrees of freedom. The value of t_c in the present case is $t_c = 1.638$ which means that the correlation is significant at the 93% level. More precisely the statistical test rejects the hypothesis that the time relation is a random scatter distribution about a constant mean at the 93% level of significance. The statistic for testing whether the slope b of the fitted line differs from some other value B is

$$t_B = \frac{b - B}{\sigma_b} \quad , \qquad (8\text{-}10)$$

where σ_b is the standard deviation of the fitted slope. In the case B = 0, t_B reduces to t_c; i.e., the statistic for testing whether the fitted slope differs from zero is the same as that for testing the correlation coefficient. Thus, the probability of obtaining a slope as large as or larger than the value 3.21×10^{-4}, if the relationship truly were a random distribution about a constant mean, is only 0.07.

The classical theory of a static universe predicts a slope of zero for the relation between Δt_c and V_r. Thus the t-test appears to reject the hypothesis that the universe is static, in spite of the great scatter in the data. But the fitted slope is

$$3.21 \times 10^{-4} \pm 1.96 \times 10^{-4} \frac{\text{degrs}}{\text{km/sec}},$$

while the prediction of the classical expanding universe hypothesis is a slope of $5.55 \times 10^{-5} \frac{\text{degrs}}{\text{km/sec}}$. Taking B equal to this latter value in equation (6-10) gives $t_B = 1.356$, a value which rejects the classical expansion hypothesis at the 91% level of significance. Clearly these data are not good enough to distinguish between the two hypotheses, but surprisingly they appear to reject both of them with a fairly high probability! Of course, all of these statistical arguments presume that the data are not biased by systematic errors in the reductions or selection effects in the observations. Therefore, the next step is to establish whether the data are contaminated by such effects.

There are three stages in the reduction of the data at which systematic errors could have been introduced: (1) the reduction of the measured light curves from the photometric system in which they were measured to the m_{pg} system, (2) the estimation of the peak magnitude m_o and time of peak t_o, and (3) the fitting of the theoretical model to the observed light curve (the program may have introduced systematic errors depending on the number of points in the fitting range). These possibilities were discussed in Chapters 6 and 7. Those chapters described tests that were made before and during the reduction process in order to assure that no systematic errors were being introduced. The results indicated that the reduction procedures would produce a consistent set of light curves, but it is still possible to test the methods further using the reduced light curves.

It is not possible to test the effects of the reductions from all of the original photometric systems to the m_{pg} system because there are not enough examples of some to give meaningful statistical comparisons. The task is further complicated by the fact that the comparisons between the various systems must be limited to sub-samples containing supernovae with similar values of V_r. It would not be correct, for example, in comparing curves originally measured in the m_{pg} system with those measured in the m_{pv} system, to choose all of the former from nearby galaxies (smaller V_r) and all of the latter from more distant galaxies (larger V_r), since the correlation between Δt_c and V_r may well be a real effect which would introduce a bias into the comparison. Taking these considerations into account, it was possible to make two comparisons. Using only supernovae with $V_r < 2000$ km/sec, there are 12 light curves that were originally measured in the m_{pg} system and 2 that were measured in the B system. The average value and standard deviation of Δt_c for the m_{pg}-curves were $\Delta t_c = 17.01 \pm 3.68$ and the corresponding values for the reduced B-curves were 18.80 ± 6.94. Since each of the two average values lies within one half of a standard deviation of the other it is probably safe to say that they do not differ significantly. In the velocity range $5000 < V_r < 8000$, there are 3 light curves that were originally measured in the m_{pg} system and 3 that were measured in the m_{pv} system. The comparison values of Δt_c for these two samples are 20.91 ± 4.59 and 20.65 ± 1.81. This is very good agreement between curves originally measured in two very different magnitude systems.

In testing the effects of the methods for estimating t_o and m_o, only supernovae with $V_r < 2000$ km/sec were used. The results of the tests

on the methods for determining t_o are given in Table 8-2. There were 8 supernovae in the sample for which the time of maximum could be determined by inspection. The average value and standard deviation of Δt_c for these 8 curves are 15.9 ± 5.2. Note that the average values

TABLE 8-2

Average Values of Δt_c for the Various Methods for Estimating t_o

Method	Number	Δt_c (Av. ± Std. Dev.)
Observed light curve	8	15.9 ± 5.2
Spectrum method (Pskovskii)	2	18.7 ± 7.1
Point-k method (Pskovskii)	3	16.3 ± 1.9
Average light curve method (Pskovskii)	4	16.3 ± 2.4
Observed color curve method (Rust)	2	19.5 ± 2.2
Average light curve method (Rust)	2	15.8 ± 1.3
All Pskovskii estimates	9	16.8 ± 3.2
All Rust estimates	4	17.7 ± 2.6

of Δt_c for all the other methods of estimating t_o lie well within one standard deviation from the average for these 8. Note also the good agreement between the 9 estimates made by Pskovskii and the 4 made by Rust. The results of the tests on the methods for determining m_o are given in Table 8-3. For 9 of the light curves the peak magnitudes were estimated directly from the observations. The average value of Δt_c for these nine curves is 15.7 ± 4.9. The reduced light curves for all of the other methods gave average values of Δt_c which are well within one standard deviation of this value.

TABLE 8-3

Average Values of Δt_c for the Various Methods of Estimating a_0

Method	Number	Δt_c (Av. ± Std. Dev.)
Observed light curve	9	15.7 ± 4.9
Average light curve method (Pskovskii)	4	16.3 ± 5.7
Point-k method (Pskovskii)	4	17.5 ± 7.9
Point-k method (Rust)	4	18.3 ± 3.8

It is especially important to check whether the number of points used in the fit had a systematic effect on the result of the fit. This is because the nearer (lower V_r) supernovae were generally more completely observed than the more distant (higher V_r) ones. All of the 8 supernovae with $V_r > 6000$ km/sec had less than 8 observed points in the fitting range; all but two of them had 4 points or less in the range. If the fitting procedure should give systematically flatter fitted light curves when the number of fitted points decreases, then the values of Δt_c would be systematically higher for larger values of V_r. In order to test this possibility, Δt_c was plotted against the number N of points for the 21 supernovae with $V_r < 2000$ km/sec. This plot is shown in Figure 8.3. The dashed line is the average value $\overline{\Delta t_c} = 16.64$ days. The solid line is the result of a least squares straight line regression of Δt_c on N which gave

$$\Delta t_c = (16.0 \pm 1.4) + (3.22 \times 10^{-2} \pm 6.15 \times 10^{-2}) \cdot N.$$

Since the slope of the fitted line is positive, the smaller values of N certainly do not produce systematically flatter fitted light curves

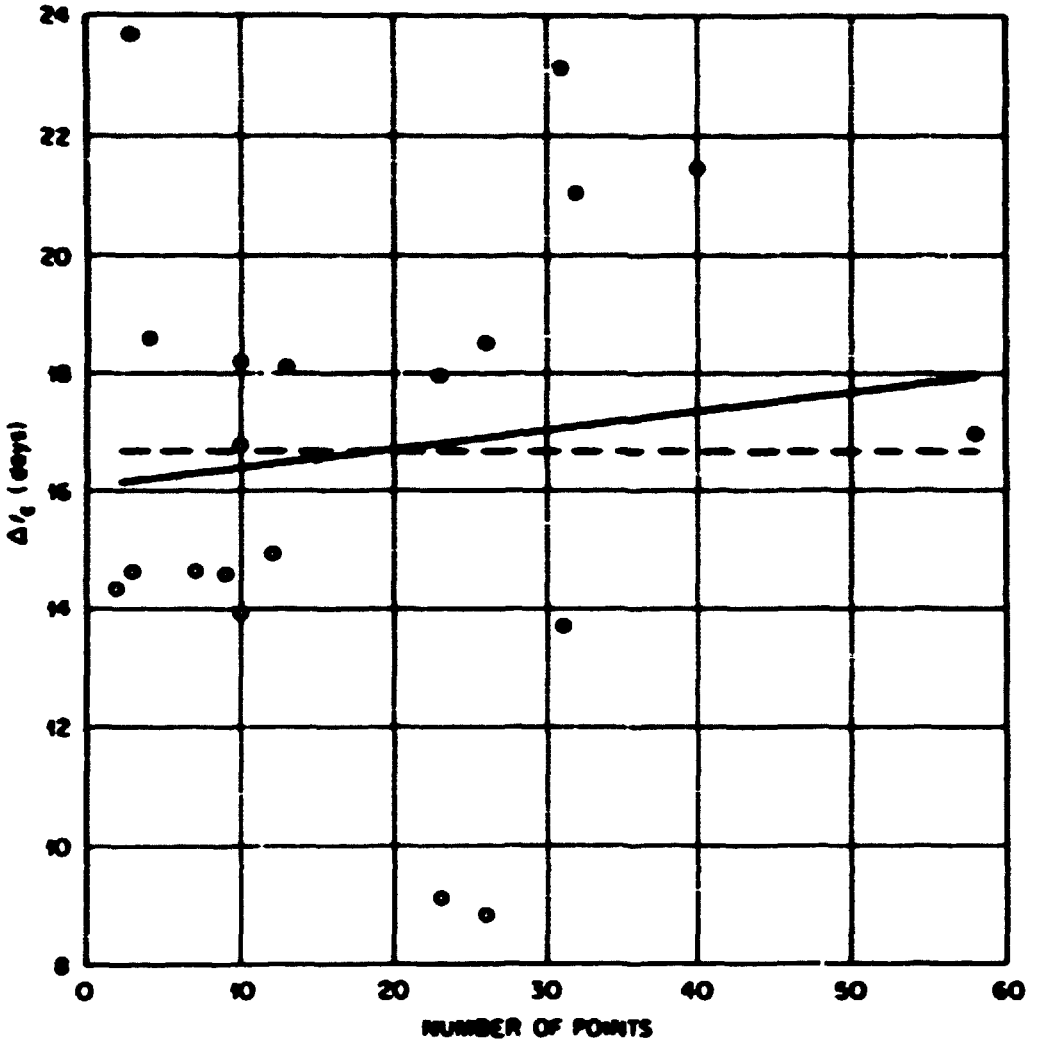

Figure 8-3. The Regression of Δt_c on the Number of Points Used for the Fit.

(larger Δt_c). Furthermore, since the slope is so small relative to its standard deviation it is safe to conclude that the value of N did not have any significant systematic effect in the other direction either. The value of the t-statistic (8-10) for testing the fitted slope against zero-slope is 0.523. This value is not significant even at the 25% level. The same value also applies for testing the significance of the correlation coefficient, which was r = 0.12, so it is clear that there is no significant correlation between Δt_c and N.

CHAPTER 9

DISTANCE MODULI, ABSOLUTE MAGNITUDES, AND THE TEST FOR OBSERVATIONAL SELECTION EFFECTS

The tests described at the end of the preceding chapter established that the $\Delta t_c - V_r$ correlation was not the result of systematic effects introduced by the data reduction or fitting procedures. There remains the possibility that systematic effects may have been introduced by the observations themselves. Photometric techniques have changed greatly since 1885, and most of the earlier observations were in relatively nearby galaxies, whereas most of the observations in the more distant galaxies have been made in more recent times. If the changes in photometric techniques have caused systematic changes in the calibration of the m_{pg} scale, then systematic effects may have been introduced into the sample. Furthermore, one must not forget the possibility that the calibration of the m_{pg} scale might, even now, have systematic errors toward the faint limit; but both of these effects are beyond the control of the present author who can only assume that the care with which the observations have been made over the years has minimized errors of this sort. It seems much more likely that systematic errors may have been introduced, not by changes or errors in the scale, but rather by observational selection effects.

Previous studies (49, 50, 137) of the peak intrinsic luminosities of type I supernovae indicate a range of about $3^m.0$ in peak absolute magnitude. It is not inconceivable that the more distant supernovae that have been observed are on the average intrinsically more luminous than the relatively nearby ones since the more luminous ones would be

BLANK PAGE

the more easily visible ones at large distances. If all the supernovae were discovered in systematic searches. this would be a very unlikely happening since a systematic search would be designed to avoid such selection effects. Some supernovae are discovered by accident in the process of observing something else; and the possibility also remains that even if a systematic search is not biased in discovering supernovae, the selection effect could enter the sample when the choice is made as to which light curves will be measured in detail. If the sample is contaminated by this effect, and if the rate of fall of the light curve is correlated with the peak absolute magnitude, the correlation between Δt_c and V_r might be explained by observational selection. Therefore it is important to obtain estimates of the absolute magnitudes of the supernovae in this sample. Such estimates are also quite interesting in themselves.

The peak absolute magnitudes of type I supernovae have previously been studied by van den Bergh (137), Pskovskii(50), and Kowal (49). Using a sample of 20 supernovae, van den Bergh obtained the values $M_0 = -18.7 \pm 1.^m1$ for the average and standard deviation of the peak photographic absolute magnitude. Using a sample of 19 supernovae, Kowal obtained $M_0 = -18.56 \pm 0.^m77$ for the same quantities. Pskovskii used a sample of 38 supernovae and grouped them according to the Hubble type of the parent galaxy. He found a slight correlation between the peak magnitude and the Hubble type, with luminosity increasing with the transition from elliptical to spiral and irregular galaxies. The average magnitude for all 38 supernovae was $M_0 = -19.2 \pm 0.^m85$.

Van den Bergh's article did not state whether the peak apparent magnitudes were corrected for absorption. Kowal corrected the apparent magnitudes for absorption within our galaxy [using 0.25 csc(b)], but made no attempt to correct for absorption within the parent galaxy. Since his average value was very close to that obtained by van den Bergh, it seems probable that the latter used the same procedure. Pskovskii corrected the apparent magnitudes for absorption both within our own and the parent galaxy. This latter correction is probably the reason that his estimate of the average peak luminosity is about $0^m.5$ brighter than those of Kowal and van den Bergh.

Nineteen of the 37 supernovae in this study had partial [and in some cases fairly complete] measured color curves, with indices (B - V) or $(m_{pg} - m_{pv})$ as a function of time. For these supernovae it was quite easy to estimate the color excesses, either

$$E(B - V) = (B - V) - (B - V)_o, \qquad (9\text{-}1)$$

or

$$E(m_{pg} - m_{pv}) = (m_{pg} - m_{pv}) - (m_{pg} - m_{pv})_o, \qquad (9\text{-}2)$$

by using the method of vertical shifts of Pskovskii's intrinsic color curves [Figures 6-1 and 6-2] to fit the observed colors. The method was described in Chapter 6, and the color excesses for the 19 supernovae are given in Table 6-4. These color excesses made it possible to estimate the total absorption of the supernovae light by using the well-known reddening relationship,

$$A_{tot} = R \cdot E(B - V), \qquad (9\text{-}3)$$

where A_{tot} is the total visual absorption and R is the ratio of total to selective absorption. Since estimates of the value of the constant R are based on data for our own galaxy, this method assumes that the

parent galaxies obey the same reddening law as our own. While there is some evidence that certain regions of our own galaxy have anomalous values of R, it is generally accepted (138, 139) that, for the absorption in the V band, the constant average value

$$R = R_{vis} = 3.1 \qquad (9\text{-}4)$$

applies over wide regions of the galaxy. As a first approximation it will be assumed here that this same value applies everywhere in all galaxies (and in the intergalactic medium as well, although intergalactic absorption is probably negligible).

In the m_{pg} system, Eq. (9-3) becomes

$$A_{pg} = R_{pg} \cdot E(B-V), \qquad (9\text{-}5)$$

where

$$R_{pg} = 4.18. \qquad (9\text{-}6)$$

This equation was used to compute the total absorptions for the 19 supernovae with measured color excesses. Measured $E(m_{pg} - m_{pv})$ color excesses were converted to $E(B-V)$ by the equation

$$E(B-V) = 0.85\, E(m_{pg} - m_{pv}). \qquad (9\text{-}7)$$

The total absorptions were used to calculate the corrected peak apparent magnitudes m_o. The absorptions within our own galaxy were also computed using the standard cosecant law (139),

$$A_{gal} = 0.25 \csc(b^{II}), \qquad (9\text{-}8)$$

where b^{II} is the galactic latitude of the parent galaxy. These values were subtracted from the total absorptions in order to determine the absorptions within the parent galaxies. For three of the supernovae

the absorptions calculated for our galaxy slightly exceeded the total absorptions computed from the color excess. Two of the three parent galaxies were ellipticals and the other was an irregular. Since elliptical galaxies have small internal absorptions, it is probable that the bulk of the absorption occurred within our own galaxy, and the slight discrepancies most likely represent small random deviations from the cosecant law, although one cannot completely rule out a small zero point error in Pskovskii's intrinsic color curves. In any case the discrepancies were small and the absorptions within the parent galaxies were taken to be zero. The cosecant law results were discarded and the corrections for m_0 were calculated solely on the basis of the color excess.

Once the absorptions within the parent galaxies had been computed for the 19 supernovae, they were divided into three groups, and the average absorptions for these groups were calculated so that they could be used as rough estimates of the absorptions for the 18 supernovae which did not have measured colors. The three groups were (1) supernovae which appeared in high absorption regions of spiral galaxies (e.g., in spiral arms), (2) supernovae which appeared in spiral galaxies but not in obviously high absorption regions, and (3) supernovae which appeared in elliptical and irregular galaxies. Extreme cases like SN1962$_1$, which occurred in an emission region, were discarded; and average values of the absorption within the parent galaxies were computed for the three groups. The results are shown in Table 9-1, which also gives the values which were adopted for correcting the apparent magnitudes of the 18 supernovae which did not have measured color excesses.

Table 9-1

Average Absorptions in Various Types of Galaxies

Group	Average Absorption	Adopted Absorption
Supernovae in elliptical and irregular galaxies.	$0^{m}.07$	$0^{m}.0$
Supernovae in spiral galaxies but not inside a spiral arm or other high absorption region.	$0^{m}.47$	$0^{m}.5$
Supernovae inside spiral arms or other high absorption regions of spiral galaxies.	$1^{m}.57$	$1^{m}.5$

These adopted corrections were applied in a conservative way according to the various observers' descriptions of the type of galaxy and the location of the supernova in it. The large $1^{m}.5$ correction was applied only if the supernovae was definitely described as having occurred inside a spiral arm. If the location was described as at the end of a spiral arm or on a projected extension of a spiral arm, or if the supernova occurred anywhere else in a spiral galaxy, then the smaller correction $0^{m}.5$ was used. After all 18 peak magnitudes were corrected in this manner for absorption within the parent galaxies, they were further corrected for absorption within our own galaxy by means of Eq. (9-8). The correction calculations are summarized in Table 9-2.

Column 1 is the supernova designation.

Column 2 is the peak photographic magnitude before the absorption correction.

Column 3 is the B - V color excess. The supernovae without entries in this column are the 18 which did not have measured colors.

Column 4 is the absorption within the parent galaxy.

Column 5 contains notes or comments describing the galaxy or the supernova's situation in the galaxy. Asterisks (*) in this column refer to notes at the end of the table.

Column 6 is the galactic latitude.

Column 7 is the absorption within our own galaxy.

Column 8 is the final corrected peak apparent magnitude.

The next step in the calculation of the peak absolute magnitudes is the estimation of the distance moduli of the parent galaxies. Van den Bergh (137) used 3 methods for estimating the distance moduli: (1) the radial velocity of the parent galaxy, (2) the mean radial velocity of the galaxy cluster containing the galaxy, or (3) the luminosity classification of the galaxy. For the Hubble constant he used H = 100 km/sec/Mpc. Kowal (49) for the most part adopted van den Bergh's estimates. Pskovskii (50) gave independent estimates using the same methods plus two other methods whenever appropriate: (1) the angular dimensions of HII regions in the parent galaxies and (2) estimates for the brightest stars in the parent galaxies. He also used H = 100 km/sec/Mpc.

Nearly two thirds of the supernovae in this study were included in one or more of the three studies described above. Whenever possible the estimates of van den Bergh and Pskovskii were averaged with independent estimates made for this study. Since it was necessary to obtain new estimates for more than one-third of the supernovae, it seemed reasonable to get new estimates for all of them. Furthermore, the final estimate for each supernova was obtained by averaging as many as possible estimates obtained from independent methods including the estimates of

Table 9-2

Summary of the Calculations of the

Corrected Peak Apparent Magnitudes m_0

SN	est. m_0	E(B-V)	Abs. in parent gal.	Notes, Comments	b^{II}	Abs. in our galaxy	correc. m_0
1885a	5.2^{m}4		0.^{m}50		-21.6°	0.^{m}68	4.06
1921c	11.0		1.50	spiral arm	55.6	0.30	9.20
1937c	8.4	0.05	0.0		79.1	0.26	8.19
1937d	12.8	0.45	1.05	edge-on gal.	-17.5	0.83	10.92
1939a	12.6	0.43	1.52	***	65.5	0.28	10.80
1939b	11.8		0.0	E-galaxy	74.4	0.26	11.54
1954a	9.5	0.13	0.28	Irreg. gal.	78.1	0.26	8.96
1954b	12.5	0.25	0.74		56.8	0.30	11.46
1959b	15.7		0.50		-75.6	0.26	14.94
1956a	12.2	0.37	1.27	spiral arm	61.9	0.28	10.65
1957a	13.85	0.68	2.53	spiral arm	44.2	0.31	11.01
1957b	12.1		0.0	E-galaxy	74.5	0.26	11.84
1959c	13.55	0.10	0.15		65.8	0.27	13.13
1960f	11.6		1.50	spiral arm	66.3	0.27	9.83
1960r	11.5	0.34	1.16		79.2	0.26	10.08
1961d	16.2	0.04	0.0	*, E-gal.	89.2	0.25	16.03
1961h	11.2		0.0	E-galaxy	73.9	0.26	10.94
1961p	14.3		0.50		-20.8	0.70	13.10
1962a	15.6	0.10	0.17	E or S0	86.5	0.25	15.18
1962e	16.4	0.0	0.0	*, bridge	68.5	0.27	16.40
1962j	13.65		0.50		-19.6	0.75	12.40
1962l	13.7	0.85	3.23	**	-50.7	0.32	10.15
1962p	14.2		0.0	E-galaxy	-28.7	0.52	13.68
1963d	15.6		0.50		80.8	0.25	14.85
1963i	12.9		0.50		71.4	0.26	12.14
1963j	12.0		0.50		59.7	0.29	11.21
1963p	13.5		0.50		-56.6	0.30	12.70
1964e	12.2		0.50		52.6	0.31	11.39
1964l	13.1		1.50	spiral arm	69.3	0.27	11.33
1965i	11.0	0.03	0.0	*, Irreg. gal.	61.7	0.28	10.87
1966j	11.1		1.50	spiral arm	54.8	0.31	9.29
1966k	16.6	0.17	0.44		68.9	0.27	15.89
1966n	14.3		0.50		-31.1	0.48	13.32
1967c	12.6	0.10	0.12		57.7	0.30	12.18
1968e	12.7	0.23	0.45		29.2	0.51	11.74
1969c	13.9^m	0.28	0.89		65.3	0.28	12.77
1971i	11.7	0.40	1.41	spiral arm	74.3	0.26	10.03

* These supernovae (1961d, 1962e, 1965i) had color excesses which gave total absorptions smaller than the absorption predicted for our own galaxy by the cosecant law. The treatment of the correction for these three is given in the text. Note that SN1962e occurred in a faint luminous bridge between two elliptical galaxies.

** 1962l: This supernova occurred in an emission region--hence the large color excess.

*** 1939a: This supernova occurred in a peculiar E0 or S0 galaxy with a gaseous envelope containing many condensations.

Pskovskiĭ and van den Bergh whenever available. The method of averaging will be described in more detail below.

The first step in obtaining independent estimates of the distance moduli was to get estimates of the apparent photographic magnitudes of the parent galaxies corrected for absorption within our own galaxy. The uncorrected apparent magnitudes were obtained by averaging several methods as described in Chapter 5 (cf. Table 5-2 and the explanation of column 8) and are given in Table 5-2. These magnitudes were corrected for absorption in our own galaxy using Eq. (9-8). No attempt was made to correct for inclination effects in the parent galaxies. The corrected apparent magnitudes are given in column 3 of Table 9-3.

The new estimates of the distance moduli were obtained by four different methods. Three methods calculated (m - M) by combining the corrected apparent magnitudes with estimates of the absolute magnitudes obtained from various luminosity functions. The other method was based on the symbolic recession velocity and the Hubble constant. The observed symbolic recession velocities are given in column 7 of Table 5-2. Only the measured values of V_r were used since the estimated values of V_r were themselves calculated using the methods based on absolute magnitudes obtained from the various luminosity functions. The observed velocities were corrected for the solar motion relative to the local group. These corrected velocities, which are given in column 4 of Table 9-3, were used for the estimates of distance moduli. The method consists essentially in combining the relation

$$m - M = 5 \log D - 5, \tag{9-9}$$

where D is the distance measured in parsecs, with the Hubble relation

$$V_r = Hr. \tag{9-10}$$

When the Hubble constant is expressed in the units km/sec/Mpc and V_r is in km/sec, then $D = 10^6 \times r$, and the combined relation becomes

$$m - M = 25 + 5 \log\left(\frac{V_r}{H}\right). \qquad (9\text{-}11)$$

Taking H = 100 km/sec/Mpc gives

$$m - M = 15 + 5 \log (V_r). \qquad (9\text{-}12)$$

The three luminosity function methods for estimating distance moduli were based upon: (1) the DDO types of the parent galaxies and van den Bergh's (140, 141) luminosity classification for late type galaxies; (2) de Vaucouleurs' (142, 143) revised types of the parent galaxies and van den Bergh's luminosity classification; and (3) the Hubble types of the parent galaxies and Holmberg's (119) luminosity classification for galaxies. Methods (1) and (3) are straightforward, consisting in assigning an absolute magnitude to each galaxy on the basis of its type in the classification scheme. Method (2) is somewhat more complicated and requires additional explanation. In his 1962 IAU Symposium paper (142), de Vaucouleurs gave a luminosity function for his revised classification system which was apparently based on a recalibration of van den Bergh's luminosity classes using a Hubble constant of 120 km/sec/Mpc. Van den Bergh's original calibration is based on the value H = 100 km/sec/Mpc which is the value adopted for this study. De Vaucouleurs also gave, in graphical form, the relationship between his revised types and van den Bergh's luminosity classes. The same relationship is given in tabular form in his 1963 Astrophysical Journal Supplement (143). This relationship was used together with van den Bergh's calibration in order to obtain a luminosity function

which gives for each revised galaxy type an absolute magnitude based on $H = 100$ km/sec/Mpc. This luminosity function was used for method (2). For most of the galaxies in this study, the revised type was obtained from the catalogue given by de Vaucouleurs in the Supplement paper. In that Supplement he also gave the correlation between his revised types and the Hubble type. For galaxies not in his catalogue, this relation was used to obtain the revised type from the Hubble type.

The distance modulus of each galaxy in this study was determined by as many as possible of the four methods just described. These determinations were then combined with the estimates of van den Bergh and Pskovskii and the final values were obtained by averaging consistent, independent estimates. That is, for each galaxy, all of the available estimates were compared for consistency and independence. If most of the estimates were fairly close in value, but one or more was very different, then the divergent value was not included in the average. Also, if two of the estimates were obtained by the same method, e.g., if Pskovskii estimate was based on the recession velocity and hence was identical to the present author's estimate using the same method, then one of them was discarded before computing the average. The average values obtained in this manner are given in column 5 of Table 9-3. The mean number of independent estimates used in calculating each of these average values was 2.6.

The estimates M_0 of the peak absolute magnitudes of the supernovae were calculated from the estimates of the distance moduli by

$$M_0 = m_0 - (m - M) \qquad (9\text{-}13)$$

where the m_o are the peak apparent magnitudes corrected for extinction. These apparent magnitudes were given in column 8 of Table 9-2. They are repeated in column 7 of Table 9-3. The calculated peak absolute magnitudes are given in column 8 of the same table.

For the seven supernovae whose parent galaxies did not have measured shifts, the estimates of the distance moduli given in column 5 were used to calculate estimates for the symbolic recession velocities by means of Eq. (9-12).

The absolute magnitudes calculated in this study were compared with those of van den Bergh, Kowal, and Pskovskii. The details of the comparisons are given in Appendix 3. In general the agreement was good when the different methods of extinction correction were taken into account. In no case were there any systematic deviations other than different average values. The average $\overline{M_o}$ for the Rust estimates was $0^m.33$ brighter than the $\overline{M_o}$ for Pskovskii's estimates, and the straight line

$$M_o(\text{Pskovskii}) = M_o(\text{Rust}) + 0^m.33$$

gave a very good fit of the plotted relation M_o(Pskovskii) vs. M_o(Rust). The $0^m.33$ difference arose from the different methods used to correct for absorption within the parent galaxy. For spiral galaxies, Pskovskii based his absorption estimates on the inclination of the plane of the galaxy, assuming a plane-parallel model for the absorbing material. It is shown in Appendix 3 that Pskovskii's estimates are in many cases not consistent with the observed color excesses in that some highly reddened supernovae had smaller extinction corrections than only slightly reddened one. The color excess method used in this study

Table 9-3

Summary of the Calculations of the Peak Absolute Magnitudes M_o

SN	Galaxy	galaxy m_{pg}	correc. V_r (Km/sec)	m - M	Notes	Supernova m_o	Supernova M_o
1885a	M31	3.65	-68	23.8	*	4.06	-19.7
1921c	NGC 3184	9.94	418	29.2		9.20	-20.0
1937c	IC 4182	13.25	554	28.6		8.19	-20.4
1937d	NGC 1003	11.18	741	30.3		10.92	-19.4
1939a	NGC 4636	10.33	778	30.3		10.80	-19.5
1939b	4621	10.74	345	30.4		11.54	-18.9
1954a	4214	9.90	311	28.8		8.96	-19.8
1954b	5668	11.90	1,732	31.2		11.46	-19.7
1955b	Anon.	15.44	16,050	34.6		14.94	-19.7
1956a	NGC 3992	10.28	1,147	30.5		10.65	-19.8
1957a	2841	9.69	671	29.7		11.01	-18.7
1957b	4374	10.09	878	30.1		11.84	-18.3
1959c	Anon.	15.57	2,980	33.5		13.13	-20.4
1960f	NGC 4496	11.66	1,665	30.5		9.83	-20.7
1960r	4382	9.80	712	29.9		10.08	-19.8
1961d	Anon.	14.75	7,706	34.3		16.03	-18.3
1961h	NGC 4564	11.91		30.8		10.94	-19.9
1961p	Anon.	12.50	3,827	32.6		13.10	-19.5
1962a	Anon.	15.75	6,152	34.2		15.18	-19.0
1962e	Anon.	15.23	14,130	34.8		16.40	-18.4
1962j	NGC 6835	12.25		32.7		12.40	-19.6
1962l	1073	11.25	1,895	31.6		10.15	-20.8
1962p	1654	13.68		32.8		13.68	-19.1
1963d	4146	13.55		33.9		14.85	-19.0
1963i	4178	11.49	140	30.6		12.14	-18.5
1963j	3913	13.91		32.5		11.21	-21.3
1963p	1084	10.80	1,448	30.8		12.70	-18.1
1964e	Anon.	14.19		32.3		11.39	-20.9
1964f	NGC 3958	10.52	919	30.2		11.33	-18.9
1965i	4753	10.42	1,252	30.3		10.87	-19.4
1966j	NGC 3198	10.51	670	29.9		9.29	-20.6
1966k	Anon.	14.43		33.5		15.89	-17.6
1966n	Anon.	15.52		34.9		13.32	-21.6
1967c	NGC 3389	11.80	1,145	30.6		12.18	-18.4
1968e	2715	12.19	5,623	32.0		11.74	-20.3
1969c	3811	12.72	3,179	32.2		12.77	-19.4
1971i	5055	9.13	600	28.4		10.05	-18.4

*SN1885a: The distance modulus adopted for this galaxy (M31) is the value given by Allen (144) in Astrophysical Quantities.

does not suffer from this shortcoming since it predicts the absorption correction from the reddening.

Although the color excess method is more consistent than the inclination method, it is important to keep in mind that 18 of the extinction corrections were only rough estimates. The average total correction for the 19 whose corrections were derived from color excesses was $\bar{A}_{pg} = 1^m.10 \pm 0^m.96$. The average of the 18 estimated corrections was $\bar{A}_{pg} = 0^m.99 \pm 0^m.53$. The smaller standard deviation for the latter group is due to the smaller range ($0 - 1^m.5$) of the estimated corrections. The good agreement between the average values demonstrates that the methods are consistent in the sense that one did not give systematically larger corrections than the other. The corrections were also checked by plotting the final corrected M_o against that part of the extinction correction attributed to the parent galaxy. The plot did not show any correlation between M_o and the correction, nor did it reveal any significant differences between the two groups of corrections.

The other large uncertainties in the M_o estimates were the estimates of the distance moduli of the parent galaxies. A plot of M_o against $(m - M)$ showed that there was no significant correlation between the two. Not only does this mean that the $(m - M)$ estimates did not introduce any systematic effects into the estimates of M_o, but it also means that there is probably no luminosity selection effect in the sample. Thus, even if there is a correlation between the absolute magnitudes M_o and the comparison parameter Δt_c, that correlation would not be responsible for the correlation between the Δt_c and the symbolic recession velocities V_r.

Before turning to the question of the relation between M_o and Δt_c, it is interesting to briefly consider two correlations originally observed by Pskovskii and confirmed by the M_o estimates in the present study. Only the results of these comparisons will be stated here, but the details can be found in Appendix 4. In his 1967 paper (140), Pskovskii found a weak correlation between the M_o and the Hubble types of the parent galaxies. The present study confirms this trend but the average values of M_o for each galaxy type differ in the two studies in two ways: (1) the averages of Rust increase more smoothly along the sequence of galaxies than do those of Pskovskii, and (2) the brightness increase along the sequence is less for the estimates of Rust than for those of Pskovskii. Thus, the correlation appears to be more regular but less pronounced for the estimates of Rust than for those of Pskovskii.

In an earlier paper (145), Pskovskii reported a correlation between M_o and the integrated absolute magnitudes of the parent galaxies, M_{gal}. The estimates in the present study confirm this correlation even though there is a wide scatter in the M_o estimates. For the present sample, the regression line is

$$M_o = -(27.9 \pm 5.1) - (0.436 \pm 0.262)\, M_{gal},$$

and the correlation coefficient is $\rho = -0.28$. The t-statistic for testing this correlation is $t = -1.67$, a value which gives significance at the 94.7% level.

The main purpose for computing the absolute magnitudes of the supernovae was to check for a correlation between them and the comparison parameter Δt_c, i.e., between the peak luminosity and the rate of fall of the light curve. The result of a straight line regression of $-M_o$

on Δt_c is shown in Figure 9-1. The horizontal dashed line is the average absolute magnitude and the solid line is the best fitting least squares line which has the equation

$$M_o = (-18.55 \pm 0.68) - (0.0512 \pm 0.0359)\Delta t_c. \qquad (9\text{-}14)$$

The correlation coefficient is 0.237 and the t-statistic for testing the significance of the correlation has the value $t = 1.43$. This latter value gives, with 34 degrees of freedom, significance at the 92% level. A closer inspection of the plot reveals that there may be an even more significant correlation than that revealed by the regression, for the points seem to fall into two separated bands, and each band by itself shows a more pronounced correlation than the totality of points. These bands will be discussed in more detail in Chapter 11. Since there does appear to be a significant relation between Δt_c and M_o, it is important to check whether M_o is correlated with the symbolic velocity of recession. The regression of $-M_o$ on V_r is shown in Figure 9-2. The broken line is the relation $M_o = \bar{M}_o$ and the solid line is the best least squares line,

$$M_o = (-19.53 \pm 0.20) + [(0.66 \pm 4.33) \times 10^{-5}]V_r.$$

Since the standard deviation of the slope is nearly seven times greater than the slope itself, it is safe to assume that the slope does not differ significantly from slope = zero. This conclusion is further reinforced by the value of the correlation coefficient, $\rho = -0.026$, and the t-statistic, $t = -0.15$. Thus, the conclusion previously drawn from the plot of M_o against $(m - M)$ is confirmed. <u>There is no significant luminosity selection in the sample</u>. This means that, though there

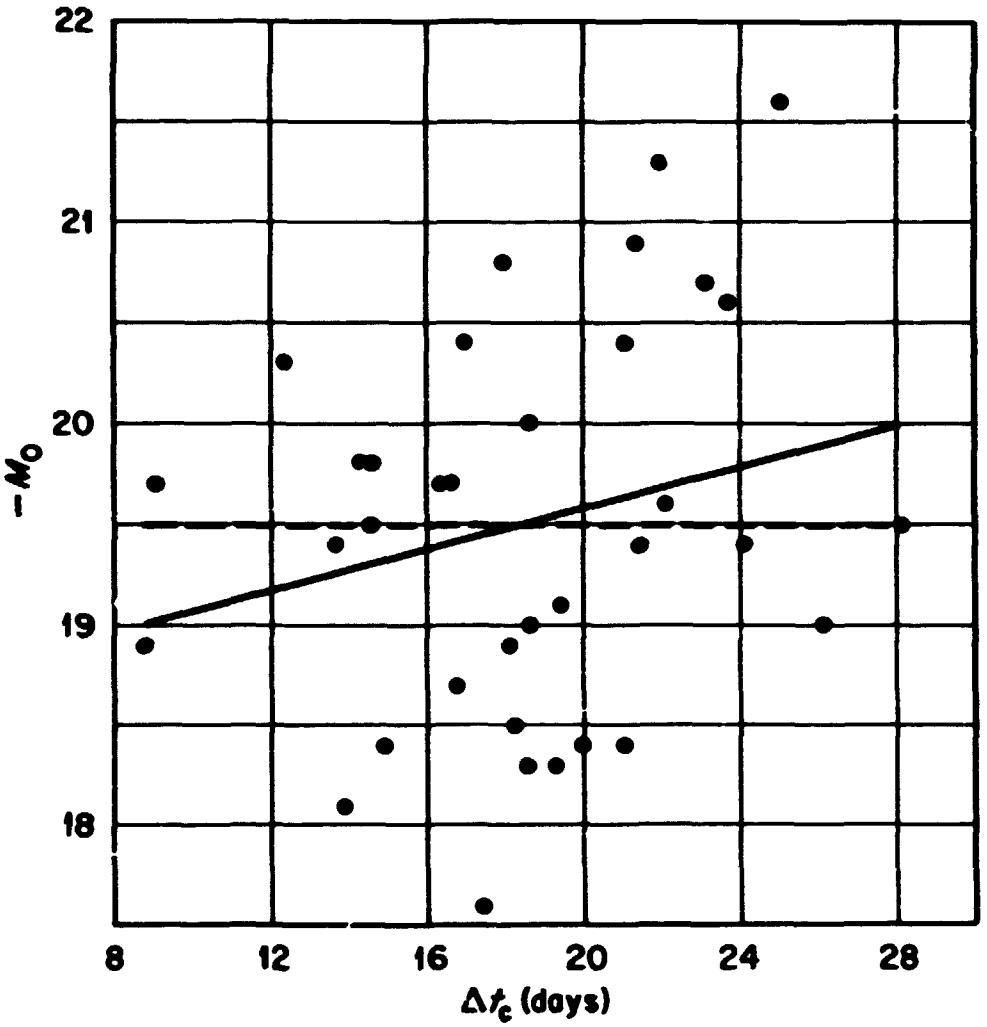

Figure 9-1. Regression of Absolute Magnitude M_o on the Comparison Parameter Δt_c.

apparently is a significant correlation between Δt_c and M_o, it is not responsible for the correlation between Δt_c and V_r.

The apparent existence of two bands in the $M_o - \Delta t_c$ relation (Figure 9-1) suggests that there might be two distinct populations of type I supernovae. The question of the reality of these two populations and their consequences in the study of supernova theory and extragalactic astronomy will be discussed in Chapters 11, 12, and 13; but first, Chapter 10 will again take up the main subject of this thesis, the $\Delta t_c - V_r$ relation.

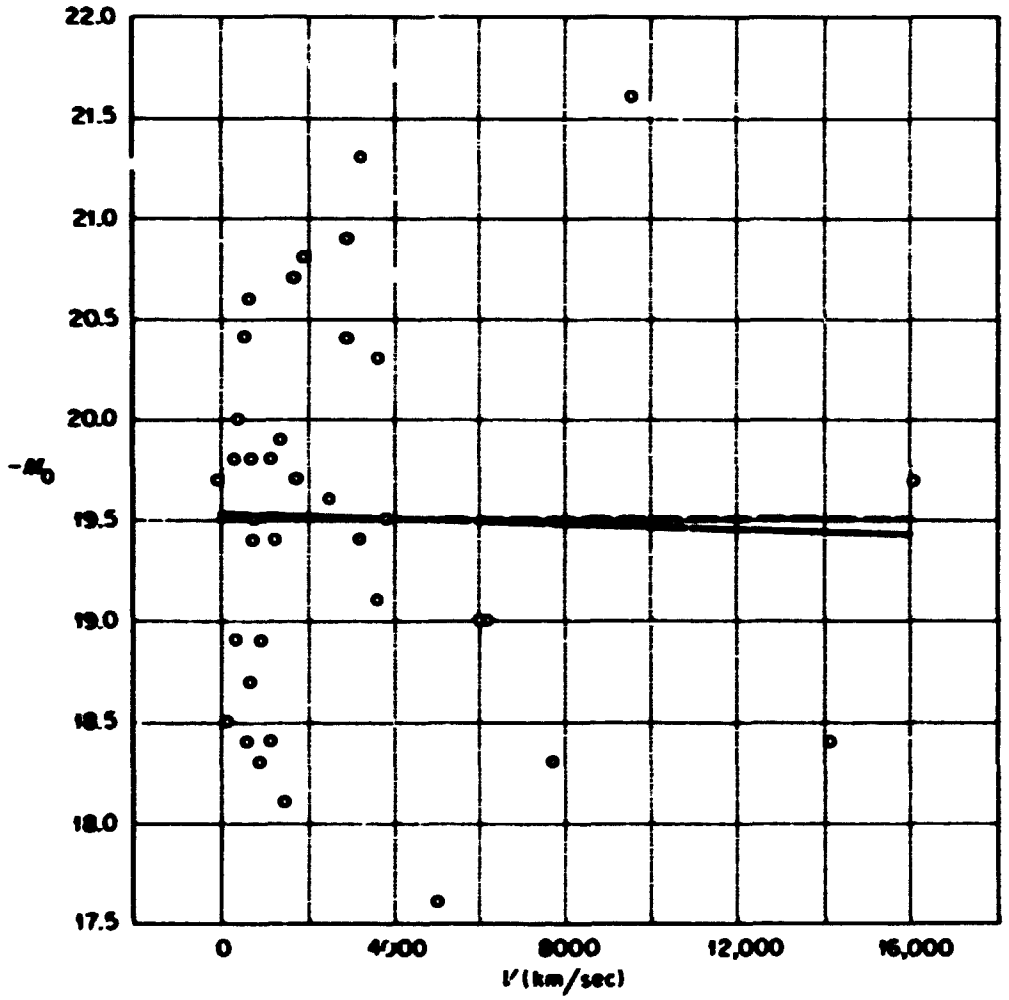

Figure 9-2. Regression of Absolute Magnitude M_o on the Symbolic Velocity of Recession.

CHAPTER 10

COMPARISON OF THE OBSERVED $\Delta t_c - V_r$ RELATION WITH THEORETICAL PREDICTIONS

In Chapter 8 a weak but marginally significant correlation was found between the comparison parameter Δt_c (number of days required for the brightness to decline from $m_o + 0^m.5$ to $m_o + 2^m.5$) and the symbolic velocity of recession V_r. It was also shown that the relation was not the result of data reduction or fitting errors. In Chapter 9 it was shown that the relation did not arise from an observational selection effect. The relation, which is shown in Figure 8-2, is poorly determined by the data, which have far too much scatter to discriminate reliably between a static Euclidean universe (slope = 0) and an expanding universe (slope = 5.55×10^{-5} days/km/sec), but the surprising result was that the slope of the regression line (slope = $3.21 \times 10^{-4} \pm 1.96 \times 10^{-4}$ days/km/sec) rejects both of them at a fairly high significance level - at the 93% level for the former and at the 91% level for the latter. Therefore, it is reasonable to ask whether there are other theories which give better agreement with the data even though the data are admittedly rather limited at the present. The important questions at this point are (1) how many theories are still consistent with the data, and (2) will it be possible, when light curves for supernovae in more distant galaxies become available, to distinguish between these alternatives?

The most commonly proposed alternatives to the expanding universe hypothesis are variants of the "tired light" theory. One of the earliest of these was the steady state theory, circa 1920, of W. D. MacMillan

BLANK PAGE

(152, 153, 154) who proposed that "radiant energy can and does disappear into the fine structure of space, and that sooner or later this energy reappears as the internal energy of an atom; the birth of an atom with its strange property of mass being a strictly astronomical affair." MacMillan suggested that the rate of energy loss is proportional to the distance traveled so that the radiant energy decreases exponentially with distance.

A similar proposal was made some 35 years later by Finlay-Freundlich (155), who suggested that the red shift is caused by a loss of energy in radiation fields (perhaps due to photon-photon interactions). He proposed the relation

$$\frac{\Delta\nu}{\nu} = -AT^4 l$$

where ν=frequency, $\Delta\nu/\nu$=redshift, T is the temperature of the radiation field, l is the path length through the field, and A is a proportionality constant. This relation is consistent with a linear Hubble law, and Freundlich combined the two in order to predict limits on the temperature of intergalactic space. His results, $1.9^{\circ}K \leq T \leq 6.0^{\circ}K$, are similar to the predictions that Gamow made at about the same time using the "big bang" theory. This prediction is almost universally overlooked by present-day cosmologists, who cite the later discovery of the cosmic microwave background as the observational confirmation of a unique prediction of the "big bang" theory.

More recent "tired light" proposals have been based on the notion that the gravitational forces have a finite range (156, 157, 158). The gravitational cut-off is achieved by introducing an exponential

attenuation into the equation for the gravitational potential. Similarly, it is assumed that the frequency of light ν observed at a distance r from the source is

$$\nu = \nu_0 \exp(-\alpha r)$$

where ν_0 is the frequency at the source and α is an attenuation constant. For small values of r, the exponential factor is well approximated by $(1 - \alpha r)$ and the relation for observed frequency can be written

$$\nu = \nu_0 (1 - \frac{H}{c} r),$$

where H is Hubble's constant and c is the velocity of light.

There are many other variants of the "tired light" hypothesis, but they all presume that the universe is static and many of them assume that it is Euclidean as well. The redshift arises not from a Doppler effect but rather from a physical interaction on the microscopic level between the light and the medium through which it passes. The distant galaxies are not receding and since in most cases space is Euclidean, there are no time dilation effects arising from the transport of signals through a curved space. Thus the prediction for the observed time lapse Δt of a macroscopic event seen at a distance is simply $\Delta t = \Delta t_0$ where Δt_0 is the time lapse that would be observed at the site of the event. This is the static Euclidean prediction which has slope = 0 in the Δt_c - Vr diagram and which was rejected at the 9σ level by the data.

Another class of theories that have been proposed as alternatives to the general relativistic expansion theories is composed of generalizations or extensions of Special Relativity. The most famous of these is Milne's Kinematic Relativity (159, 160). A very lucid exposition of Milne's theory of time has been given by Martin Johnson (161). Milne

proposed that there are two time scales in the universe. One, called t-time or kinematic time, is the time which applies on the atomic scale. The other, called τ-time or dynamic time, is the time which applies to events on the macroscopic level. The two time scales are related by the differential equation

$$\frac{dt}{t} = \frac{d\tau}{t_o}, \tag{10-1}$$

where t_o is the present age of the universe on the t-scale. Taking as boundary conditions $\tau = -\infty$ for $t = 0$ and $\tau = t = t_o$ at the present epoch, the differential equation is solved to give

$$\tau = t_o \log\left(\frac{t}{t_o}\right) + t_o. \tag{10-2}$$

Atoms emit and absorb radiation frequencies which are constant in t-measure. According to Milne the question of whether or not the red shift should be interpreted as a Doppler effect depends on whether the measurement of light from distant galaxies is governed by t-time or τ-time. More precisely, Milne showed that in t-time the number N of galaxies per unit volume decreases according to

$$N = \frac{Bt}{c^3\left(t^2 - \frac{d^2}{c^2}\right)^2},$$

where t is the epoch of observation, d is the distance, and B is a constant. Thus in the t-time scale the universe is expanding. On the other hand, he showed that in τ-time, $N \propto 1/c^3t_o^3$ which is independent of τ, so there is no expansion. There is a red shift since by Equation (10-1) the observed wavelength λ_{obs} is related to the emission wavelength λ_{em} by

$$\frac{\lambda_{em}}{t} = \frac{\lambda_{obs}}{t_o}, \text{ or } \frac{\lambda_{obs}}{\lambda_{em}} = \frac{t_o}{t}.$$

Because the t-time of observation, t_o, is later than the time t of emission, it follows that $\lambda_{obs} > \lambda_{em}$. Thus the important question for Milne's theory is not whether the universe is expanding or static--it is expanding in t-time and static in τ-time. The important question is "Which time scale are we using when we observe the distant galaxies?"

The event under consideration in this thesis is the decline in luminosity of a distant supernova. This is an event whose occurrence is presumably governed by the macroscopic τ-time scale. It follows quite readily from Equation (10-2) that for an event whose duration Δt is short compared to the present age of the universe, i.e., for an event such that $\Delta t << t_o$, the time lapse measured at the event is the same in either time scale, i.e., $\Delta t = \Delta\tau$. When the event occurs in a distant galaxy, there is a long time lapse between occurrence and observation so the two time-scales have time to diverge and give different observed time lapses. In the τ-system, the universe is static and the light travel time between the occurrence and observation of the beginning of the event is the same as the travel time between the occurrence and observation of the end of the event. This means that $\Delta\tau$ (observed) = $\Delta\tau$ (occurrence), which is the same as the prediction of the conventional static, Euclidean theory.

In the t-system, the universe is expanding so the light travel time between occurrence and observation increases between the beginning and end of the event. In this case it is easy to show that if the light travel time is much smaller than the present age of the universe, the observed time lapse is given by

$$\Delta t \text{ (observed)} = \left(1 + \frac{V_r}{c}\right)\Delta\tau \text{ (occurrence)}, \qquad (10\text{-}3)$$

where V_r is the radial velocity of the galaxy of occurrence. Since all of the supernovae in this study occurred in relatively nearby galaxies, i.e., in galaxies whose distances are small fractions of the maximum distances that have been observed, the light travel times involved are certainly much less than the age of the universe; so the above formula applies. The prediction is the same as that of the standard expanding universe hypothesis. Obviously, the present test cannot, even in principle, distinguish between Milne's theory and the standard theories; but if it could be shown by some other means that Milne's theory is valid, then the test could be used to determine which of the two time-scales we use in observing the distant galaxies.

A more recent variation of the special relativistic theories is that of Stanislaw Bellert (162, 163) who assumed that "the space of events is a static space, and the red shift is a consequence of the geometry of that space." Using two postulates which he called: (1) the postulate of equivalence of stationary frames of reference, and (2) the postulate of uniqueness concerning the measurement of electromagnetic wavelength, he argued that the red shift $\Delta\lambda/\lambda_0$ is related to the luminosity distance D by

$$\frac{\Delta\lambda}{\lambda_0} = \frac{kD}{1 - kD} \qquad (10\text{-}4)$$

where $k = H/c$, H being the Hubble constant and c being the velocity of light. He called the constant k the <u>coefficient of radial elongation</u> because objects seen from a distance have their apparent radial dimensions Δr lengthened according to

$$\Delta r = \frac{\Delta r'}{1 - kr_0},$$

where $\Delta r'$ is the length measured at the object and r_o is the distance from the observer to the object. The apparent transverse dimensions of the object are not changed by the distance, but time lapses are altered by

$$\Delta t = \frac{\Delta t'}{1 - kr_o}, \tag{10-5}$$

where $\Delta t'$ is the time lapse observed at the site of the occurrence and Δt is the apparent time lapse observed at distance r_o from the occurrence. Bellert identified the distance r_o with the luminosity distance D between the occurrence and the observation. Combining equations (10-4) and (10-5), then, gives

$$\Delta t = \left(1 + \frac{\Delta\lambda}{\lambda_o}\right)\Delta t',$$

or, taking $z = \Delta\lambda/\lambda_o$,

$$\Delta t = (1 + z)\Delta t'. \tag{10-6}$$

According to Bellert's theory the universe is static, but given an observed red shift z one can still define a symbolic recession velocity V_r by $V_r = cz$, and using this symbolic velocity, the prediction of Bellert's theory for the test of this thesis is

$$\Delta t_c = \left(1 + \frac{V_r}{c}\right)\left(\Delta t_c\right)_o, \tag{10-7}$$

which is the same as the prediction of the expanding universe theories.

All of the theories that have been discussed so far have made the same prediction as either the static Euclidean theory or the classical expansion theory. There is one recent theory, however, which gives a quite different prediction. That theory is the covariant chronogeometry of I. E. Segal (164, 165). Chronogeometry was initiated by A. A. Robb (166) who called it time-space geometry. The name chronogeometry was coined by A. D. Fokker (167) who regarded it as an alternate

approach to relativity theory. Segal replaced the Minkowski space-time M of special relativity with a particular chronogeometry $\tilde{M}$ which is locally identical to M but geometrically different from M in the large.

Segal's treatment of the theory is very abstruse. He describes $\tilde{M}$ as "... the chronogeometry of apparently maximal symmetry, among those which do not admit simultaneity." He contrasted $\tilde{M}$ to M as follows: "This model $\tilde{M}$ admits the fifteen-parameter conformal group (more exactly, a doubly-infinite-sheeted covering of this group) as its group of causality-preserving symmetries, while Minkowski space M admits only the eleven-parameter group of Lorentz and scale transformations. This necessitates a modified definition of time, as the parameter of a one-parameter group of temporal displacements distinct from (non-conjugate to) that employed in special relativity. The locally negligible disparity between relativistic time and this new time becomes significant at large distances."

An exposition of the development of Segal's theory is far outside the scope of this thesis, and the present author has found it almost impossible to assess the validity of the theory because of Segal's highly esoteric development. It was, however, fairly easy to determine the prediction of the theory for the $\Delta t_c - V_r$ relation, which is the main subject of this thesis. According to the theory, there is a unique, invariant time τ which in the local neighborhood of an event is closely approximated by special relativistic time t. Suppose that the event in question is the emission of a light ray occurring at time $\tau = t = 0$. According to the theory, the variation of the two time scales along the light ray is given by the equation

$$t = \tan \tau \qquad (10\text{-}8)$$

where τ is measured in "natural" units (units for which the velocity of light is unity) and varies between $-\frac{\pi}{2}$ and $+\frac{\pi}{2}$ as t varies between $-\infty$ and $+\infty$. At any later point of observation the two time scales are related by

$$\frac{\partial \tau}{\partial t} = \frac{1}{1+t^2}, \tag{10-9}$$

in terms of the local special relativistic coordinates at that point. Even though the universe is static, there is a red shift which arises because of the discrepancy between the two time scales. According to Segal, this red shift is given by

$$z = \tan^2\left(\frac{\tau}{2}\right). \tag{10-10}$$

For small values of t the approximate formula

$$z = \frac{t^2}{4} \tag{10-11}$$

is valid. Since the red shifts of all the supernovae in the present sample are relatively small ($z < .06$), this latter formula will be used.

Using Equations (10-9) and (10-11) it is quite easy to work out the prediction of the theory for the $\Delta t_c - V_r$ relation. Taking $\Delta\tau = (\Delta t_c)_o$ as the time lapse of occurrence and Δt_c as the observed time lapse, and using the relation

$$\Delta t = \frac{\partial t}{\partial \tau} \Delta\tau$$

from elementary calculus it follows that

$$\Delta t_c = \frac{1}{\partial\tau/\partial t} (\Delta t_c)_o.$$

Substituting equation (10-9) into this result gives

$$\Delta t_c = (1+t^2)(\Delta t_c)_o.$$

Now by Eq. (10-11), $t^2 = 4z$ so this last expression becomes

$$\Delta t_c = (1+4z)(\Delta t_c)_o. \tag{10-12}$$

Finally, defining a symbolic velocity V_r by $V_r = cz$ (even though the universe is static), the prediction becomes

$$\Delta t_c = \left(1 + 4\,\frac{V_r}{c}\right)(\Delta t_c)_o. \qquad (10\text{-}13)$$

It should be emphasized that this prediction is based on the present author's interpretation of Segal's theory and is not attributed to Segal himself who may have different ideas about the workings of the two time scales. (There may, for example, be problems of interpretation similar to those that arose in connection with Milne's theory.) In the remainder of this thesis, however, the term "Segal's chronogeometry" will be used as a shorthand notation for "Rust's interpretation of Segal's chronogeometry."

The above prediction is quite different from that of both the Static Euclidean theory and the classical expansion theory. It predicts a linear relationship between Δt_c and V_r with a slope four times greater than that of the straight line relation predicted by the expansion hypothesis. Using the estimate $(\Delta t_c)_o/c = 5.55 \times 10^{-5}$ days/km/sec obtained in Chapter 8 from the 21 supernovae with $V_r < 2000$ km/sec, the slope predicted by Segal's chronogeometry is 2.22×10^{-4} days/km/sec. This latter value is much closer to the slope of the regression line (slope = $3.21 \times 10^{-4} \pm 1.96 \times 10^{-4}$) than the former. A plot of the data together with the regression line and the three predictions are given in Figure 10-1. Each of the three prediction lines is the best fitting straight line having the slope predicted by the corresponding theory. All have slopes less than the least squares regression line. The prediction of Segal's chronogeometry gives the best agreement with the regression line. The t-statistic for testing whether the slope

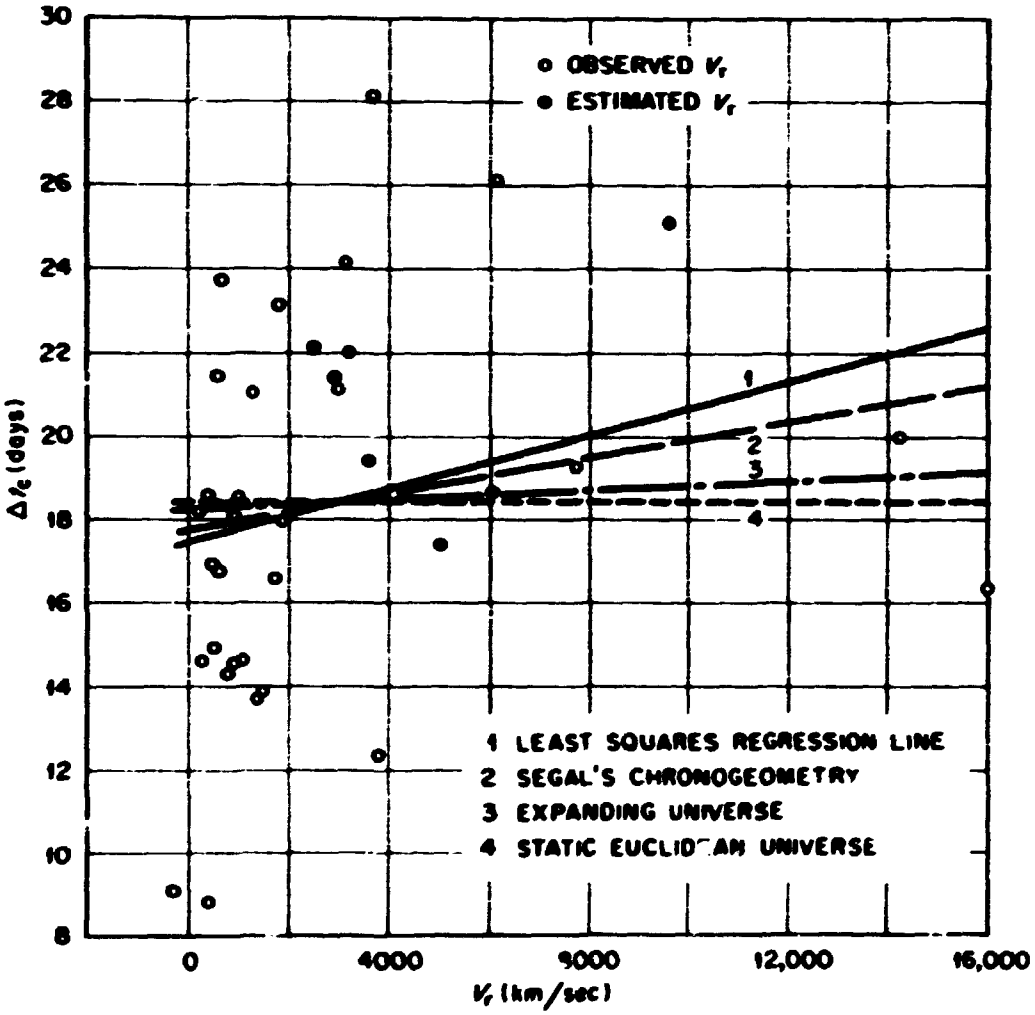

Figure 10-1. Comparison of the $\Delta t_c - V_r$ Regression Line with the Predictions of the Various Theories.

of the regression line is significantly greater than the slope of Segal's prediction has the value $t = 0.51$. With 34 degrees of freedom, this t-value rejects Segal's prediction at only the 69% level. Said another way, if Segal's theory were true, then one could expect to obtain a fitted slope as great or greater than the one actually obtained about 31% of the time (if 36 sample points were used each time). On this basis it is reasonable to say that Segal's theory is consistent with the observed data.

Although the predictions of the Expanding Universe and the Static Euclidean Universe were rejected by the t-test at the 93% and 91% significance levels, respectively, one cannot in all fairness say that they are inconsistent with the data in this sample. The scatter in the data is extremely large and the points are not scattered uniformly over the range in V_r. There are only 15 points in the sample with $V_r > 2000$ km/sec and 7 of these did not have measured V_r [cf. Fig. 10-1]. For those 7 points the symbolic velocities were obtained from estimates of the distance moduli and the Hubble relation using the value $H = 100$ km/sec/Mpc. Because they comprise such a large fraction of the points with $V_r > 2000$ km/sec, it is important to determine how sensitive the fitted slope is to the value of those estimates. This sensitivity was tested by recalculating the 7 V_r estimates using both $H = 75$ and $H = 125$ km/sec/Mpc and repeating the regression for each of these two sets of estimates. The results of these tests are summarized in Table 10-1. The first row contains the slope of the fitted regression line together with its standard deviation. All of these slopes are greater than those predicted by any of the theories. The second row contains the correlation

Table 10-1

Sensitivity Study of the Effect of the Value Adopted for H on the Regression of Δt_c on V_r

	H = 75	H = 100	H = 125
Slope of Regression Line	$(2.96 \pm 2.05) \times 10^{-4}$	$(3.21 \pm 1.96) \times 10^{-4}$	$(3.30 \pm 1.84) \times 10^{-4}$
Correlation Coefficient	0.24	0.27	0.29
Comparison* with Static Euclidean	t = 1.44 92%	t = 1.64 95%	t = 1.79 96%
Comparison** with Expanding Universe	t = 1.17 87%	t = 1.36 91%	t = 1.49 92%
Comparison*** with Segal's Chronogeometry	t = 0.36 64%	t = 0.51 69%	t = 0.59 72%

* The Static Euclidean Universe predicts slope = 0.
Tired Light theories and Milne's theory with observations in τ-time (macroscopic time scale) make the same prediction.

** The Expanding Universe predicts slope = 5.55×10^{-5}.
Milne's theory with observations in t-time (atomic time) and Bellert's theory make the same prediction.

*** Segal's Covariant Chronogeometry predicts slope = 2.2×10^{-4}.

coefficients. The degree of correlation clearly increases with increasing H, but even the minimum value ($\rho = 0.24$ for $H = 75$) is significant at the 92% level. Rows 3, 4, and 5 contain the comparisons with the theoretical predictions. In each case the value of the t-statistic for comparing the fitted slope to the predicted slope is given together with the corresponding significance level. The Static Euclidean model is rejected in all cases with significance levels exceeding 90%.

All of these tests indicate that reasonable changes in the value of H do not produce qualitatively different results in the comparison of the regression line and the predictions of the three theories; but both the slope of the regression line and the correlation coefficient are sensitive to the value adopted for H, both of them increasing with increasing values of H. Estimates of H are usually obtained from a regression of apparent magnitude m on $\log(V_r)$ for large samples of galaxies which hopefully have similar intrinsic luminosities. Supernovae can be used for this regression also, and, in fact, using supernovae avoids some of the difficulties which arise from using galaxies. This subject will be discussed more fully in Chapter 13 where a new method for determining the Hubble constant will also be given.

In Chapter 9 it was shown that the $M_o - \Delta t_c$ relation for the present sample of supernovae apparently consists of two distinct bands which are well separated [cf. Figure 9-1]. The presence of these bands suggests that there are two distinct populations of Type I supernovae. If that is true, then the effect of these two populations must be taken into account in making the $\Delta t_c - V_r$ test [Figure 10-1]. The next chapter will discuss the reality of the two populations and Chapter 12 will discuss a method for taking them into account in the $\Delta t_c - V_r$ relation.

CHAPTER 11

THE TWO LUMINOSITY GROUPS

Returning to the apparent existence of two separated bands in the $M_o - \Delta t_c$ relation, consider Figure 11-1, which illustrates the results of performing regressions separately for the two bands. The upper band, plotted as solid circles, is well separated from the lower band, which is plotted as open circles. The gap between the two is everywhere greater than or equal to $0^m.8$. The straight lines are the least squares regression lines: for the upper band,

$$M_o = (-18.08 \pm 0.35) - (0.122 \pm 0.020)\ \Delta t_c \qquad (11\text{-}1)$$

and for the lower band,

$$M_o = (-16.74 \pm 0.58) - (0.101 \pm 0.029)\ \Delta t_c \qquad (11\text{-}2)$$

In the following text, the upper band will be called the more luminous group and the lower band the less luminous group, though it is not yet established whether the separation into two groups is a true luminosity effect or the result of a systematic bias in the reductions and calculations of the estimates of M_o. Table 11-1 gives the membership of the two groups together with the corresponding values of Δt_c and M_o.

Table 11-2 gives some of the parameters which characterize the relations between M_o and Δt_c for the two groups, taken separately and together. Note that the difference between the mean M_o for the two groups is $1^m.43$, a value more than twice the standard deviation in both cases. The statistic for testing the consistency of two means, $\bar{x}_1$, $\bar{x}_2$, is

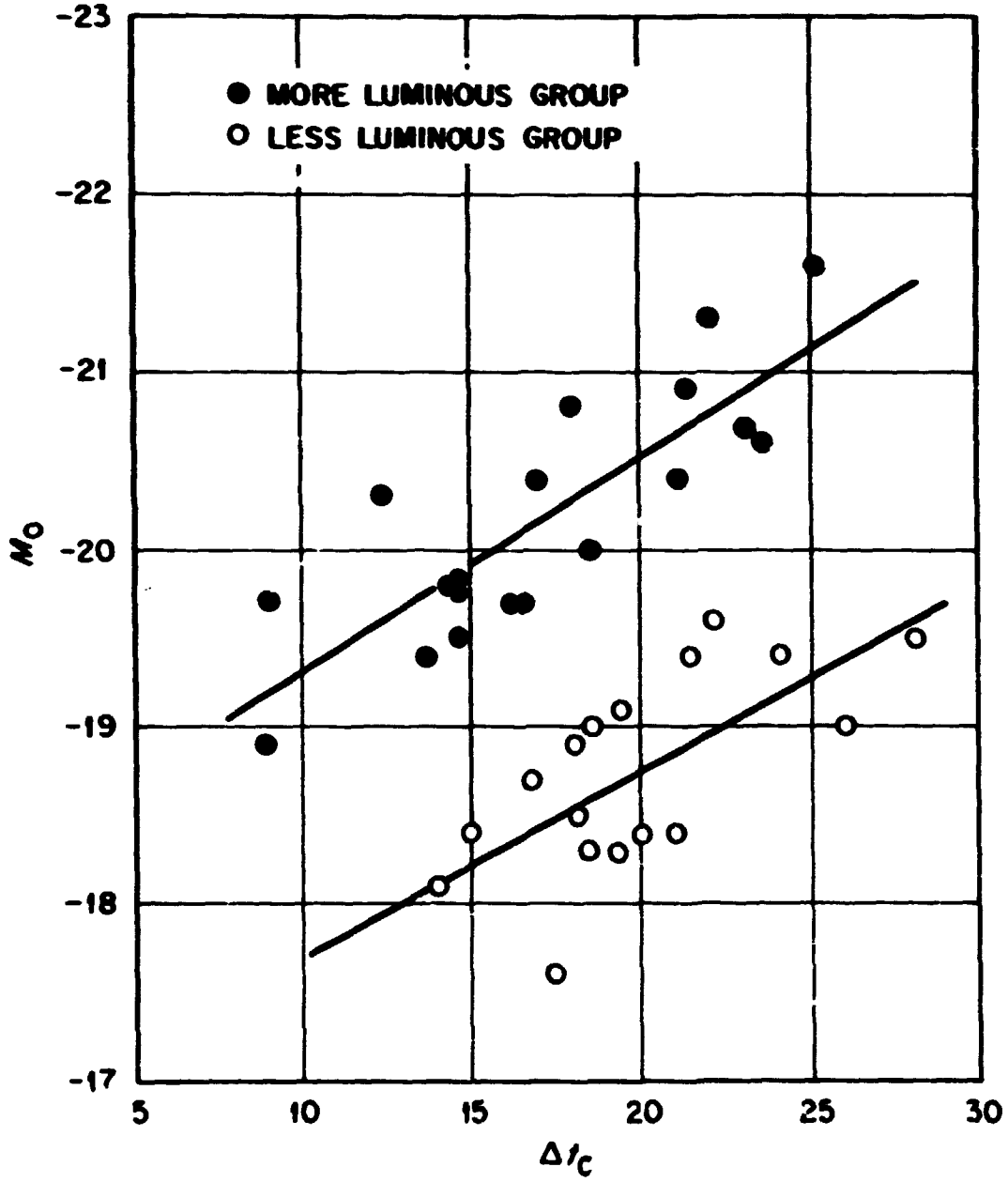

Figure 11-1. Regressions of Absolute Magnitude on the Comparison Parameter for the Two Luminosity Groups.

Table 11-1

The Two Groups of Supernovae

More Luminous Group				Less Luminous Group		
SN	Δt_c	M_0		SN	Δt_c	M_0
1885a	9.1	-19.7		1937d	21.4	-19.4
1921c	18.6	-20.0		1957a	16.8	-18.7
1937c	17.0	-20.4		1957b	18.5	-18.3
1939a	14.6	-19.5		1961d	19.3	-18.3
1939b	8.8	-18.9		1961p	28.1	-19.5
1954a	14.6	-19.8		1962a	26.1	-19.0
1954b	16.6	-19.7		1962e	19.9	-18.4
1955b	16.3	-19.7		1962j	22.1	-19.6
1956a	14.6	-19.8		1962p	19.4	-19.1
1959c	21.1	-20.4		1963d	18.6	-19.0
1960f	23.1	-20.7		1963i	18.2	-18.5
1960r	14.3	-19.8		1963p	13.9	-18.1
1962*l*	18.0	-20.8		1964*l*	18.1	-18.9
1963j	22.0	-21.3		1966k	17.4	-17.6
1964e	21.4	-20.9		1967c	21.0	-18.4
1965i	13.7	-19.4		1969c	24.1	-19.4
1966j	23.7	-20.6		1971i	14.9	-18.4
1966n	25.1	-21.6				
1968e	12.4	-20.3				

Table 11-2

Parameters of the Relations between M_0 and Δt_c for the Groups, Taken Separately and Together

	More Luminous Group	Less Luminous Group	Both Groups Taken Together
Number	19	17	36
$\bar{M}_0 \pm \sigma(M_0)$	$-20.17 \pm 0.^{m}69$	$-18.74 \pm 0.^{m}56$	$-19.51 \pm 0.^{m}94$
Intercept of Regression Line	$-18.08 \pm 0.^{m}35$	$-16.74 \pm 0.^{m}58$	$-18.55 \pm 0.^{m}68$
Slope of Regression Line	-0.122 ± 0.020	-0.101 ± 0.029	-0.0512 ± 0.0359
Correlation Coefficient ρ	0.832	0.670	0.237
t-Statistic for Testing ρ	6.188	3.499	1.425
Significance Level of Test	greater than 99.95%	99.7%	92%
$\overline{\Delta t}_c \pm \sigma(\Delta t_c)$	17.10 ± 4.70	19.87 ± 3.71	$18.4\text{?} \pm 4.33$

$$t_m = \frac{\bar{x}_1 - \bar{x}_2}{S} \sqrt{\frac{n_1 n_2}{n_1 + n_2}} \qquad (11\text{-}3)$$

where n_1, n_2 are the two sample sizes, and

$$S = \sqrt{\frac{(n_1 - 1)\sigma_1^2 + (n_2 - 1)\sigma_2^2}{n_1 + n_2 - 2}} \ , \qquad (11\text{-}4)$$

with σ_1, σ_2 being the two standard deviations. This statistic has a t-distribution with $(n_1 + n_2 - 2)$ degrees of freedom. For the present case $t_m = 6.8$ with 34 degrees of freedom, indicating that the difference between the two means is significant at a level exceeding 99.95%.

The slopes of the regression lines differ by only 0.021, a value comparable to the standard deviation of the slope in each case. The correlation coefficients are highly significant in both cases.

The difference between the average values of Δt_c for the two groups is 2.77 days. This difference might not seem significant when compared to the two standard deviations, ±4.70 days and ±3.71 days, but the two samples together contain 36 points, and the t-statistic for comparing the two means has the value $t_m = 1.95$. This value, with 34 degrees of freedom, gives a significance level of 97% for the difference.

The minimum width in the Δt_c direction of the gap between the two groups is about 5.5 days. Chapter 8 contained a thorough sensitivity analysis of the effects on the estimated Δt_c values of the various techniques used in the reduction and fitting of the light curves. That study did not reveal any systematic differences large enough to account for the gap between the two groups. Furthermore, there does

not seem to be any exclusive association of either group with one of the particular reduction techniques. If the gap does not represent a real effect, it must be the result of a bias in the estimates of M_o rather than in Δt_c.

The estimates of M_o were calculated by the formula

$$M_o = m_c - (m - M),$$

where the $(m - M)$ is the estimated distance modulus of the galaxy and m_o is the corrected peak apparent magnitude. A plot of M_o as a function of $(m - M)$ did not show any hint of a separation into two luminosity groups or of any correlation of M_o with $(m - M)$. Thus if the gap were caused by systematic biases in estimating the M_o, they most likely would have arisen in the estimation and/or the correction of the m_o.

The four different methods for estimating the original uncorrected m_o were tested for systematic differences. The details of these tests are given in Appendix 3. They revealed no strongly exclusive association of either luminosity group with any of the methods. Furthermore, the average values of the M_o for the various methods are very similar. Similar tests of the methods of correcting for absorption within the parent galaxies (described in Appendix 5) also showed no significantly exclusive association of either group with any of the methods of calculating or estimating the correction. The average total correction for the more luminous group was $A_{ML} = 1^m.13 \pm 0^m.01$ and for the less luminous group was $A_{LL} = 0^m.96 \pm 0^m.04$. The difference, $0^m.17$, is not statistically significant.

Another approach to the effect of the corrections on the final $M_o - \Delta t_c$ relation is to consider the relation that arises when the M_c are calculated using the uncorrected estimates of m_c. This plot is shown in Figure 11-2. The abscissa is the same as before, but the ordinate is based upon the original m_o without correction for absorption either in our own galaxy or in the parent galaxy. The two groups are plotted with the same symbols as before. Two parallel lines have been drawn which essentially separate the points into two groups. There is only one point in the gap between the two lines. The gap itself has a vertical separation of about $0^m.3$. All of the points above the gap belong to the more luminous group, and all of the members of the less luminous group lie below the gap together with four members of the more luminous group. Thus, aside from the five members of the more luminous group that lie in or below the gap, the uncorrected magnitudes themselves display a tendency to separate into two groups when plotted against Δt_c.

The separation into two groups in Figure 11-2 would probably have gone unnoticed had there not been some a priori means of identifying the points. It appears, then, that it is the correction for absorption that sharpens the separation into two groups. There are two possible opposing interpretations: (1) The separation into two groups is essentially already present in the uncorrected plot and the correction for absorption within the parent galaxy brings it to a sharper focus by reducing the random scatter due to the absorption error, or (2) the apparent separation into two groups in the uncorrected plot is a random fluctuation that is unfortunately emphasized by the small difference, $0^m.17$, in the average total correction for the two groups. The latter

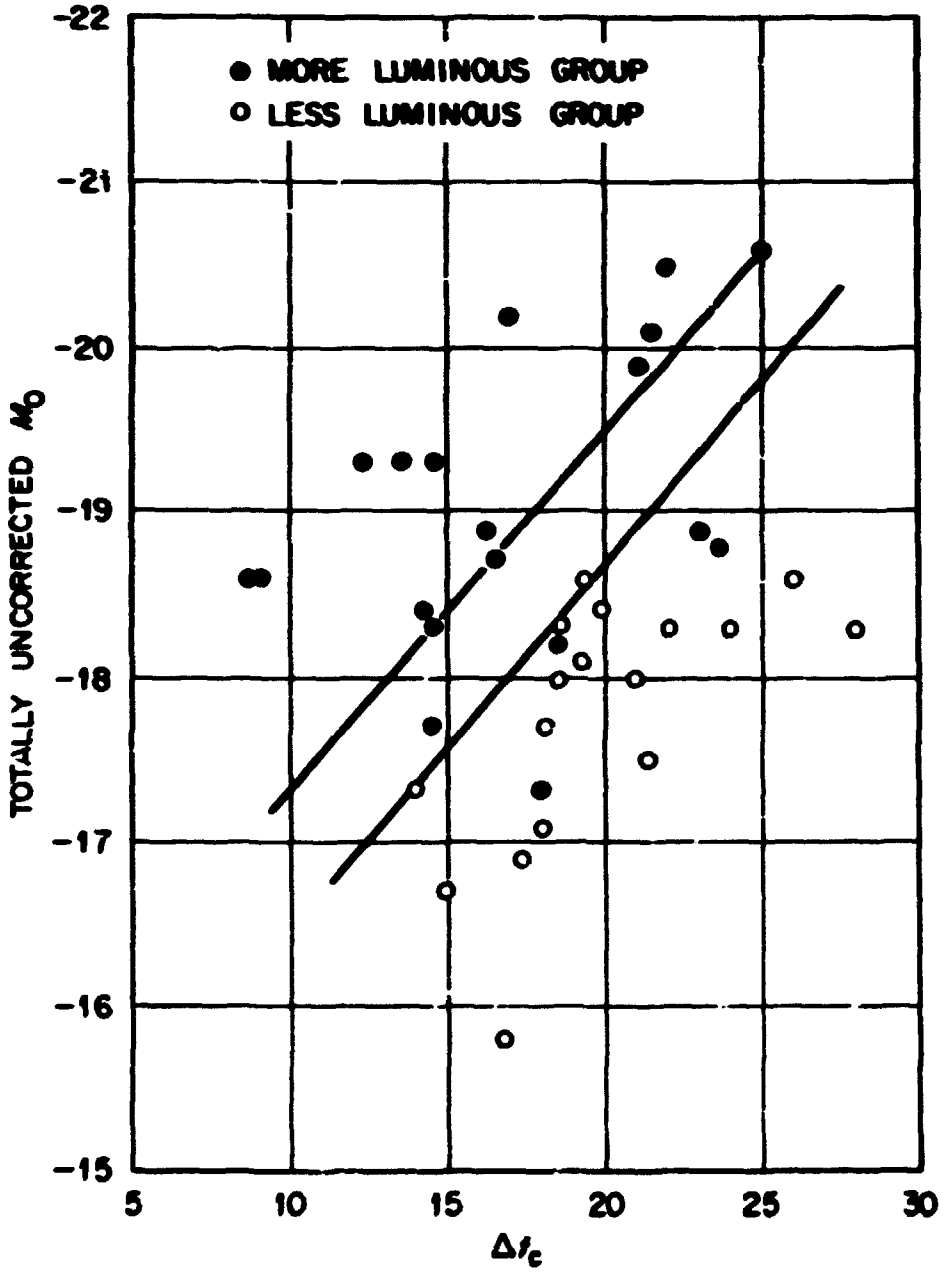

Figure II-2. Absolute Magnitude as a Function of Δt_c for Totally Uncorrected Magnitudes, with the Two Groups Distinguished.

view presupposes a chain of coincidences that taken altogether is highly improbable. Even if the gap in Figure 11-2 were assumed to be a random fluctuation, the correction process was designed to satisfy consistently other criteria which have nothing to do with the location of the points in that plot. As a further check on this line of reasoning, Figure 11-1 was plotted again using only supernovae with measured color excesses or which occurred in elliptical galaxies. Although there may be considerable errors in the absorption corrections for this subsample, the corrections are surely all consistent. The two bands were well defined in the plot with exactly half of the 22 points in each band. The remaining 14 supernovae were corrected by either $1^{m}.5$ or by $3^{m}.0$ depending on whether or not they occurred in a spiral arm. Since there was no strongly exclusive association of either of these corrections with one of the luminosity groups (cf. Appendix 5), it is almost certain that the addition of those supernovae to the sample did not introduce any systematic effects either.

It would appear then that the two bands and the correlation within each band were not caused by flaws or inconsistencies in applying the estimation and correction procedures. There remains the possibility that some of the assumptions in the procedures are incorrect. These assumptions concern the meaning of the Hubble relation, the value of the Hubble constant, and the various techniques used in constructing luminosity functions for galaxies. Even the measurements of the integrated apparent magnitudes of the parent galaxies were based on the assumption that the Hubble relation is truly linear, this assumption being needed in order to give the proper aperture adjustments so that the integrated magnitudes are consistent for galaxies at various distances. The

linearity of the relation for galaxies within 30 Mpc has recently been challenged by de Vaucouleurs (146), who found two different parabolic laws for the North and South Galactic Hemispheres. Although a plot of the positions of the supernovae (cf. Appendix 6) shows that both luminosity groups coexist in the same parts of the sky so that the separation into luminosity groups was not caused by some anisotropy in the Hubble law, the correlation within each group may have been affected by local non-linear perturbations in the law. The question of linearity of the Hubble law will be discussed in more detail in Chapters 13 and 14.

For the present, with regard to the question of the reality of the two luminosity groups, the arguments that have been given here indicate that the consistent reduction of the best available data using the currently accepted, conventional assumptions support the conclusion that the groups represent two distinct populations of Type I supernovae. If one accepts the admittedly speculative hypothesis that normal distributions have some fundamental significance in nature, then some further support for this conclusion is given by the distribution of the magnitudes for the two groups taken together and separately. These distributions are shown in Figure 11-3. In each case the distribution was plotted as a histogram of 5 boxes with the width of the boxes being approximately equal to the standard deviation of the magnitudes in that group. The distribution for the two groups taken together appears to be distinctly skewed from a normal distribution, but the two distributions taken separately appear to be reasonable approximations to normal distributions, considering the small sizes of the two samples. The distribution for the groups taken together becomes more sensible, then, when it is regarded as the sum of two normal distributions.

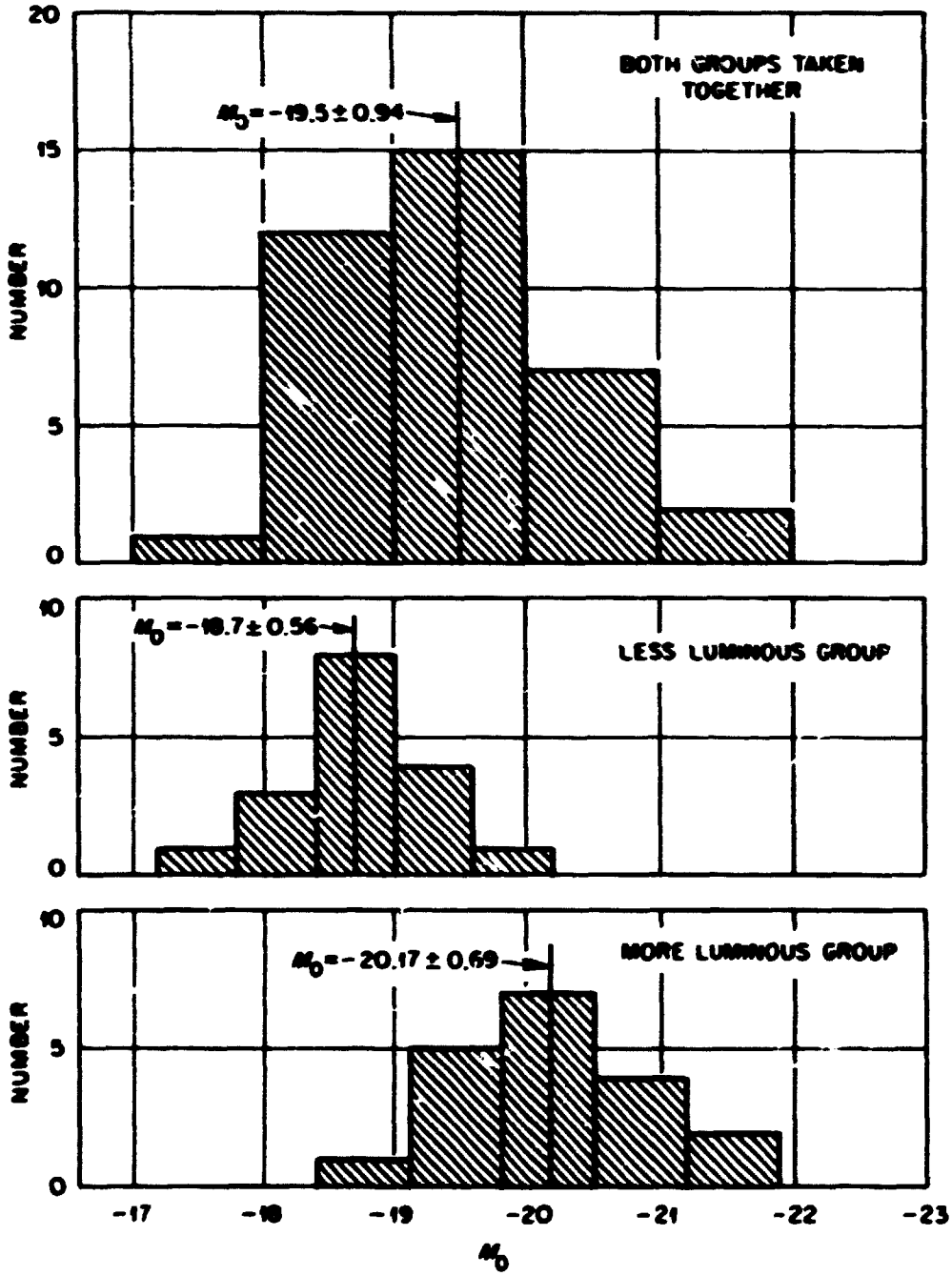

Figure 11-3. The Distribution of M_o for the Two Groups Taken Together and Separately.

The idea that there are two populations of Type I supernovae is actually not a new one. In [illegible] Baade and Zwicky (1938) suggested that there are two kinds of Type I supernovae associated with Population I and Population II stars, citing as evidence an analysis of the frequency of occurrence in different kinds of galaxies. Using a sample of [illegible] supernovae, they obtained a distribution having two frequency maxima corresponding to E and to S(B)c galaxies. The present sample, which probably has many supernovae in common with their sample, has a similar distribution. A comparison of the two distributions together with an analysis of the relative frequency of the two luminosity groups in different types of galaxies is given in Appendix 7. Both luminosity groups occur in elliptical galaxies, thus ruling out an identification of the two groups with Population I and II stars. There appears to be a slight trend for the more luminous group to occur more often in galaxies of later types (Sb, Sc, Irr) and for the less luminous group to predominate in earlier types (E, SO, Sa), but the numbers in the various types are too small to judge whether the trend is statistically significant. Such a tendency would explain the correlation of M_p with galaxy type first noticed by Pskovskii and confirmed by this study (cf. Appendix 4).

Another more recent attempt to identify two distinct subtypes of type I supernovae has been described by Barbon, Ciatti, and Rosino (1970) who collected the light curves of 26 supernovae and divided them into two groups which they characterized as being "fast" or "slow" supernovae. Their criterion for determining whether a given supernova was fast or slow was somewhat subjective, "fast" supernovae being

described as showing "peaked maxima with large amplitude," while "slow" supernovae have "broad and shallow maxima." They arrived at this distinction by intercomparing light curves, superimposing them and shifting them along both the time and the brightness axes in order to obtain agreement. In this way they obtained two "average" light curves which characterize the two groups. In other words, they tried to divide the light curves into two self-consistent groups which they characterized as being fast or slow according to the parameters of the final average light curves for the groups. Such a procedure is necessarily subjective if there is an underlying continuum of forms of the light curves. This arbitrariness was probably compounded by their comparison procedure, allowing unconstrained shifts of the light curves in both directions. Furthermore, they made no attempt to convert light curves measured in the B-system to the m_{pg}-system.

There is little correlation between the groups of Barbon et al. and those of the present study. Table II-3 compares the group memberships for the 21 supernovae common to the two studies.

Table II-3

Comparison of the "Fast" and "Slow" Groups of Barbon, Ciatti, and Rosino with the Luminosity Groups of the Present Study

Rust \ Barbon et al.	"Fast" Supernovae	"Slow" Supernovae
More Luminous Group	3	8
Less Luminous Group	5	5

Figure 11-4 shows the distribution in Δt_c of the 21 common supernovae with the "fast" and "slow" groups indicated by different shadings. The large overlap between the two groups indicates that the distinction between fast and slow is somewhat arbitrary. The average Δt_c for the two groups are significantly different, however. The average values, $\overline{\Delta t}_c$ = 17.14 days for the "fast" group and $\overline{\Delta t}_c$ = 19.95 days for the "slow" group, are very close to the averages for the two luminosity groups in the present study: $\overline{\Delta t}_c$ = 17.10 days for the more luminous group and $\overline{\Delta t}_c$ = 19.87 for the less luminous group. The difference between these latter two averages is significant at the 97% level. Barbon et al. also found little difference in the average M_0 for their groups, with $\overline{M_0}$ = -18.82 and $\overline{M_0}$ = -18.50 for the "fast" and "slow" groups, respectively. The present study gives different averages for the two luminosity groups, $\overline{M_0}$ = -20.17 and $\overline{M_0}$ = -18.74. On the basis of these considerations, the luminosity groups of this study are much more likely to represent a true division of Type I supernovae into distinct groups than are the "fast" and "slow" categories of Barbon et al.

If the luminosity groups are real, and if the correlations of M_0 with Δt_c are also real, then these relations will have far-reaching consequences both in the study of supernovae theory and in extra-galactic astronomy. Any successful supernova model will have to explain the existence of two groups having similar correlations between the peak luminosity and the rate of fall of the light curve, but different total energy releases. That the peak luminosity and the rate of fall in luminosity might be correlated is not at all surprising. A similar

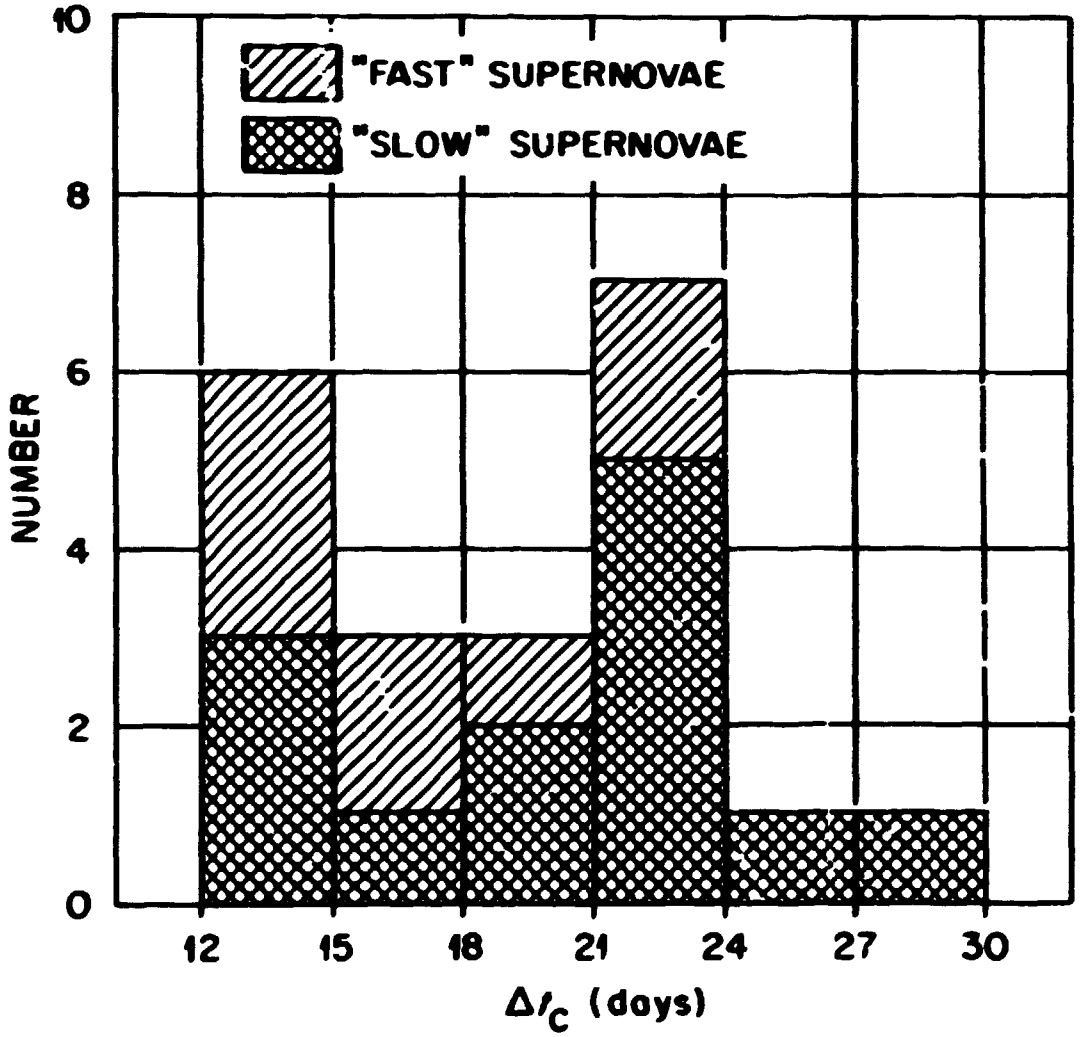

Figure 11-4. Distribution of the Δt_c for the 21 Supernovae Common to the Present Study and the Study of Barbon et al.

correlation has been found for ordinary novae (151), but in that case the relation between the peak luminosity and the logarithm of the rate of fall is linear and in the opposite sense, with the more luminous novae having the more rapidly falling light curves.

The relations between M_0 and Δt_c within the two bands are very much analagous to the period-luminosity relations for Cepheid variable stars. Thus they should provide a relatively precise distance indicator that can be extended to much larger distances than the currently available methods of similar precision. This new method of distance estimation will be discussed in Chapter 14.

CHAPTER 12

FURTHER REFINEMENTS AND FUTURE PROSPECTS FOR THE $\Delta t_c - V_r$ TEST

In Chapter 11 it was shown that the present sample of supernovae was drawn from two different parent populations. The two subsamples have different average absolute magnitudes $\bar{M}_o$ and different average values $\overline{\Delta t_c}$ of the comparison parameter. The power for discriminating among cosmological models of the $\Delta t_c - V_r$ test has undoubtedly been lessened by this mixing of populations. As more data become available, the test will surely be performed on the two groups separately. For the present there are not enough light curves available in either group to give a meaningful statistical test. Because of this fact, a more refined test was simulated by translating the less luminous group so that it was consistent with the more luminous group. This was possible because of the basic similarity of the $M_o - \Delta t_c$ relations for the two groups.

The slope of the $M_o - \Delta t_c$ regression line for the more luminous group was 0.122 ± 0.020, and the average point was $(\overline{\Delta t_c} = 17.09, \bar{M}_c = -20.17)$. The corresponding values for the less luminous group were slope $= 0.101 \pm 0.029$ and average point $= (\overline{\Delta t_c} = 19.87, \bar{M}_o = -18.74)$. Because the slopes were so similar, it seemed natural to rectify the less luminous group by subtracting 2.78 days from all of the Δt_c and subtracting $1^m.43$ from all of the M_o. The result of this adjustment is shown in Figure 12-1. The basic similarity of the two distributions is emphatically demonstrated by the overlap of the two groups. The line is the least-squares regression line

$$M_o = -(18.2 \pm 0.28) - (0.115 \pm 0.016)\ \Delta t_c$$

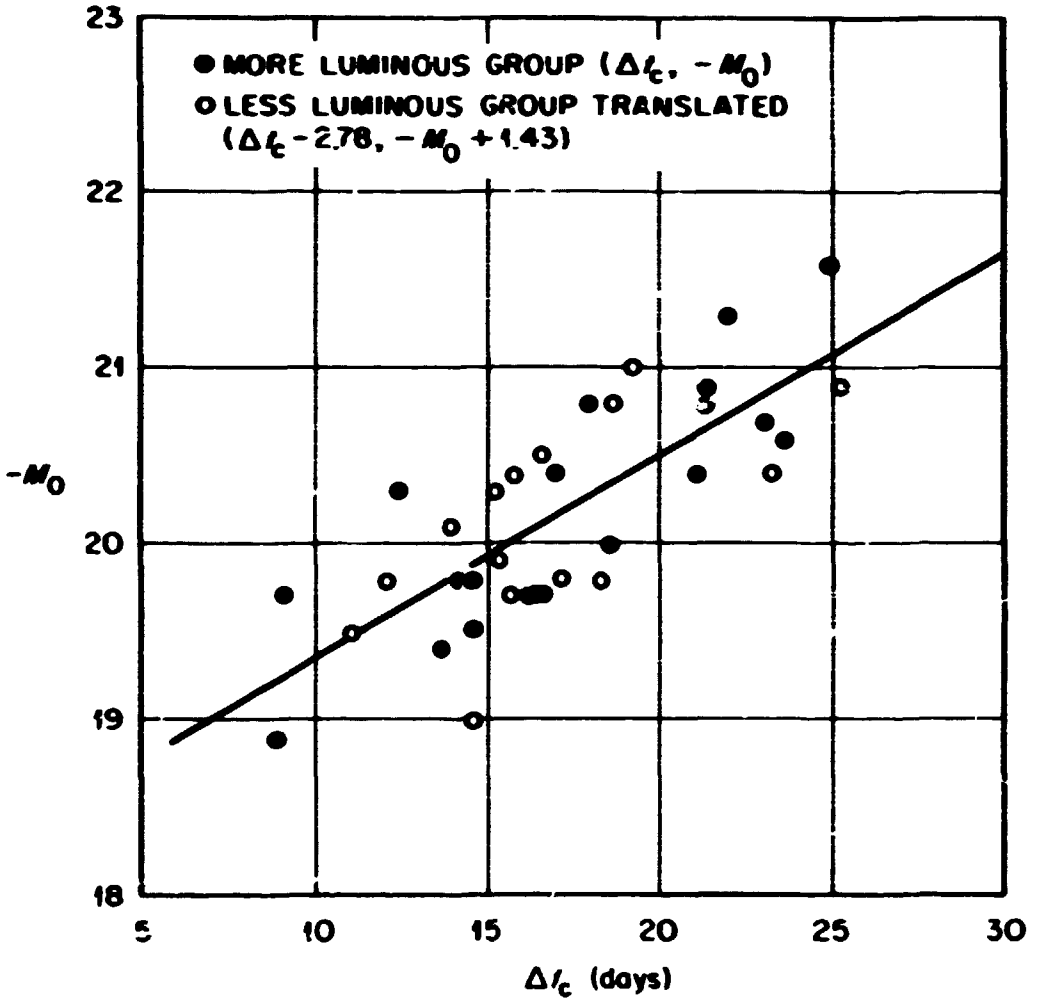

Figure 12-1. Reconciled M_o - Δt_c Relation.

The reconciled magnitudes were regressed on V_r in order to check for luminosity selection effects, and none were found. The reconciled sample was therefore judged to be appropriate for the $\Delta t_c - V_r$ test.

The $V_r - \Delta t_c$ relation for the reconciled sample is shown in Figure 12-2. The results are completely similar to those obtained with the unreconciled sample with Segal's chronogeometry giving much better agreement with the regression line than the other predictions. The values of the t-statistics for comparing the various predictions to the regression line are not very meaningful since this is only a simulation. The exercise suggests that the agreement between Segal's theory and the observed data in the original sample did not arise as an accidental side effect of using a sample from mixed parent populations. It further gives an idea of the kind of scatter to be expected in a refined sample from either of the populations alone. This in turn gives information on the kind of data that should be obtained in the future in order to strengthen the test.

The t-statistic for comparing a fitted slope b to a predicted slope B is

$$t_B = \frac{b - B}{\sigma(b)} = \frac{b - B}{\sigma\left[(\Delta t_c)_o\right]} \sqrt{\Sigma\left(V_{r_i} - \bar{V}_r\right)^2} \qquad (12\text{-}1)$$

where $\sigma\left[(\Delta t_c)_o\right]$ is the standard deviation of the intrinsic variation in Δt_c. For the reconciled sample, the 21 supernovae with $V_r < 2000$ km/sec have $\sigma\left[(\Delta t_c)_o\right] = 3.80$ days. This is probably a good estimate of the value that would be obtained from a refined sample drawn from only one of the parent populations. It will be used as such in the following to calculate the number of points needed to give 95%

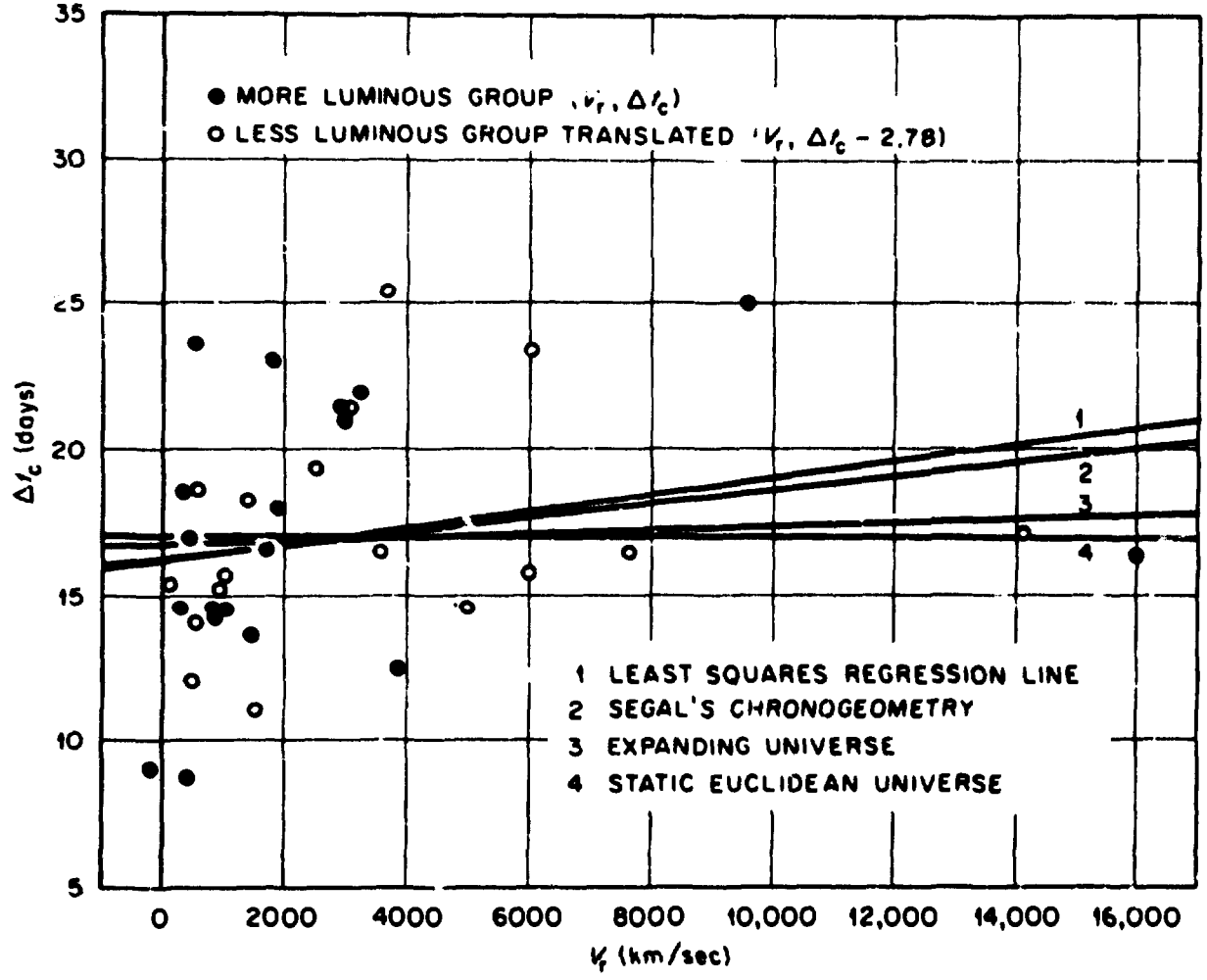

Figure 12-2. Reconciled Δt_c - V_r Relation.

tests between various pairs of theoretical predictions. Equation (12-1) can be used for these calculations by assuming that a given pair predicts slopes b and B. Once the values of b, B, and $\sigma[(\Delta t_c)_o]$ are fixed, the value the t-statistic, and hence the significance level of the test, can be varied only by choosing the sample to vary the quantity

$$S = \sqrt{\Sigma(V_{r_i} - \bar{V}_r)^2} \quad . \tag{12-2}$$

For the present sample, the range is $-299 < V_r < 16{,}000$ km/sec, but the sample points are heavily concentrated toward the lower end, a fact reflected by the average and standard deviation, $\bar{V}_r = 3009 \pm 3732$ km/sec. The value of S is $S = 2.21 \times 10^4$. This value can be used, together with the slopes of the various predictions, in Eq. (12-1) to calculate the power of a true refined sample with the same V_r distribution to discriminate between the various pairs of predictions.

The present reconciled sample had $\overline{(\Delta t_c)_o} = 15.56 \pm 3.80$ days. Using this average value to calculate the predicted slopes gives:

(1) slope $= \dfrac{\overline{(\Delta t_c)_o}}{c} = 5.2 \times 10^{-5}$, for the classical expansion hypothesis, and

(2) slope $= 4\,\dfrac{\overline{(\Delta t_c)_o}}{c} = 2.8 \times 10^{-4}$, for Segal's chronogeometry.

The prediction of the static Euclidean hypothesis is, of course, slope = 0. The t-statistics and corresponding significance levels for testing the various predictions against one another are given in Table 12-1. None of the tests is close to the traditional 95% value though the test of Segal's chronogeometry against the static Euclidean hypothesis is close to the less strict 90% level which is accepted as adequate by some statisticians.

TABLE 12-1

The Power of a Sample with the Same V_r-Distribution as the Present one to Discriminate Between Alternative Theoretical Predictions

Test	t-statistic	Significance Level
Expansion Hypothesis against Static Euclidean Hypothesis	.303	62%
Segal's Chronogeometry against Static Euclidean Hypothesis	1.21	88%
Segal's Chronogeometry against Expansion Hypothesis	0.905	81%

All of the regressions of Δt_c on V_r that have been performed in both this chapter and the previous ones gave fitted slopes greater than any of the predicted values. These larger slopes may have resulted from the deficiency of data at larger values of V_r, but the possibility is open that the true slope actually is greater. If the greater slope persists as more data become available, then the tests of that greater slope against the static Euclidean and the classical expansion hypotheses become more powerful than any of those shown in Table 12-1. More precisely, if the future data should continue to give slopes approximately the same as the results so far obtained (slope $\cong 3.0 \times 10^{-4}$ days/km/sec, say), then not too many more data points will be required to reject the static Euclidean and the classical expansion hypotheses at the 95% level since the tests are almost powerful enough to reject them already with the present sample. The test for discriminating against Segal's

chronogeometry would be quite difficult, however, unless the new data give a slope very much greater than that given by the present sample. All of this is only speculation, and for the present it is interesting to assume that one of the three predictions is correct and to determine how many more data will be required to discriminate between them.

There are three ways to increase the quantity S [Eq. (12-2)] and hence the significance level of a given test: (1) increase the number of points in the sample, (2) increase the dispersion of the sample points within a given range, and (3) increase the range of sample points. In the present sample the value of S would have been greater if so many of the points had not been clustered at the lower end of the range. If they had been scattered uniformly over the range, S would have been 2.77×10^4 rather than 2.21×10^4. Consider the general case of a sample containing N points spread uniformly over a range $0 \leq V_r \leq V_m$. The mean value of such a sample is $\bar{V}_r = V_m/2$. The value of S is given by

$$S \equiv S_u = \int_0^{V_m} \left(V - \frac{V_m}{2} \right)^2 \frac{N}{V_m} \, dV,$$

which gives

$$S_u = V_m \sqrt{\frac{N}{12}} \quad . \tag{12-3}$$

A uniform sample would give the most pleasing $V_r - \Delta t_c$ plot, but a more effective sample for increasing S would be one with half of the sample points clustered at each end of the fitting range. The mean of such an end-points sample would still be $\bar{V}_r = V_m/2$, but the value of S would be

$$S \equiv S_{EP} = \sqrt{\Sigma\left(\frac{V_m}{2}\right)^2} = \frac{V_m}{2}\sqrt{N} \quad . \qquad (12\text{-}4)$$

Combining Eqs. (12-3) and (12-4) it is easy to see that if N_u is the number of points with a uniform distribution in V_r required to give a certain value $S = S_u$, then the number N_{EP} of points in an end-points distribution which would be required to give the same value of S is only $N_{EP} = N_u/3$.

The range of the present reconciled sample extends to 16,000 km/sec. At this distance, the deviation between the best fitting straight line for the expansion hypothesis and the slope = 0 straight line for the static Euclidean hypothesis is only 0.83 days. The standard deviation of the intrinsic variation of Δt_c is 3.80 days, a value 4.6 times greater than the deviation between the two predictions. To extend the range of the observations to the point where the deviation between the predictions is equal to the intrinsic standard deviation would require observing out to V_r = 73,000 km/sec. Assuming H = 100 km/sec/Mpc gives

$$m - M = 5 \log\left(\frac{V_r}{H}\right) - 5 = 39.5$$

as the distance modulus corresponding to this velocity. The average absolute magnitudes of the two luminosity groups are $\bar{M}_o = -20.2$ and $\bar{\bar{M}}_o = -18.7$. The corresponding peak apparent magnitudes when the supernovae are at distance m - M = 39.5 are $\bar{m}_o = 19.1$ and $\bar{\bar{m}}_o = 20.6$. In order to obtain light curves for the kind of analysis done in this thesis, it is necessary to measure down to about $\bar{m}_o + 2\overset{m}{.}5$. Allowing 1.0 mag.

for extinction in our own and the parent galaxies means that the observing equipment must be able to reach the limits m = 22.6 for the more luminous group and m = 24.1 for the less luminous group. These limits are within the capabilities of present equipment at large observatories.

The V_r = 73,000 km/sec range is quite arbitrary and the tests can all be made with samples taken out to smaller limiting V_r, but the smaller the range, the greater is the sample size required to make any of the given tests definitive. Table 12-2 gives, for various limiting V_r the sample requirements for discriminating at the 95% level of significance between pairs of the three alternative hypotheses that have been discussed. The numbers of sample points required are given in each case for both a uniform sample and an end-points sample. These numbers (which should be regarded as approximate indicators rather than rigid specifications) were obtained by using Eqs. (12-1, 12-2, 12-3, 12-4) and a table of the t-distribution (172). The numbers enclosed in parentheses should be regarded as "formal" estimates since, in actual practice, more sample points would probably be required to eliminate the possibility of spurious small sample effects.

The numbers in the table indicate that if Segal's chronogeometry is truly the correct hypothesis, then the present sample can be easily extended to verify this even without going to a fainter limiting V_r. At V_{max} = 16,000 km/sec only 16 points in an end-point sample would be required to eliminate the static Euclidean hypothesis. Of these, the 8 points at lower end of the range are already in the sample (in fact, there are 21 supernovae with V_r < 2000 km/sec), and two of the points at the higher end (SN1959b and SN1962e) have already been

TABLE 12-2

Sample Requirements for Discriminating at the 95% Level of Significance Between Pairs of Alternate Predictions for the Slope of the $V_r - \Delta t_c$ Relation

Upper Limit of Sample Range, V_{max} =			16,000	25,000	36,500	73,000
Limiting Magnitude Required	More Luminous Group		19.3	20.3	21.1	22.6
	Less Luminous Group		20.8	21.8	22.6	24.1
Number of Sample Points Required to Reliably Discriminate Between Alternative Hypotheses	Classical Expansion Hypothesis vs. Static Euclidean Hypothesis	Uniform Sample	680	280	130	35
		End-points Sample	228	94	44	12
	Segal's Chrono-geometry vs. Static Euclidean Hypothesis	Uniform Sample	45	20	12	(5)
		End-points Sample	16	8	(4)	(2)
	Segal's Chrono-geometry vs. Classical Expansion Hypothesis	Uniform Sample	75	35	17	(7)
		End-points Sample	26	12	(6)	(3)

obtained. So the sample needs only six more light curves for supernovae with $V_r \sim 16{,}000$ km/sec. The limiting magnitudes required to obtain these light curves are attainable with telescopes of intermediate size equipped with image tube devices. According to Drake Deming (173) the 40 inch telescope at Prairie Observatory could be used to obtain the basic light curve measurements, although, if photographic techniques were used, the photoelectric comparison sequence would have to be obtained using a larger instrument. The radial velocities would also have to be measured with a larger instrument.

The test of Segal's chronogeometry against the classical expansion hypothesis would be slightly more difficult since 11 more light curves at the upper end of the range would be required. Both of the tests become much easier with instruments which can measure light curves out to $V_r = 25{,}000$ km/sec, and in fact there is little need to go further out to verify or disprove Segal's theory.

If the additional data produces fitted slopes more in agreement with the classical expansion hypothesis or the static Euclidean hypothesis, it is absolutely essential to sample out to a greater limiting V_r in order to discriminate between the two. Even with $V_{max} = 36{,}500$ km/sec, an end-points sample would require 22 light curves at the upper end of the range. But at $V_{max} = 73{,}000$ km/sec only 6 new light curves would be required and this is well within the capabilities of a large telescope. Not all of the observations would require the large telescope since the peak apparent magnitude is $2^m.5$ brighter than the faintest that must be reached. Any effort of this sort would require the close cooperation of the various systematic supernova search projects.

The Palomar supernova search in 1972 (174) discovered 13 new supernovae, seven of which were in anonymous galaxies with $m_{pg} \geq 16.5$. These seven would certainly have been good candidates for the tests involving Segal's chronogeometry. It would probably be necessary to search to even fainter magnitudes than is currently done in order to reach the V_{max} needed for testing the expansion hypothesis against the static Euclidean hypothesis, although two of the supernovae that were discovered occurred in galaxies of magnitude 18.5.

The peak magnitudes obtained in the process of gathering further light curves for the $V_r - \Delta t_c$ relation will also be very useful for determining the correct slope of the $\log (V_r) - m_o$ relation. This relation, which is one of the most important observational relations in cosmology, is the subject of the next chapter.

CHAPTER 13

THE RED SHIFT-MAGNITUDE RELATION AND A NEW METHOD FOR DETERMINING THE HUBBLE CONSTANT

The most fundamental relation in modern cosmology has been the velocity-distance formula. Although some of the earlier workers believed that the relation is a quadratic [cf. Lundmark (169)], it has been almost universally accepted since the time of Hubble's fundamental work in the 1930's that the relation is locally linear, having the form

$$V_r = Hr \qquad (13\text{-}1)$$

where H is the Hubble constant. A great deal of work in the last decade has been devoted to seeking the departures from linearity which are predicted for very large redshifts by the conventional Friedmann expansion models, but almost no one has questioned the linearity for red shifts z less than about 0.3.

Estimates of H are usually obtained from a regression of $\log(V_r)$ on apparent magnitude m for large samples of galaxies which hopefully have similar intrinsic luminosities. Following the development of T. A. Agekyan (168), let m be the measured apparent magnitude, Δm be any correction needed in that measured value, M be the absolute magnitude and r be the distance to the galaxy measured in parsecs. Then,

$$(m - \Delta m) - M = 5 \log r - 5. \qquad (13\text{-}2)$$

According to the Hubble law, this expression can be written

$$(m - \Delta m) = 5 \log (V_r) - 5 - 5 \log (H) + M.$$

Taking a whole collection of galaxies with average absolute magnitude $\bar{M}$, one can write for each of them

$$(m_i - \Delta m_i) = 5 \log (V_{r_i}) + (\bar{M} - 5 - 5 \log H) + (M_i - \bar{M}). \qquad (13\text{-}3)$$

These expressions are the equations of condition for a regression of $(m_i - \Delta m_i)$ on $\log(V_r)$. The result of such a regression is a straight line

$$(m - \Delta m) = A \cdot \log(V_r) + B, \qquad (13\text{-}4)$$

where A and B are the parameters of the fit. The $M_i - \bar{M}$ behave like random errors, averaging out to zero, so one can estimate H from the expression

$$B = \bar{M} - 5 - 5 \log H, \qquad (13\text{-}5)$$

if one knows the value of $\bar{M}$.

Note that the value of A should turn out to be very nearly 5 or else the linear Hubble law is not valid. It has been a common practice in recent years to assume the validity of the Hubble law and hold the constant A fixed while performing the fit. When galaxy magnitudes are used for $(m_i - \Delta m_i)$, such a procedure <u>does not</u> provide an independent test of the linear Hubble law no matter how well the resulting line fits the data and no matter how small the scatter in the data. This point has been demonstrated by Segal (165), who pointed out that the measurement of the galaxy magnitudes m_i requires an assumption of a cosmological model in order to determine the aperture corrections needed to give consistent magnitudes of galaxies at varying distances.

The basic problem is that galaxies have finite angular extent and diffuse boundaries. If the same aperture is used for both distant and nearby galaxies, the magnitudes of the distant galaxies will be

systematically too bright because a greater portion of the luminous disks will be included. The form of the correction unfortunately depends on the geometry of space-time, i.e., on the assumption of a cosmological model. Segal showed that this problem cannot be avoided even by confining the sample by observing only very narrow central portions of galaxies with small red shifts (say $z < 0.1$). In particular, he proved that such low z observations cannot distinguish between the Hubble Law, $z \propto r$, and the quadratic, "Lundmark Law," $z \propto r^2$, [cf. (169)]. He did this by showing that if either one of the two laws is actually valid and if the observations are made twice, once with the aperture correction designed for the Hubble law and once for the Lundmark Law, then both sets of observations will agree with the corresponding law no matter which of the two is actually valid. Thus, galaxy observations cannot provide a model-independent test of the linearity of the relation. The recent monumental work of Sandage and his collaborators proves that if the observations and reductions are made in accordance with the Friedmann models, then the results are consistent with a linear Hubble law. It is still possible that if the same observations are made and reduced in accordance with some other theory, the result might be a completely different velocity-distance relation, e.g., a quadratic law.

Segal's Covariant Chronogeometry predicts a quadratic law for small redshifts. In (165) he showed that if the observations are made in a frequency range where the spectral function of the source is of the form $f(\nu) \propto 1/\nu^{\alpha}$, where α is called the spectral index, then apparent magnitude m is related to red shift z by

$$m = 2.5 \log z - 2.5(2 - \alpha)\log(1 + z) + C$$

where C is a constant whose value depends on the absolute magnitude M. For all reasonable values of α and for small values of z, this expression reduces to

$$m \cong 2.5 \log z + \text{const.}, \quad 0 < z < 0.1. \tag{13-6}$$

To see that this expression actually corresponds to a quadratic velocity distance law, it is easiest to substitute such a law into Eq. (13-2). Taking $z = k^2 r^2$ where k^2 is a constant gives $r = z^{\frac{1}{2}}/k$ which, when substituted into Eq. (13-2) gives

$$(m - \Delta m) - M = 5 \log (z^{\frac{1}{2}}/k) - 5,$$

or

$$m = 5 \log (z^{\frac{1}{2}}) + [M + \Delta m - 5 \log k - 5],$$

which can be written

$$m = 2.5 \log z + \text{const.}$$

To support his claim that the local red shift-distance relation is quadratic, Segal cites a 1962 paper by G. S. Hawkins (170) and a 1972 paper by de Vaucouleurs (146). Hawkins used the galaxies in the classic study of Humason, Mayall and Sandage (118) to obtain the regression line

$$m = 2.26 \log z + 4.63,$$

which gives a red shift-distance law of the form $z \propto r^{2.22}$, and interpreted the result as evidence for a quadratic law though he admitted that, "A linear law can only be obtained from these data by postulating that systematic biases, such as selection effects, exist; and by weighting the observations in some way so as to remove the suspected bias." De Vaucouleurs calculated the distance moduli of a sample of nearby groups of galaxies ($r < 30$ Mpc) using several methods and extensive

cross-checking to obtain consistency. When he plotted red shifts against his final distance estimates he obtained an apparent quadratic variation which he attributed to a local anistropy in the expansion law (presumably caused by the "local supercluster").

Both of the above studies involved galaxies and hence are subject to the same criticisms that Segal invoked in his arguments about the aperture effects. One way to avoid some of these difficulties is to use supernovae for the analysis. Supernovae are point sources, so there is no need to worry about aperture corrections. Thus they are ideal candidates for determining the redshift-magnitude relation.

The redshift-magnitude relation for supernovae has previously been studied by Kowal (49), who followed the usual practice of holding the slope A fixed at the value 5.0. The 29 supernovae in this study with measured red shifts were subjected to the $m - \log(V_r)$ analysis, but both parameters were allowed to vary in the regression. The peak apparent magnitudes m_o of the supernovae were used as the m_i. The symbolic velocities were corrected for the solar motion relative to the local group. In working with galaxies the corrections Δm_i consist of: (1) the aperture effect, (2) the light travel time effect, (3) the K-correction for the effect of the red shift on the spectrum of the galaxy, and (4) the correction for absorption [cf. Humanson, Mayall, and Sandage (118)]. The first correction is unnecessary for supernovae. The second correction is only required for $z \geq 1.0$ and hence does not apply for this study. A great deal of work has been done on deriving K-corrections for galaxies, but the spectrum of a supernova is very different from the spectrum of a galaxy; so the same K-corrections cannot be used. The red shifts in the present sample are all relatively small ($V_r < 16{,}000$ km/sec), and

the pass band for the m_{pg} system is fairly broad; so the K-corrections were assumed to be negligible. In the case of galaxies, the fourth correction is accomplished easily using the cosecant law, but for supernovae the absorption correction is more difficult because of absorption within the parent galaxies. This problem was discussed in detail in Chapter 9. The corrections that were calculated there were used to correct the magnitudes for the $m_o - \log(V_r)$ analysis.

Taking the corrected peak apparent magnitudes for $m_i + \Delta m_i$ in Equation (13-3) gives

$$m_{o_i} = 5 \log (V_{r_i}) + (\bar{M} - 5 - 5 \log H) + (M_i - \bar{M}), \qquad (13\text{-}7)$$

and Equation (13-4) becomes

$$m_o = A \log (V_r) + B. \qquad (13\text{-}8)$$

The results of the regression of m_o on $\log(V_r)$ are shown in Figure 13-1, which follows the standard convention of plotting $\log(V_r)$ on the y-axis and m_o on the x-axis even though $\log(V_r)$ was taken as the independent variable in the regression. The two different luminosity groups [cf. Chapter 11] are indicated by different symbols. The supernova SN1961h was also included in the regression even though its light curve was not complete enough to give an accurate value of Δt_c so that it could be classified into one of the luminosity groups. The two supernovae SN1939b and SN1963i (indicated by arrows) were judged to be outliers and were not included in the regression. Their symbolic recession velocities were 345 and 140 km/sec, values of the same order of magnitude as the random peculiar velocities of galaxies; so it is not surprising that they deviate so far from the fitted curve.

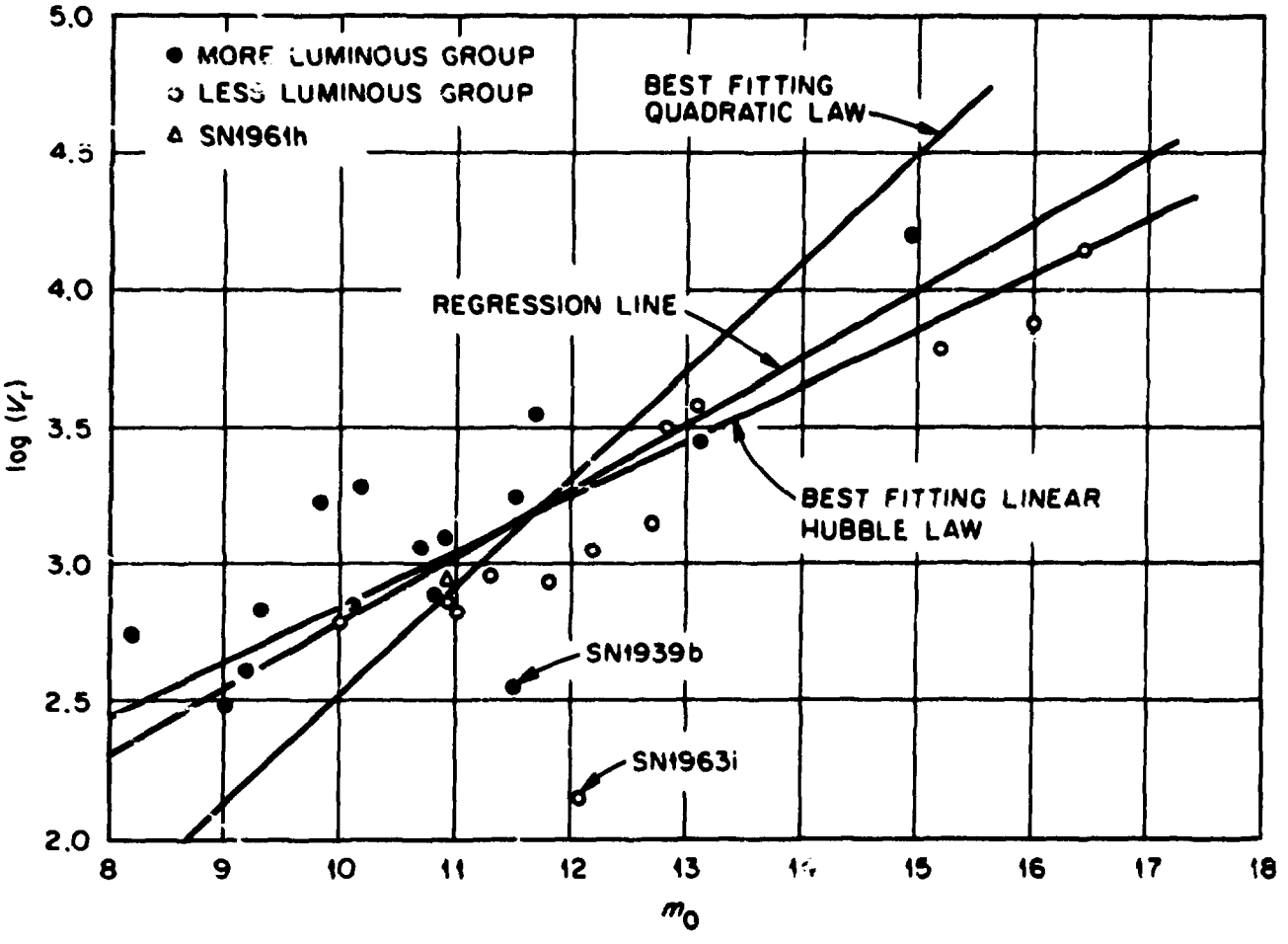

Figure 13-1. The Regression of m_o on log (V_r) Compared with the Best-Fitting Linear and Quadratic Laws.

Figure 13-1 also shows the best fitting lines for a linear Hubble law (slope = 5.0) and a quadratic Lundmark law (slope = 2.5). The quadratic law clearly fails to fit the data, but the agreement between the best fitting linear law and the regression is not as good statistically as the figure might lead one to believe, although it is obvious that the linear law gives a much better fit to the data than does the quadratic one. The slope of the regression is $A = 4.16 \pm 0.44$, a result which is comparable to some of the slopes obtained for galaxies by Humason, Mayall and Sandage (118). [They obtained, for example, a slope $A = 4.33 \pm 0.38$ using a sample of 90 Sc and SBc galaxies with $2.2 < \log(V_r) < 4.0$.] The correlation coefficient for the regression is 0.884, and the t-statistic for testing it is 9.476, giving significance at a level greater than 99.95%. The t-statistic for testing the slope against slope = 5.0 is $t = -1.904$, a value which rejects the linear Hubble law at about the 96.4% level. More precisely, if the Hubble law were truly valid, then the probability of obtaining a slope as low as $A = 4.164$ by chance is only 3.6%. The quadratic law is rejected at an even greater level of significance (greater than 99.95%).

At this point one should not attach too much significance to the apparent statistical rejection of the linear Hubble law. The sample does not extend to very large red shifts. For the smaller values of $\log(V_r)$, the random motions of the galaxies are comparable to the systematic distance effects. Because of the weighting introduced by taking logarithms of the V_r, variations introduced by these random motions will be unsymmetrical and predominantly downward in the diagram. Another possible source error is the absorption corrections. These should not

cause systematic effects in a large sample, but in a small sample there is a slight probability that 2 or 3 very inaccurate corrections in the same direction at one end of the diagram could introduce a bias.

Another intrinsic source of error in the present sample is the large scatter in absolute magnitudes which was introduced by combining the two distinct luminosity groups. It is apparent from Figure 13-1 that the two groups do have distinct luminosity characteristics, for even though they are not widely separated in the diagram, the points for the more luminous group lie systematically to the left of those for the less luminous group. In Chapter 11 the means and standard deviations for the absolute magnitudes of the two groups were estimated as $\bar{M}_o = -20.17 \pm 0.^m69$ and $\bar{M}_o = -18.74 \pm 0.^m56$. Taken separately, each group gives a much better approximation to the ideal single-luminosity class. The $\log(V_r) - m_o$ analysis was therefore performed on the two groups separately even though the number of sample points in each case was small. The results of all of the regressions are compared in Table 13-1. The correlation coefficient was improved in both cases by taking the groups separately, but both of them rejected the linear Hubble model at a high level of statistical significance. The analysis was also performed on the reconciled sample discussed in the preceding chapter. The results, which are illustrated in Figure 13-2, are very similar to those given in Table 13-1, with both the linear and quadratic laws being rejected at high levels of significance.

Although the present data seem to indicate that the true velocity-distance relation lies somewhere between a linear and a quadratic law, it is important to keep in mind that the present sample is dominated

Table 13-1

Results of the $m_v - \log(V_e)$ Regressions

	The Two Groups Taken Together	More Luminous Group	Less Luminous Group
n	27	14	12
A = slope of regression line	4.164 ± 0.459	3.558 ± 0.499	4.265 ± 0.565
B = intercept	-1.606 ± 1.413	-0.428 ± 1.568	-1.259 ± 1.215
ρ = correlation coefficient	0.884	0.900	0.965
t-statistic for testing ρ	9.476	7.147	11.687
significance level	greater than 99.95%	greater than 99.95%	greater than 99.99%
B for best fitting line with slope = 5	-4.270	-4.882	-3.680
Comparison of Regression line to best fitting line with slope = 5	t = -1.904 rejected at the 96.4% level	t = -2.868 rejected at the 99.2% level	t = -2.015 rejected at the 96.3% level

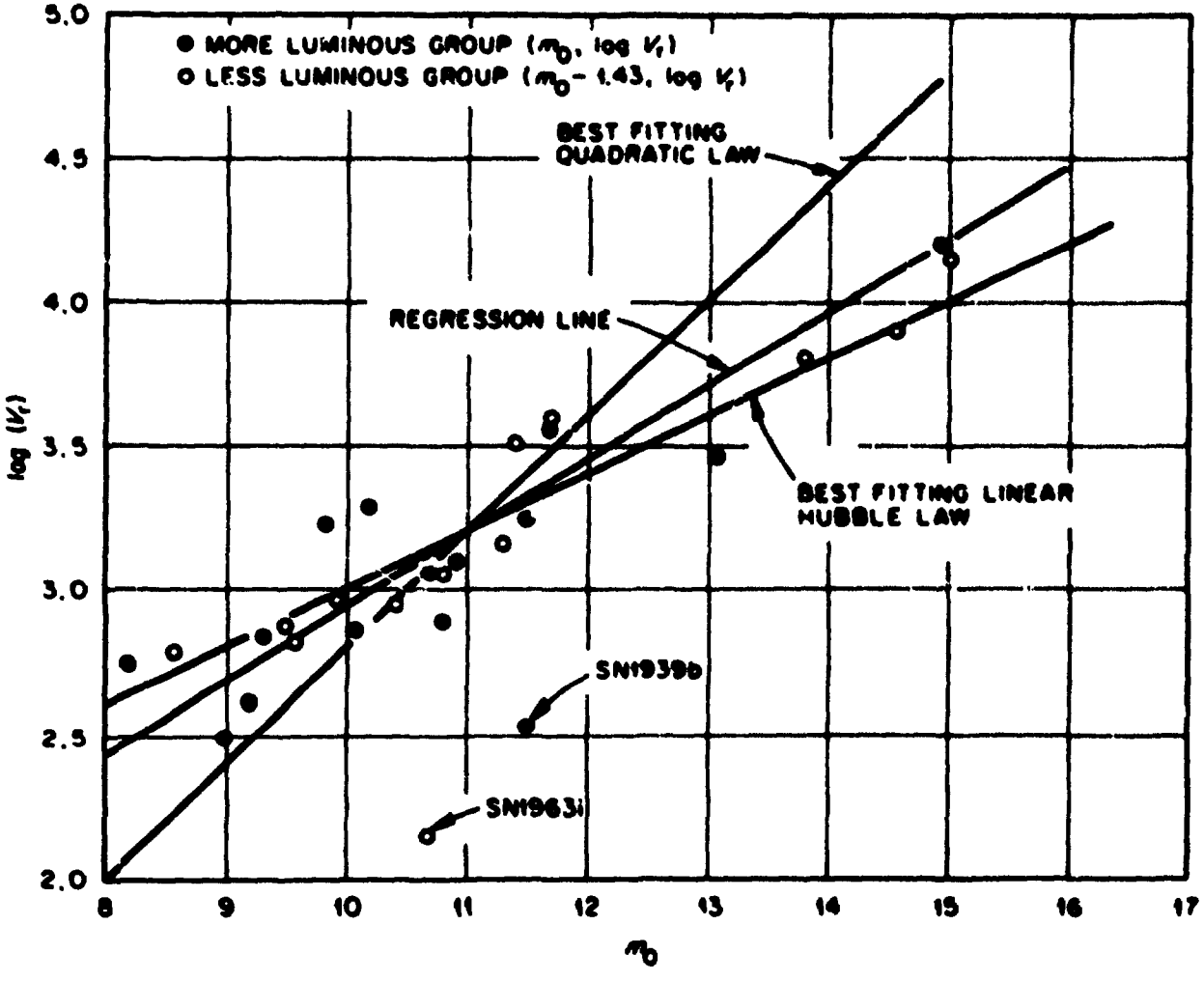

Figure 13-2. The m_o - log(V_r) Relation for the Reconciled Sample.

by relatively low red shifts. Not only are the relative errors due to random motions greater for low red-shift galaxies, but they are also given an inordinately high statistical weight by the use in the regression of the logarithmic scale for the V_r. The relative weights of the points are quite different when plotted in linear scales as V_r[km/sec] against r[Mpc]. Furthermore, there is a growing body of evidence [cf. de Vaucouleurs (146), Rubin et al. (171)] that the velocity-distance relation for local galaxies deviates significantly from that of the general field. Therefore, until more data are available on supernovae with symbolic velocities greater than, say, 2500 km/sec, it would be premature to rule out the linear Hubble law. By the same reasoning, it is also too soon to reject the quadratic Lundmark law.

If the linear Hubble law is accepted, then the best fitting line of slope = 5 for each of the luminosity groups, combined with the $M_o - \Delta t_c$ regression line for that group, provides a new method for estimating the Hubble constant. Figure 13-3 shows the two best-fitting lines with slope = 5. Together they appear to give an adequate fit of the two luminosity groups. The idea for estimating the Hubble constant is based on Equation (13-5), [$B = \bar{M} - 5 - 5 \log H$], although that equation cannot itself be used because the average absolute magnitude $\bar{M} = \bar{M}_o$ is not known. In Chapter 9 estimates were given for the values of M_o for the supernovae, but these estimates were calculated on the assumption that H = 100 km/sec/Mpc. The basic equation for estimating M_o had the form

$$M_o = m_o + 5 \log\left(\frac{V_r}{H}\right) + \text{constant}$$

$$= m_o + 5 \log (V_r) - 5 \log (H) + \text{constant}.$$

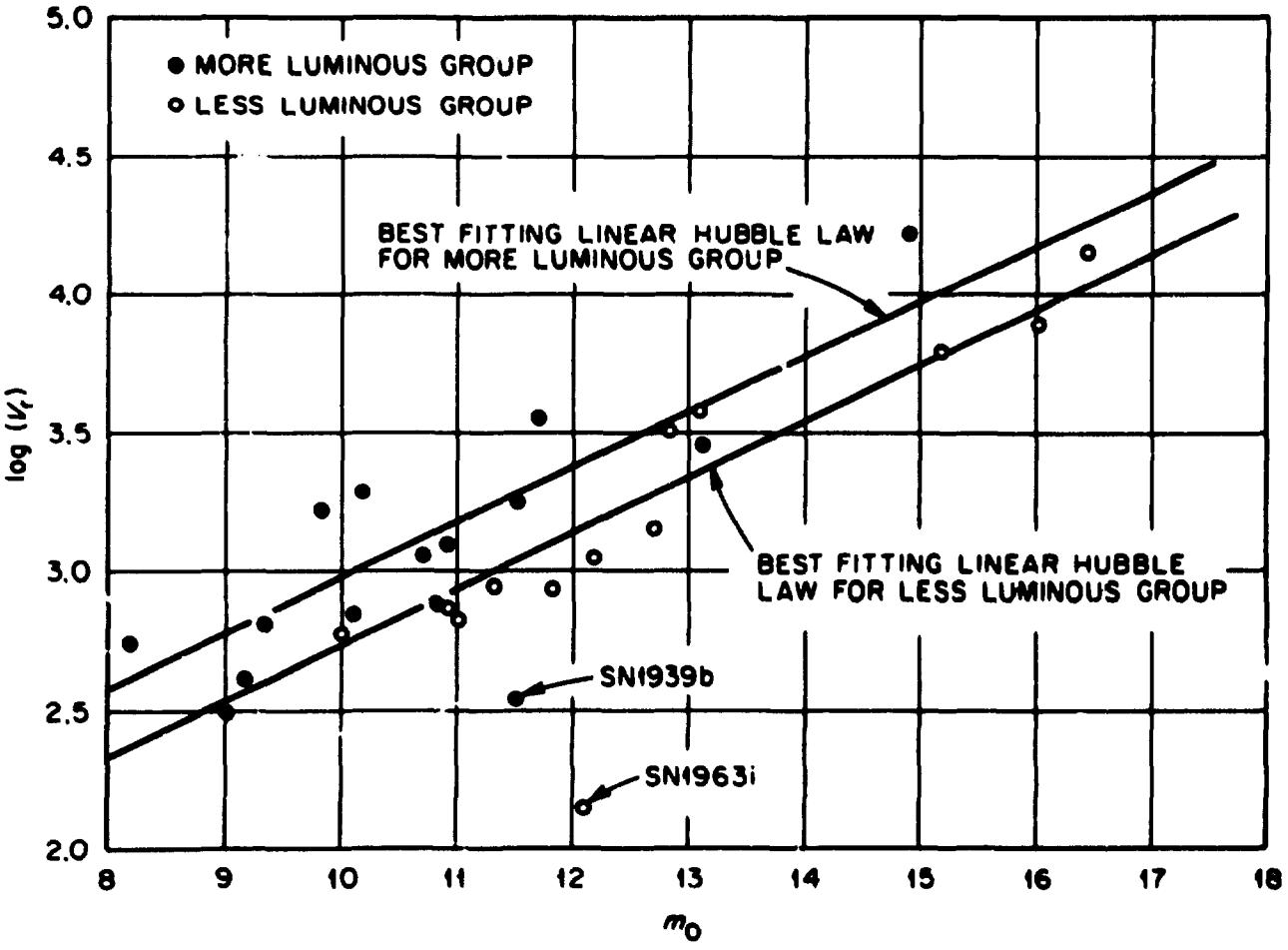

Figure 13-3. The Best-Fitting Linear Hubble Law for Each of the Two Luminosity Groups.

Of course, some of the estimates were obtained from galaxy luminosity functions, but most of these were calibrated using an assumed value of H, and the formula for changing the calibration value is derived from the above equation. The important thing to notice about the equation is that any error in H produces the same constant error in all of the M_o. This means that the $M_o - \Delta t_c$ relations defined by the two luminosity groups may have zero-point errors, but the slopes are not affected by variations in H. Thus, the slope, a, of the regression line

$$M_o = a\Delta t_c + b \qquad (13\text{-}9)$$

for each group is correctly determined by the data, but the intercept b is in error by an amount which depends on the error in H.

The regression line (13-9) passes through the average point $(\overline{\Delta t_c}, \overline{M_o})$ so Eq. (13-9) can be substituted into Eq. (13-5); solving for log(H) and at the same time converting H to units of km/sec/Mpc gives

$$\log H = 1/5\ (a\overline{\Delta t_c} + b - 5 - B) + 6. \qquad (13\text{-}10)$$

The only unknown on the right hand side of the equation is b.

In order to use Eq. (13-10) it is necessary to find a method for estimating b independently of H. In particular, what is needed are supernovae occurrences in galaxies whose distance moduli can be determined by some independent means. If $(m-M)_k$ is such a known distance modulus, then substitution of Eq. (13-9) into the identity $m_o - M_o = (m-M)_k$ leads to

$$b = m_o - a\Delta t_c - (m-M)_k. \qquad (13\text{-}11)$$

The values of m_o and Δt_c are measured and the value of a is correctly determined by the regression of the estimated M_o on Δt_c. Computing a

corrected $\underline{b}$ by this method amounts to shifting the regression line (13-9) vertically along the M_o axis until the absolute magnitude that it predicts for the supernova in question is consistent with the magnitude calculated by $M_o = m_o - (m-M)_k$. The final estimate of $\underline{b}$ should be the mean of several independent determinations of this kind in order to average out the intrinsic luminosity variation of the supernovae.

The method just outlined for determining H removes one of the principal difficulties associated with the classical methods which use the relation $V_r = Hr$. That difficulty is to select galaxies that are near enough so that their distances can be determined by primary distance indicators like cepheid variables, novae, brightest stars, angular dimensions of HII regions, etc., and at the same time are far enough away so that their peculiar velocities ($\sim$ 300 km/sec) do not significantly contaminate their red shifts. This is a problem that may not even be amenable to a solution by averaging if the red shift-magnitude relation for local galaxies actually does deviate significantly from that of more distant ones. The present method avoids the problem because it does not require the symbolic velocities. It must be used with care, however, because of the apparent coorelation between Δt_c and V_r. The value of the slope, $\underline{a}$, in Eqs. (13-10,11) and the value of $\overline{\Delta t_c}$ in (13-10) should be determined by samples of relatively local supernovae. The latter parameter is more sensitive to this effect than the former. If there is no luminosity selection in the sample, then a subsample containing the more distant supernovae will have the same proportions of low Δt_c and high Δt_c values as a subsample of nearer ones. The Δt_c value for all of the supernovae in the former subsample will, however, be systematically

higher than the ones in the latter because of the $\Delta t_c - V_r$ correlation. The net effect on the $M_o - \Delta t_c$ diagram will be to increase the scatter in the direction of the Δt_c-axis. As long as the sample does not extend to such large distance that the $M_o - \Delta t_c$ correlation is destroyed, the inclusion of moderately more distant supernovae should not produce a bias in the estimate of the slope $\underline{a}$. The estimate of $\overline{\Delta t_c}$, by contrast, should be determined by a sample of local supernovae, since otherwise the value of H predicted by Eq. (13-10) would depend on how far out the sample extended.

An ideal sample for determining the parameter $\underline{b}$, using Eq. (13-11), would be a collection of supernovae in Local Group galaxies since these galaxies are the ones with the best determined distances. Unfortunately, there was only one such supernova in the present study (SN1885a), and the absorption correction for its peak magnitude was rather crude. The sample that was used consisted of the six supernovae which occurred in the Virgo cluster. The value adopted for the distance modulus of the cluster was "the best current estimate" given recently by de Vaucouleurs (146) who obtained it by averaging several independent determinations [cf. (146) and the references given there]. That value is $(m - M)_k = 30.65$.

Four of the six supernovae used belong to the more luminous group and two belong to the less luminous group. The values of $\underline{a}$ for these two groups were taken directly from the regressions of M_o on Δt_c [cf. Chapter 11]. The two average values of $\underline{b}$ obtained by Eq. (13-11) were $b_{ML} = -18.24$ and $b_{LL} = -16.85$ for the more luminous and the less luminous group, respectively. These values compare favorably with the values originally obtained from the regressions, -18.08 and -16.74.

The average values $\overline{\Delta t_c}$ for the two groups were calculated using only the 21 supernovae with $V_r < 2000$ km/sec. Of these, 13 belong to the more luminous group and had $(\overline{\Delta t_c})_{ML} = 15.89$ days. The eight belonging to the less luminous group had $(\overline{\Delta t_c})_{LL} = 17.85$ days. Combining these values with the b_{ML} and b_{LL} and with the two values of B obtained from the separate regressions of m_o on $\log(V_r)$ [cf. Table 13-1] gives by Eq. (13-10) the estimates $H_{ML} = 87.1$ and $H_{LL} = 101.4$ km/sec/Mpc. Taking a weighted average of these two values gives for the final estimate H = 92 km/sec/Mpc.

This value of H should be regarded as a provisional determination by the present method. The obvious shortcomings of the determination are the smallness of the samples involved in the regressions of m_o on $\log(V_r)$, the regressions of M_o on Δt_c, and in calibrating the zero point of the $M_o - \Delta t_c$ relation. In spite of this, the value obtained is extremely close to the value obtained by de Vaucouleurs in his survey of nearby groups of galaxies (146). Using $(m - M) = 30.65$ for the Virgo cluster, he obtained H = 94 km/sec/Mpc. If the average value of $(m - M)$ is replaced by the extreme estimates used in obtaining that average, then the present method gives H = 69 and H = 107 km/sec/Mpc corresponding to $(m - M)_{max} = 31.25$ and $(m - M)_{min} = 30.3$. Both of these values are in reasonable agreement with the current best estimates by other methods. If the debate about the slope of the $\log V_r - m$ relation is finally settled in favor of the linear Hubble law, then as more supernova light curves become available, the present method will provide a powerful means for estimating H. Furthermore, the accurate calibration of the zero point of the $M_o - \Delta t_c$ relation will provide a significant refinement in the use of that relation as an extragalactic distance indicator--a possibility that will be discussed in the next chapter.

CHAPTER 14

A NEW METHOD FOR ESTIMATING EXTRAGALACTIC DISTANCES

In Chapter 11 it was shown that there are two distinct luminosity groups of type I supernovae and that each of these groups has a well-defined $M_0 - \Delta t_c$ relation. In Chapter 13 it was shown that the estimates of the slopes of these two relations are not affected by an error in the value of H used for computing the M_0 or by the variation in Δt_c introduced by the $\Delta t_c - V_r$ relation, so long as the sample is confined to relatively local supernovae; but these errors do introduce inaccuracies into the determinations of the intercepts. Fortunately, these zero-point errors can be removed by recalibrating the intercepts using supernovae which occurred in galaxies whose distances can be determined by other methods. This was done in the preceding chapter using the six occurrences in the Virgo Cluster. The resulting recalibrated relations are

$$(M_0)_{ML} = -0.122\Delta t_c - 18.24, \qquad (14\text{-}1)$$

and

$$(M_0)_{LL} = -0.101\Delta t_c - 16.85, \qquad (14\text{-}2)$$

for the more luminous and the less luminous groups, respectively.

The above relations can be considered to be the supernova analogues of the period-luminosity relations for Cepheid variable stars. They can be used to estimate the distance to a given supernova. The method consists essentially of measuring its light curve and using the value of Δt_c thus determined to predict its absolute magnitude and hence its distance modulus from the appropriate $M_0 - \Delta t_c$ regression line. Of course,

BLANK PAGE

it is necessary to assign the supernova to its proper luminosity group so that the correct regression line is used. This choice can probably be made from a rough estimate of the distance modulus of the parent galaxy like the ones used earlier to determine the two $M_0 - \Delta t_c$ relations. Since the gap between the two bands is so pronounced, the estimate would probably give an unambiguous determination in most cases, though a more ideal situation would be to have some independent means of distinguishing between the two groups. Such a technique may be developed from systematic studies of supernova spectra or the time variation of their color curves.

There is one other complication in the method. That is the dependence of Δt_c on V_r and hence on distance. This variation appears almost certainly to be significant, even though the exact slope is still uncertain. It will not have much effect on estimates of the distances to local supernovae, but it will have to be taken into account for more distant ones.

In order to test the method, the distances to the supernovae in the present sample were calculated using the recalibrated relations (14-1, 2). The observed values of Δt_c were corrected before substituting them into these relations. The correction equation,

$$(\Delta t_c)_{correc.} = (\Delta t_c)_{obs.} - (2.80 \times 10^{-4})V_r,$$

was obtained from the regression relation for the reconciled sample [Figure 12-2]. These corrections were not very large for the nearby supernovae (out to 30 Mpc, for example), but they were significant for the more distant ones. In view of the present uncertainty in the correction relation, the latter estimates should probably not be given too much credence.

For $r < 30$ Mpc, the velocity-distance relation defined by the new distant estimates is quite interesting. A plot of the relation is given in Figure 14-1. The plot of the supernova relation is superimposed on a plot of the velocity-distance relation for nearby groups in the north galactic hemisphere given in the study by de Vaucouleurs (146). With the exception of the two outliers SN1939b and SN1963i, which have been discarded in all the $m_b - \log(V_r)$ regressions, the agreement between the two different samples is exceptionally good. The two independent methods yield the same quadratic relation even down to the magnitude of the scatter! Thus, the new method of calculating distances is consistent with the averaging methods for clusters used by de Vaucouleurs, and the new distance estimates support his claim that locally the velocity-distance law is quadratic rather than linear.

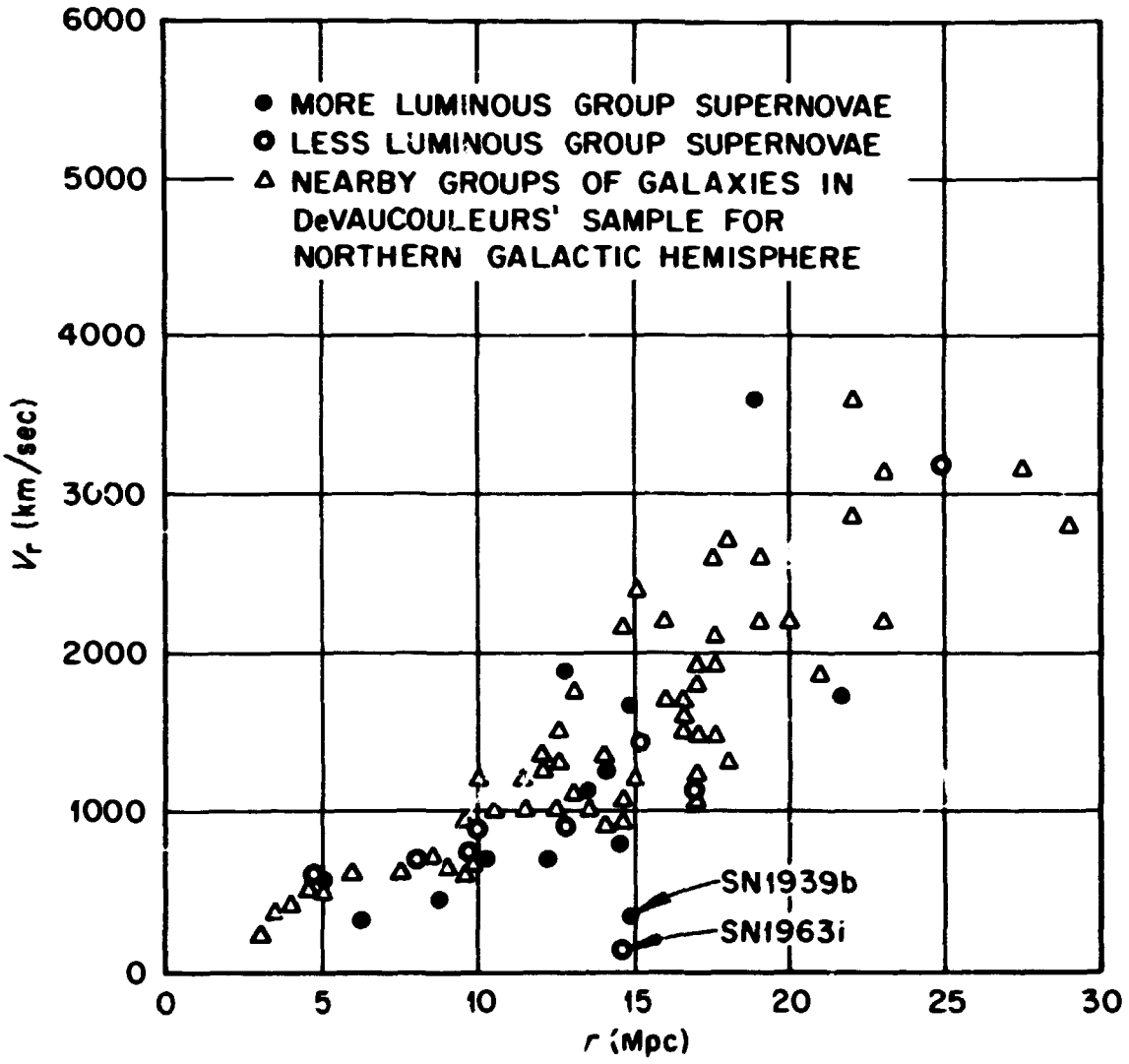

Figure 14-1. The Velocity-Distance Relation for the Local Neighborhood.

CHAPTER 15

SUMMARY AND DISCUSSION OF RESULTS

The analysis in this thesis has been based on 37 light curves observed during an 86 year period beginning with the first extragalactic supernova discovery (SN1885a). This sample contains every light curve that could be found which had a well observed initial rapidly declining segment, including one (SN1971i) observed by the author and his colleagues at Prairie Observatory. The light curves were originally measured in several different photometric systems, but they were all reduced to the international m_{pg} system. The resulting light curves, given in Appendices 1 and 2, constitute a consistent sample for statistical studies.

The reduction procedure made extensive use of Pskovskii's fundamental work on the time evolution of supernova colors combined with photometric conversion formulas originally derived for normal stars. Many of the light curves were measured in both the m_{pg} and in other systems. The agreement obtained in these cases between the measured and the converted m_{pg} magnitudes validate the reduction procedures. Pskovskii's work on the form of the type I light curve was used extensively in estimating the parameters of the brightness peak for fragmentary light curves measured in the m_{pg} system. An iterative method was developed which combines these techniques with the color curve to simultaneously convert to m_{pg} and estimate the parameters of the peak for fragmentary light curves measured in other photometric systems.

More than half of the supernovae in the sample had measured colors. For these supernovae, Pskovskii's color curve was combined with the absorption-reddening relation to give estimates of the absorptions

within the parent galaxies and peak magnitudes corrected for absorption. These absorption corrections represent the first attempt known to the present author to obtain corrected magnitudes for which the correction in each case is consistent with the observed reddening. An analysis of the average corrections within various types of galaxies gave rough estimates of the absorption corrections for the supernovae which did not have measured colors. The corrected peak magnitudes thus obtained were used to calculate estimates of the corrected peak absolute magnitudes M_0. Extensive tests of the magnitudes obtained indicated the consistency of the two methods of correcting for absorption.

Each of the light curves in the sample was fitted with the optical reverberation model of Morrison and Sartori. Previously this model has been used only for fitting the later, slowly declining segment of the light curve, but in the present study it was applied, with good results, to the early, rapidly declining segment. Tests of the model showed that it gives excellent fits to either segment taken alone, but it cannot fit the two together or the transition region between the two segments. If the model is valid, then these results can be interpreted as evidence that there are two distinct regions in the responding medium (e.g., a circumstellar envelope and the interstellar medium).

Regardless of whether or not the Morrison-Sartori model is valid, it provided a fitting function which does an excellent job of "filling in" or extrapolating fragmentary light curves. The fitted curves were also used to define a comparison parameter Δt_c (the number of days required for the apparent brightness to decline from $m_0 + 0^m.5$ to $m_0 + 2^m.5$), which gives a consistent measure of the rates of decline of the light

curves that is relatively insensitive to errors in the estimates of the parameters of peak brightness (m_0 = peak apparent magnitude and t_0 = date of peak).

The estimates of M_0 and Δt_c for the supernovae in this sample provide a data base containing much useful information both for supernova theory and cosmological tests. Although the Δt_c apparently do increase with increasing symbolic velocity V_r, it was possible to get a good estimate of the intrinsic distribution by considering the supernovae in the sample with $V_r < 2000$ km/sec. The estimates of M_0 provided confirmatory evidence for two correlations previously reported by Pskovskii [cf. Appendix 4]: (1) a correlation between M_0 and the Hubble type of the parent galaxy and (2) a correlation between M_0 and the luminosity of the parent galaxy.

The estimates of M_0 and Δt_c taken together provide very strong evidence that there are two distinct populations of type I supernovae having different average values $\overline{M_0}$ and $\overline{\Delta t_c}$. The two groups, which were called the more luminous group ($\overline{M_0} = -20.17$, $\overline{\Delta t_c} = 17.1$ days) and the less luminous group ($\overline{M_0} = -18.74$, $\overline{\Delta t_c} = 19.9$ days), were extensively tested [cf. Appendix 5] to determine whether or not they might have been the result of systematic errors in estimating the M_0 rather than being real distinct populations. No systematic effects were found. The two groups were compared with subgrouping schemes proposed by previous authors, and it was shown that the present scheme gives a more significant subdivision than the preceding ones.

It is the relationship between M_0 and Δt_c that defines the division into two luminosity groups and indicates the significance of the division. The groups appear in the plot of M_0 against Δt_c as two well separated

bands with a highly significant linear correlation within each band. These two linear relations should have far-reaching consequences for future research on supernovae. They will provide validating relations for theoretical models. They can also be used for distance estimation in a manner analagous to the use of the period-luminosity relations for Cepheid variables.

In order to use the $M_0 - \Delta t_c$ relations for distance estimation, it was necessary to recalibrate them. The original estimates of M_0 were obtained using an assumed value of the Hubble constant H. Also, since the Δt_c are correlated with V_r, variation in the latter parameter introduces scatter in the $M_0 - \Delta t_c$ relation. In Chapter 13 it was shown that these uncertainties do not affect the slope of the $M_0 - \Delta t_c$ relation. Therefore it was necessary to correct only the intercept. This was done by using the six supernovae which occurred in the Virgo cluster together with de Vaucouleurs' "best" average estimate of the distance modulus of that cluster. This recalibrated relation can then be used to estimate the absolute magnitude of a given supernova from the measured value of the comparison parameter Δt_c.

There are two complications in using the above described method. One is determining the group membership for the given supernova. Until some independent method is found, an initial estimate of M_0 using the same techniques that were used to determine the $M_0 - \Delta t_c$ relations will probably suffice to determine which group to use. The other complication arises from the correlation between Δt_c and V_r. The measured Δt_c must be corrected for this effect. The correction is negligible for relatively local supernovae, but it may be significant for distant ones.

The chief task of this thesis was to examine the $\Delta t_c - V_r$ relation in order to test the expansion hypothesis. In Chapter 8 the correlation between these two quantities for the present sample was shown to be significant at the 93% level, but the slope of the regression line was much larger than the values predicted by both the static Euclidean and the classical expansion hypotheses. Chapter 10 gave a review of some of the theories that have been proposed as alternatives, and it was shown that only one of them gave a prediction that differed from those two hypotheses. That one was derived by the present author using the covariant chronogeometry proposed recently by the mathematician I. E. Segal. The resulting prediction gave much better agreement with the regression line than the other two predictions.

In Chapter 8 extensive tests were described which show that the unexpectedly large slope of the $\Delta t_c - V_r$ relation did not arise from systematic errors in the data reduction, and in Chapter 9 it was shown that the result was not caused by a luminosity selection effect. In Chapter 12 a reconciled sample was constructed by combining the two luminosity groups so that they simulated a single luminosity population. The $\Delta t_c - V_r$ regression for the reconciled sample gave essentially the same results as the original sample, so the unexpected slope was not caused by a population effect.

Although the regression line of Δt_c on V_r gives the best agreement with Segal's theory and rejects the classical expansion hypothesis at the 91% level, one cannot make the claim that the former theory is correct and the latter is wrong. There is a very wide scatter in the Δt_c data and the sample points are clustered toward the lower end of the V_r

range, which extends out to only V_r = 16,000 km/sec. The t-statistics for computing the significance levels of the various tests take all of these factors into account. Thus, the 91% level obtained for rejecting the expansion hypothesis is a valid value, but it is considerably less than the traditionally acceptable 95% level. Even so, the level is large enough to encourage some doubt as to the validity of the expansion hypothesis and to emphasize the need for further work in order to verify or disverify it.

Another method for distinguishing between cosmological theories is the redshift-magnitude relation. The slope of this relation determines the form of the velocity-distance relation. The classical expansion hypothesis predicts the linear Hubble law. Segal's theory predicts a quadratic law ($V_r \sim r^2$). Observations of galaxies cannot be used to give an independent estimate of the slope because they require aperture corrections which in turn require assumptions about the geometry of space-time and hence about the form of the velocity-distance relation. Because they are highly luminous point sources, supernovae are the ideal candidates for this analysis.

When (in Chapter 13) the supernovae in the present sample were subjected to the M_0, $\log(V_r)$ analysis, the resulting regression line had a slope intermediate between the values corresponding to the linear Hubble law and the quadratic law. The correlation was highly significant and both laws were rejected at significance levels exceeding 95%! The sample was dominated by low-z and hence relatively local supernovae. In view of the recent work that has been done on local anisotropies in and deviations from the Hubble law, one must consider the possibility

that the result reflects a purely local effect. If so, it is premature to rule out the Hubble law--but it is also premature to rule out a quadratic law.

In Chapter 14 the new method of distance estimation using the recalibrated $M_0 - \Delta t_c$ relations was applied to the supernovae in the sample with distances less than about 30 Mpc in order to construct the local velocity-distance relation. Since the V_r for the supernovae involved were all relatively small, the corrections to the Δt_c, required by the $\Delta t_c - V_r$ correlation, were small; it did not matter that the exact slope of the $\Delta t_c - V_r$ relation is not yet well determined. The resulting velocity-distance relation gave extremely good agreement with the quadratic relation recently found by de Vaucouleurs using averages for nearby groups and clusters of galaxies. This result gives confirming evidence for his result, indicates that the new method of distance estimation is consistent with the older methods, and suggests that the results obtained in Chapter 13 were indeed more indicative of a local effect than of the true velocity-distance relation for the general field.

If the validity of the linear Hubble law is accepted, then the recalibrated $M_0 - \Delta t_c$ relation can be combined with the $m_0 - \log(V_r)$ analysis to give a new method for estimating the Hubble constant. Older methods, based on the formula $V_r = Hr$, require primary distance indicators (like Cepheids) close enough to be visible and yet far enough away so that the V_r are not dominated by random motions. This would be a difficult problem even in the absence of local anomalies in the Hubble relation. The new method avoids the problem because it does not use the value of V_r in the determination. When it was applied to the present sample, the resulting estimate was $H = 92$ km/sec/Mpc.

Most of the analyses and tests performed in this thesis have been provisional or not completely conclusive because the present sample of light curves is not extensive enough. In particular, the $\Delta t_c - V_r$ tests were only marginally significant because there were not enough light curves for larger values of V_r. In Chapter 12 the reconciled sample was used to estimate the sample requirements for discriminating at the 95% level between various pairs of alternative hypotheses. The results were quite encouraging. They indicate that if Segal's theory is correct, only a medium-large telescope will be needed to gather the light curves required to reject the static Euclidean and the classical expansion hypotheses, and furthermore, only a few more light curves will be needed. If one of the latter two hypotheses is correct, a really large telescope will be required, but again only a few more light curves will be needed to distinguish between them. In view of the preliminary indications of the results obtained from the present analysis, it would seem that the collection of these additional light curves should be given a high priority. Not only would they make the $\Delta t_c - V_r$ test definitive, but they also might resolve the question of the form of the velocity-distance relation, give a better estimate of H, and refine the new method of distance estimation. The author will consider this thesis a great success if it hastens the gathering of these new data.

LIST OF REFERENCES

(1) North, J. D., 1965, The Measure of the Universe (Oxford University Press, London).

(2) McVittie, G. C., 1961, Fact and Theory in Cosmology (The Macmillan Company, New York).

(3) Minkowski, R. and Wilson, O. C., 1956, The Astrophysical Journal, 123, 373.

(4) Wilson, O. C., 1949, Publications of the Astronomical Society of the Pacific, 61, 132.

(5) Kerr, F. J., Hindman, J. V., and Robinson, B. J., 1954, Australian Journal of Physics, 7, 297.

(6) van de Hulst, H. C., Raimond, E., van Woerden, H., 1957, Bulletin of the Astronomical Institutes of the Netherlands, 14, 1.

(7) Ford, W. K., Rubin, V. C., and Roberts, M. S., 1971, The Astronomical Journal, 76, 22.

(8) Arp, H. C., 1971, Science, 174, 1189.

(9) Arp, H. C., 1970, in External Galaxies and Quasi-Stellar Objects, D. S. Evans, Ed., (International Astronomical Union Symposium No. 44, Uppsala), 380-392

(10) Schmidt, M., 1963, Nature, 197, 1040.

(11) Jeffreys, W. H., 1964, The Astronomical Journal, 69, 255.

(12) Luyten, W. J., and Smith, J. A., 1966, The Astrophysical Journal, 145, 366.

(13) Hoyle, F., and Burbidge, G. R., 1966, Nature, 210, 1346.

(14) Abell, G. O., 1958, The Astrophysical Journal Supplement Series, 3, 211.

(15) Bahcall, J. N., 1969, The Astrophysical Journal, 158, L87.

(16) Gunn, J. E., 1971, The Astrophysical Journal, 164, L113.

(17) Robinson, L. B. and Wampler, E. J., 1972, The Astrophysical Journal, 171, L83-L86.

(18) Arp, H. C., 1970, The Astrophysical Journal, 162, 811-813.

(19) Arp, H. C., 1966, The Astrophysical Journal Supplement Series, 14, 1-20.

(20) Arp, H. C., 1970. The Astronomical Journal, 75, 1.

(21) Arp, H. C., 1967, The Astrophysical Journal, 148, 321.

(22) Arp, H. C., 1971, Astrophysical Letters, 9, 1-4.

(23) Burbidge, E. M., Burbidge, G. R., Solomon, P. M., and Strittmatter, P. A., 1971, The Astrophysical Journal, 170, 233-240.

(24) Arp, H. C., Burbidge, E. M., Mackay, C. D., and Strittmatter, P. A., 1972, The Astrophysical Journal, 171, L41-L43.

(25) Zwicky, F., 1956, in Ergebnisse der Exakten Naturwissenschaften, Band XXIX, S. Flugge and F. Trendelenburg, Eds., (Springer-Verlag, Berlin).

(26) Sargent, W. L. W., 1968, The Astrophysical Journal, 153, L135-L137.

(27) Burbidge, E. M. and Burbidge, G. R., 1961, The Astrophysical Journal, 134, 244-247.

(28) Arp, H. C., 1970, Astrophysical Letters, 5, 257-260.

(29) Arp, H. C., 1971, Astrophysical Letters, 7, 221-224.

(30) Arp, H. C., 1970, Nature, 225, 1033-1035.

(31) Lewis, B. M., 1971, Nature Physical Science, 230, 13-15.

(32) Arp, H. C., 1971, Nature Physical Science, 231, 103-104.

(33) Jaakkola, T., 1971, Nature, 234, 534-535.

(34) McCrea, W. H., 1935, Zeitschrift fur Astrophysik, 9, 290-314.

(35) Wilson, O. C., 1954, The Astrophysical Journal, 120, 634-636.

(36) Milford, S. N., 1955, The Astrophysical Journal, 122, 13-23.

(37) Milford, S. N., 1953, The Astronomical Journal, 58, 43-44.

(38) Pinzi, A., 1961, Annales D'Astrophysique, 24, 68-70.

(39) Burbidge, E. M., Burbidge, G. R., Fowler, W. A., and Hoyle, F., 1957, Reviews of Modern Physics, 29, 547-649.

(40) Mihalas, D., 1965, Publications of the Astronomical Society of the Pacific, 75, 256-268.

(41) Pecker, J. C., Roberts, A. P., and Vigier, J. P., 1972, Nature, 237, 227-229.

(42) Page, T., 1961, Proceedings of the Fourth Berkeley Symposium on Mathematical Statistics and Probability, 3, 2[illegible].

(43) Page, T., 1970, The Astrophysical Journal, 159, 791.

(44) Zwicky, F., 19[illegible], Handbuch der Physik, 51, S. Flugge, Ed., 7[illegible]-765 (Springer-Verlag, Berlin).

(45) Zwicky, F., 19[illegible], Stars and Stellar Systems, Vol. VIII, Stellar Structure, Aller and McLaughlin, Eds., 3[illegible]-25 (The University of Chicago).

(46) Karpowicz, M. and Rudnicki, K., 19[illegible], Preliminary Catalogue of Supernovae Discovered Till the End of 19[illegible], Publications of the Astronomical Observatory of the Warsaw University, Volume 15 (Warsaw University Press).

(47) Kowal, C. T. and Sargent, W. L. W., 19[illegible], The Astronomical Journal, 76, 756-764.

(48) Minkowski, R., 19[illegible], Annual Reviews of Astronomy and Astrophysics, Vol. 2 (Annual Reviews, Inc., Palo Alto), p. 2[illegible].

(49) Kowal, C. T., 19[illegible], The Astronomical Journal, 73, 1021-1024.

(50) Pskovskii, Yu. P., 19[illegible], Soviet Astronomy - AJ, 11, 63-69.

(51) Pskovskii, Yu. P., 19[illegible], Soviet Astronomy - AJ, 14, 798-805.

(52) Deming, D., Rust, B., and Olson, E., 19[illegible], Publications of the Astronomical Society of the Pacific, 82, 521-527.

(53) Dunlap, J. R., 1971, International Astronomical Union Circular No. 2330, June 2, 1971.

(54) van de Hulst, H. C., 1971, International Astronomical Union Circular No. 2334, June 18, 1971.

(55) van Herk, G. and Schoenmaker, A. A., 1972, Astronomy and Astrophysics, 17, 146-147.

(56) Huruhata, M., 1971, International Astronomical Union Circular No. 2332, June 2, 1971.

(57) Parenago, P. P., 1949, Peremennye Zvezdy, 7, 109-123.

(58) Gaposchkin, S., 1961, Sky and Telescope, 21, 526-527.

(59) Shapley, H., 1939, Proceedings of the National Academy of Science USA, 25, 569-571.

(60) Baade, W. and Zwicky, F., 1938, The Astrophysical Journal, 88, 411-421.

(61) Deutsch, A. N., 1939, Poulkovo Observatory Circular No. 28, 73-75.

(62) Miclas, H. L., 1939, Publications of the Astronomical Society of the Pacific, 51, 166-168.

(63) Bertaud, C., 1941, Astronomie, 55, 161-162.

(64) Shapley, H., 1939, Harvard College Observatory Announcement Card No. 437, June 1, 1939.

(65) Wild, P., 1960, Publications of the Astronomical Society of the Pacific, 72, 97-105.

(66) Pietra, S.. 1955, Memorie della Societa Astronomica Italiana, 26, 181-188.

(67) Zwicky, F., 1956, Publications of the Astronomical Society of the Pacific, 68, 271-272.

(68) Zwicky, F. and Karpowicz, M., 1964, The Astronomical Journal, 69, 759-761.

(69) Zwicky, F. and Karpowicz, M., 1965, The Astronomical Journal, 70, 564-565.

(70) Bertola, F., 1964, The Astronomical Journal, 69, 236-242.

(71) Wenzel, W., 1957, Nachrichtenblatt der Astronomischen Zentralstelle Astronomischen Rechen-Institut Heidelberg, 11, 14.

(72) Gotz, W., 1958, Astronomische Nachrichten, 284, 141-142.

(73) Li Tzin, 1957, Acta Astronomica Sinica, 5, 321-323.

(74) Mihalas, D., 1962, Publications of the Astronomical Society of the Pacific, 74, 116-124.

(75) Romano, G., 1957, La Ricerca Scientifica, 27, N. 10, 3-5.

(76) Huth, H., 1960, Circulaire, Bureau Centrale Internationale des Telegrammes Astronomiques, No. 1723.

(77) Kulikov, V. I., 1960, Astronomicheskii Tsirkular No. 215, 2-4.

(78) Tempesti, P., 1961, Memorie della Societa Astronomica Italiana, 32, 249-255.

(79) Mannino, G., 1962, Memorie della Societa Astronomica Italiana, 33, 147-149.

(80) Zaitseva, G. V., 1961, Astronomicheskii Tsirkular No. 223, 1-2.

(81) Gates, H. S., 1961, Harvard College Observatory Announcement Card No. 1521.

(82) Zwicky, F., 1961, Publications of the Astronomical Society of the Pacific, 73, 185-190.

(83) Romano, G., 1962, Memorie della Societa Astronomica Italiana, 33, 17-37.

(84) Zwicky, F. and Barbon, R., 1967, The Astronomical Journal, 72, 1366.

(85) Rudnicki, K. and Zwicky, F., 1967, The Astronomical Journal, 72, 407-409.

(86) Bertola, F., 1965, Memorie della Societa Astronomica Italiana, 36, 299-307.

(87) Bertola, F., 1964, Annales D'Astrophysique, 27, 319-326.

(88) Rosino, L., 1963, Coelum, 31, 52-53.

(89) Rosino, L., 1963, Information Bulletin on Variable Stars of Commission 27, International Astronomical Union, No. 37.

(90) Rosino, L., 1964, Annales D'Astrophysique, 27, 314.

(91) Zaitseva, C. V., 1964, Peremennye Zvezdy, 15, 107-108.

(92) Lochel, K., 1963, Information Bulletin on Variable Stars of Commission 27, International Astronomical Union, No. 30.

(93) Lochel, K., 1965, Sterne, 41, 118-122.

(94) Zwicky, F., 1964, Publications of the Astronomical Society of the Pacific, 76, 326.

(95) Wild, P., 1963, Harvard College Observatory Announcement Card No. 1601.

(96) Chincarini, G. and Margoni, R., 1964, Memorie della Societa Astronomica Italiana, 35, 129-132.

(97) Bertola, F., Mammano, A. and Perinotto, M., 1965, Contributi Dell'Osservatorio Astrofisico Dell'Universita di Padova in Asiago, No. 174.

(98) Kaho, S., 1967, Tokyo Astronomical Bulletin, Second Series, No. 176.

(99) Lovas, M., 1964, Information Bulletin on Variable Stars of Commission 27, International Astronomical Union, No. 50.

(100) Ahnert, P., 1964, Information Bulletin on Variable Stars of Commission 27, International Astronomical Union, No. 56.

(101) Chuadze, A. D., 1964, Astronomicheskii Tsirkular No. 291, 1-2.

(102) Zaitseva, C. V., 1964, Astronomicheskii Tsirkular No. 301, 1.

(103) Lochel, K., 1966, Mitteilungen uber Veranderliche Sterne, 2, 195-197.

(104) Van Lyong, L. and Panarin, J. P., 1966, Peremennye Zvezdy, 16, 90-91.

(105) Ciatti, F. and Barbon, R., 1971, Memorie della Societa Astronomica Italiana, 42, 145-161.

(106) Wild, P., 1966, International Astronomical Union Circular No. 1986.

(107) Chincarini, G. and Perinotto, M., 1968, Memorie della Societa Astronomica Italiana, 39, 189-199.

(108) Kaho, S., 1968, Tokyo Astronomical Bulletin, Second Series, No. 189.

(109) Rudnicki, K., 1967, Astronomische Nachrichten, 290, 135-139.

(110) de Vaucouleurs, G., Solheim, J. E. and Brown, R., 1967, Astrofizika, 1, 565.

(111) Marx, S. and Pfau, W., 1967, Information Bulletin on Variable Stars of Commission 27, International Astronomical Union, No. 206.

(112) Borzov, G. G., Dibai, E. A., Esipov. V. F. and Pronik, V. I., 1969, Soviet Astronomy - AJ, 13, 423-426.

(113) Chuadze, A. D. and Barblishvili, T. I., 1969, Byull. Abastumansk Astrofiz. Obs. No. 37, 9-12.

(114) Chavira, E., 1968, International Astronomical Union Circular No. 2061.

(115) Bertola, F. and Ciatti, F., 1971, Memorie della Societa Astronomica Italiana, 42, 67-72.

(116) Scovil, C. E., 1971, International Astronomical Union Circular No. 2338, July 2, 1971.

(117) Vaucouleurs, G. de and Vaucouleurs, A. de, 1964, Reference Catalogue of Bright Galaxies, (University of Texas Press, Austin).

(118) Humason, M. L., Mayall, N. U. and Sandage, A. R., 1956, The Astronomical Journal, 61, 97-162.

(119) Holmberg, E., 1964, Arkiv for Astronomi, 3, 387-438.

(120) Holmberg, E., 1958, Lund Meddelanden, II, No. 136.

(121) Pettit, E., 1954, The Astrophysical Journal, 120, 413-438.

(122) Bigay, J. H., 1951, Annales d'Astrophysique, 14, 319-366.

(123) Zwicky, F., Herzog, E. and Wild, P., 1961, Catalogue of Galaxies and Clusters of Galaxies, Vol. 1, (California Institute of Technology, Pasadena).

(124) Zwicky, F. and Herzog, E., 1963, Catalogue of Galaxies and Clusters of Galaxies, Vol. 2, (California Institute of Technology, Pasadena).

(125) Pskovskii, Yu. P., 1968, Soviet Astronomy - AJ, 11, 570-575.

(126) Beyer, M., 1939, Astronomische Nachrichten, 268, 350-354.

(127) Beyer, M., 1954, Nachrichtenblatt der Astronomischen Zentralstelle, 8, 34.

(128) Wellman, P., 1955, Zeitschrift fur Astrophysik, 35, 205-209.

(129) Morrison, P. and Sartori, L., 1966, Physical Review Letters, 16, 414.

(130) Morrison, P. and Sartori, L., 1969, The Astrophysical Journal, 158, 541-570.

(131) Arnett, W. D., 1971, The Astrophysical Journal, 163, 11-16.

(132) Householder, A. S., 1964, The Theory of Matrices in Numerical Analysis (Random House (Blaisdell), New York).

(133) Golub, G., 1965, Numerische Mathematik, 7, 206-216.

(134) IBM, Technical Publications Department, 1967, System/360 Scientific Subroutine Package, Version II, Programmer's Manual, 360A-CM-03X, (IBM, Technical Publications, White Plains, New York), pp. 191-195.

(135) Ibid, pp. 161-163.

(136) Grubb, F. E., 1950, Annals of Mathematical Statistics, 21, 27-58.

(137) van den Bergh, S., 1960, Zeitschrift fur Astrophysik, 49, 201-205.

(138) Sharpless, S., 1963, Stars and Stellar Systems, Vol. III, Basic Astronomical Data, K. A. A. Strand, Ed., 225-240, (The University of Chicago Press).

(139) Mihalas, D., 1968, Galactic Astronomy, 68-77, (W. H. Freeman and Co., San Francisco).

(140) van den Bergh, S., 1960, The Astrophysical Journal, 131, 215-223.

(141) van den Bergh, S., 190, The Astrophysical Journal, 131, 558-573.

(142) de Vaucouleurs, G., 1962, Problems of Extra-Galactic Research, IAU Symposium No. 15, G. C. McVittie, Ed., 3-21, (MacMillan).

(143) de Vaucouleurs, G., 1963, The Astrophysical Journal Supplement Series, Supplement Number 74, Vol. VIII, 31-98.

(144) Allen, C. W., 1963, Astrophysical Quantities, 2nd Edition, (The Althone Press, Univ. of London).

(145) Pskovskii, Yu. P., 1962, Soviet Astronomy - AJ, 5, 498-502.

(146) de Vaucouleurs, G., 1972, External Galaxies and Quasi-Steller Objects, IAU Symposium No. 44, D. S. Evans, Ed., 353-366, (D. Reidel Publ. Co.).

(147) Bertola, F. and Sussi, M. G., 1965, Contributi Dell'Osservatorio Astrofisico Dell'Universita di Padova in Asiago, No. 176.

(148) Zwicky, F., 1960-65, Circular Letter on Supernovae, No. 1-8.

(149) Zwicky, F., 1964, List of Supernovae Discovered since 1885, California Institute of Technology.

(150) Barbon, R., Ciatti, F. and Rosino, L., 1973, Astronomy and Astrophysics, 25, 241-248.

(151) Schmidt, T., 1957, Zeitschrift fur Astrophysik, 41, 182.

(152) MacMillan, W. D., 1918, The Astrophysical Journal, 48, 35-49.

(153) MacMillan, W. D., 1923, Scientia, 33, 3-12, 103-112.

(154) MacMillan, W. D., 1925, Science, 62, 63-72, 96-99, 121-127.

(155) Finlay-Freundlich, E., 1954, Philosophical Magazine, 45, 303-319.

(156) Gerasim, A., 1969, Astrophysical Letters, 4, 51-54.

(157) Freund, P. G. O., Maheshwari, A. and Schonberg, E., 1969, The Astrophysical Journal, 157, 857-867.

(158) Yourgrau, W. and Woodward, J. F., 1971, Acta Physica Academiae Scientiarum Hungaricae, 30, 323-329.

(159) Milne, E. A., 1935, Relativity, Gravitation and World-Structure, (Oxford University Press, London).

(160) Milne, E. A., 1948, Kinematic Relativity, (Oxford University Press, London).

(161) Johnson, M., 1947, Time, Knowledge and the Nebulae, (Dover Publications, New York).

(162) Bellert, S., 1969, Astrophysics and Space Science, 3, 268-282.

(163) Bellert, S., 1970, Astrophysics and Space Science 7, 211-230.

(164) Segal, I., 1972, Astronomy and Astrophysics, 18, 143-148.

(165) Segal, I. E., 1973, Covariant Chronogeometry and Extragalactic Astronomy, (in manuscript, Massachusetts Institute of Technology).

(166) Robb, A. A., 1936, Geometry of Time and Space, (Cambridge University Press, Cambridge).

(167) Fokker, A. D., 1965, Time and Space, Weight and Inertia, (Pergamon Press, Oxford).

(168) Agekyan, T. A., 1969, Physics of Stars and Stellar Systems, A. A. Mikhailov, ed., (Israel Program for Scientific Translations, Jerusalem, NASA TT F-506) 631-703.

(169) Lundmark, K., 1925, Monthly Notices of the Royal Astronomical Society, 85, 865-895.

(170) Hawkins, G. S., 1962, Nature, 194, 563-564.

(171) Rubin, V. C., Ford, W. K. and Rubin, J. S., 1973, The Astrophysical Journal, 183, L111-L115.

(172) Fisher, R. A. and Yates, F., 1970, Statistical Tables for Biological, Agricultural, and Medical Research, 6th Edition, (Hafner Publ. Co., Darien, Conn.).

(173) Deming, D., 1974, (Private communication).

(174) Koval, C. T., Zwicky, F., Sargent, W. L. W. and Searle, L., 1973, Publications of the Astronomical Society of the Pacific, 427-435.

APPENDIX 1

THE OBSERVED AND REDUCED DATA

Tables A1-1.1 through A1-1.37 give the observed and reduced data used for constructing the light curves in this study. The original observations are given on the left side of the tables with the source and magnitude system identified at the top of each column. The abbreviations for the magnitude systems are the same as those used in Tables 5-2, 6-3, and 6-4. The date given for each observation is in the form given by the original observer, sometimes in Julian days and sometimes in the mo/da/yr notation. The times which are given with some of the dates are in the U.T. system. The estimates m_o and t_o of peak photographic brightness and date of peak are given at the head of each table. The reduced data used for constructing the light curves are given in the final two columns of each table. The column labeled t gives the time in days relative to t_o of the observation, and the column labeled m_{pg} gives the magnitude reduced to the m_{pg} system. The steps of the conversion techniques used in each case are summarized in Tables 6-3 and 6-4. For some supernovae, some of the observed magnitudes were not used in constructing the final light curves so there are missing entries in the final two columns. In most of these cases the unused observations were used, however, in calculating the color excesses given in Table 6-4 so they are included in the following tables.

Table A1 - 1.1

SN1885A		t_0 = JD2409776		m_0 = 5.2
Date	Obs. m_{vis}	Source	t	m_{pg}
JD2409771	7.0	Gaposhkin (58)	-5	6.4
JD2409774	6.0	Parenago (57)	-2	5.5
779	6.0		3	5.6
781	7.0		5	6.7
783	7.3		7	7.0
785	7.77		9	7.6
786	7.85		10	7.7
787	7.95		11	7.8
788	8.06		12	8.0
789	8.27		13	8.2
790	8.27		14	3.3
791	8.40		15	8.5
792	8.37		16	8.5
793	8.54		17	8.7
794	8.60		18	8.8
795	8.82		19	9.1
796	8.88		20	9.2
797	9.00		21	9.4
798	9.02		22	9.4
799	9.05		23	9.5
800	9.11		24	9.6
801	9.07		25	9.7
802	9.22		26	9.9
803	9.29		27	10.0
804	9.34		28	10.1
805	9.54		29	10.4
806	9.60		30	10.4
807	9.59		31	10.5

Table A1 - 1.1 (Continued)

SN1885A		t_0 = JD2409776		m_0 = 5.2
Date	Obs. m_{vis}	Source	t	m_{BK}
808	9.54		32	10.4
809	9.68		33	10.6
JD2409810	9.67	Parenago (57)	34	10.6
811	9.79		35	10.7
812	9.76		36	10.6
813	9.97		37	10.8
814	10.08		38	10.9
815	10.05		39	10.9
816	10.20		40	11.0
817	10.18		41	11.0
818	10.26		42	11.1
819	10.46		43	11.3
820	10.36		44	11.2
821	10.41		45	11.2
822	10.53		46	11.3
824	10.54		48	11.3
825	10.52		49	11.3
826	10.57		50	11.3
827	10.56		51	11.3
828	10.68		52	11.4
829	10.66		53	11.4
830	10.69		54	11.4
831	10.59		55	11.3
832	10.37		56	11.0
833	10.72		57	11.4
834	10.96		58	11.6
836	10.74		60	11.4
837	10.68		61	11.3

Table A1 - 1.1 (Continued)

SN1885A		t_0 = JD2409776		m_0 = 5.2
Date	Obs. m_{vis}	Source	t	m_{BK}
838	10.8		62	11.4
839	11.00		63	11.6
840	11.20		64	11.8
841	11.17		65	11.7
842	11.03		66	11.6
844	11.25		68	11.8
845	11.0		69	11.5
JD2409846	11.33	Parenago (57)	70	11.8
848	11.25		72	11.7
849	11.05		73	11.5
850	11.18		74	11.6
851	11.18		75	11.6
852	11.4		76	11.8
853	11.05		77	11.5
856	11.4		80	11.8
858	11.6		82	12.0
860	11.5		84	11.8
862	11.4		86	11.7
864	11.8		88	12.1
869	11.5		93	11.7
870	11.8		94	12.0
871	12.0		95	12.2
874	11.95		98	12.1
876	12.05		100	12.2
877	12.0		101	12.2
878	12.3		102	12.4
880	12.2		104	12.3
882	11.9		106	12.0

Table A1 - 1.1 (Continued)

SN1885A		t_0 = JD2409776		m_0 = 5.2
Date	Obs. m_{vis}	Source	t	m_{PE}
886	12.4		110	12.5
887	12.7		111	12.8
894	12.9		118	12.9
904	13.1			
905	13.3			
906	13.7			
908	14.7			
909	13.75			
912	14.0			
937	15.7			
938	14.6			
942	15.3			
945	15.7			
972	15.8			

Table A1 - 1.2

SN1921c		t_0 = 12/9/21		m_0 = 11.0
Date	Obs. m_{pg}	Source	t	m_{pg}
12/5/21	11.1	Shapley (59)	-4	11.1
12/7/21	11.1		-2	11.1
12/8/21	11.1		-1	11.1
12/8/21	11.0		-1	11.0
12/11/21	11.0		2	11.0
12/19/21	11.2		10	11.2
12/21/21	11.5		12	11.5
12/27/21	11.8		18	11.8
1/1/22	12.8		23	12.8
1/26/22	14.1		48	14.1

Table A1 - 1.3

SN1937c t_0 = JD2428768.0 m_0 = 8.4

Date	Baade & Zwicky(60) m_{pg}	Parenago (57) m_{pg}	Deutsch (61) m_{pg}	Beyer (126) m_{vis}	t	m_{pg}
JD2428762.4		8.85			-5.6	8.85
772.7		8.4			4.7	8.40
774.7	8.48	8.58			6.7	8.58
775.7	8.63	8.63			7.7	8.63
776.7	8.62	8.62			8.7	8.62
777.5		8.68			9.5	8.68
777.7	8.64				9.7	8.64
778.5		8.74			10.5	8.74
778.7	8.74				10.7	8.74
779.3				8.76		
779.5		8.93			11.5	8.93
779.6	8.83				11.6	8.83
779.7	8.98				11.7	8.98
780.3			9.2	8.90	12.3	9.20
780.6	9.25				12.6	9.25
780.6		9.15			12.6	9.15
780.7	9.14				12.7	9.14
781.3				8.79		
781.6		9.13			13.6	9.13
781.7	9.13				13.7	9.13
781.7	9.09				13.7	9.09
781.7	9.24				13.7	9.24
782.3			9.3		14.3	9.30
782.4				8.95		
782.5		9.31			14.5	9.31
782.7	9.50				14.7	9.50
783.3				8.99		

Table A1 - 1.3 (Continued)

SN1937c	t_0 = JD2428768.0					m_0 = 8.4
Date	Baade & Zwicky (60) m_{pg}	Parenago (57) m_{pg}	Deutsch (61) m_{pg}	Beyer (126) m_{vis}	t	m_{pg}
JD2428783.4				9.09		
783.5		9.55			15.5	9.55
783.7	9.54				15.7	9.54
783.7	9.55				15.7	9.55
JD2428784.3				9.03		
784.4		9.55			16.4	9.55
784.6	9.58				16.6	9.58
784.6	9.55				16.6	9.55
785.4				9.19		
785.5		9.72			17.5	9.72
785.6	9.78				17.6	9.78
785.6	9.77				17.6	9.77
786.3			9.9		18.3	9.90
786.3				9.21		
786.6	9.81				18.6	9.81
786.6	9.89				18.6	9.89
786.6		9.87			18.6	9.87
787.3			9.9		19.3	9.90
787.3				9.26		
787.6	9.93				19.6	9.93
787.6	9.93				19.6	9.93
787.6		9.92			19.6	9.92
788.3			10.0		20.3	10.00
788.6	10.08				20.6	10.08
788.6	10.30				20.6	10.30
788.6		10.08			20.6	10.08
788.7	9.92				20.7	9.92

Table A1 - 1.3 (Continued)

SN1937c	t_0 = JD2428768.0					m_0 = 8.4
Date	Baade & Zwicky(60) m_{pg}	Parenago (57) m_{pg}	Deutsch (61) m_{pg}	Beyer (126) m_{vis}	t	m_{pg}
JD2428789.6	10.11				21.6	10.11
789.6	10.45				21.6	10.45
789.6		10.27			21.6	10.27
789.7	10.24				21.7	10.24
790.3				9.49		
790.6	10.22				22.6	10.22
790.6	10.37				22.6	10.37
790.6		10.30			22.6	10.30
790.7	10.32				22.7	10.32
791.6	10.37				23.6	10.37
791.6	10.54				23.6	10.54
JD2428791.6		10.46			23.6	10.46
792.6	10.56				24.6	10.56
792.6	10.41				24.6	10.41
792.6		10.48			24.6	10.48
793.4				9.67		
793.6	10.52				25.6	10.52
793.6	10.56				25.6	10.56
793.6		10.54			25.6	10.54
794.3				9.72		
794.6	10.79				26.6	10.79
794.6	10.68				26.6	10.68
794.6		10.74			26.6	10.74
797.3		10.7		9.80	29.3	10.70
798.0		11.0			30.0	11.00
798.3			11.0	9.91	30.3	11.00
799.6	11.12				31.6	11.12

Table A1 - 1.3 (Continued)

SN1937c t_0 = JD2428768.0 m_0 = 8.4

Date	Baade & Zwicky(60) m_{pg}	Parenago (57) m_{pg}	Deutsch (61) m_{pg}	Beyer (126) m_{vis}	t	m_{pg}
JD2428799.6	11.31				31.6	11.31
799.6		11.22			31.6	11.22
800.3				10.3		
800.6	11.25				32.6	11.25
800.6	11.19				32.6	11.19
800.6		11.18			32.6	11.18
801.3				10.20		
801.6	11.30				33.6	11.30
801.6	11.16				33.6	11.16
801.6		11.23			33.6	11.23
802.5		11.31			34.5	11.31
802.6	11.27				34.6	11.27
802.6	11.25				34.6	11.25
803.3			11.3		35.3	11.30
803.5		11.32			35.5	11.32
803.6	11.31				35.6	11.31
803.6	11.26				35.6	11.26
804.3			11.4	10.33	36.3	11.40
JD2428804.5		11.35			36.5	11.35
804.6	11.33				36.6	11.33
805.3		11.40			37.3	11.40
805.3			11.4		37.3	11.40
806.3				10.36		
806.6	11.29				38.6	11.29
806.6	11.31				38.6	11.31
806.6		11.30			38.6	11.30
807.2			11.4		39.2	11.40

Table A1 - 1.3 (Continued)

SN1937c	t_0 = JD2428768.0				m_0 = 8.4	
Date	Baade & Zwicky(60) m_{pg}	Parenago (57) m_{pg}	Deutsch (61) m_{pg}	Meyer (126) m_v	t	m_{pg}
JD2428807.3				10.48		
807.5		11.40			39.5	11.40
807.6	11.42				39.6	11.42
807.6	11.39				39.6	11.39
808.5		11.43			40.5	11.43
808.6	11.36				40.6	11.36
808.6	11.35				40.6	11.35
809.2			11.5		41.2	11.50
809.3		11.50			41.3	11.50
810.2			11.5		42.2	11.50
810.4		11.51			42.4	11.51
810.6	11.52				42.6	11.52
811.2		11.5			43.2	11.50
811.2			11.5		43.2	11.50
812.2		11.5			44.2	11.50
812.2			11.5		44.2	11.50
812.3				10.59		
813.3				10.56		
813.6	11.46	11.46			45.6	11.46
814.2		11.50	11.5		46.2	11.50
814.3				10.72		
815.6	11.62	11.62			47.6	11.62
817.3				10.74		
818.3				10.74		
818.6	11.72	11.72			50.6	11.72
819.3		11.70		10.76	51.3	11.70
820.6	11.86	11.86			52.6	11.86
822.3				10.89		

Table A1 - 1.3 (Continued)

SN1937c t_0 = JD2428768.0 m_0 = 8.4

Date	Baade & Zwicky (60) m_{pg}	Parenago (57) m_{pg}	Deutsch (61) m_{pg}	Beyer (126) m_{vis}	t	m_{pg}
JD2428826.2		11.9	11.9		58.2	11.90
827.2				11.12		
829.3				11.19		
830.2		11.8	11.8		62.2	11.80
831.0	11.94				63.0	11.94
831.1		11.92			63.1	11.92
831.2			11.9	11.03	63.2	11.90
833.0	12.03	12.03			65.0	12.03
833.2				11.13		
836.6		12.00			68.6	12.00
837.0	12.02				69.0	12.02
840.2				11.26		
340.6				11.22		
842.0	12.05				74.0	12.05
842.0		12.07			74.0	12.07
842.1			12.1		74.1	12.10
853.6				11.62		
854.6				11.71		
862.9	12.38	12.38			94.9	12.38
865.0	12.40				97.0	12.40
865.0	12.46				97.0	12.46
865.0	12.42				97.0	12.42
865.0	12.43	12.43			97.0	12.43
865.6				11.93		
866.0	12.49				98.0	12.49
866.0	12.43				98.0	12.43
866.0		12.46			98.0	12.46

Table A1 - 1.3 (Continued)

SN1937c	t_0 = JD2428768.0					m_0 = 8.4
Date	Baade & Zwicky (60) m_{pg}	Parenago (57) m_{pg}	Deutsch (61) m_{pg}	Beyer (126) m_{vis}	t	m_{pg}
JD2428871.9	12.47	12.47			103.9	12.47
873.9	12.47	12.47			105.9	12.47
879.8		12.60			111.8	12.60
JD2428880.9	12.64				112.9	12.64
880.9		12.60			112.9	12.60
895.9	13.13				127.9	13.13
896.0	13.15				128.0	13.15
896.0	13.15				128.0	13.15
896.0	13.11				128.0	13.11
896.0		13.14			128.0	13.14
897.0	13.03	13.03			129.0	13.03
898.9		13.12			130.9	13.12
899.0	13.13				131.0	13.13
904.9	13.13	13.13			136.9	13.13
906.9	13.05	13.05			138.9	13.05
907.9	13.17	13.17			139.9	13.17
908.5			13.2		140.5	13.20
908.7		13.30			140.7	13.30
908.9	13.39				140.9	13.39
910.0	13.23	13.23			142.0	13.23
910.9	13.30	13.30			142.9	13.30
921.9	13.48	13.48			153.9	13.48
923.4				13.17		
926.5				13.12		
929.5				13.07		
934.8		14.00			166.8	14.00
935.6				13.13		

Table A1 - 1.3 (Continued)

SN1937c t_0 = JD2428768.0 m_0 = 8.4

Date	Baade & Zwicky (60) m_{pg}	Parenago (57) m_{pg}	Deutsch (61) m_{pg}	Beyer (126) m_{vis}	t	m_{pg}
JD2428937.8		13.60			169.8	13.60
946.3		14.00	14.0		178.3	14.00
947.8	13.65	13.65			179.8	13.65
948.4				13.24		
949.4				13.29		
949.8	13.71	13.71			181.8	13.71
950.3			14.0		182.3	14.00
950.5				13.39		
950.6		13.86			182.6	13.86
950.8	13.72				182.8	13.72
JD2428951.4			13.9		183.4	13.90
951.6		13.80			183.6	13.80
951.8	13.71				183.8	13.71
952.5				13.39		
952.8	14.13	14.13			184.8	14.13
953.8	14.13				185.8	14.13
954.0		14.12			186.0	14.12
954.5				13.44		
954.8	13.92				186.8	13.92
955.0		14.01			187.0	14.01
955.6			13.8	13.44	187.6	13.80
955.8	13.94				187.8	13.94
956.0		13.96			188.0	13.96
960.4		14.0	14.0		192.4	14.00
963.6		14.05			195.6	14.05
963.9	14.10				195.9	14.10
967.5		14.1	14.1		199.5	14.10

Table A1 - 1.3 (Continued)

SN1937c t_0 = JD2428768.0 m_0 = 8.4

Date	Baade & Zwicky (60) m_{pg}	Parenago (57) m_{pg}	Deutsch (61) m_{pg}	Beyer (126) m_{vis}	t	m_{pg}
JD2428978.4				13.56		
981.3			14.3		213.3	14.30
981.6		14.31			213.6	14.31
981.8	14.32				213.8	14.32
982.4		14.3	14.3		214.4	14.30
983.8		14.3			215.8	14.30
985.7	14.35				217.7	14.35
985.7		14.37			217.7	14.37
988.7	14.34				220.7	14.34
988.7	14.44				220.7	14.44
988.7		14.39			220.7	14.39
989.7	14.21	14.21			221.7	14.21
990.4				13.79		
990.8	14.57	14.57			222.8	14.57
992.8	14.66	14.66			224.8	14.66
994.8		14.3			226.8	14.30
JD2429007.4		14.7	14.7		239.4	14.70
JD2429010.8	14.68	14.68				
012.5			14.9			
012.6		14.90				
012.7	14.90					
016.5				14.00		
017.4		14.75				
020.3		15.0	15.0			
020.4				14.06		
024.6	15.07	15.07				
026.5		15.0	15.0			

Table A1 - 1.3 (Continued)

SN1937c	t_0 = JD2428768.0					m_0 = 8.4
Date	Baade & Zwicky (60) m_{pg}	Parenago (57) m_{pg}	Deutsch (61) m_{pg}	Beyer (126) m_{vis}	t	m_{pg}
JD2429038.5				14.1		
040.8	15.28	15.28				
048.8	15.57	15.57				
049.8	15.57	15.57				
058.0		15.6				

Table A1 - 1.4

SN1937d t_0 = JD2428792.0 m_0 = 12.8

Date	Baade & Zwicky (60) m_{pg}	Wachmann (60) m_{pg}	Parenago (57) m_{pg}	Beyer (126) m_{vis}	t	m_{pg}
JD2428776.8			12.70		-15.?	12.70
777.8			12.40		-14.2	12.40
782.6		13.73			- 9.4	13.73
782.8			13.00		- 9.2	13.00
784.5		13.28			- 7.5	13.28
787.8	12.98		12.98		- 4.2	12.98
788.8	13.01				- 3.2	13.01
788.8			13.06		- 3.2	13.06
788.9	13.12				- 3.1	13.12
789.8	13.16		13.16		- 2.2	13.16
790.8	12.85				- 1.2	12.85
790.8			12.84		- 1.2	12.84
790.9	12.84				- 1.1	12.84
791.8			12.84		- 0.2	12.84
791.9	12.67				- 0.1	12.67
791.9	12.89				- 0.1	12.89
792.7			12.97		0.7	12.97
792.9	12.90				0.9	12.90
793.9	13.11		13.11		1.9	13.11
794.5				12.16		
794.9	13.00		13.00		2.9	13.00
795.3				12.18		
795.8			13.00		3.8	13.00
795.9	13.00				3.9	13.00
796.7			13.00		4.7	13.00
797.3				(11.9)		
797.6			13.03		5.6	13.03

Table A1 - 1.4 (Continued)

SN1937d t_0 = JD2428792.0 m_0 = 12.8

Date	Baade & Zwicky (60) m_{pg}	Wachmann (60) m_{pg}	Parenago (57) m_{pg}	Beyer (126) m_{vis}	t	m_{pg}
JD2428798.3				12.59		
798.5				12.52		
798.8			13.20		6.8	13.20
799.7	13.19				7.7	13.19
JD2428799.7	12.93				7.7	12.93
799.7			13.07		7.7	13.07
800.3				12.56		
800.7	13.10				8.7	13.10
800.7			13.20		8.7	13.20
801.3				12.60		
801.7	13.39				9.7	13.39
801.7			13.30		9.7	13.30
801.8	13.20				9.8	13.20
802.5			13.68		10.5	13.68
802.7	13.69				10.7	13.69
803.5			13.67	12.93	11.5	13.67
803.7	13.66				11.7	13.66
804.4				13.05		
804.5			13.81		12.5	13.81
804.8	13.79				12.8	13.79
805.8	13.90		13.90		13.8	13.90
806.4				13.11		
806.5				13.11		
806.6			14.01		14.6	14.01
807.4				13.17		
807.7			14.20		15.7	14.20
807.9	14.26				15.9	14.26

Table A1 - 1.4 (Continued)

SN1937d	t_0 = JD2428792.0					m_0 = 12.8
Date	Baade & Zwicky (60) m_{pg}	Wachmann (60) m_{pg}	Parenago (57) m_{pg}	Beyer (126) m_{vis}	t	m_{pg}
JD2428808.6			14.21		16.6	14.21
808.8	14.27				16.8	14.27
808.9	14.27				16.9	14.27
809.6			14.35		17.6	14.35
810.5			14.30		18.5	14.30
811.6			14.35		19.6	14.35
812.3				13.46		
812.7	14.68				20.7	14.68
812.8			14.64		20.8	14.64
812.9	14.61				20.9	14.61
813.3				13.47		
813.9	14.61				21.9	14.61
JD2428813.9			14.62		21.9	14.62
814.0	14.64				22.0	14.64
814.3				13.52		
814.6			14.64		22.6	14.64
814.7	14.71				22.7	14.71
815.5			14.90		23.5	14.90
816.5				13.74		
816.5				13.76		
817.4				13.84		
818.5				13.82		
819.2			15.13		27.2	15.13
820.8	15.03		15.03		28.8	15.03
821.7			15.20		29.7	15.20
822.4				13.87		
822.5			15.33		30.05	15.33

Table A1 - 1.4 (Continued)

SN1937d t_0 = JD2428792.0 m_0 = 12.8

Date	Baade & Zwicky (60) m_{pg}	Wachmann (60) m_{pg}	Parenago (57) m_{pg}	Beyer (126) m_{vis}	t	m_{pg}
JD2428824.7			15.30		32.7	15.30
829.3				(13.5)		
830.4				13.98		
830.5			15.80		38.5	15.80
831.5				~14.0		
832.5			15.63		40.5	15.63
834.2			15.75		42.2	15.75
834.3				(13.8)		
837.2			15.73		45.2	15.73
838.8			15.69		46.8	15.69
838.9	15.80				46.9	15.80
838.9	15.68				46.9	15.68
840.5				14.16		
840.8	15.69				48.8	15.69
840.8			15.71		48.8	15.71
840.9	15.73				48.9	15.73
844.7			16.20		52.7	16.20
847.3				(14.1)		
848.7			16.20		56.7	16.20
861.7			16.50		69.7	16.50
JD2428863.7	16.42		16.42		71.7	16.42
865.7	16.47		16.47		73.7	16.47
872.6	16.55				80.6	16.55
872.7			16.52		80.7	16.52
895.6	16.93				103.6	16.93
895.7			16.94		103.7	16.94
895.8	16.95				103.8	16.95

Table A1 - 1.4 (Continued)

SN1937d	t_0 = JD2428792.0					m_0 = 12.8
Date	Baade & Zwicky (60) m_{pg}	Wachmann (60) m_{pg}	Parenago (57) m_{pg}	Beyer (126) m_{vis}	t	m_{pg}
JD2428897.8	16.91		16.91		105.8	16.91
898.7	16.99		16.99		106.7	16.99
929.8	17.05		17.05		137.8	17.05
954.6	17.41		17.41		162.6	17.41
955.6	17.42		17.42		163.6	17.42
990.6	17.43		17.43		198.6	17.43

Table A1 - 1.5

SN1939a t_0 = JD2429290.0 m_0 = 12.60

Date	Hoffleit (63) m_{pg}	Giclas (62) m_{pg}	Baade (48) m_{pg}	Beyer (126) m_{vis}	t	m_{pg}
JD242928[illegible]			14.8		-9.0	14.8
282			13.4		-8.0	13.4
284	12.5				-6.0	13.0
284			12.8		-6.0	12.8
286	12.2		12.7		-4.0	12.7
287			12.7		-3.0	12.7
287.9		12.8			-2.1	12.9
288.7				12.35		
288.9		13.0			-1.1	13.0
289	12.5				-1.0	13.0
289.6				12.24		
289.9		12.8			-0.1	12.8
290			12.6		0.0	12.6
290.9		12.8			0.9	12.8
291	12.3				1.0	12.8
291	11.8				1.0	12.3
292.9		12.9			2.9	12.9
293.5				12.25		
294			12.6		4.0	12.6
294			12.7		4.0	12.7
297.0		13.1			7.0	13.1
297			12.8		7.0	12.8
304.8		14.0			14.8	14.0
306			14.7		16.0	14.7
306.9		14.3			16.9	14.3
307		14.6			17.0	14.6
308.6				13.79		

Table A1 - 1.5 (Continued)

SN1939a	t_0 = JD2429290.0				m_c = 12.60	
Date	Hoffleit (63) m_{pg}	Giclas (62) m_{pg}	Baade (48) m_{pg}	Beyer (126) m_{vis}	t	m_{pg}
JD2429308.8		14.6			18.8	14.6
309			14.8		19.0	14.8
310.9		14.6			20.9	14.6
315.8		15.0			25.8	15.0
316.8		14.7			26.8	14.7
JD2429318			15.2		28.0	15.2
343			15.6		53.0	15.6
344			15.5		54.0	15.5
347			15.7		57.0	15.7
375			16.2		85.0	16.2
399			16.7		109.0	16.7
400			16.7		110.0	16.7
431			17.0		141.0	17.0
432			17.1		142.0	17.1
458			17.7		168.0	17.7

Table A1 - 1.6

SN1939b t_0 = JD2429385.0 m_0 = 11.8

Date	Shapley (64) m_{pg}	Baade (48) m_{pg}	t	m_{pg}
JD2429376		13.9	-9	13.9
4/23/39	13.6		-8	13.6
JD2429379	12.7	12.7	-6	12.7
5/6/39	12.2		5	12.2
5/6/39	12.1		5	12.1
5/7/39	12.6		6	12.6
JD2429391		12.2	6	12.2
5/8/39	12.9		7	12.9
JD2429392		12.6	7	12.6
393		13.0	8	13.0
5/10/39	13.5		9	13.5
5/11/39	13.2		10	13.2
JD2429395		13.5	10	13.5
395		13.8	10	13.8
5/12/39	13.6		11	13.6
5/12/39	13.3		11	13.3
JD2429396	13.7		11	13.7
396	14.0		11	14.0
5/13/39	13.7		12	13.7
JD2429397		14.2	12	14.2
5/14/39	13.9		13	13.9
JD2429398		14.1	13	14.1
5/15/39	13.8		14	13.8
5/16/39	13.7		15	13.7
5/16/39	13.8		15	13.8

Table A1 - 1.6 (Continued)

SM1939b	t_0 = JD2429385.0			m_0 = 11.8
Date	Shapley (64) m_{pg}	Baade (48) m_{pg}	t	m_{pg}
JD2429402		15.3	17	15.3
403		15.2	18	15.2
406		15.3	21	15.3
424		15.9	39	15.9
427		16.2	42	16.2
428		16.1	43	16.1
JD2429430		16.2	45	16.2
432		16.2	47	16.2
435		16.1	50	16.1
437		16.3	52	16.3
458		16.3	73	16.3
458		16.4	73	16.4
612		18.8	227	18.8

Table A1 - 1.7

SN1954a t_0 = JD2434851.0 m_0 = 9.50

Date	Wild (65) m_{pg}	Hoffmeister (66) m_{pg}	Pietra (65, 66) m_{pg}	Beyer (128) m_{pv}	t	m_{pg}
JD2434843.0		10.8			-8.0	10.8
855.9		10.1			4.9	10.1
857.9		10.4			6.9	10.4
867.4			11.7		16.4	11.7
888.9		12.4			37.9	12.4
5/30/54, 7^h 09^m	12.43				42.3	12.43
5/31/54, 9 35	12.32				43.4	12.32
6/1/54, 5 15	12.66				44.2	12.66
6/1/54, 7 11	12.59				44.3	12.59
6/2/54, 5 03	12.57				45.2	12.57
6/2/54, 6 08	12.65				45.3	12.65
6/2/54, 6 51	12.56				45.3	12.56
6/2/54, 7 25	12.66				45.3	12.66
6/4/54				11.8		
6/4/54, 5^h 20^m	12.67				47.2	12.67
6/4/54, 6 00	12.68				47.3	12.68
6/4/54, 6 11	12.67				47.3	12.67
6/4/54, 6 27	12.69				47.3	12.69
6/5/54				11.8		
JD2434899.4			12.2		48.4	12.2
6/6/54				11.9		
JD2434900.4			12.4		49.4	12.4
901.4			12.5		50.4	12.5
6/8/54				11.9		

Table A1 - 1.7 (Continued)

SN1954a	t_0 = JD2434851.0					m_0 = 9.50
Date	Wild (65) m_{pg}	Hoffmeister (66) m_{pg}	Pietra (65, 66) m_{pg}	Beyer (128) m_{pv}	t	m_{pg}
JD2434902.4			12.4		51.4	12.4
6/9/54, 6^h 00^m	12.76				52.3	12.76
6/10/54				12.0		
6/10/54, 7^h 55^m	12.75				53.3	12.75
6/11/54				12.0		
6/11/54, 4^h 42^m	12.72				54.2	12.72
6/12/54, 7 55	12.69				55.3	12.69
6/13/54				12.1		
6/14/54				12.0		
6/16/54				12.1		
6/17/54, 7^h 12^m	12.82				60.3	12.82
JD2434915.4			12.6		64.4	12.6
6/22/54				12.2		
JD2434916.4			12.4		65.4	12.4
919.4			12.9		68.4	12.9
6/27/54				12.3		
6/28/54				12.2		
JD2434922.4			12.9		71.4	12.9
6/30/54				12.3		
6/30/54, 5^h 56^m	13.01				73.2	13.01
JD2434924.4			12.8		73.4	12.8
7/1/54				12.3		
7/2/54				12.4		

Table A1 - 1.7 (Continued)

SN1954a	t_0 = JD2434851.0					m_0 = 9.50
Date	Wild (65) m_{pg}	Hoffmeister (66) m_{pg}	Pietra (65, 66) m_{pg}	Beyer (128) m_{pv}	t	m_{pg}
JD2434926.4			13.0		75.4	13.0
7/5/54				12.4		
7/6/54				12.4		
7/9/54, 4^h 36^m	13.19				82.2	13.19
7/10/54				12.4		
JD2434945.4			13.3		94.4	13.3
947.4			13.1		96.4	13.1
948.4			13.5		97.4	13.5
953.4			13.2		102.4	13.2
7/31/54, 4^h 45^m	13.42				104.2	13.42
JD2434957.4			13.9		106.4	13.9
959.4			13.8		108.4	13.8
8/5/54, 4^h 00^m	13.48				109.2	13.48
JD2434961.4			13.9		110.4	13.9
8/29/54, 3^h 35^m	14.03				133.1	14.03
8/29/54, 4 20	14.39				133.2	14.39
JD2434987.3			14.2		136.3	14.2
10/25/54, 12^h 34^m	15.11				190.5	15.11
JD2435043.6			15.6		192.6	15.6
050.6			15.7		199.6	15.7
067.6			15.8		216.6	15.8
JD2435096.6			16.4			
100.6			16.3			
101.6			16.4			

Table A1 - 1.7 (Continued)

SH1954e	t_0 = JD2434851.0				m_0 = 9.50	
Date	Wild (65) m_{pg}	Hoffmeister (66) m_{pg}	Pietra (65, 66) m_{pg}	Beyer (128) m_{pv}	t	m_{pg}
1/28/55, 9^h 39^m	16.88					
2/14/55, 9 23	17.08					
3/2/55, 10 34	17.58					
JD2435185.5		17.7				
3/27/55, 8^h 12^m	17.66					

Table A1 - 1.8

SN1954b t_0 = 5/3/54 m_0 = 12.50

Date		Wild (65) m_{pg}	Pietra (65, 66) m_{pg}	Wild (65) B-V	t	m_{pg}
5/2/54	8^h 11^m	12.44			-0.7	12.44
5/3/54	8 37	12.75			0.4	12.75
	8 46	12.88			0.4	12.88
5/4/54	8 59	12.65			1.4	12.65
	9 37	12.57			1.4	12.57
5/5/54	5 41	12.45			2.2	12.45
	6 11	12.67			2.3	12.67
	6 33	12.62			2.3	12.62
	6 36	12.78			2.3	12.78
	7 15	12.98			2.3	12.98
5/6/54	9 44	13.02			3.4	13.02
5/7/54	10 30	13.33			4.4	13.33
5/8/54	6 53	13.07			5.3	13.07
JD2434871.4			13.6		5.4	13.6
5/9/54	7^h 45^m	13.03		0.27	6.3	13.03
	8 25	13.30			6.4	13.30
	8 30	13.19			6.4	13.19
	8 53	13.05			6.4	13.05
	9 20	13.46			6.4	13.46
5/10/54	5 50	13.06		0.20	7.2	13.06
	8 00	12.95			7.3	12.95
	9 53	13.52			7.4	13.52
5/11/54	5 50	13.20		0.36	8.2	13.20
5/12/54	5 36	13.24		0.26	9.2	13.24
5/21/54	5 16	14.22			18.2	14.22
	5 32	14.36			18.2	14.36

Table A1 - 1.8 (Continued)

SN1954b		t_0 = 5/3/54			m_J = 12.50	
Date		Wild (65) m_{pg}	Pietra (65, 66) m_{pg}	Wild (65) B-V	t	m_{PG}
5/22/54	5 23	14.43			19.2	14.43
	5 28	14.63			19.2	14.63
	6 05	13.71			19.3	13.71
	6 35	14.54			19.3	14.54
5/24/54	6 54	14.68			21.3	14.68
5/24/54	7^h 00^m	14.75			21.3	14.75
	7 13	14.57			21.3	14.57
JD2434888.4			14.3		22.4	14.3
5/26/54	7^h 28^m	15.24			23.3	15.24
JD2434889.4			14.4		23.4	14.4
5/28/54	7^h 47^m	15.26			25.3	15.26
JD2434892.4			15.2		26.4	15.2
5/30/54	7^h 18^m	15.32		1.05	27.3	15.37
5/31/54	8 20	15.36			28.3	15.36
JD2434895.4			15.3		29.4	15.3
6/2/54	7^h 53^m	15.63			30.3	15.63
JD2434896.4			15.3		30.4	15.3
899.5			15.4		33.5	15.4
900.5			15.5		34.5	15.5
902.4			15.4		36.4	15.4
6/11/54	5^h 04^m	15.65			39.2	15.65
JD2434915.4			15.4		49.4	15.4
919.4			15.5		53.4	15.5
6/28/54	8^h 02^m	15.79			56.3	15.79

Table A1 - 1.8 (Continued)

SN1954b	t_0 = 5/3/54			m_0 = 12.50	
Date	Wild (65) m_{PG}	Pietra (65, 66) m_{PG}	Wild (65) B-V	t	m_{PG}
JD2434922.4		15.6		56.4	15.6
923.4		15.7		57.4	15.7
7/2/54 $7^h\ 58^m$	15.97			60.3	15.97
JD2434926.5		15.8		60.5	15.8
7/9/54 $4^h\ 45^m$	16.11			67.2	16.11
JD2434945.4		16.2		79.4	16.2
948.4		16.0		82.4	16.0
949.4		15.9		83.4	15.9
7/31/54 $5^h\ 10^m$	16.53			89.2	16.53
JD2434955.4		16.2		89.4	16.2
8/1/54 $5^h\ 30^m$	16.17			90.2	16.17
JD2434958.4		16.2		92.4	16.2
8/26/54 $3^h\ 48^m$	16.96			115.2	16.96

Table A1 - 1.9

SN1955b	t_0 = 10/3/55	m_0 = 15.7
Date	t	Zwicky (67) m_{pg}
9/22/55	-11	17.6
10/11/55	8	16.3
10/12/55	9	16.4
10/24/55	21	17.9
11/18/55	46	19.8
12/15/55	73	21.4

Table A1 - 1.9

SN1955b	t_0 = 10/3/55		m_0 = 15.70
Date	Zwicky (67) m_{pk}	t	m_{pg}
9/22/55	17.6	-11	17.6
10/11/55	16.3	8	16.3
10/12/55	16.4	9	16.4
10/24/55	17.9	21	17.9
11/18/55	19.8	46	19.8
12/15/55	21/4	73	21.4

Table A1 - 1.10

SN1956a		t_0 = 3/14/56		m_0 = 12.20	
Date		Zwicky and Karpowicz (68)		t	m_{pg}
		m_{pg}	m_{pv}		
3/8/56	9^h 13^m	13.08		-5.6	13.08
3/31/56	3 10	13.30		17.1	13.30
	3 33		13.11		
	7 15		13.25		
4/4/56	3 56	14.38		21.2	14.38
	4 57	13.89		21.2	13.89
	5 02		13.14		
	6 33		13.20		
4/5/56	4 36	14.08		22.2	14.08
4/6/56	5 29		13.20		
4/7/56	4 09	14.24		24.2	14.24
	7 57	14.43		24.3	14.43
4/9/56	10 55	14.72		26.5	14.72
4/17/56	—	15.07		34.0	15.07
5/1/56	4 38	15.40		48.2	15.40
	6 49	15.80		48.3	15.80
5/3/56	4 08	15.20		50.2	15.20
5/4/56	3 59		14.31		
5/16/56	9 29	15.93		63.4	15.93
6/3/56	5 14	15.90		81.2	15.90
6/16/56	8 19	15.88		94.3	15.88
7/10/56	5 55	16.12		118.2	16.12
8/1/56	5 17	16.25		140.2	16.25
8/6/56	4 44	16.74		145.2	16.74
10/6/56	11 57	17.50		206.5	17.50
10/31/56	10 34	17.60		231.4	17.60
12/4/56	12 36	18.6			

Table A1 - 1.10 (Continued)

SN1956a		t_0 = 3/14/56		m_0 = 12.20
Date		Zwicky and Karpowicz (68)	t	m_{pg}
		m_{pg} m_{pv}		
12/5/56	9 27	18.7		
	9 40	18.8		
3/29/57	6 54	20.0		
4/25/57	6 47	21.2		
6/26/57	4 56	21.4		
6/26/57	5^h 29^m	21.4		
6/28/57	5 40	21.5		

Table A1 - 1.11

SN1957a			t_0 = 2/27/57					m_0 = 13.85
Date			Zwicky and Karpowicz (69)		Bertola (70)	Wenzel (71)	t	m_{pg}
			m_{pg}	m_{pv}	m_{pg}	m_{pg}		
2/26/57	4^h	27^m	15.2				-0.8	15.2
3/1/57	—		14.0				2.0	14.0
3/5/57	21	50				14.4	6.9	14.6
3/6/57	0	21				14.4	7.0	14.6
3/7/57	3	44	14.7				8.2	14.7
	4	37		13.8				
3/8/57	4	25	15.2				9.2	15.2
	4	52		13.9				
3/9/57	1	05				14.8	10.0	15.0
3/11/57	3	01				15.3	12.1	15.5
3/20/57	19	49				16.2	21.8	16.4
3/21/57	21	14				16.3	22.9	16.5
3/22/57	19	55				16.3	23.8	16.5
3/23/57	19	40				16.4	24.8	16.6
3/26/57	21	12				16.4	27.9	16.6
3/28/57	6	52		15.4				
	7	05	16.8				29.3	16.8
3/29/57	5	38		15.6				
	6	02	16.6				30.3	16.6
3/30/57	5	29	16.8				31.2	16.8
	6	50		15.4				
3/31/57	6	23	16.9				32.3	16.9
	6	30		15.4				
3/31/57	21	29				16.7	32.9	16.9
4/1/57	4	10	16.7				33.2	16.7
4/1/57	19	46				16.6	33.8	16.8
4/2/57	20	47				16.5	34.9	16.7

Table A1 - 1.11 (Continued)

SN1957a t_0 = 2/27/57 m_0 = 13.85

Date			Zwicky and Karpowicz (69) m_{pg}	Zwicky and Karpowicz (69) m_{pv}	Bertola (70) m_{pg}	Wenzel (71) m_{pg}	t	m_{pg}
4/3/57	21	31				16.4	35.9	16.6
4/4/57	22	33				16.6	36.9	16.8
4/9/57	20	47				16.6	41.9	16.8
4/16/57	20	42				17.1	48.9	17.3
4/18/57	23	09			17.40		51.0	17.40
4/22/57	23^h	23^m				17.3	55.0	17.5
4/23/57	0	15			17.45		55.0	17.45
4/23/57	22	42				17.3	55.9	17.5
4/23/57	22	43			17.40		55.9	17.40
4/25/57	5	39	17.3				57.2	17.3
	6	45		16.2				
4/26/57	23	25			17.65		59.0	17.65
4/29/57	0	15				17.3	61.0	17.5
4/29/57	5	28	17.2				61.2	17.2
5/2/57	1	00				17.4	64.0	17.6
5/3/57	5	50		16.6				
	6	24	17.5				65.3	17.5
5/5/57	1	53			17.75		67.1	17.75
5/5/57	7	25		16.4				
	7	43	17.8				67.3	17.8
5/22/57	23	30			18.00		85.0	18.00
5/29/57	22	36				17.9	91.9	18.1
5/30/57	4	29		17.2				
	4	46	18.1				92.2	18.1
6/1/57	22	40			18.20		94.9	18.20
6/1/57	23	42				17.9	95.0	18.1
6/27/57	4	39	18.3				120.2	18.3
6/27/57	4	46		17.4				

Table A1 - 1.12

SN1957b t_0 = 5/9/57 m_0 = 12.10

Date	Bertola (70) m_{pg}	Romano (75) m_{pg}	Gotz (72) m_{pg}	Li Tzin (73) m_{pg}	t	m_{pg}
JD2435952.3		14.0			-15.0	14.8
955.4		13.6			-12.0	14.4
957.4		13.0			-10.0	13.8
5/3/57 $22^h\ 35^m$			12.5		- 5.1	12.5
$23^h\ 06^m$			12.5		- 5.0	12.5
JD2435977.4		12.2			10.0	13.0
978.4		12.2			11.0	13.0
5/21/57 $23^h\ 17^m$	13.20				13.0	13.20
5/22/57 22 59	13.30				14.0	13.30
5/23/57 21 53			13.4		14.9	13.4
JD2435982.4		12.6			15.0	13.4
5/23/57 $23^h\ 31^m$			13.4		15.0	13.4
5/25/57 20 38				13.16	16.9	13.24
5/25/57 21 57			13.6		16.9	13.6
5/25/57 22 48			13.7		17.0	13.7
5/26/57 21 57			13.8		17.9	13.8
5/28/57 21 49			13.9		19.9	13.9
5/29/57 21 30			14.1		20.9	14.1
5/29/57 21 59				13.87	20.9	13.95
5/30/57 22 03			14.2		21.9	14.2
5/31/57 22 26				14.18	22.9	14.26
5/31/57 22 59			14.2		23.0	14.2
JD2435990.4		13.5			23.0	14.3
5/31/57 23 01	14.45				23.0	14.45
JD2435991.4		13.6			24.0	14.4
6/1/57 $23^h\ 06^m$	14.60				24.0	14.60

Table A1 - 1.12 (Continued)

SN1957b t_0 = 5/9/57 m_J = 12.10

Date			Bertola (70) m_{pg}	Romano (75) m_{pg}	Gotz (72) m_{pg}	Li Tzin (73) m_{pg}	t	m_{pg}
6/2/57	21	13				14.96	24.9	14.96
6/2/57	22	16			14.6		24.9	14.6
JD2435992.4				13.6			25.0	14.4
6/6/57	23h	11m			14.3		29.0	14.3
6/8/57	21	35				14.98	30.9	15.06
6/12/57	21	49				15.06	34.9	15.14
6/16/57	21h	48m			14.7		38.9	14.7
6/17/57	21	30				15.22	39.9	15.30
6/17/57	22	46	15.20				39.9	15.20
6/17/57	23	12	15.15				40.0	15.15
6/18/57	21	18				15.56	40.9	15.64
6/20/57	22	11			15.4		42.9	15.4
6/28/56	20	40				15.61	50.9	15.69
6/28/57	21	51			15.5		50.9	15.5
6/28/57	22	30	15.60				50.9	15.60
6/29/57	21	30				15.59	51.9	15.67
7/4/57	20	51				15.49	56.9	15.57
7/4/57	22	36			15.6		56.9	15.6
7/9/57	20	30				15.53	61.9	15.61
7/9/57	20	39				15.54	61.9	15.62
7/16/57	20	47				15.61	68.9	15.69
7/19/57	20	46				15.90	71.9	15.98
7/20/57	22	01	15.90				72.9	15.90
7/21/57	20	48				15.97	73.9	16.05
7/30/57	21	46	16.00				82.9	16.00

Table A1 - 1.13

SN1959c			t_0 = 7/1/59			m_0 = 13.55	
			Mihalas (74)				
Date			m_{pg}	B	V	t	m_{pg}
6/28/59	21^h	20^m	13.55	14.1		-2.1	13.55
7/1/59	21	09	13.60	14.15		0.9	13.60
7/2/59	21	01	13.65	14.2		1.9	13.65
7/3/59	20	25	13.75	14.25		2.9	13.75
7/5/59	20	30	13.75	14.25		4.9	13.75
7/7/59	20	44		14.35	14.30	6.9	13.78
7/8/59	20	37		14.25	14.15	7.9	13.69
7/10/59	21	04		14.64	14.42	9.9	14.10
7/10/59	22	20	14.15	14.60		9.9	14.15
7/11/59	22	38	14.25	14.70		10.9	14.25
7/12/59	20	31		14.78	14.54	11.9	14.24
7/13/59	20	33		14.84	14.55	12.9	14.31
7/27/59	20	20	15.75	16.10		26.8	15.75
7/28/59	20	21		16.18	15.27	27.8	15.76
8/2/59	20	10	16.10	16.45		32.8	16.15
8/3/59	20	11		16.52	15.59	33.8	16.11
8/3/59	20	31	15.90	16.2		33.9	15.90
8/26/59	19	38	15.40	15.8		56.8	15.40
1/31/60	5	01		19.7			

Table A1 - 1.14

SN1960f t_0 = 4/16/60 z_c = 11.60

Date		Bertola (70) m_{pg}	Huth (76) m_{pg}	Kulikov (77) m_{pg}	Tempesti (78) m_{pg}	Mannino (79) m_{pg}	t	m_{pg}
4/14/60	9^h 06^m		10.6				-1.6	11.45
4/15/60	9 36		10.8				-0.6	11.65
4/16/60	9 51		11.1				0.4	11.95
4/19/60	9 36		10.8				3.4	11.65
4/20/60	9 36		10.8				4.4	11.65
JD2437046.4						11.53	5.4	11.53
4/21/60	20^h 17^m	11.6					5.8	11.6
JD2437047.3						11.74	6.3	11.74
4/22/60	19^h 55^m			11.42			6.8	11.84
JD2437048.4						12.05	7.4	12.05
049.4						12.16	8.4	12.16
050.5						12.10	9.5	12.10
4/25/60	20^h 24^m			11.55			9.8	11.97
4/26/60	19 55			11.91			10.8	12.33
4/27/60	19 41			11.62			11.8	12.04
JD2437056.5						12.52	15.5	12.52
5/1/60	21^h 00^m	12.55					15.9	12.55
JD2437057.4						12.68	16.4	12.68
5/3/60	0^h 00^m				12.10		17.0	12.71
JD2437058.4						12.78	17.4	12.78
069.3						13.68	28.3	13.68
070.4						14.05	29.4	14.05
5/16/60	22^h 21^m	14.10					30.9	14.10
JD2437072.4						14.11	31.4	14.11
5/17/60	19^h 26^m			13.56			31.8	13.98

Table A1 - 1.14 (Continued)

Sm1960f t_0 = 4/16/60 m_0 = 11.60

Date	Bertola (70) m_{pg}	Huth (76) m_{pg}	Kulikov (77) m_{pg}	Tempesti (78) m_{pg}	Mannino (79) m_{pg}	t	m_{pg}
JD2437073.4					14.21	32.4	14.21
5/19/60 $19^h\ 41^m$			13.53			33.8	13.95
JD2437075.4					14.27	34.4	14.27
076.4					14.37	35.4	14.37
5/21/60 $21^h\ 50^m$				13.75		35.9	14.36
JD2437077.4					14.42	36.4	14.42
5/22/60 $19^h\ 55^m$			13.92			36.8	14.34
JD2437078.5					14.42	37.5	14.42
5/23/60 $19^h\ 41^m$			14.02			37.8	14.44
JD2437079.4					14.53	38.4	14.53
5/24/60 $18^h\ 53^m$			14.10			38.8	14.52
JD2437080.4					14.48	39.4	14.48
5/25/60 $18^h\ 58^m$			14.26			39.8	14.68
5/26/60 21 36				14.05		40.9	14.66
5/26/60 22 58	14.48					41.0	14.48
JD2437082.4					14.60	41.4	14.60
5/28/60 $20^h\ 53^m$				13.85		42.9	14.46
JD2437085.4					14.75	44.4	14.75
5/30/60 $23^h\ 46^m$				14.05		45.0	14.66
JD2437086.4					14.75	45.4	14.75
6/1/60 $19^h\ 12^m$			14.30			46.8	14.72
JD2437098.4					15.05	57.4	15.05
JD2437099.4					14.97	58.4	14.97
6/13/60 $19^h\ 41^m$			14.64			58.8	15.06

Table A1 - 1.14 (Continued)

SN1960f t_0 = 4/16/60 m_0 = 11.50

Date	Bertola (70) m_{pg}	Huth (76) m_{pg}	Kulikov (77) m_{pg}	Tempesti (78) m_{pg}	Mannino (79) m_{pg}	t	m_{pg}
JD2437100.4					14.90	59.4	14.90
6,14/60 19^h 41^m			14.60			59.8	15.02
6/16/60 19 41			14.90			61.8	15.32
JD2437103.4					14.90	62.4	14.90
6/17/60 19^h 41^m			14.92			62.8	15.34
JD2437104.4					14.97	63.4	14.97
6/18/60 23^h 46^m				14.70		64.0	15.31
6/20/60 19 26			14.90			65.8	15.32
6/26/60 21 28	15.20					71.9	15.20
6/26/60 21 40	15.20					71.9	15.20
6/27/60 19 41			15.01			72.8	15.43
6/27/60 21 46	15.20					72.9	15.20
JD2437114.4					15.12	73.4	15.12
115.4					15.12	74.4	15.12
7/12/60 19^h 12^m			15.23			87.8	15.65

Table A1 - 1.15

SN1960r t_0 = 12/19/60 m_0 = 11.50

Date	Bertola (70) m_{pg}	Zaitseva (80) m_{pg}	Gates (81) B	Gates (81) V	t	m_{pg}
12/20/60			12.00		1.0	11.75
JD2437312.5		13.71			24.5	13.71
314.5		13.97			26.5	13.97
1/19/61 0^h 55^m	14.28				28.0	14.29
1/16/61			14.35	13.08	31.0	14.28
1/22/61 0 02	14.55				34.0	14.55
1/22/61 2 01	14.40				34.1	14.40
1/23/61 0 34	14.65				35.0	14.65
JD2437326.6		14.73			38.6	14.73
1/27/61 3^h 09^m	14.60				39.1	14.60
1/27/61 3 34	14.58				39.1	14.58
1/28/61 3 42	14.70				40.2	14.70
2/8/61 22 36	14.90				51.9	14.90
2/10/61 22 00	14.82				53.9	14.82
2/11/61 22 18	15.00				54.9	15.00
2/12/61 22 20	14.93				55.9	14.93
2/14/61 0 56	14.80				57.0	14.80
2/14/61 22 11	14.85				57.9	14.85
JD2437354.6		15.08			66.6	15.08
377.4		15.44			89.4	15.44
377.5		15.38			89.5	15.38
377.5		15.25			89.5	15.25
378.5		15.28			90.5	15.28
378.5		15.29			90.5	15.29
3/23/61 22^h 47^m	15.63				94.9	15.63
3/26/61 1 39	15.20				97.1	15.20

Table A1 - 1.15 (Continued)

SN1960r t_c = 12/19/60 m_0 = 11.50

Date			Bertola (70) m_{pg}	Zaitseva (80) m_{pg}	Gates (81) B	Gates (81) V	t	m_{pg}
4/6/61	23	04	15.57				109.0	15.57
4/7/61	23	39	15.60				110.0	15.60
4/8/61	23	28	15.65				111.0	15.65
JD2437405.3				15.90			117.3	15.90
4/19/61	20^h	41^m	15.80				121.9	15.80
4/19/61	23	55	15.78				122.0	15.78
5/2/61	19^h	47^m	15.90				134.8	15.90
5/5/61	21	56	16.03				137.9	16.03
5/7/61	22	37	15.93				139.9	15.93
5/7/61	23	25	15.90				140.0	15.90
5/9/61	23	06	15.95				142.0	15.95
5/10/61	23	21	15.98				143.0	15.98
5/13/61	0	25	16.05				145.0	16.05

Table A1 - 1.16

SN1961d	t_0 = 1/17/61			m_0 = 16.20
Date	Zwicky (82)		t	m_{pg}
	m_{pg}	m_{pv}		
12/22/60		21		
12/23/60		21.0		
12/24/60		20.4		
1/15/61		16.70	-2.0	16.23
1/21/61		16.95	4.0	16.64
1/24/61		17.05	7.0	16.83
2/11/61	18.75		25.0	18.75
2/13/61		18.20	27.0	18.96
2/21/61		18.50	35.0	19.41
2/22/61		18.45	36.0	19.36
2/23/61		18.45	37.0	19.35
3/11/61		18.80	53.0	19.55
3/11/61	19.55		53.0	19.54

Table A1 - 1.17

Sd1961h	t_0 = 5/8/61		m_0 = 11.20
Date	Romano (83) m_{pg}	t	m_{pg}
5/2/61	11.4	-6.0	11.4
5/5/61	11.3	-3.0	11.3
5/7/61	11.2	-1.0	11.2
5/9/61	11.2	1.0	11.2
5/10/61	10.9	2.0	10.9
5/11/61	11.3	3.0	11.3
5/12/61	11.4	4.0	11.4
5/18/61	11.8	10.0	11.8
6/1/61	12.7	24.0	12.7
6/2/61	13.0	25.0	13.0

Table A1 - 1.18

SN1961p		t_0 = 9/11/61		m_0 = 14.30
Date		Bertola (70) m_{pg}	t	m_{pg}
9/1/61	22^h 36^m	14.95	-9.1	14.95
9/3/61	21 14	14.63	-7.1	14.63
9/4/61	23 58	14.40	-6.0	14.40
9/6/61	23 24	14.50	-4.0	14.50
9/8/61	0 46	14.42	-3.0	14.42
9/9/61	23 02	14.05	-1.0	14.05
9/10/61	22 59	14.35	0.0	14.35
9/13/61	22 25	14.28	2.9	14.28
9/13/61	23 07	14.35	3.0	14.35
9/15/61	23 00	14.32	5.0	14.32
9/16/61	22 58	14.32	6.0	14.32
9/17/61	23 59	14.38	7.0	14.38
9/18/61	1 50	14.45	7.1	14.45
9/19/61	0 25	14.48	8.0	14.48
9/20/61	1 09	14.68	9.0	14.68
9/21/61	1 57	14.70	10.1	14.70
9/22/61	2 10	14.70	11.1	14.70
10/2/61	22 27	15.63	21.9	15.63
10/9/61	22 48	16.28	28.9	16.28
10/10/61	23 20	16.18	30.0	16.18
10/11/61	23 49	16.23	31.0	16.23
10/31/61	21 03	17.12	50.9	17.12
11/1/61	19 19	17.30	51.8	17.30
11/1/61	19 58	17.30	51.8	17.30
11/2/61	23 40	17.25	53.0	17.25
11/5/61	18 07	17.20	55.8	17.20
11/10/61	23 12	17.32	61.0	17.32

Table A1 - 1.18 (Continued)

SN1961p t_0 = 9/11/61 m_0 = 14.30

Date			Bertola (70) m_{pg}	t	m_{pg}
11/14/61	22	15	17.30	64.9	17.30
11/15/61	22	18	17.30	65.9	17.30
11/15/61	22	55	17.25	66.0	17.25
11/17/61	1	18	17.35	67.1	17.35
11/17/61	19	03	17.35	67.8	17.35
11/18/61	1^h	17^m	17.52	68.1	17.52
11/19/61	2	13	17.55	69.1	17.55
11/28/61	17	36	17.50	78.7	17.50
12/8/61	20	22	17.48	88.8	17.48
12/11/61	17	13	17.75	91.7	17.75
12/12/61	17	46	17.65	92.7	17.65
12/15/61	0	42	17.90	95.0	17.90
1/6/62	17	22	18.00	117.7	18.00
1/8/62	17	44	17.90	119.7	17.90
1/8/62	21	55	17.95	119.9	17.95
1/24/62	18	41	18.10	135.8	18.10
1/25/62	19	09	18.10	136.8	18.10
1/31/62	18	47	18.10	142.8	18.10
2/6/62	21	37	18.42	148.9	18.42

Table A1 - 1.19

SN1962a			t_0 = 1/15/62			m_0 = 15.60
Date			Zwicky and Barbon (84)		t	m_{PE}
			m_{BK}	m_{PV}		
1/6/62	10^h	54^m		18.65	-8.5	18.06
1/8/62	10	20		18.10	-6.6	17.56
1/9/62	10	43	17.64		-5.5	17.64
1/9/62	10	58		17.84	-5.5	17.32
2/2/62	9	50		16.05	18.4	16.34
2/3/62	10	48	16.25		19.5	16.25
2/3/62	11	04		15.86	19.5	16.21
3/2/62	10	08		17.24	46.4	18.11
3/6/62	7	51		17.87	50.3	18.70
3/28/62	6	37	18.70		72.3	18.70
3/29/62	7	15		18.47	73.3	19.04
3/31/62	8	20	18.85		75.3	18.85
4/8/62	8	00		18.67	83.3	19.12
5/1/62	5	46	19.20		106.2	19.20
5/3/62	8	25		19.22	108.4	19.40
5/5/62	4	50		19.22	110.2	19.38
5/6/62	7	24	19.49		111.3	19.49
5/29/62	7	10		20.00	134.3	19.92
5/30/62	5	27	19.56		135.2	19.56
6/30/62	6	12	19.44		166.3	19.44

Table A1 - 1.20

SN1962e			t_0 = 2/19/62		m_0 = 16.40	
Date			Rudnicki and Zwicky (85)		t	m_{pg}
			m_{pg}	m_{pv}		
3/2/62	9^h	46^m		17.5	11.4	17.37
3/6/62	7	30		17.8	15.3	17.85
3/28/62	4	06	19.4		37.2	19.4
3/28/62	4	31		19.0	37.2	19.85
3/29/62	6	07		18.7	38.3	19.54
4/9/62	7	44		19.0	49.3	19.74
4/29/62	5	42		18.8	69.2	19.32

Table A1 - 1.21

SH1962j		t_0 = 9/2/62		m_0 = 13.00
Date		Bertola (86) m_{pg}	t	m_{pg}
8/30/62	22^h 20^m	13.65	-2.1	13.65
9/3/62	20 37	13.65	1.9	13.65
9/5/62	20 42	13.85	3.9	13.85
9/8/62	22 40	13.95	6.9	13.95
9/18/62	18 38	14.66	16.8	14.66
9/20/62	18 40	14.64	18.8	14.64
9/24/62	20 45	15.15	22.9	15.15
9/25/62	18 29	15.32	23.8	15.32
9/30/62	20 55	15.74	28.9	15.74
10/4/62	18 32	15.95	32.8	15.95
10/19/62	19 04	16.36	47.8	16.36
10/22/62	18 16	16.48	50.8	16.48
10/24/62	19 30	16.45	52.8	16.45
10/26/62	18 20	16.50	54.8	16.50
11/2/62	17 43	16.60	61.7	16.60
11/16/62	17 21	16.80	75.7	16.80
11/23/62	17 27	16.90	82.7	16.90
11/24/62	17 43	16.80	83.7	16.80
11/29/62	17 33	16.85	88.7	16.85
12/17/62	17 24	17.00	106.7	17.00

Table A1 - 1.22

SN1962L t_0 = 12/5/62 m_0 = 13.20

Date			Bertola (57) B	Bertola (57) V	Bunine (58) m_{pg}	t	m_{pg}
11/23/62	22[h]	31[m]	15.20		15.0	-11.1	15.0
11/26/62	18	01			14.3	-8.2	14.3
	18	40	14.49		14.2	-8.2	14.2
	21	32			14.2	-8.1	14.2
11/29/62	18	36			14.1	-5.2	14.1
	21	38			13.8	-5.1	13.8
	23	55	14.24	13.66		-5.0	14.35
11/30/62	1	21	14.20			-4.9	14.02
	1	43			14.0	-4.9	14.0
	18	33			14.1	-4.2	14.1
	23	49	14.12			-4.0	13.94
12/1/62	0	12			14.0	-4.0	14.0
12/2/62	0	18			13.8	-3.0	13.8
	0	20	14.10			-3.0	13.92
	17	50	14.05			-2.3	13.88
	20	35			14.1	-2.1	14.1
	23	40	14.08	13.88		-2.0	13.92
12/3/62	22	26	14.01			-1.1	13.84
	22	57			13.9	-1.0	13.9
	23	00	14.03	13.33		-1.0	13.87
12/4/62	22	24			13.9	-0.1	13.9
12/5/62	22	30	13.97	13.28		0.9	13.80
	24	00			13.4	1.0	13.4
12/6/62	1	12	13.95			1.0	13.79
12/7/62	1	07			13.6	2.0	13.6
12/14/62	17	46			14.2	9.7	14.2
12/15/62	19	16	14.31			10.8	14.20

Table A1 - 1.22 (Continued)

SN1962ℓ t_0 = 12/5/62 m_0 = 13.20

Date			Bertola (87) B	Bertola (87) V	Rosino (88) m_{PG}	t	m_{PG}
12/15/62	19	46			14.3	10.8	14.3
12/16/62	18	52			14.5	11.8	14.5
	21	00	14.94	13.39		11.9	14.40
12/17/62	19	50	14.50			12.8	14.40
	20	16			14.7	12.8	14.7
12/17/62	21^h	50^m	14.61	13.46		12.9	14.53
12/18/62	19	06			14.9	13.8	14.9
	20	40	14.76	13.57		13.9	14.68
12/20/62	18	57			15.1	15.8	15.1
	20	35	14.99			15.9	14.91
12/21/62	19	10			15.1	16.8	15.1
	23	00	15.05	13.79		17.0	14.99
12/22/62	19	51			15.1	17.8	15.1
	20	06	15.21			17.8	15.15
	21	30	15.10	13.82		17.9	15.04
12/25/62	19	18	15.55			20.8	15.51
	19	43			15.3	20.8	15.3
12/26/62	18	33			15.5	21.8	15.5
	19	50	15.63	14.21		21.8	15.60
12/27/62	17	50			15.5	22.7	15.5
	21	00	15.95	14.43		22.9	15.93
1/14/63	17	59			16.1	40.7	16.1
	18	20	16.32			40.8	16.35
1/15/63	18	12			16.2	41.8	16.2
1/16/63	18	29			16.1	42.8	16.1
1/19/63	19	03			16.1	45.8	16.1
	20	28	16.31			45.9	16.33

Table A1 - 1.22 (Continued)

SN1962ℓ t_0 = 12/5/62 m_0 = 13.20

Date			Bertola (87) B	Bertola (87) V	Rosino (88) m_{pg}	t	m_{pg}
1/20/63	17	49			16.2	46.7	16.2
	20	09	16.35			46.8	16.37
1/22/63	18	29			16.2	48.8	16.2
1/24/63	18	13			16.4	50.8	16.4
	18	21	16.35			50.8	16.37
1/25/63	18	10			16.4	51.8	16.4
1/26/63	18	48			16.4	52.8	16.4
1/27/63	18	31	16.41			53.8	16.42
2/23/63	19	23	16.95			80.8	16.92
2/25/63	19	20	16.89			82.8	16.85

Table A1 - 1.23

SN1962p	t_0 = 10/29/62		m_0 = 14.2
Date	Rosino (89) m_{pg}	t	m_{pg}
10/9/62	16.9	-20	16.9
10/24/62	15.0	-5	15.0
11/23/62	16.5	25	16.5
11/26/62	16.5	28	16.5
11/30/62	17.1	32	17.1
12/3/62	17.2	35	17.2
12/5/52	17.2	37	17.2
12/20/62	17.4	52	17.4
12/22/62	17.4	54	17.4
1/14/63	17.6	77	17.6
1/24/63	17.6	87	17.6

Table A1 - 1.24

SN1963d t_0 = 1/20/63 a_0 = 15.60

Date			Bertola (86) m_{pg}	Rosino (90) m_{pg}	t	m_{pg}
1/22/63				15.5	2	15.5
1/25/63	0^h	08^m		15.90	5.0	15.90
1/27/63	0	09		16.00	7.0	16.00
1/28/63	0	14		16.10	8.0	16.10
1/31/63	0	30		16.40	11.0	16.40
2/24/63	0	03		18.85	35.0	18.85
2/25/63	23	59		18.90	37.0	18.90
3/1/63	0	25		18.95	40.0	18.95
3/14/63	22	37		19.05	53.9	19.05
3/17/63	22	45		19.05	56.9	19.05
4/30/63	8	37		19.35	100.4	19.35

Table A1 - 1.25

SM19531 t_0 = 5/5/63 m_0 = 12.90

Date		Zaitseva (91) m_{PG}	Lochel (92) m_{PG}	Bertaud (93) m_{PG}	t	m_{PG}
4/22/63			15.8		-13	15.8
4/27/63				14.3	-8	14.3
5/14/63	19^h 00^m	13.90			9.8	13.9
	21 00	13.90			9.9	13.90
5/16/63	20 00	14.01			11.8	14.01
	21 00	13.98			11.9	13.98
5/20/63			14.3		15	14.3
5/21/63	19 00	14.57			16.8	14.57
5/22/63	20 00	14.68			17.8	14.68
5/23/63	21 00	14.81			18.9	14.81
5/25/63	20 00	15.07			20.8	15.07
5/26/63	19 00	15.16			21.8	15.16
6/10/63	20 00	15.71			36.8	15.71
6/16/63	20 00	15.80			42.8	15.80

Table A1 - 1.26

SN1963j t_0 = 5/10/63 m_0 = 12.0

Date			Zwicky (94) m_{pg}	Wild (95) m_{pg}	Chincarini and Margoni (96) m_{pg}	t	m_{pg}
5/18/63			12.5			8	12.5
5/20/63				13.0		10	13.0
5/21/63	24^h	13^m			13.85		
5/25/63	20	56			13.7	15.9	13.7
5/26/63	23	04			13.75	17.0	13.75
5/28/63	24	01			13.8	19.0	13.8
5/30/63	24	59			13.8	21.0	13.8
5/31/63	25	08			13.9	22.0	13.9
6/9/63	21	14			14.3	30.9	14.3
6/12/63	23	08			14.8	34.0	14.8
6/17/63	22	44			14.9	38.9	14.9
6/23/63	22	52			15.4	44.9	15.4
6/25/63	23	35			15.5	47.0	15.5
6/26/63	23	13			15.4	48.0	15.4
7/14/63	21	33			16.1	65.9	16.1
7/16/63	21	56			16.3	67.9	16.3
7/18/63	21	07			16.4	69.9	16.4
7/19/63	21	50			16.4	70.9	16.4

Table A1 - 1.27

SN1963p t_0 = 9/27/63 m_0 = 13.30

Date		Bertola et al (97) B	Kaho (98) m_K	t	m_{pg}
9/22/63	$00^h\ 25^m$	14.25			
9/23/63	23 53	14.15		-3.0	13.81
9/27/63	0 24	14.05		0.0	13.72
10/9/63	23 34	14.70		13.0	14.43
10/13/63	0 04	15.15		16.0	14.90
JD2438321.1			15.33	21.1	15.45
322.1			15.88	22.1	16.04
10/19/63	$3^h\ 17^m$	15.95		22.1	15.74
10/22/63	0 01	16.45		25.0	16.27
10/23/63	3 19	16.50		26.1	16.33
10/25/63	23 34	16.70		29.0	16.55
10/26/63	23 37	16.70		30.0	16.76
	23 58	16.85		30.0	16.71
JD2438345.1			16.67	45.1	17.18
345.1			16.76	45.1	17.33
346.1			16.62	46.1	17.09
346.2			16.72	46.2	17.26
11/17/63	$23^h\ 12^m$	17.50		52.0	17.37
11/22/63	22 50	17.55		57.0	17.41
12/12/63	21 18	17.80		76.9	17.63
JD2438382.1			17.04	82.1	17.83
383.0			16.92	83.0	17.54
383.0			17.00	83.0	17.73
1/8/64	$19^h\ 51^m$	18.50		103.8	18.28
	20 13	18.60		103.8	18.38
1/19/64	19 30	18.80		114.8	18.56

Table A1 - 1.27 (Continued)

SN1963p	t_0 = 9/27/63			m_0 = 13.50
Date	Bertola et al (97)	Kaho (98) m_K	t	m_{PG}
JD2438414.9		17.08	114.9	17.89
415.0		17.18	115.0	18.35
1/20/64 19^h 38^m	18.95		115.8	18.71

Table A1 - 1.28

SN1964e t_0 = 2/27/64 m_0 = 11.90

Date		Lovas (99)	Ahnert (100)	Chuadze (101)		Zaitseva (102)	Lochel (103)	t	
		m_{pg}	m_{pg}	m_{pv}	m_{pg}	m_{pg}	m_{pg}		m_{pg}
2/14/64			14.3					-13	13.7
2/19/64	$1^h\ 42^m$			14.0					
2/20/64			13.2					-7	12.6
2/20/64	$0^h\ 19^m$			13.2					
	0 36			13.1					
3/2/64			12.85					4	12.25
3/8/64			13.3					10	12.7
3/10/64			13.1					12	12.5
3/10/64	$0^h\ 00^m$					12.90		12.0	12.9
3/12/64	1 36					13.05		14.1	13.05
3/13/64		13.21						15	13.21
3/14/64	$21^h\ 36^m$					13.30		16.9	13.3
3/15/64	0 09				13.6			17.0	13.25
	0 25				13.7			17.0	13.35
3/16/64		13.52						18	13.52
3/16/64	$20^h\ 28^m$				13.9			18.9	13.55

Table A1 - 1.28

SN1964e t_0 = 2/27/64 m_0 = 11.90

Date		Lovas (99) m_{pg}	Ahnert (100) m_{pg}	Chuadze (101) m_{pv}	Chuadze (101) m_{pg}	Zaitseva (102) m_{pg}	Lesnel (103) m_{pg}	t	m_{pg}
3/17/64		13.47						19	13.47
3/19/64		13.40						21	13.40
3/22/64	$0^h\ 23^m$				14.5			24.0	14.15
4/10/64							15.80	43	15.2
4/13/64	$20^h\ 39^m$					15.00		46.9	15.0
4/14/64	22 33					15.10		47.9	15.1
4/16/64	0 00					15.27		49.0	15.27
4/18/64							15.65	51	15.05
4/19/64	$0^h\ 00^m$					15.35		52.0	15.35
5/9/64							15.90	72	15.3
5/17/64							16.0	80	15.4
5/31/64							16.0	94	15.4
6/4/64							16.9	98	16.3
6/8/64							16.75	102	16.15
7/2/64							17.0	126	16.4
7/7/64							17.1	131	16.5
9/12/64							18.0	198	17.4

Table A1 - 1.29

SN1964L			t_0 = 12/8/64		m_0 = 13.10
Date			Bertola et al (97) m_{pg}	t	m_{pg}
12/12/64	2^h	00^m	13.45	4.1	13.45
	2	27	13.60	4.1	13.60
12/13/64	1	23	13.50	5.1	13.50
12/23/64	2	03	14.50	15.1	14.50
12/24/64	0	31	14.65	16.0	14.65
	0	35	14.70	16.0	14.70
12/31/64	0	37	15.55	23.0	15.55
	2	40	15.40	23.1	15.40
	23	15	15.55	24.0	15.55
1/5/65	0	32	15.65	28.0	15.65
1/6/65	0	22	16.05	29.0	16.05
	22	15	16.05	29.9	16.05
1/7/65	0	04	16.05	30.0	16.05
1/8/65	22	44	16.25	31.9	16.25
1/10/65	1	12	16.10	33.0	16.10
1/11/65	0	58	16.40	34.0	16.40
1/23/65	22	33	16.25	46.9	16.25
1/25/65	22	42	16.40	48.9	16.40
2/2/65	21	31	16.45	56.9	16.45
2/4/65	0	08	16.65	58.0	16.65
2/4/65	23	19	16.60	59.0	16.60
2/8/65	23	53	16.60	63.0	16.60
2/21/65	23	01	16.60	76.0	16.60
2/27/65	2	27	16.65	81.1	16.65
2/27/65	4	45	16.75	81.2	16.75
3/7/65	1	30	16.80	89.1	16.80
3/12/65	0	11	17.00	94.0	17.00

Table A1 - 1.29 (Continued)

SH1964ℓ t_0 = 12/8/64 a_0 = 13.10

Date			Bertola et al (97) a_{DE}	t	a_{DE}
3/25/65	23	55	17.05	108.0	17.05
3/27/65	23	32	17.05	110.0	17.05
3/31/65	21	47	17.15	113.9	17.15
4/6/65	22	42	17.10	119.9	17.10
5/3/65	23	42	17.35	147.0	17.35
5/6/65	23	38	17.50	150.0	17.50

Table A1 - 1.30

SH1965I	t_0 = 6/13/65			m_0 = 11.0
Date	Van Lyong and Pomerin (104) m_{pg}	Ciatti and Barton (105) B	V	t	m_{pg}
JD2438915.3	16.09			-9.7	16.09
916.3	15.67			-8.7	15.67
6/18/65 21^h 31^m			11.80	5.9	11.56
JD2438932.3	12.58			7.3	12.58
6/20/65 21^h 00			12.45	7.9	12.27
21 21			12.55	7.9	12.37
JD2438933.4	12.46			8.4	12.48
6/22/65 21^h 08^m			12.70		
21 22		12.60		9.9	12.50
21 28		12.65		9.9	12.55
22 04		12.70		9.9	12.60
22 12			12.75		
JD2438935.4	12.70			10.4	12.70
6/23/65 21^h 08^m			12.80		
21 26		12.75		10.9	12.65
JD2438936.3	12.73			11.13	12.73
6/24/65 20^h 34^m			12.80		
21 10			12.85		
21 11		12.80		11.9	12.72
21 20		12.95		11.9	12.87
21 30		12.90		11.9	12.82
6/25/65 21 10			12.95		
21 16			12.90		
21 25		13.10		12.9	13.03
21 30		13.00		12.9	12.93
JD2438938.3	13.00			13.3	13.00
939.3	12.81			14.3	12.81

Table A1 - 1.30 (Continued)

SN1965i t_0 = 6/13/65 m_0 = 11.0

Date	Van Lyong and Pennarin (104) m_{pg}	Cietti and Barbon (105) B	Cietti and Barbon (105) V	t	m_{pg}
6/27/65 21h 00m			13.10		
21 15		13.35		14.9	13.30
21 20		13.30		14.9	13.25
JD2438940.3	13.29			15 3	13.29
941.3	13.33			16.3	13.33
6/29/65 21h 11m			13.25		
21 20		13.40		16.9	13.34
21 25		13.45		16.9	13.39
JD2438942.3	13.38			17.3	13.38
943.3	13.39			18.3	13.39
944.3	13.81			19.3	13.81
956.3	14.80			31.3	14.80
959.3	15.08			34.3	15.08
960.3	15.62			35.3	15.62
963.3	15.78			38.3	15.78

Table A1 - 1.31

SN1966j		t_0 = 11/23/66			m_0 = 11.0	
Date		Wild (106) m_{pg}	Chincarini and Perinotto (107) B	Kaho (108) m_K	[illegible] et al (112) ~ B	t	m_{pg}
12/18/66		13.0				25	13.0
12/21/66	1^h 47^m		13.30			28.1	13.18
12/22/66	3 00		13.25			29.1	13.13
12/24/66	3 27		13.50			31.1	13.39
1/3/67	22 56		14.20			42.0	14.08
1/5/67	0 28		14.2			43.0	14.08
JD2439500.1				14.36		47.1	14.25
500.2				14.42		47.2	14.30
500.2				14.35		47.2	14.24
500.2				14.44		47.2	14.31
501.2				14.32		48.2	14.21
501.2				14.28		48.2	14.18
501.2				14.55		48.2	14.41
1/11/67	0^h 10^m		14.3			49.0	14.17
JD2439503.3				14.48		50.3	14.35
503.3				14.42		50.3	14.30
1/13/67	2^h 00^m		14.45			51.1	14.31
23 38			14.50			52.0	14.36
1/19/67	0 40		14.5			57.0	14.36
2/2/67	23 08		14.6			72.0	14.43
JD2439528.1				14.83		75.1	14.63
528.2				14.76		75.2	14.56
528.3				14.74		75.3	14.54
2/7/67	23^h 13^m		14.7			77.0	14.52
2/9/67					14.75		

Table A1 - 1.31 (Continued)

SN1966J t_0 = 11/23/66 m_0 = 11.10

Date	Wild (106) m_{pg}	Chincarini and Perinotto (107) B	Kaho (108) m_K	Borzov et al (112) ~ B	t	m_{PG}
2/15/67 20 12		15.00			84.8	14.81
2/27/67				14.95		
JD2439553.1			15.09		106.1	14.84
557.1			14.98		104.1	14.72
3/8/67				15.10		
3/9/67				15.30		
JD2439564.2			15.32		111.2	15.05
3/14/67 23^h 56^m		15.20			112.0	14.96
JD2439565.1			15.27		112.1	15.00
565.1			15.11		112.1	14.84
565.1			15.35		112.1	15.08
3/17/67 2^h 35^m		15.30			114.9	15.06
4/14/67				15.70		
JD2439608.0			16.12			
608.0			16.10			
5/1/67				15.60		
5/1/67				16.00		
5/3/67				16.10		
JD2439626.1			16.05			
626.2			16.38			
643.0			16.57			
643.1			16.43			
646.0			16.50			
6/11/67				15.80		
7/1/67				16.10		

Table A1 - 1.32

SN1966k t_0 = JD2439489.0 m_0 = 16.60

Date	Rudnicki (109) m_{pg}	Rudnicki (109) m_{pv}	t	m_{pg}
JD2439478.9		18.4	-10.1	17.9
479.9	17.8		-9.1	17.8
479.9		18.2	-9.1	17.7
505.0		17.6	16.0	17.9
506.9	18.1		17.9	18.1
534.0		19.0	45.0	20.0
551.8		18.9	62.8	19.7
552.7		19.2	63.7	20.0
564.7		19.5	75.7	20.1
564.8	19.6		75.8	19.6

Table A1 - 1.33

SH1966n	t_0 = 10/7/66		m_0 = 14.3
Date	Cietti and Barbon (105) m_{BK}	t	m_{pg}
10/14/65 0^h $3\frac{1}{2}^m$	14.70	7.0	14.70
11/7/66 22 3½	16.90	31.9	16.90
11/14/66 0 05	16.95	38.0	16.95
11/16/66 0 17	17.10	40.0	17.10
11/19/66 0 3½	17.30	43.0	17.30
12/6/66 22 35	17.60	60.9	17.60
12/8/66 21 35	17.65	62.9	17.65
12/9/66 22 04	17.70	63.9	17.70
12/10/66 21 10	17.70	64.9	17.70
12/11/66 21 06	17.80	65.9	17.80
1/4/67 19 11	18.00	89.8	18.00

Table A1 - 1.34

SN1967c t_0 = 2/22/67 m_0 = 12.60

Date		de Vaucouleurs et al (110) B	de Vaucouleurs et al (110) V	Marx and Prau (111) b	Borsov et al (112) ~ B	Chuadse et al (113) m_{pv}	Kaho (108) m_K	t	m_{pg}
2/28/67	18h 26m					12.47		6.8	12.69
3/1/67	17 12					12.52		7.7	12.71
	17 32					12.69		7.7	12.88
3/3/67	17 00					12.58		9.7	12.86
	17 11					12.46		9.7	12.74
	17 36					12.64		9.7	12.92
3/6/67					13.40			12.0	13.14
JD2439556.8		13.55	13.28					12.8	13.31
3/7/67	17h 38m					12.94		13.7	13.38
	17 50					12.79		13.7	13.23
	17 59					12.67		13.8	13.11
	18 07					12.90		13.8	13.34
3/8/67					14.05			14.0	13.81
3/8.1/67				13.65				14.1	13.44
3/8/67	17h 52m					12.87		14.7	13.34

Table A1 - 1.34 (Continued)

SN1967c t_0 = 2/22/67 m_0 = 12.60

Date		de Vaucouleurs et al (110) B	de Vaucouleurs et al (110) V	Marx and Pfau (111) b	Borsov et al (112) ~ B	Chuadse et al (113) m_{pv}	Kaho (108) m_v	t	m_{pg}
3/8/67	18^h 15^m					12.79		14.8	13.26
	18 25					12.90		14.8	13.37
3/9.0/67				13.70				15.0	13.50
3/9/67					13.95			15.0	13.71
JD2439559.7		13.83	13.48					15.7	13.60
561.9		13.97	13.60					17.9	13.75
3/12.0/67				14.10				18.0	13.95
JD2439562.8		14.06	13.62					18.8	13.85
3/12/67	19^h 21^m					13.00		18.8	13.70
3/12.9/67				13.95				18.9	13.81
3/13/67	19^h 49^m					13.17		19.8	13.89
JD2439564.2							13.76	20.2	13.96
564.2							13.77	20.2	13.97
564.8		14.18	13.69					20.8	13.98

Table A1 - 1.34 (Continued)

SN1967c t_0 = 2/22/67 m_0 = 12.60

Date	de Vaucouleurs et al (110) B	de Vaucouleurs et al (110) V	Marx and Pfau (111) b	Borisov et al (112) B	Chuadze et al (113) m_{pv}	Kaho (108) m_K	t	m_{pg}
3/14/67 20h 07m					13.17		20.8	13.92
20 20					13.20		20.8	13.95
JD2439565.1						13.79	21.1	13.99
565.8	14.34	13.74					21.8	14.16
566.8	14.50	13.85					22.8	14.33
569.9	14.89	14.10					25.9	14.74
3/29.8/67			14.90				35.8	14.92
3/30/67 18h 02m					13.63		36.8	14.96
18 14					13.90		36.8	15.23
4/1/67 19 08					14.23		38.8	15.54
19 16					14.22		38.8	15.43
4/6/67 18 32					14.34		43.8	15.60
18 40					14.38		43.8	15.64
4/7.8/67			15.60				44.8	15.60
JD2439589.8	16.11	15.31					45.8	15.96
4/8/67 20h 03m					14.51		45.8	15.75

Table A1 - 1.34 (Continued)

SN1967- t_0 = 2/22/67 m_0 = 12.60

Date	de Vaucouleurs et al (110) B	de Vaucouleurs et al (110) V	Marx and Pfau (111) b	Borzov et al (112) ~ B	Chuadze et al (113) m_{pv}	Kaho (108) m_K	t	m_{pg}
JD2439591.7	16.23	15.33					47.7	16.10
4/10.8/67			15.90				47.8	15.89
4/10/67 19^h 48^m					14.39		47.8	15.64
4/11.8/67			15.65				48.8	15.64
4/12/67 18^h 31^m					14.60		49.8	15.80
JD2439594.6	16.33	15.43					50.6	16.20.
4/13/67 19^h 41^m					14.20		50.8	15.40
4/14/67				16.10			51.0	15.96
4/14/67 20^h 07^m					14.24		53.8	15.42
JD2439608.0						16.35	64.0	16.58
608.0						16.22	64.0	16.42
4/29/67				15.85			66.0	15.69
4/30/67				16.0			67.0	15.84
4/30.9/67			16.20				67.9	16.13
5/1/67				16.40			68.0	16.24

Table A1 - 1.34 (Continued)

SN1967c t_0 = 2/22/67 m_0 = 12.60

Date	de Vaucouleurs et al (110) B	de Vaucouleurs et al (110) V	Marx and Pfau (111) b	Borzov et al (112) ~ B	Chuadze et al (113) m_{pv}	Kaho (108) m_K	t	m_{pg}
JD2439613.7	16.35						69.7	16.19
613.7	16.43						69.7	16.27
616.7	16.65						72.7	16.48
618.7	16.45						74.7	16.28
5/7.9/67			16.20				74.9	16.11
JD2439619.7	16.85						75.7	16.68
621.7	16.73						77.7	16.56
5/10.9/67			16.20				77.9	16.10
5/11.9/67			16.30				78.9	16.20
JD2439623.7	16.94	16.33					79.7	16.76
643.7	17.50						99.7	17.29
645.7	17.40						101.7	17.19
646.0						16.60	102.0	16.90
646.0						16.57	102.0	16.85
JD2439649.7	17.38						105.7	17.16
650.7	17.78						106.7	17.56

Table A1 - 1.35

SN1968e t_0 = 3/15/68 m_0 = 12.70

Date	Chavira (114) m_{PG}	Rusev (51) m_{PG}	Ciatti and Barbon (105) B	Ciatti and Barbon (105) V	t	m_{PG}
3/21/68	13.5				6	13.5
3/25/68 $21^h\ 30^m$			15.50	14.85	10.9	14.43
JD2439943		14.7			12	14.7
3/27/68 $20^h\ 30^m$			15.60	15.00	12.[illegible]	14.65
JD2439944		14.8			13	14.8
3/29/68 $22^h\ 07^m$			15.60	15.25	13.9	14.95
JD2439945		14.75			14	14.75
946		14.9			15	14.9
3/30/68 $20^h\ 35^m$			15.70	15.[illegible]	15.9	15.08
4/3/68 24 00			16.10	15.65	20.0	15.63
JD2439963		15.8			32	15.8
966		15.95			35	15.95
4/23/68 $20^h\ 13^m$			17.20			

Table A1 - 1.36

SN1969c			t_0 = 1/31/69				m_0 = 13.94
Date			Bertola and Ciatti (115)			t	m_{PG}
			B	V	m_{PG}		
1/20/69	21^h	15^m			16.35	-10.1	16.35
2/9/69	22	04		(14.10)			
	22	18			14.60	9.9	14.60
2/13/69	19	50			15.10	13.8	15.10
	20	08	15.30			13.8	15.10
	21	15		14.60		13.9	14.89
2/17/69	23	03	15.35			18.0	15.18
	23	18		14.82		18.0	15.30
	25	36	15.50			18.1	15.33
2/21/69	23	01	15.80			22.0	15.66
	23	16		14.95		22.0	15.63
	25	26	15.85			22.1	15.71
	27	39		14.85		22.2	15.53
3/6/69	19	17	16.65			34.8	16.59
	19	33		15.45		34.8	16.66
3/8/69	19	25	16.70			36.8	16.64
	22	43	16.65			36.9	16.59
	23	01		15.45		37.0	16.65
3/9/69	19	55	16.75			37.8	16.68
	20	12		15.55		37.8	16.73
	22	01		15.45		37.9	16.63
	22	19	16.70			37.9	16.63
4/7/69	23	58	17.35			67.0	17.24
4/0/69	26	13	17.55			69.1	17.43
4/10/69	24	03	17.60			70.0	17.48
4/14/69	25	17	17.60			74.1	17.48
4/17/69	25	21	17.10			77.1	16.97

Table A1 - 1.36 (Continued)

SN1969c			t_0 = 1/31/69				m_0 = 13.94
Date			Bertola and Ciatti (115)			t	m_{pg}
			B	V	m_{pg}		
4/23/69	25	28	17.70			83.1	17.56
5/12/69	20	08	17.80			101.8	17.63

Table A1 - 1.37

SN1971i t_0 = 5/27/71 m_c = 11.70

Date		Deming et al (52)			Ishida (56)		Van Herk et al (54, 55)	Scovil (116)	t	m_{pg}
		B	V	m_{pg}	V	B-V	m_{pg}	m_{pv}		
5/20.95/71							12.87		-6	12.87
5/25/71	$12^h\ 00^m$				12.09	0.16			-1.5	11.99
5/30/71				12.10					3	12.10
5/30/71		12.45	12.10						3	12.22
5/31/71				11.75					4	11.75
5/31/71		12.29	11.98						4	12.06
6/1/71				11.70					5	11.70
6/1/71		11.94	11.51						5	11.73
6/3/71				12.30					7	12.30
6/9/71		13.13	12.20						13	13.00
6/10/71		13.45	12.30						14	13.37
6/11/71								12.2	15	13.27
6/12/71								12.3	16	13.39
6/14/71		13.95	12.70						18	13.88
6/16/71		13.95	12.75						20	13.88
6/17/71				14.10					21	14.10
6/17/71								13.4	21	14.61

Table A1 - 1.37 (Continued)

SN1971i t_0 = 5/27/71 m_0 = 11.70

Date	Deming et al (52)			Ishida (56)		Van Herk et al (54, 55)	Scovil (116)	t	m_{pg}
	B	V	m_{pg}	V	B-V	m_{pg}	m_{pv}		
6/22/71	14.70	13.35						26	14.65
6/22/71			14.60					26	14.60
6/23/71	14.58	13.39						27	14.50
6/27/71							13.7	31	14.91
6/29/71	15.06	13.83						33	14.99
7/3/71	14.83	13.97						37	14.69
7/14/71	15.25	14.05						48	15.18
7/16/71	15.35	14.50						50	15.21
7/16/71			15.25					50	15.25
7/29/71	15.45	14.90						63	15.26
7/31/71	15.50	15.00						65	15.30
8/2/71	15.50	14.90						67	15.32
8/3/71	15.30	15.05						68	15.06
8/14/71	15.8							79	15.47

APPENDIX 2

THE REDUCED LIGHT CURVES

Figures A2 - 1.1 through A2 - 1.37 give the final reduced light curves used for the analysis. All magnitudes have been converted to the m_{pg} system and any necessary zero-point corrections have been applied. Different symbols have been used for the different observers in each curve. The vertical straight lines at t=0 represent the estimates of m_o. The fitted curves are the fits of the Morrison-Sartori model which were used to estimate the values of the comparison parameter Δt_c. The values of the parameters C and A which define these fitted curves are given in columns 9 and 10 of Table 8-1.

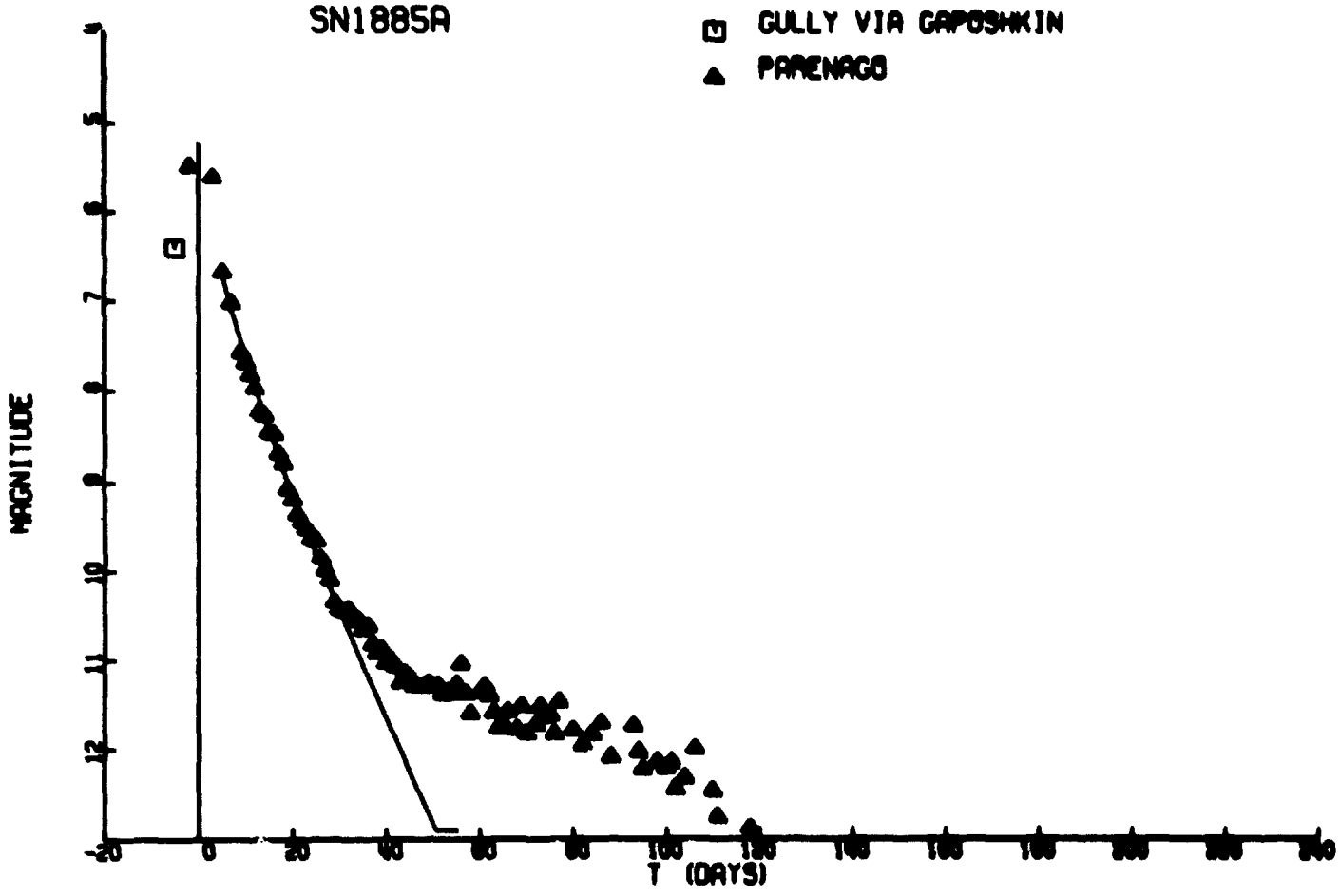

Figure A2-1.1

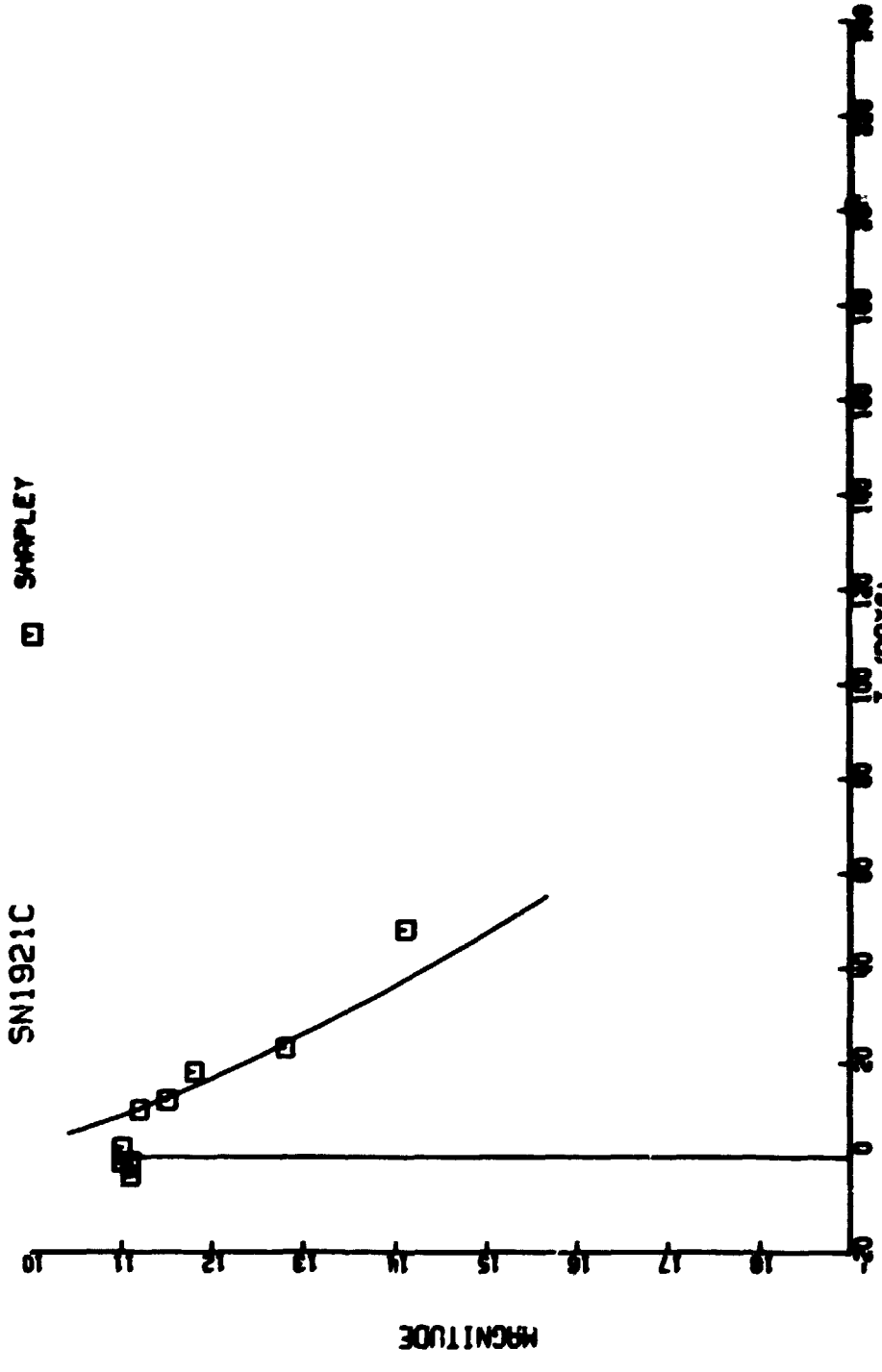

Figure A2-1.2

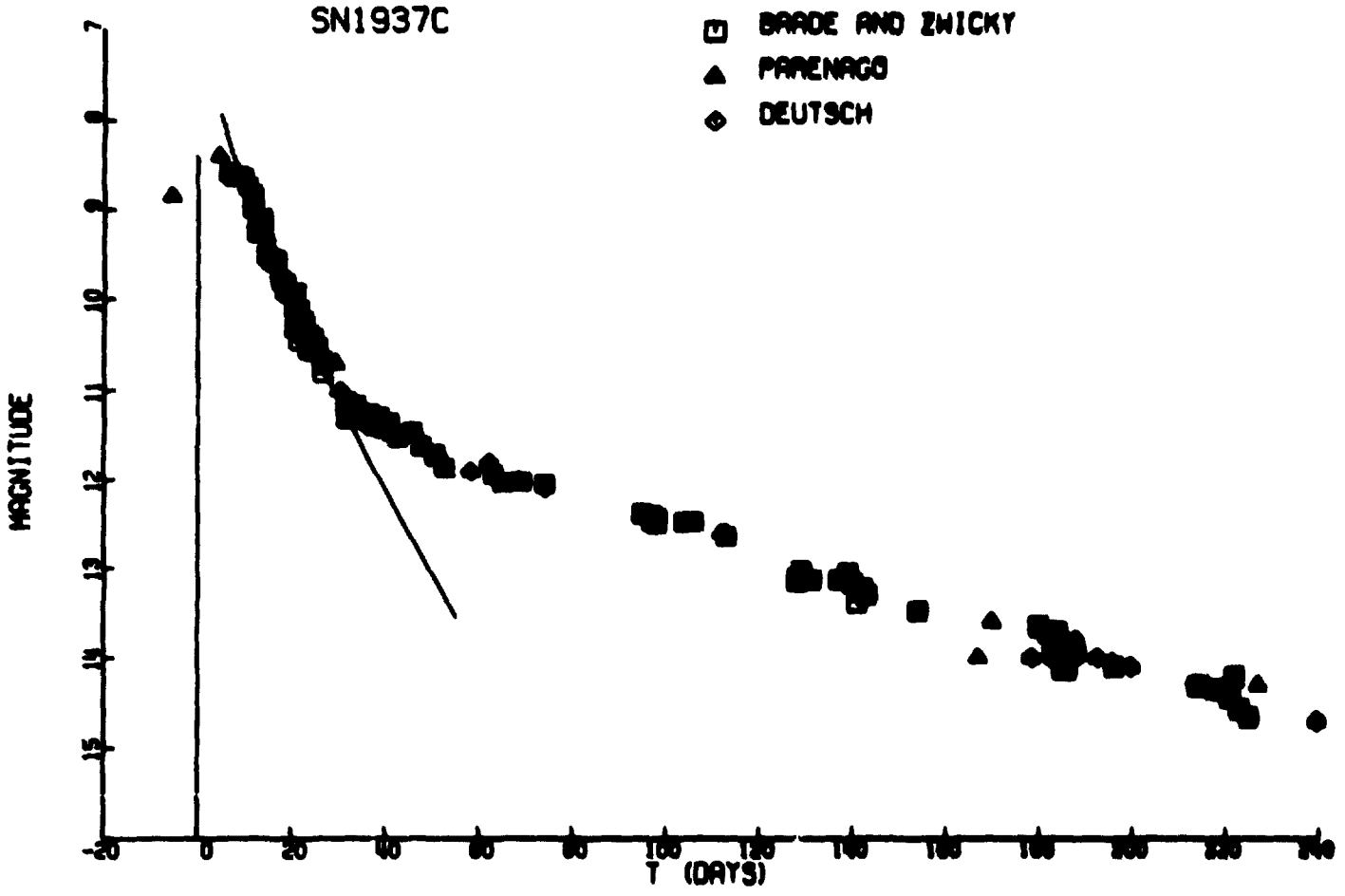
SN1937C
BAADE AND ZWICKY
PARENAGO
DEUTSCH
MAGNITUDE
T (DAYS)

Figure A2-1.3

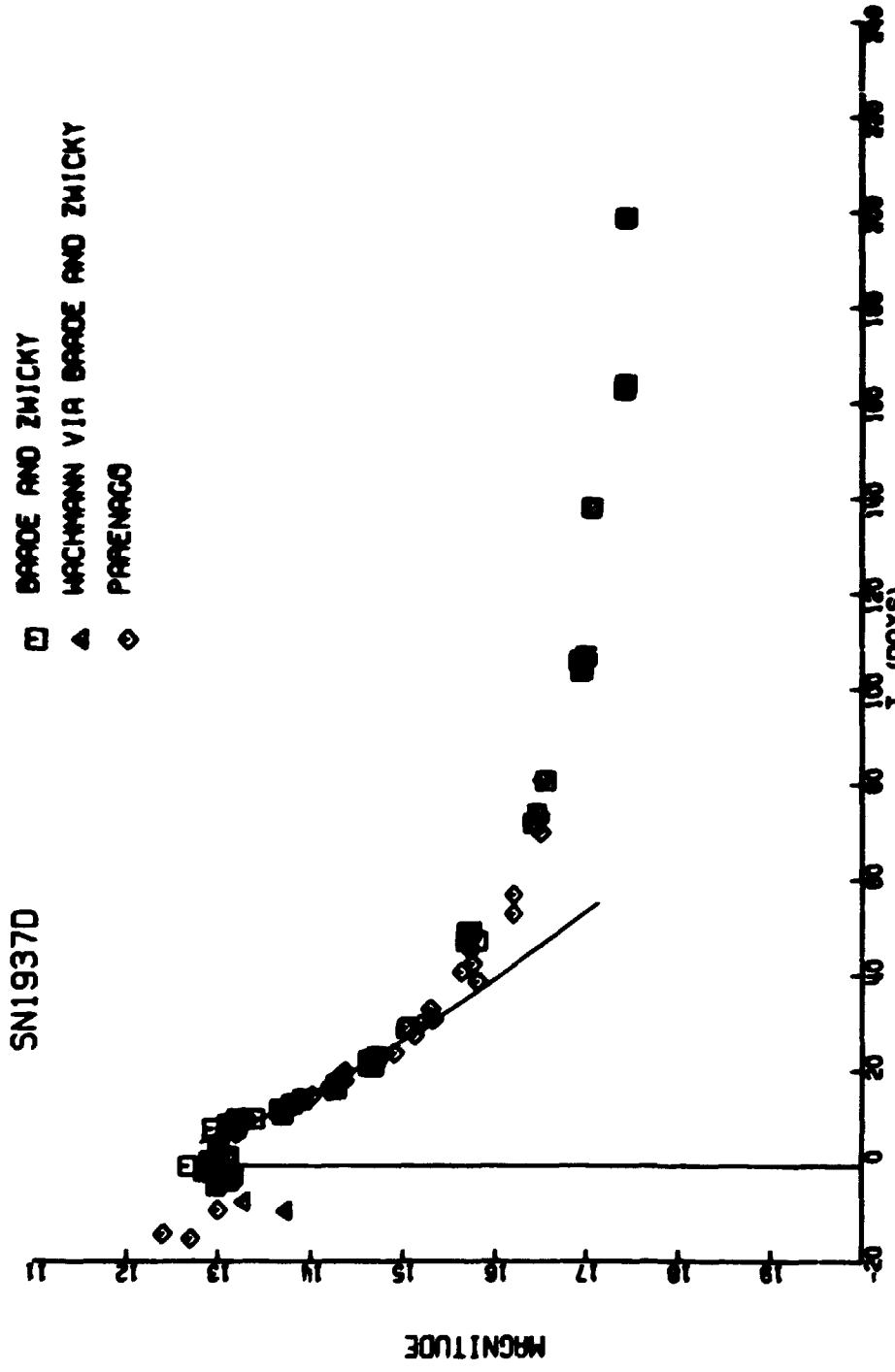
SN1937D
BARDE AND ZWICKY
WACHMANN VIA BARDE AND ZWICKY
PARENAGO
MAGNITUDE
T (DAYS)

Figure A2-1.4

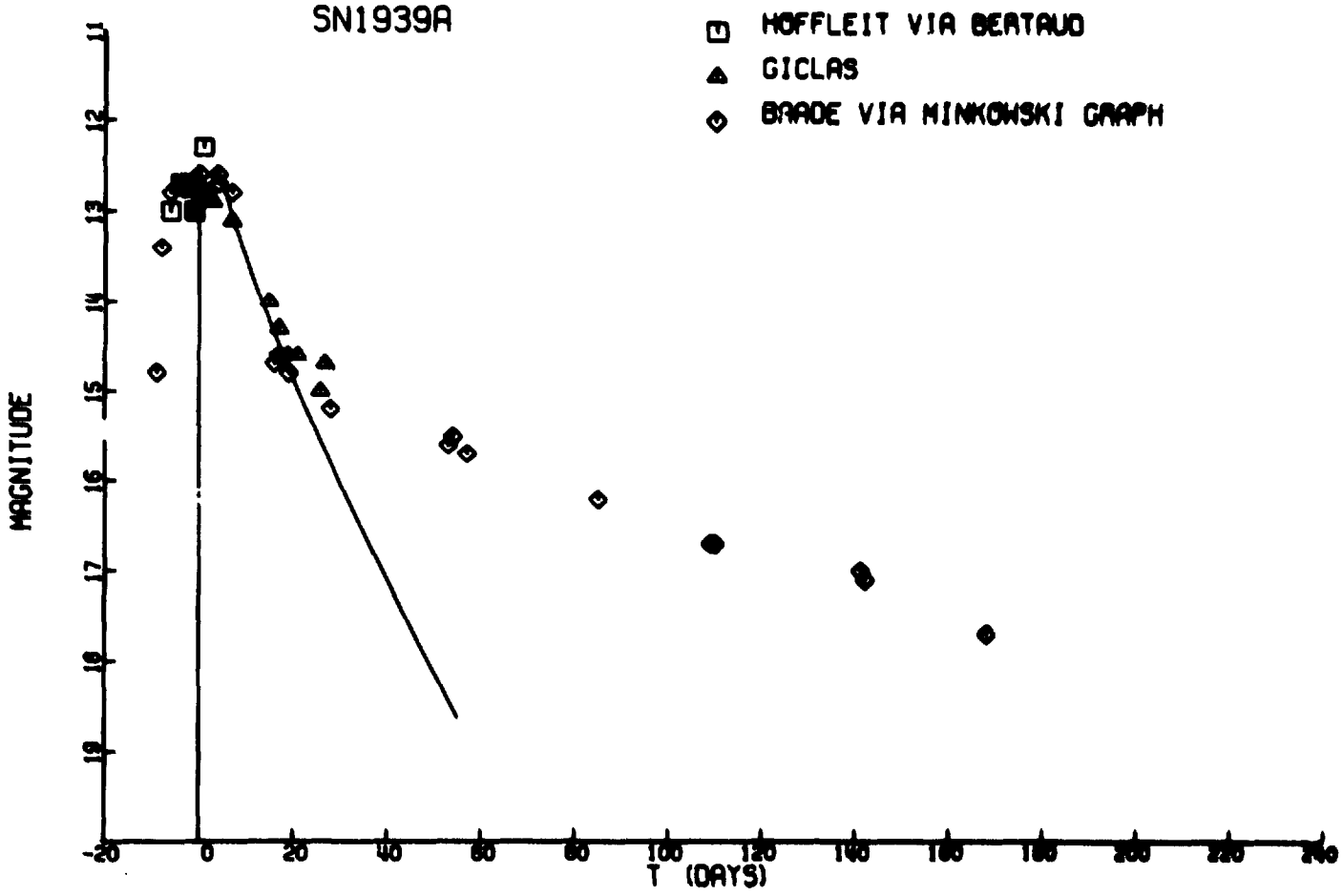
SN1939A
HOFFLEIT VIA BERTAUD
GICLAS
BAADE VIA MINKOWSKI GRAPH
MAGNITUDE
T (DAYS)

Figure A2-1.5

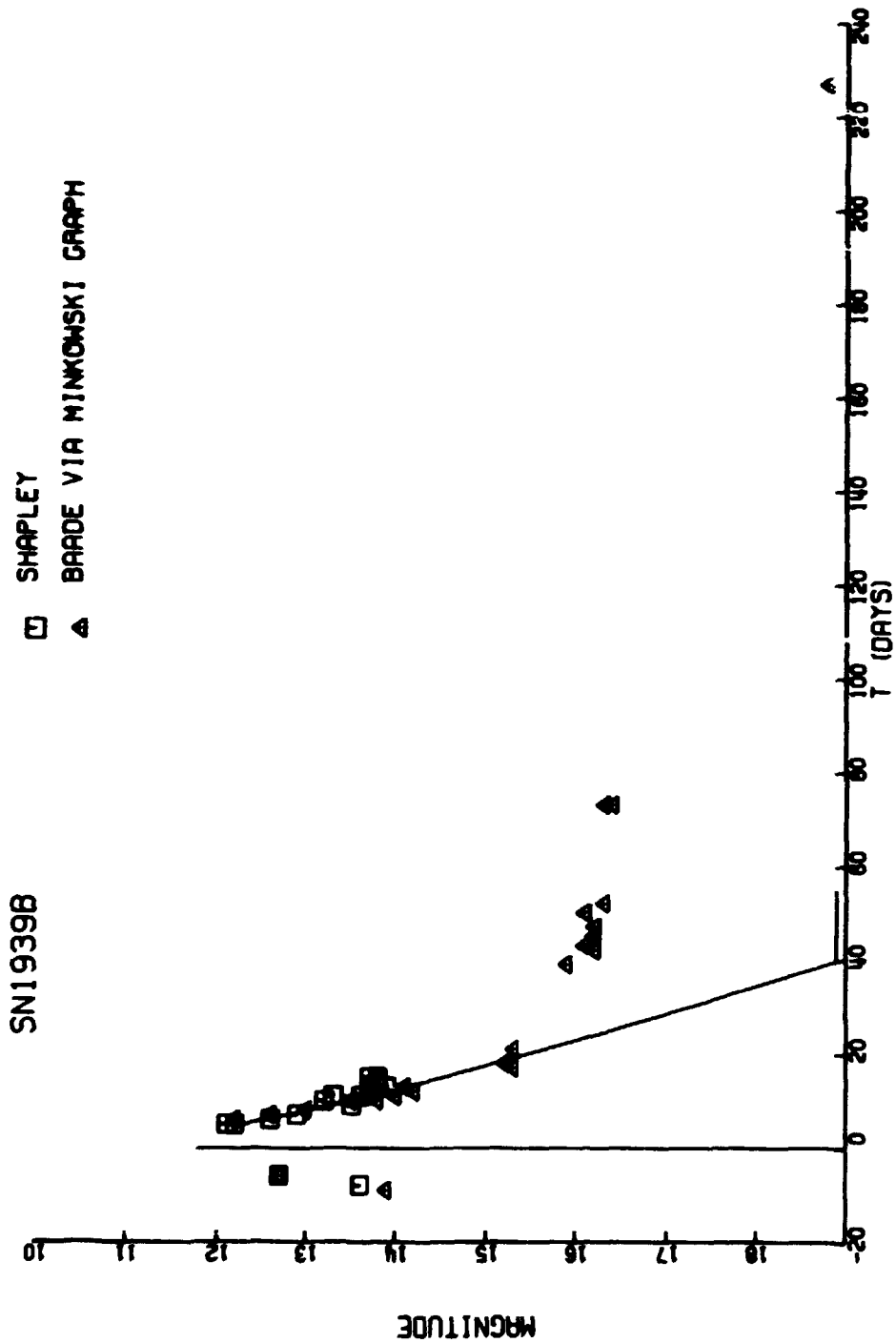
SN1939B
SHAPLEY
BAADE VIA MINKOWSKI GRAPH
MAGNITUDE
T (DAYS)
10
11
12
13
14
15
16
17
18
-20
0
20
40
60
80
100
120
140
160
180
200
220
240

Figure AP-1.6

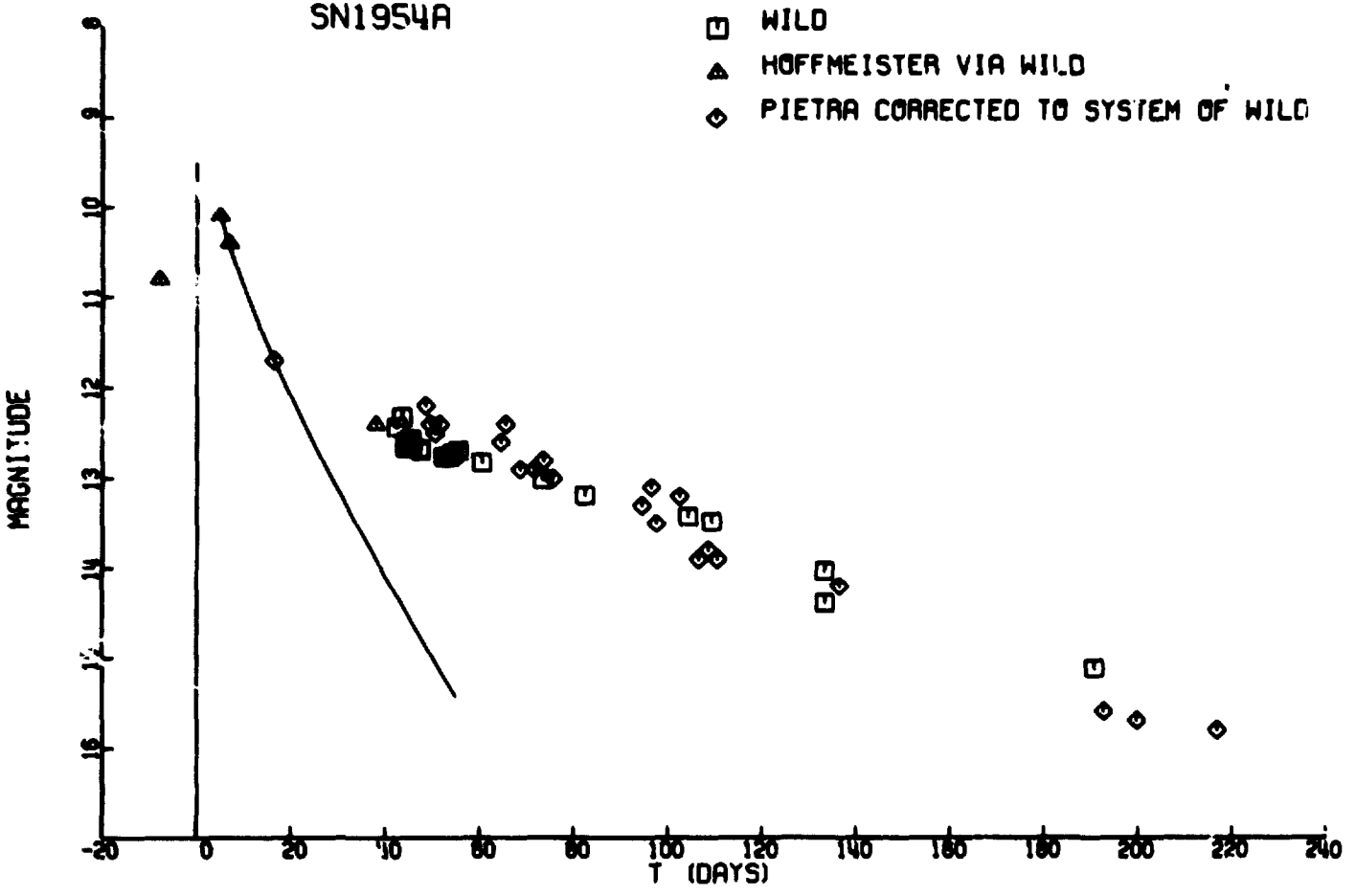
SN1954A
WILD
HOFFMEISTER VIA WILD
PIETRA CORRECTED TO SYSTEM OF WILD
MAGNITUDE
T (DAYS)
-20
0
20
40
60
80
100
120
140
160
180
200
220
240

Figure A2-1.7

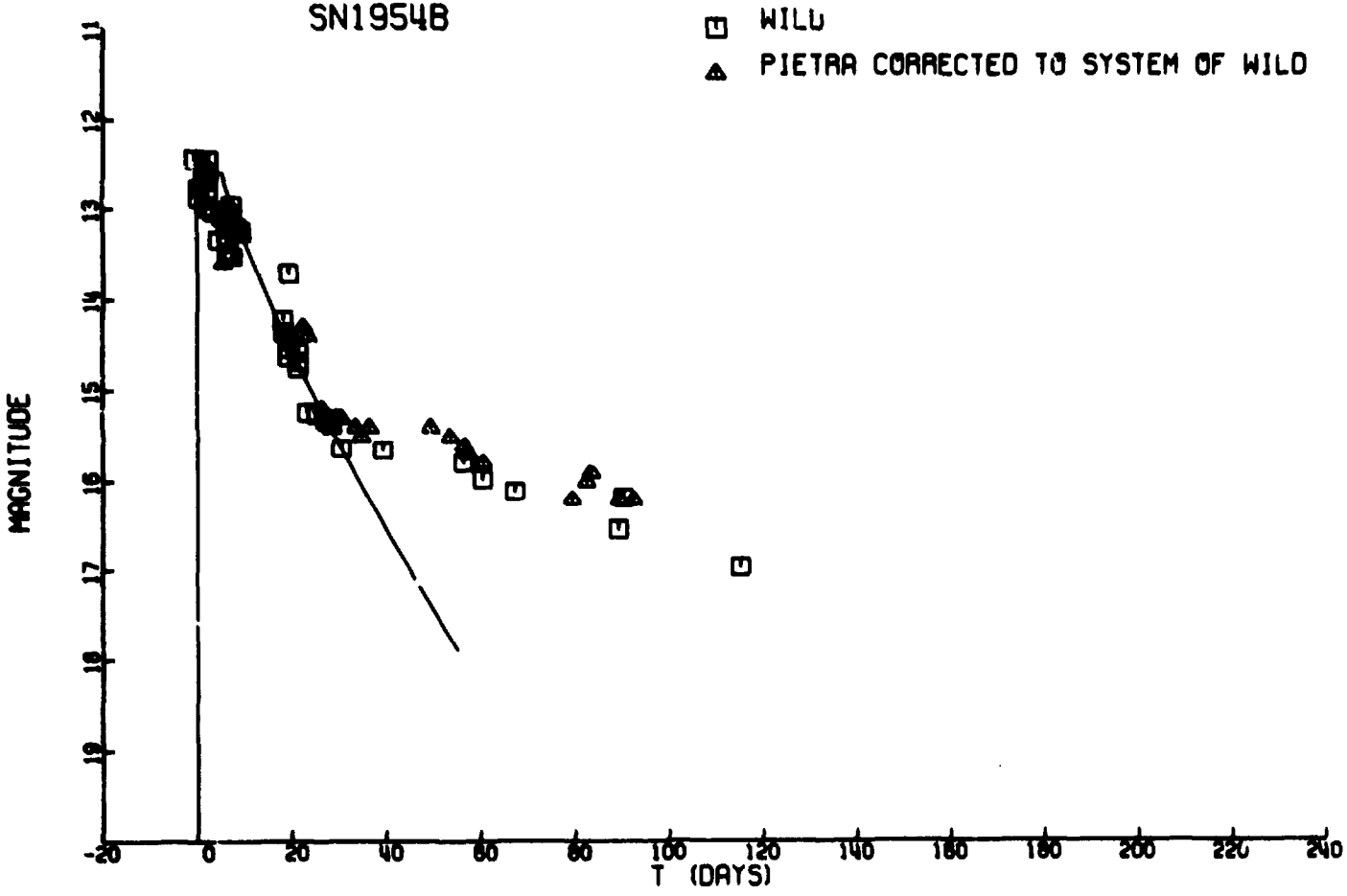
SN1954B
WILD
PIETRA CORRECTED TO SYSTEM OF WILD
MAGNITUDE
T (DAYS)
11
12
13
14
15
16
17
18
19
-20
0
20
40
60
80
100
120
140
160
180
200
220
240

Figure A2-1.8

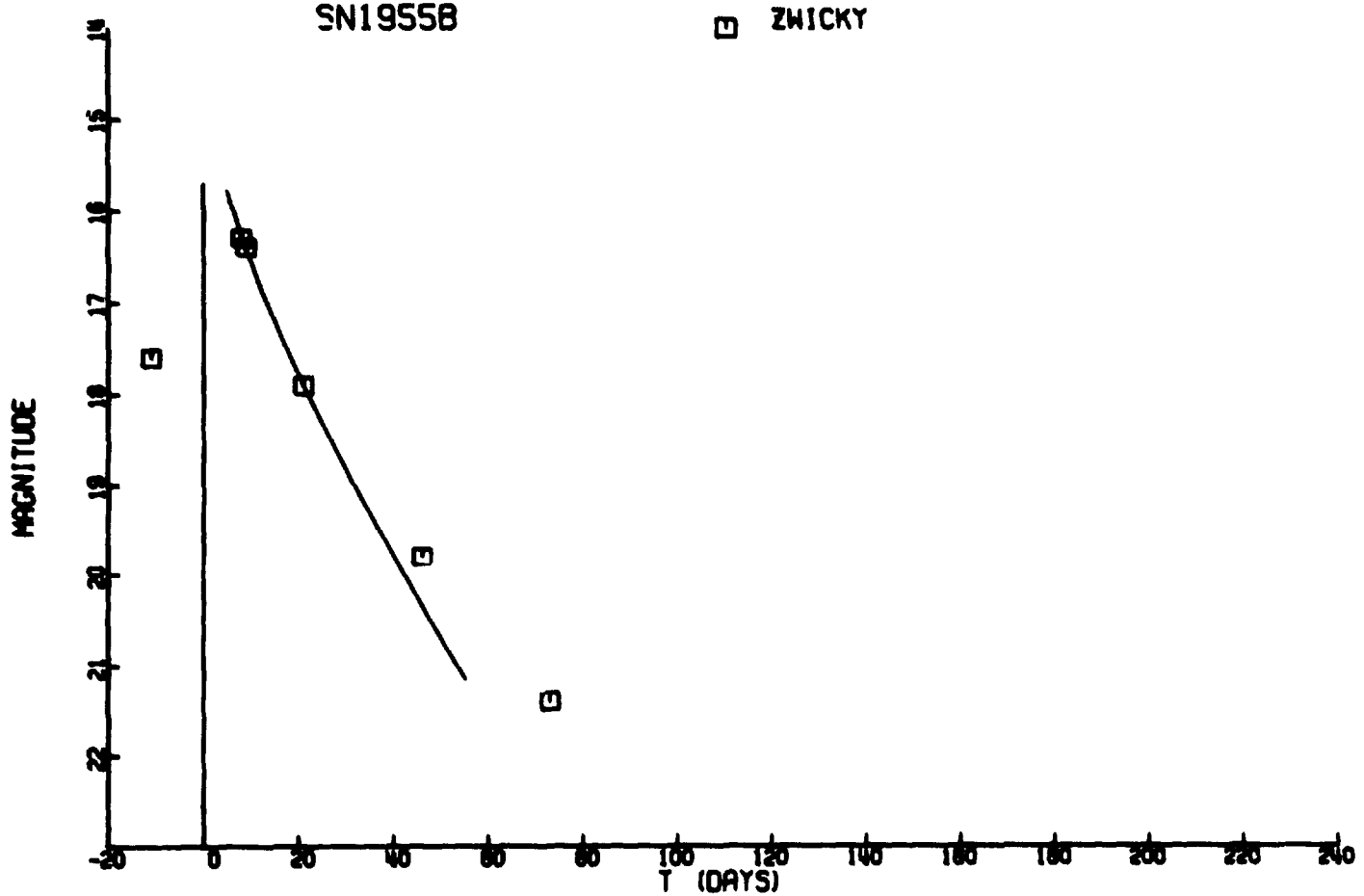
SN1955B
ZWICKY
MAGNITUDE
T (DAYS)
-20
0
20
40
60
80
100
120
140
160
180
200
220
240

Figure A2-1.9

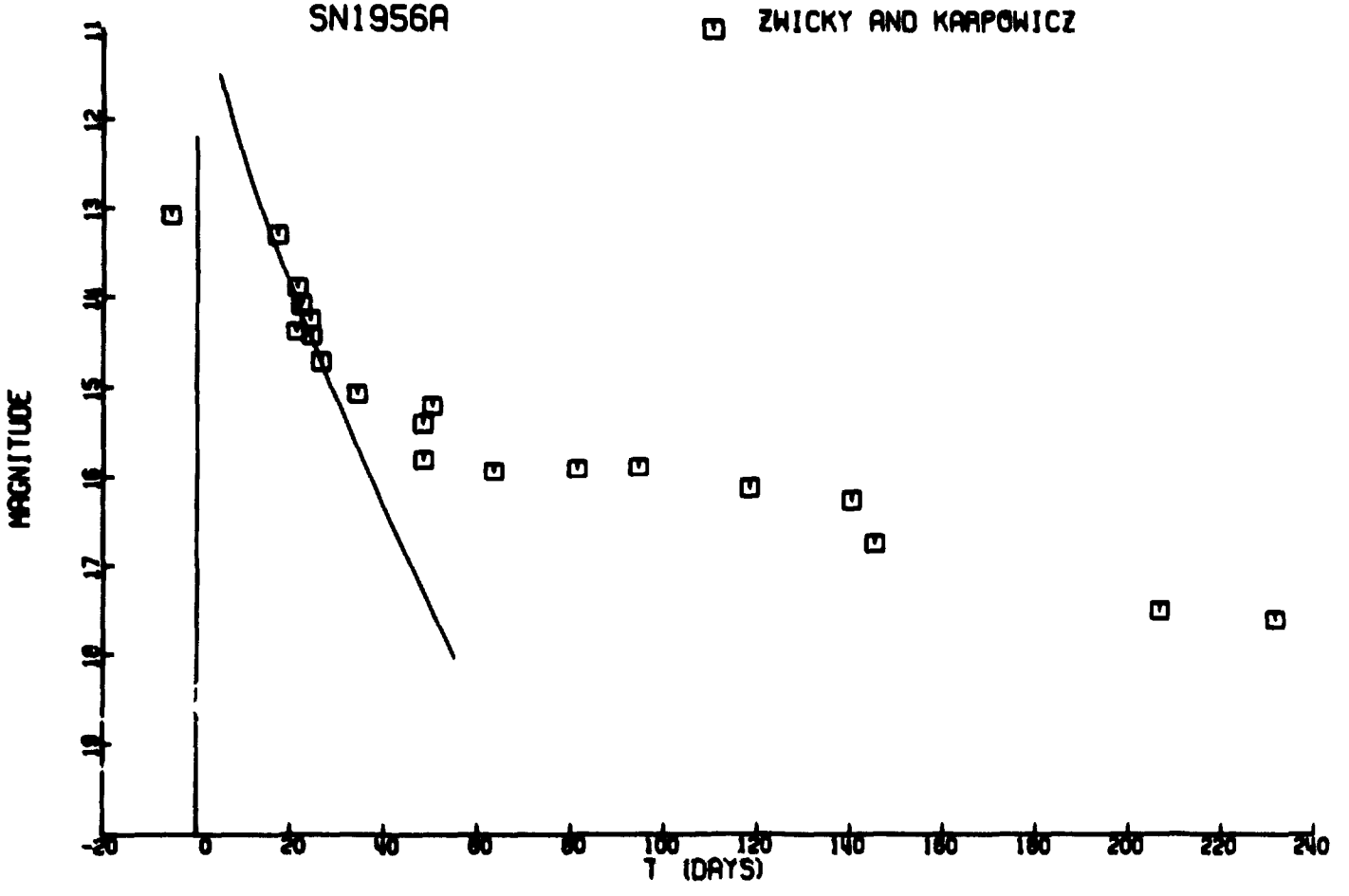

Figure A2-1.10

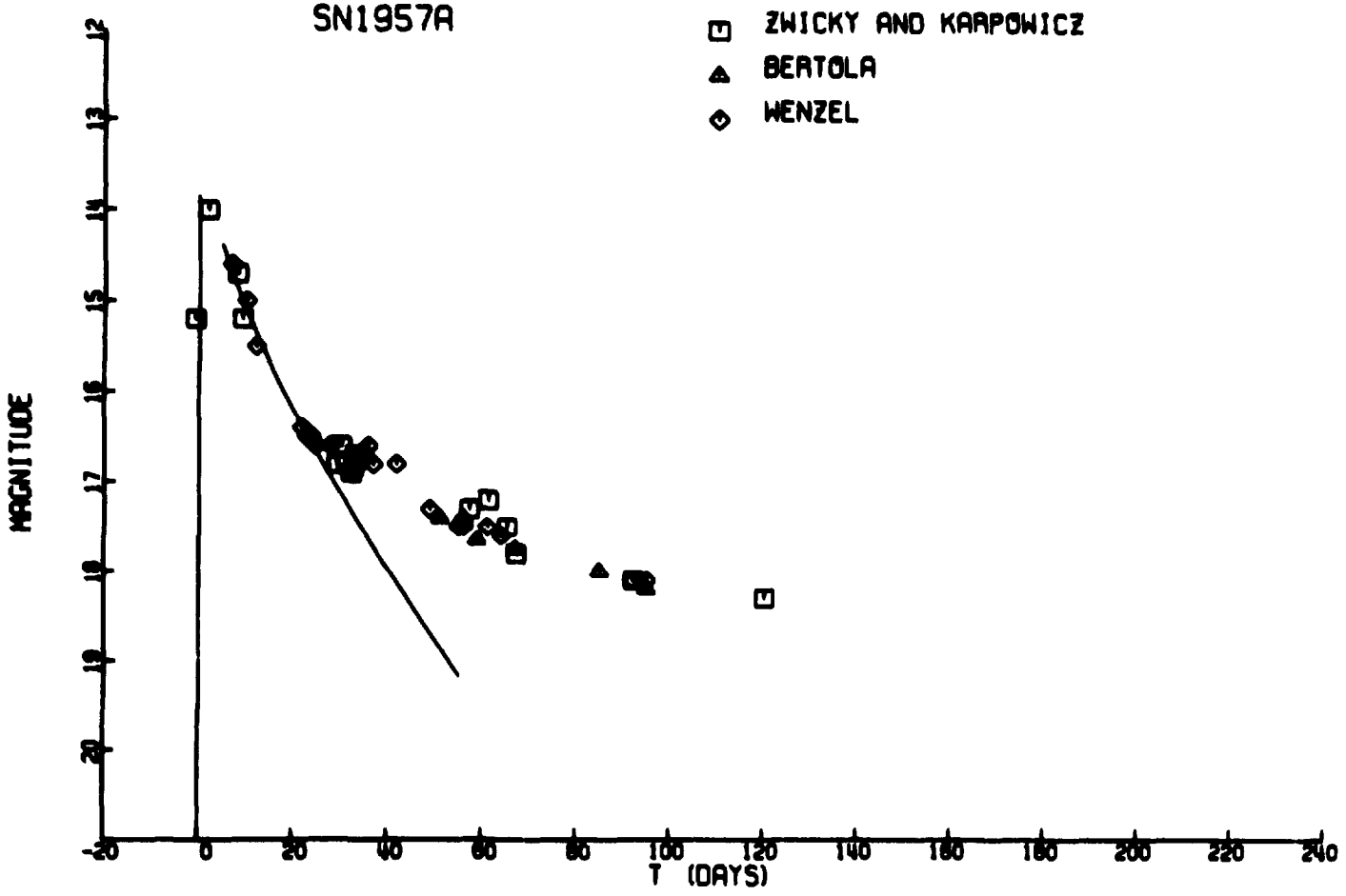

Figure A2-1.11

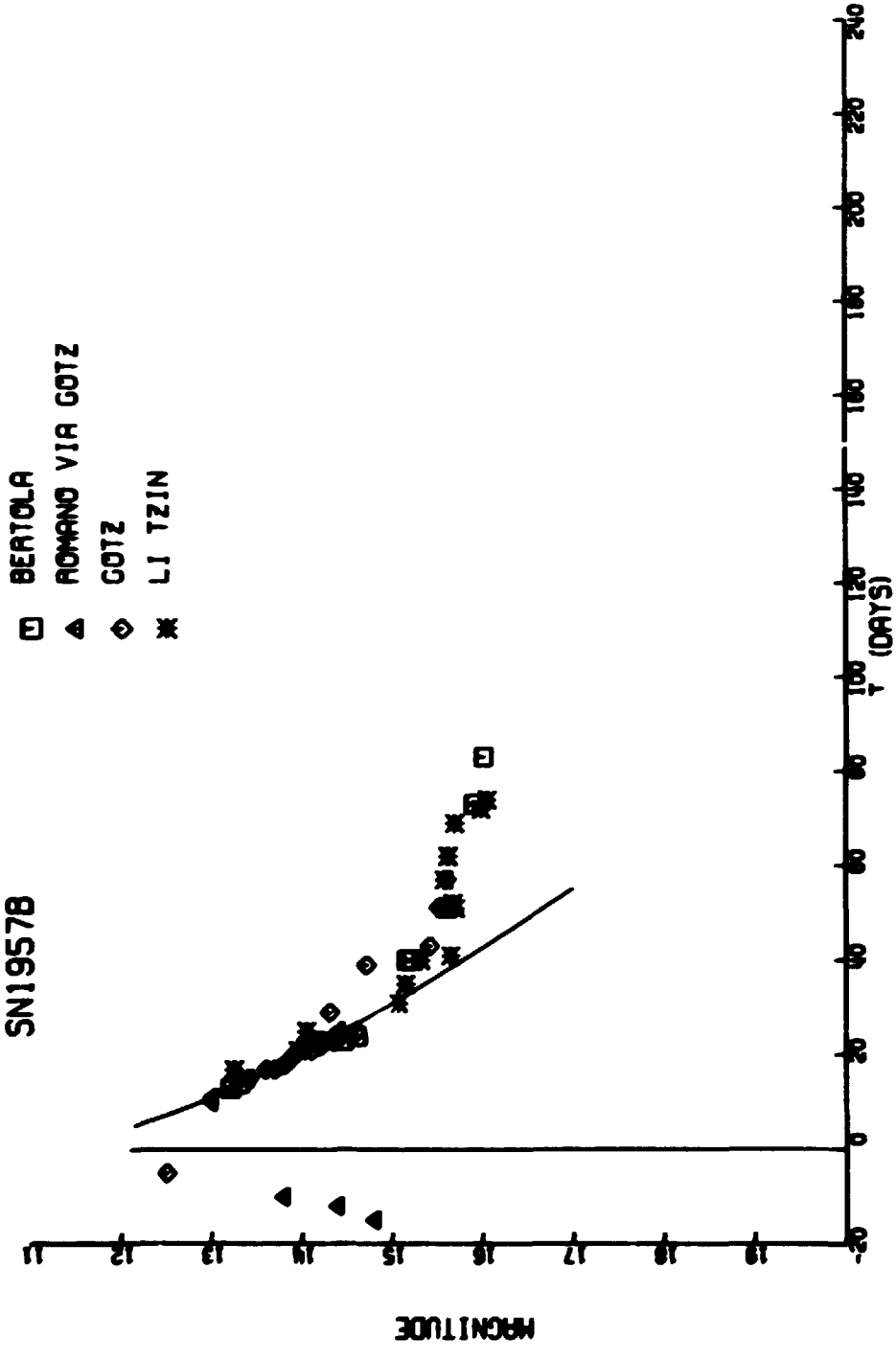

Figure A2-i.12

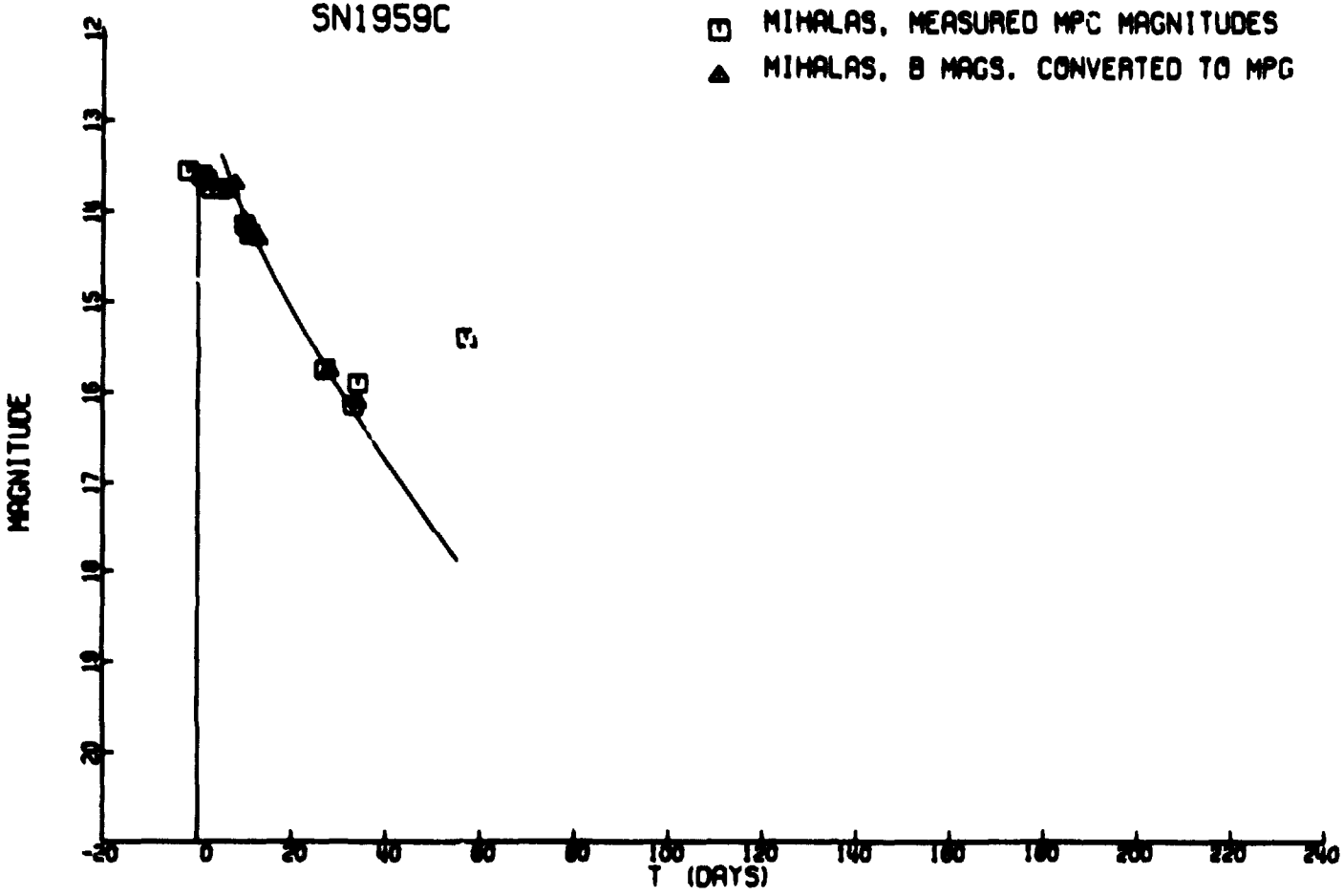

Figure A2-1.13

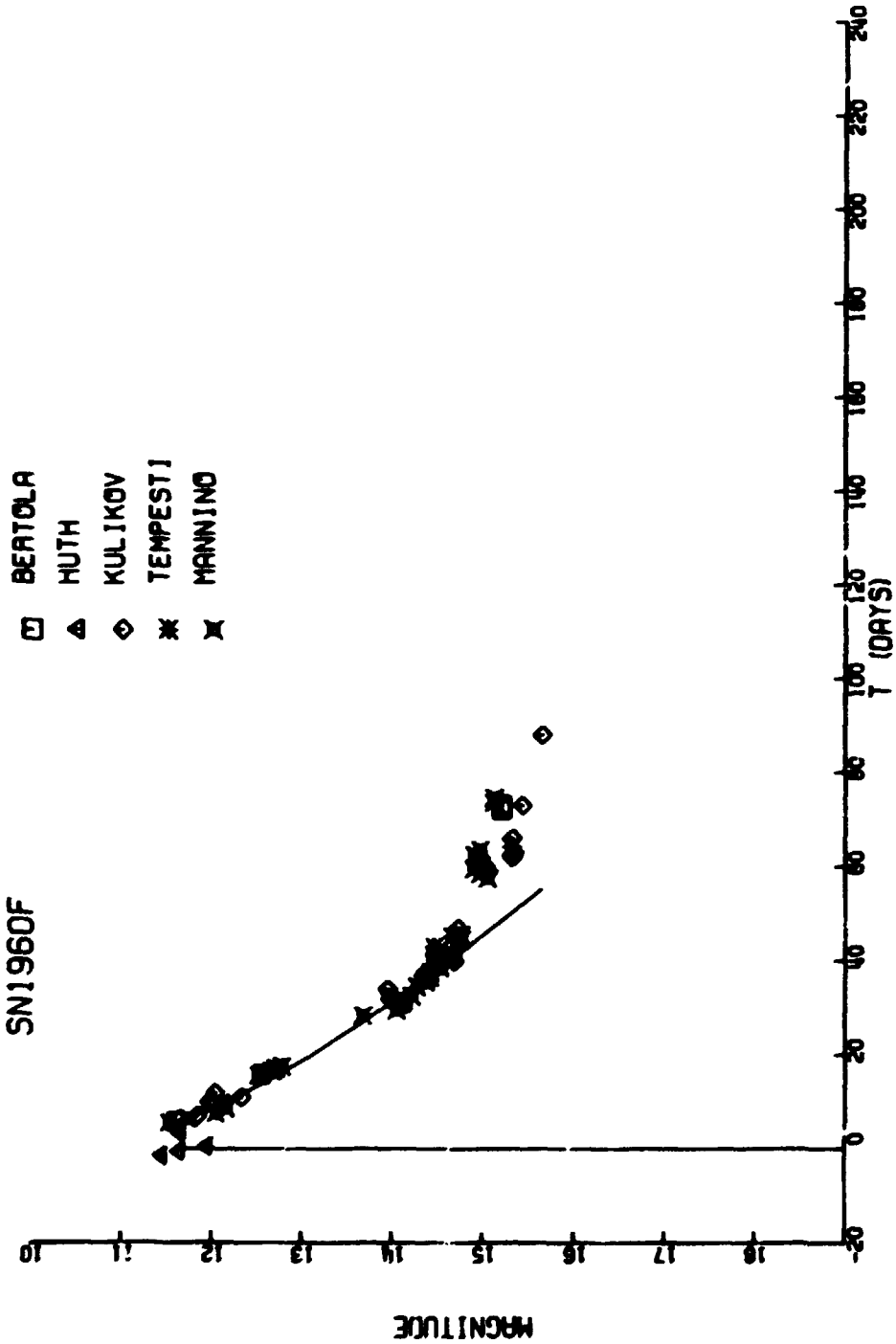

Figure A5-1.14

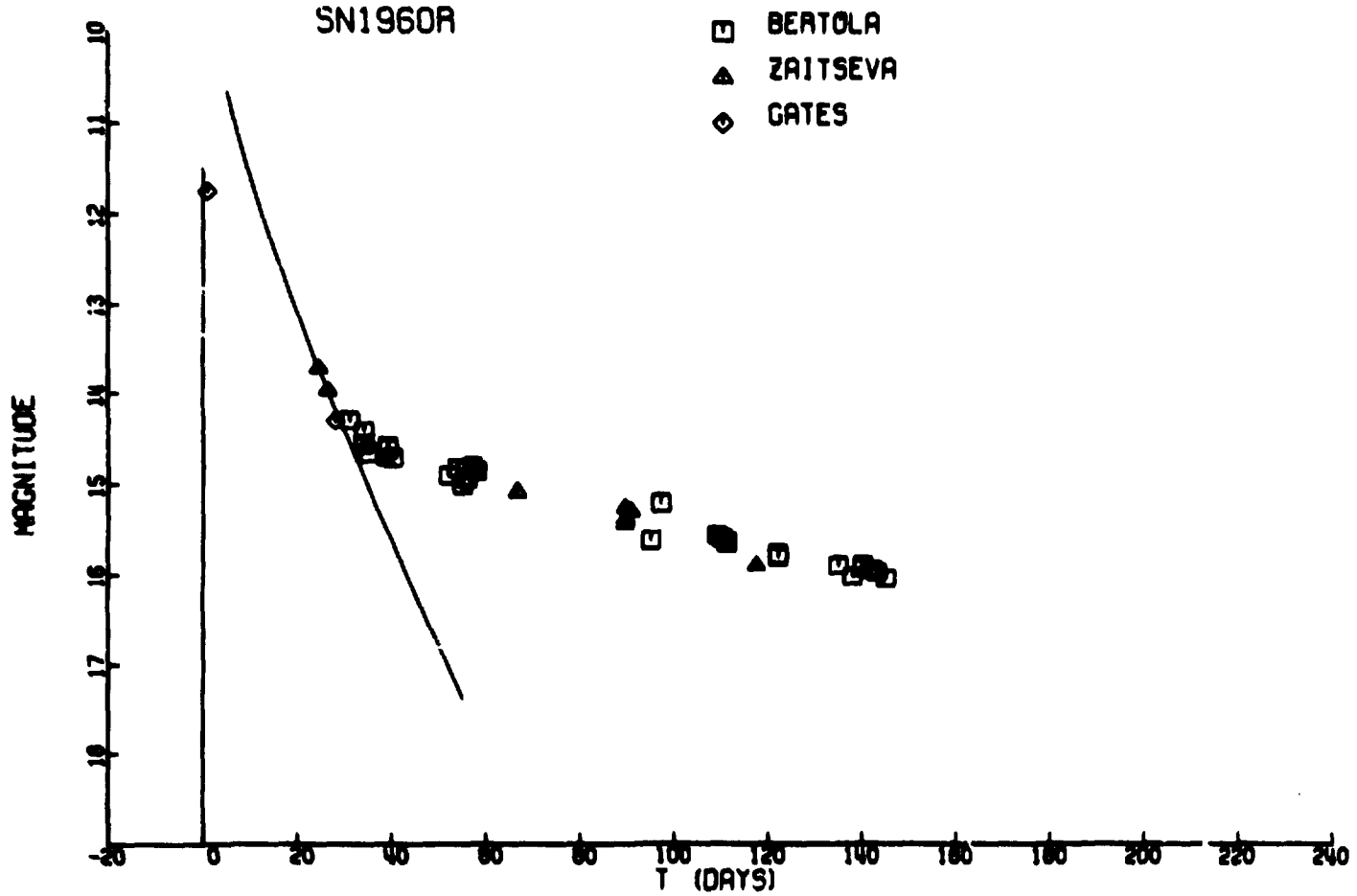

Figure A2-1.15

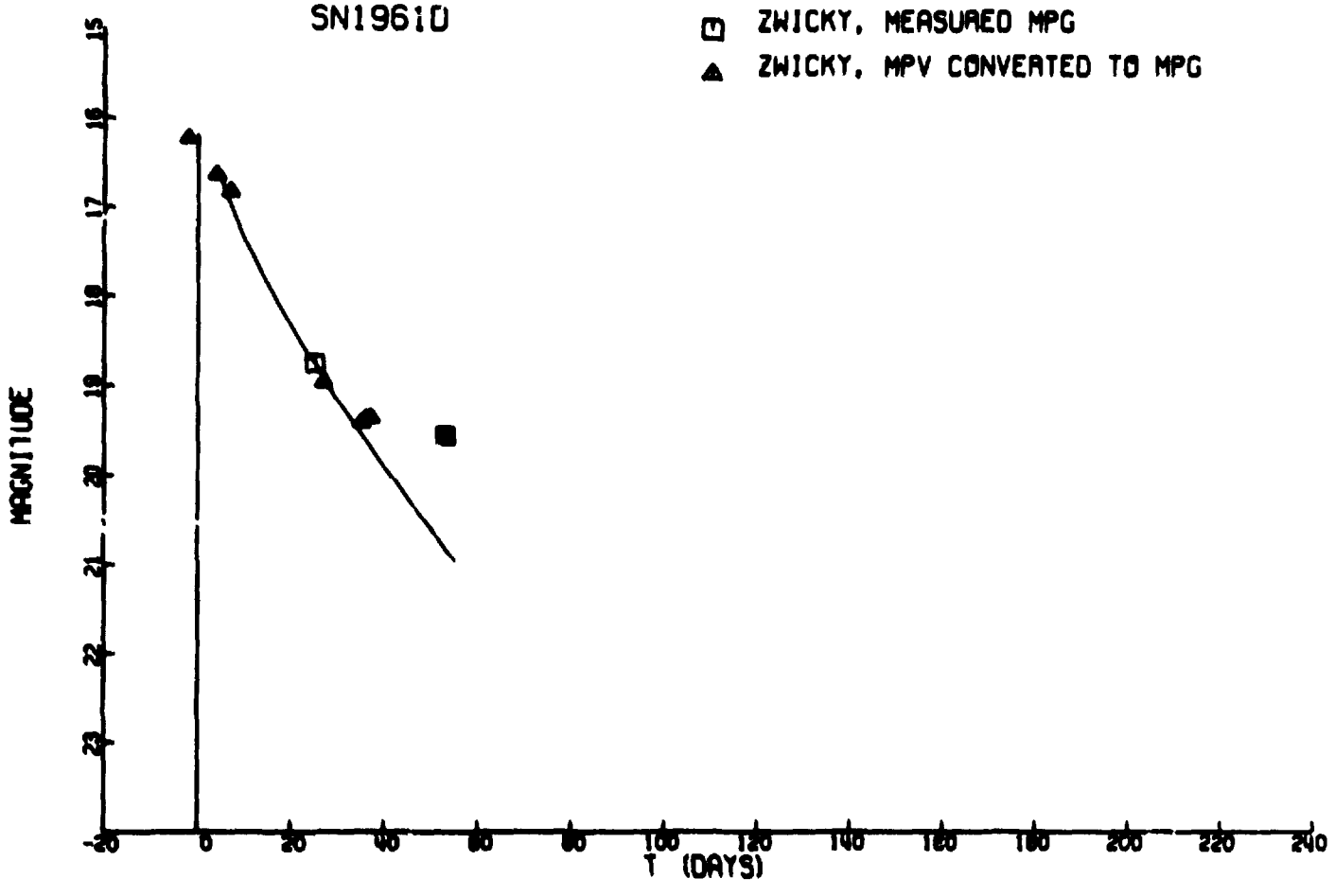

Figure A2-1.16

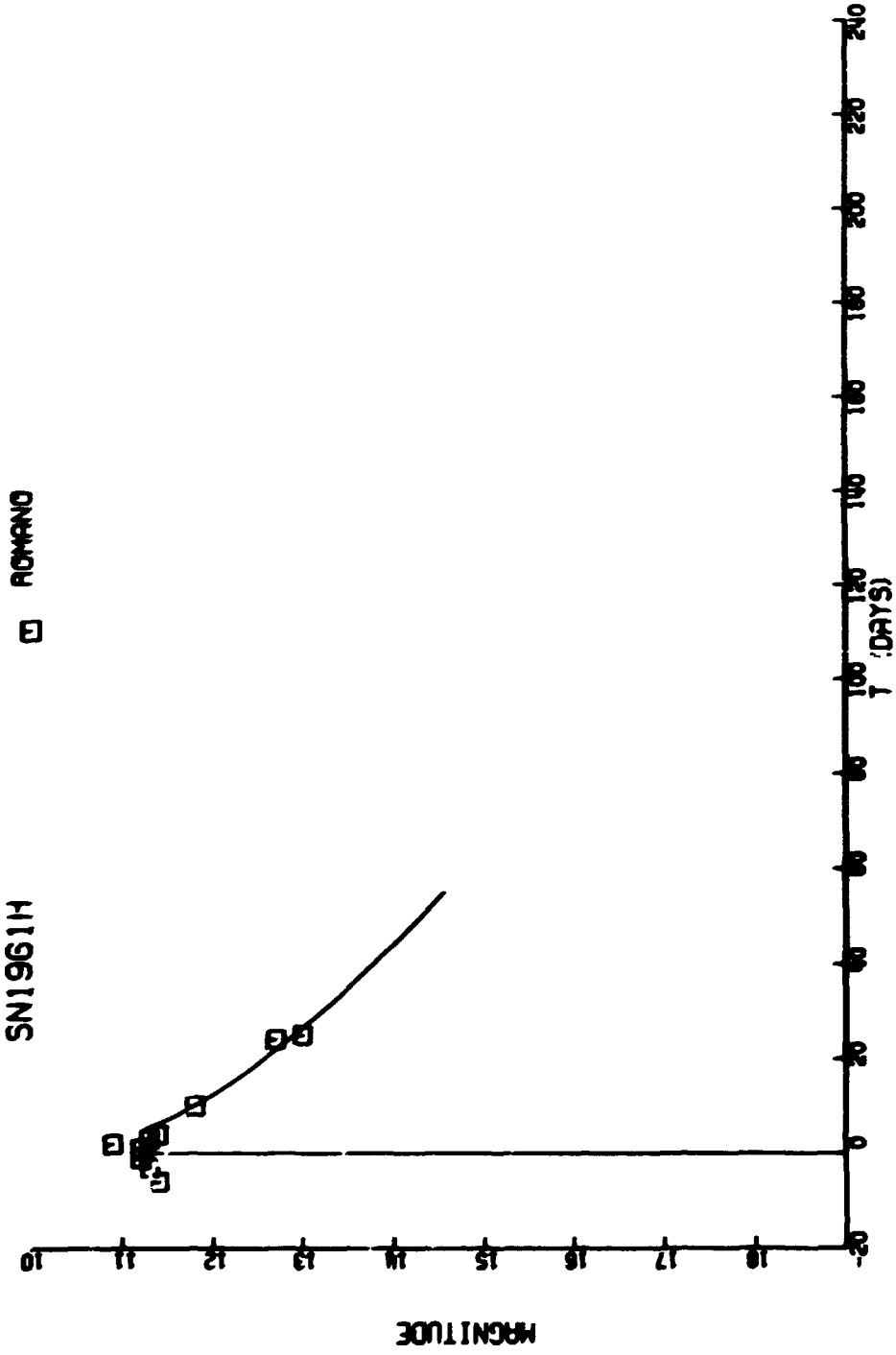

Figure A2-1.17

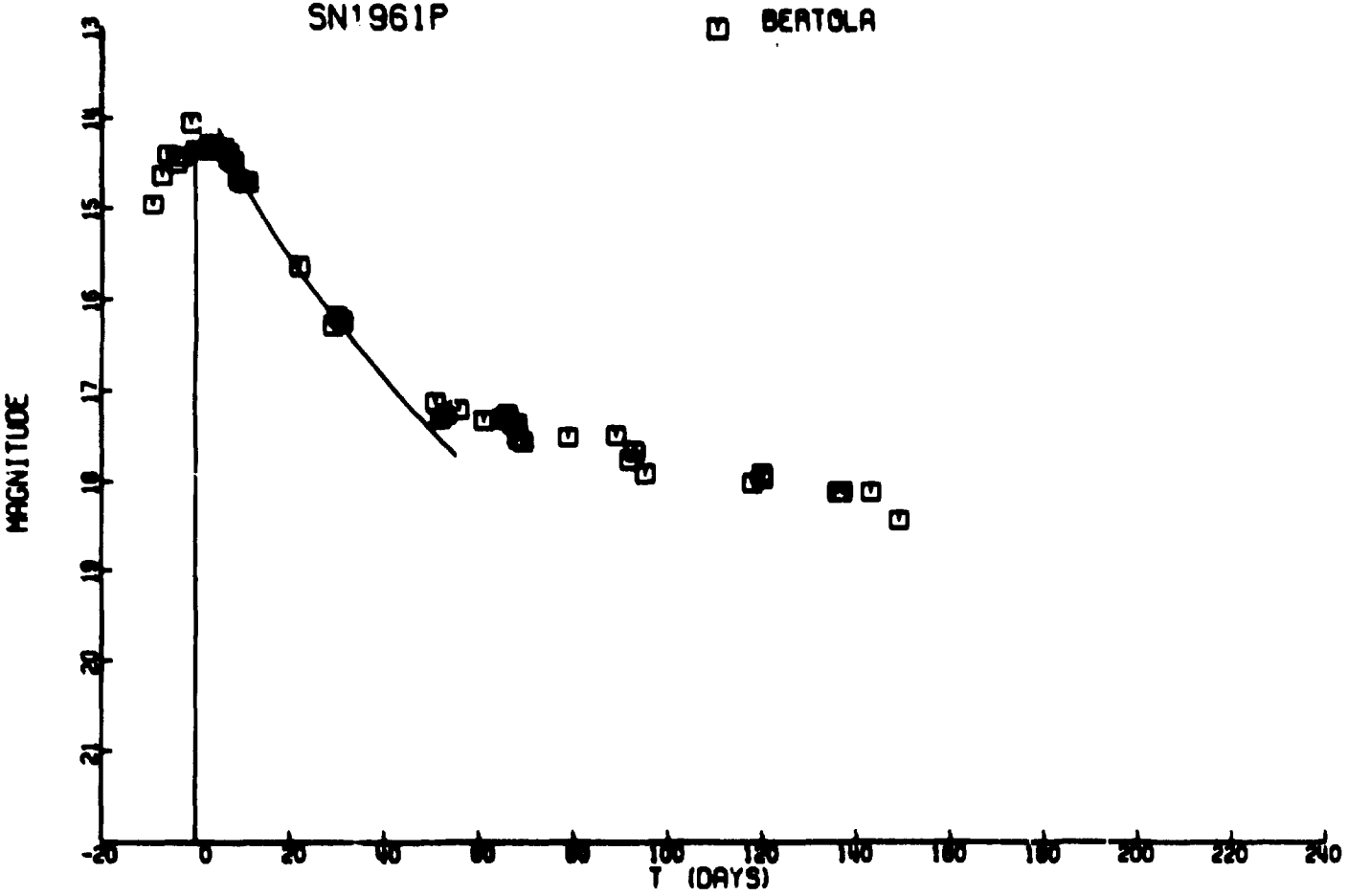

Figure A2-1.4

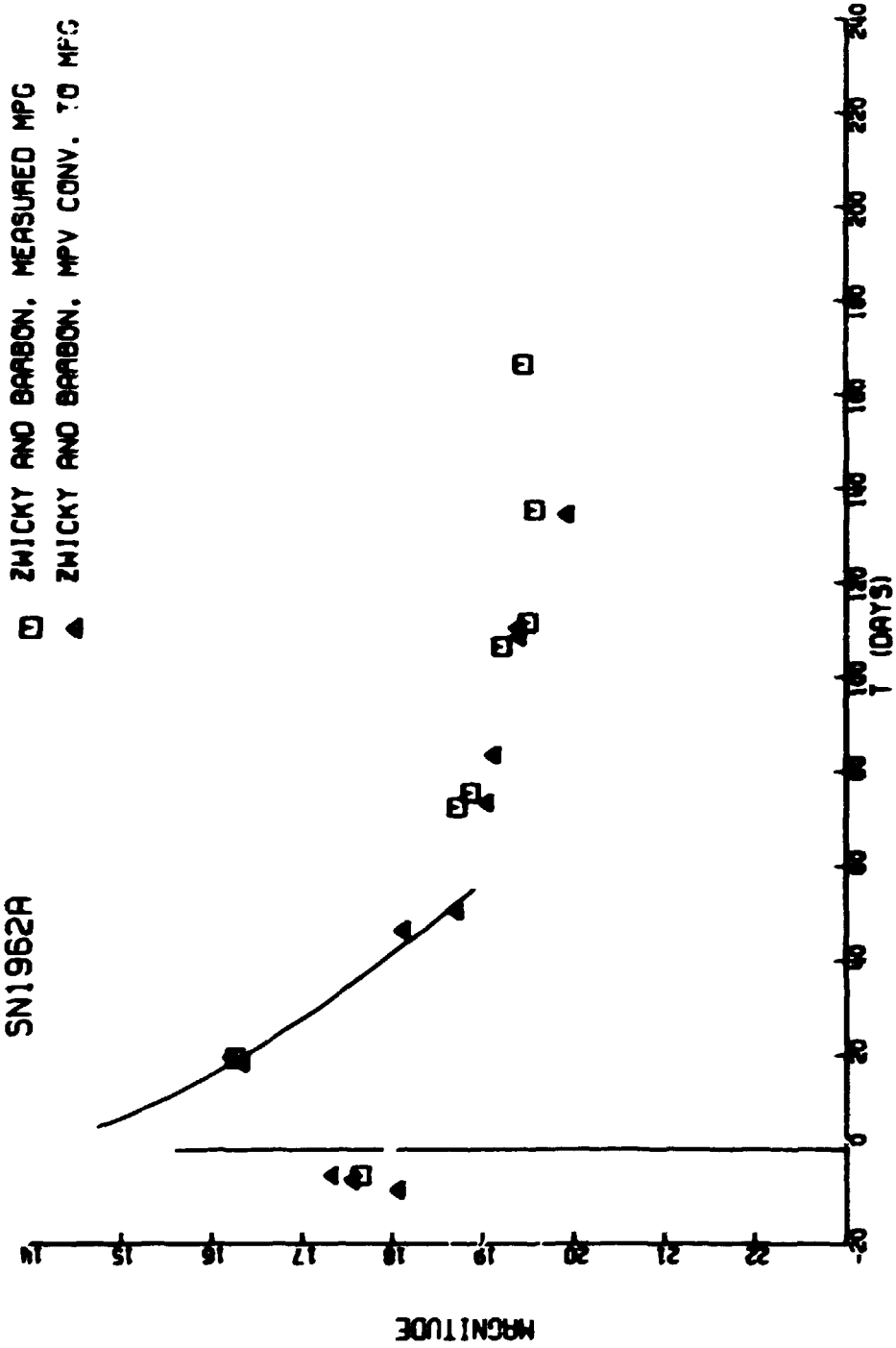

Figure A2-1.19

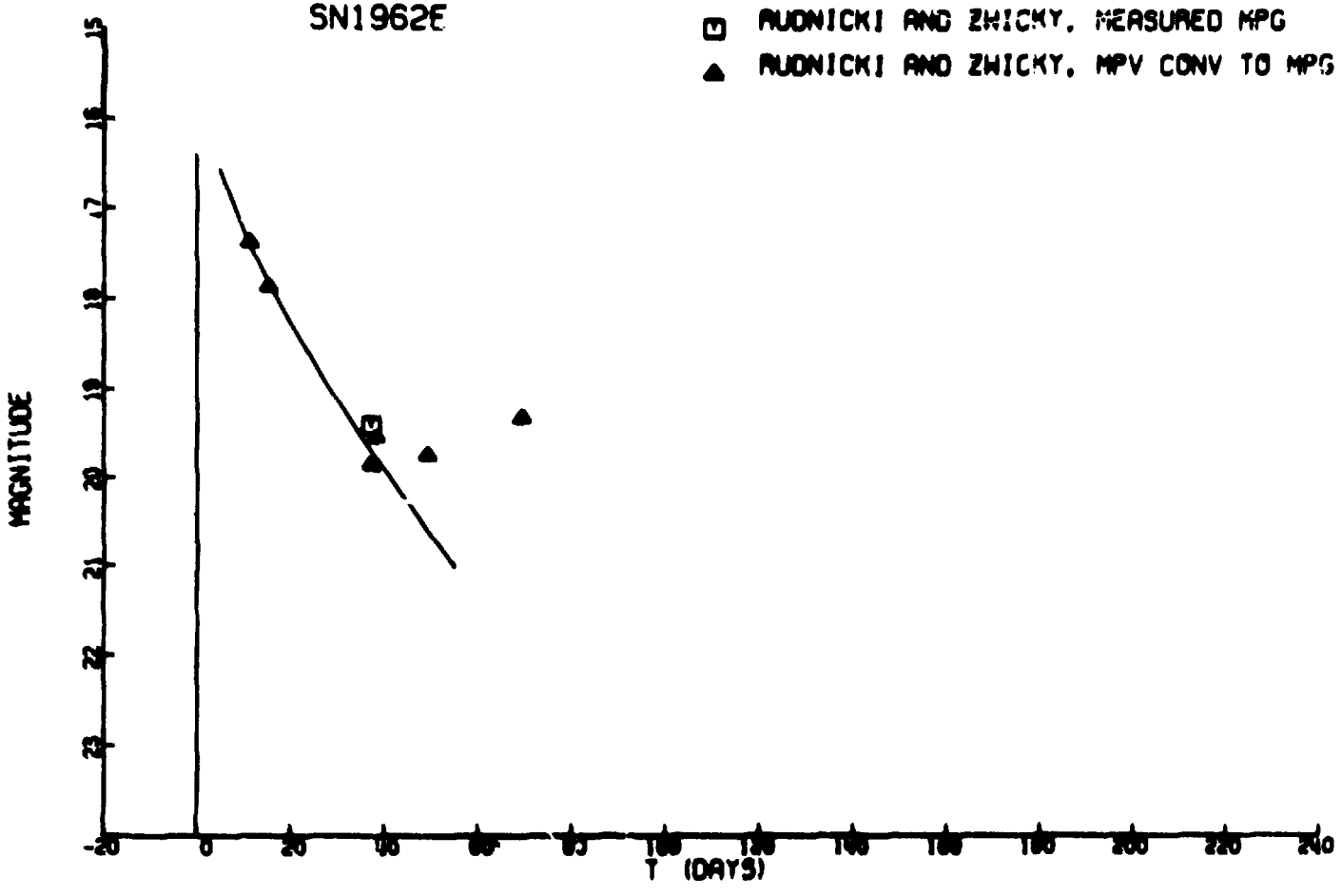
SN1962E
RUDNICKI AND ZWICKY, MEASURED MPG
RUDNICKI AND ZWICKY, MPV CONV TO MPG
MAGNITUDE
T (DAYS)

Figure A?-1.20

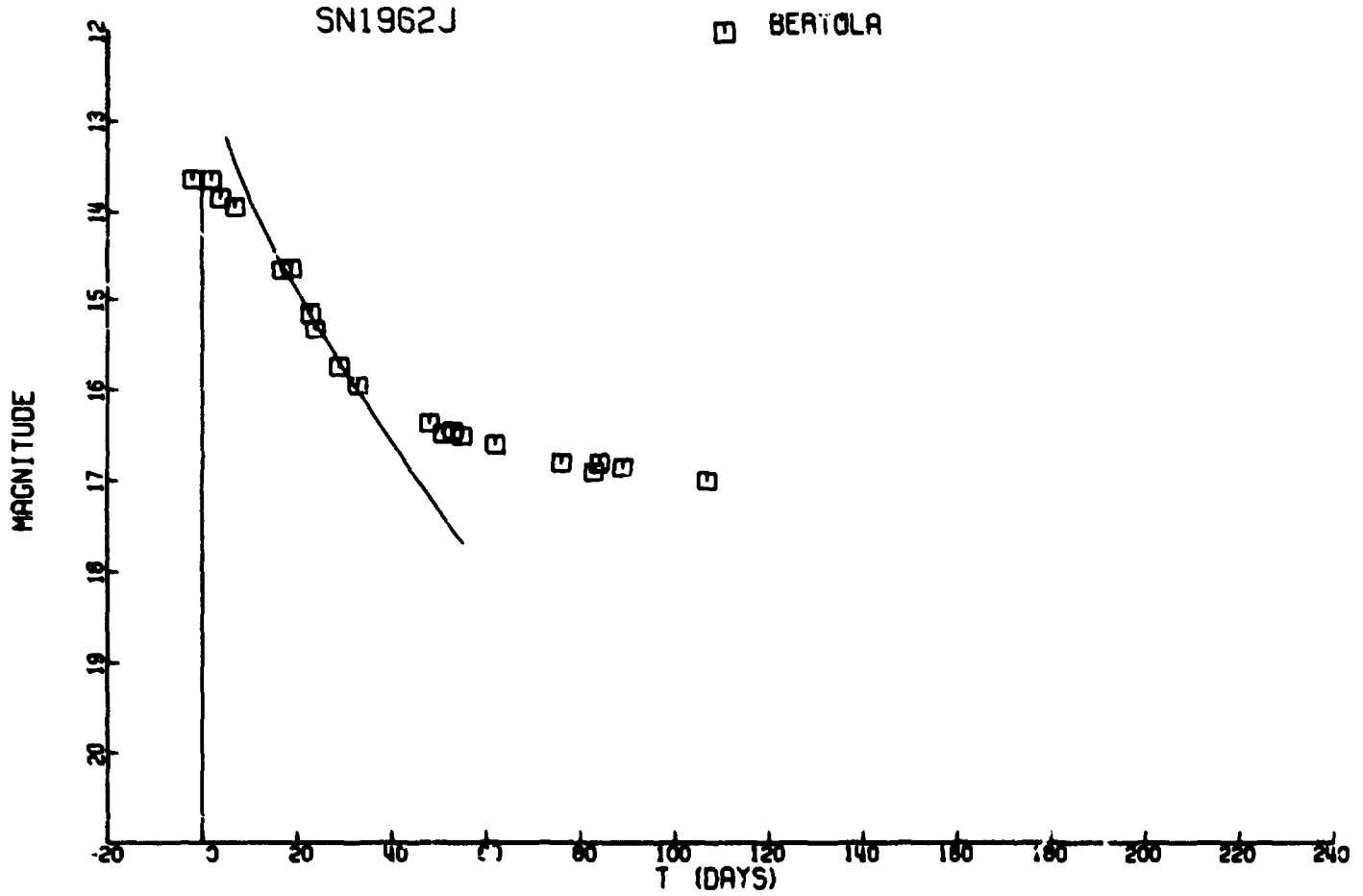

Figure A2-1.21

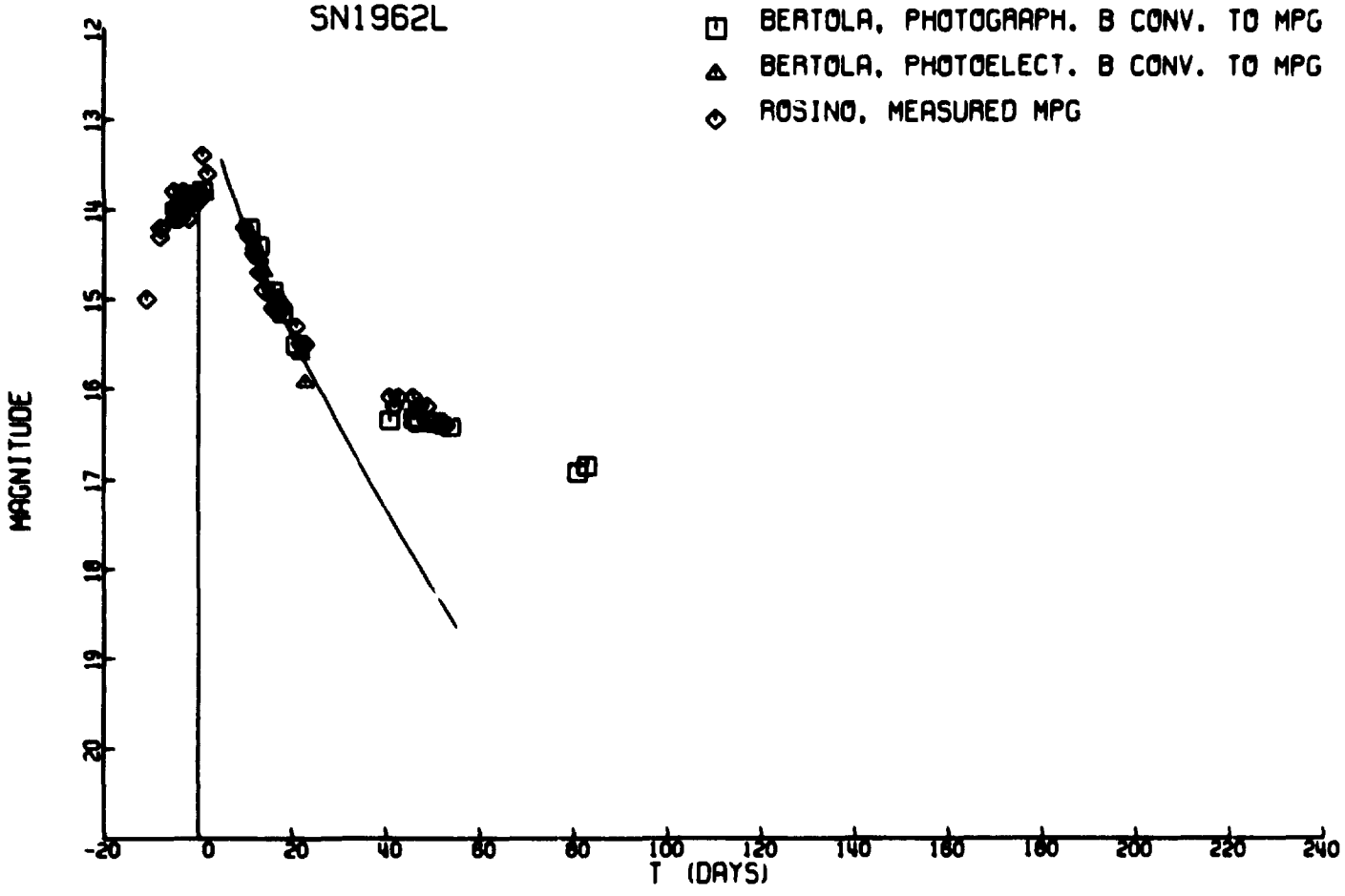

Figure A2-1.22

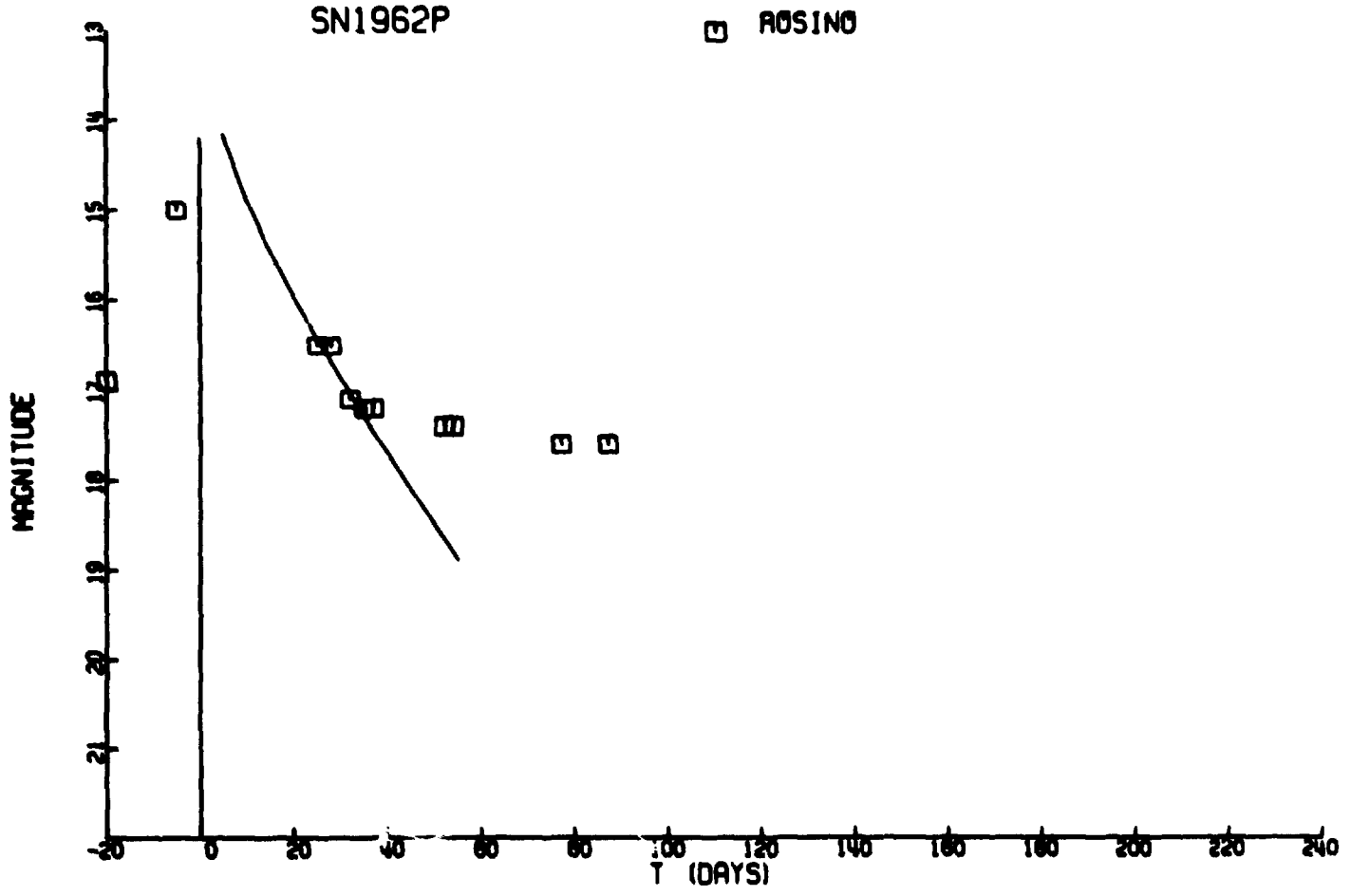

Figure A2-1.23

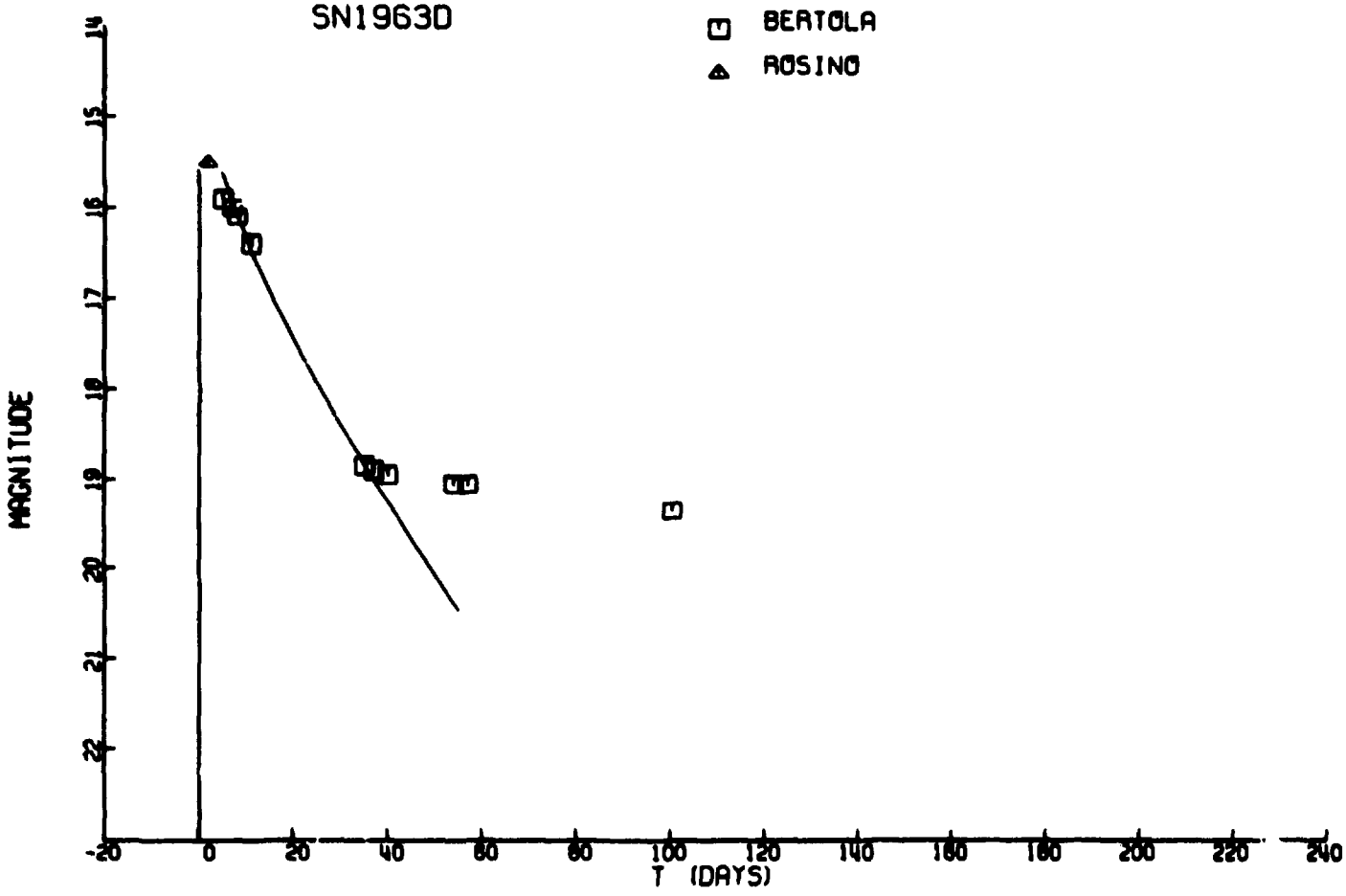

Figure A2-1.24

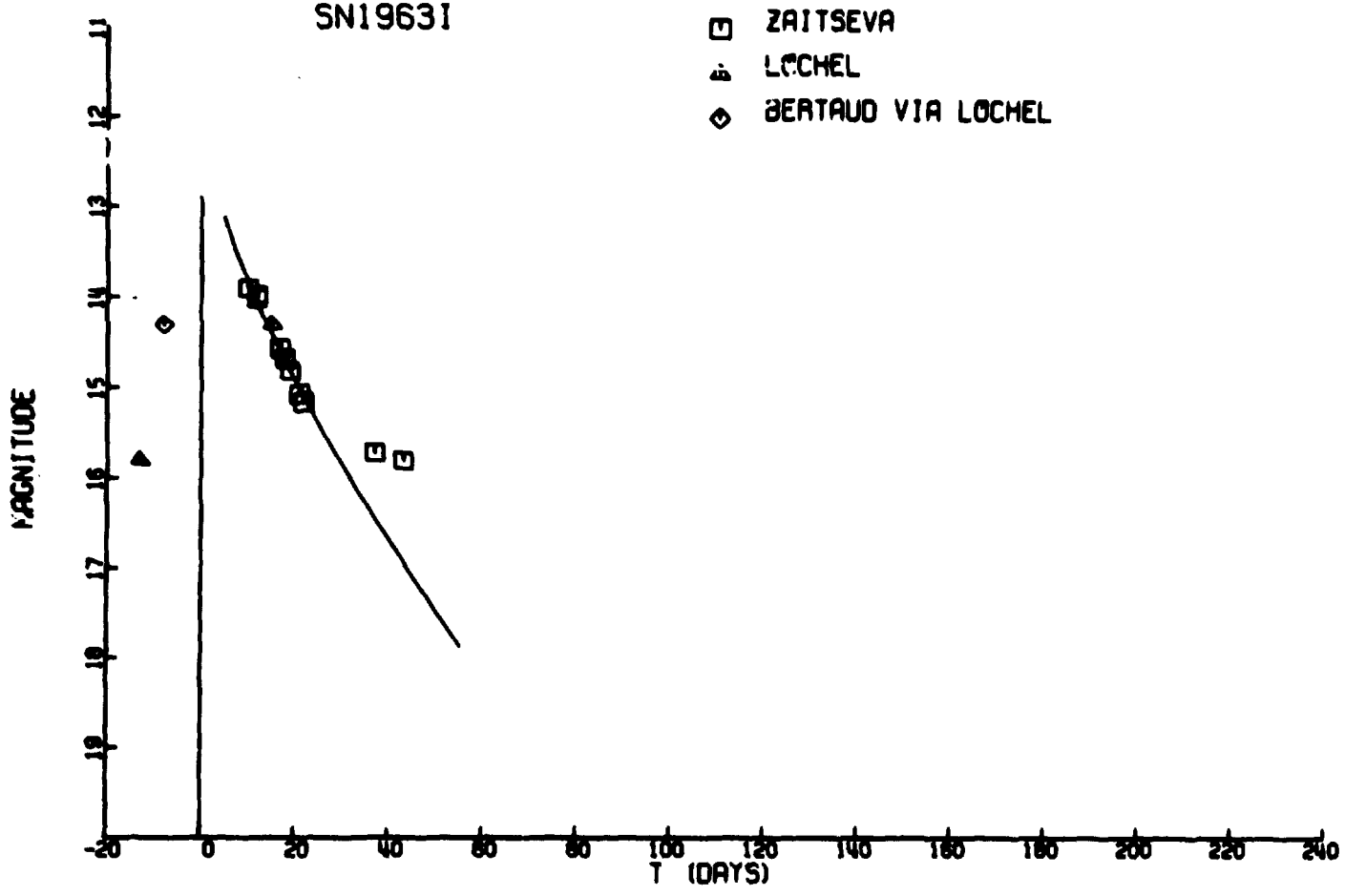

Figure A2-1.25

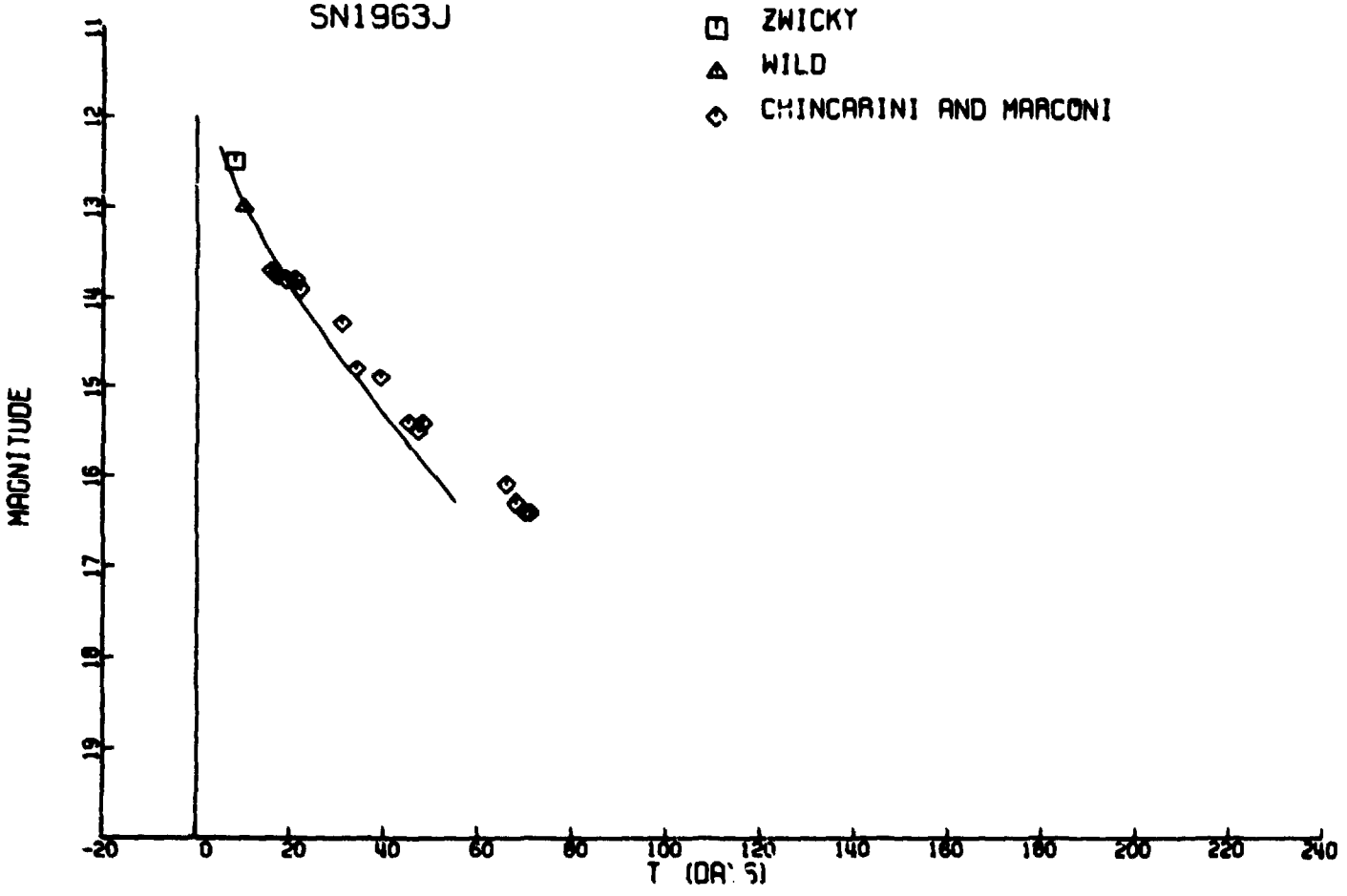

Figure A2-1.26

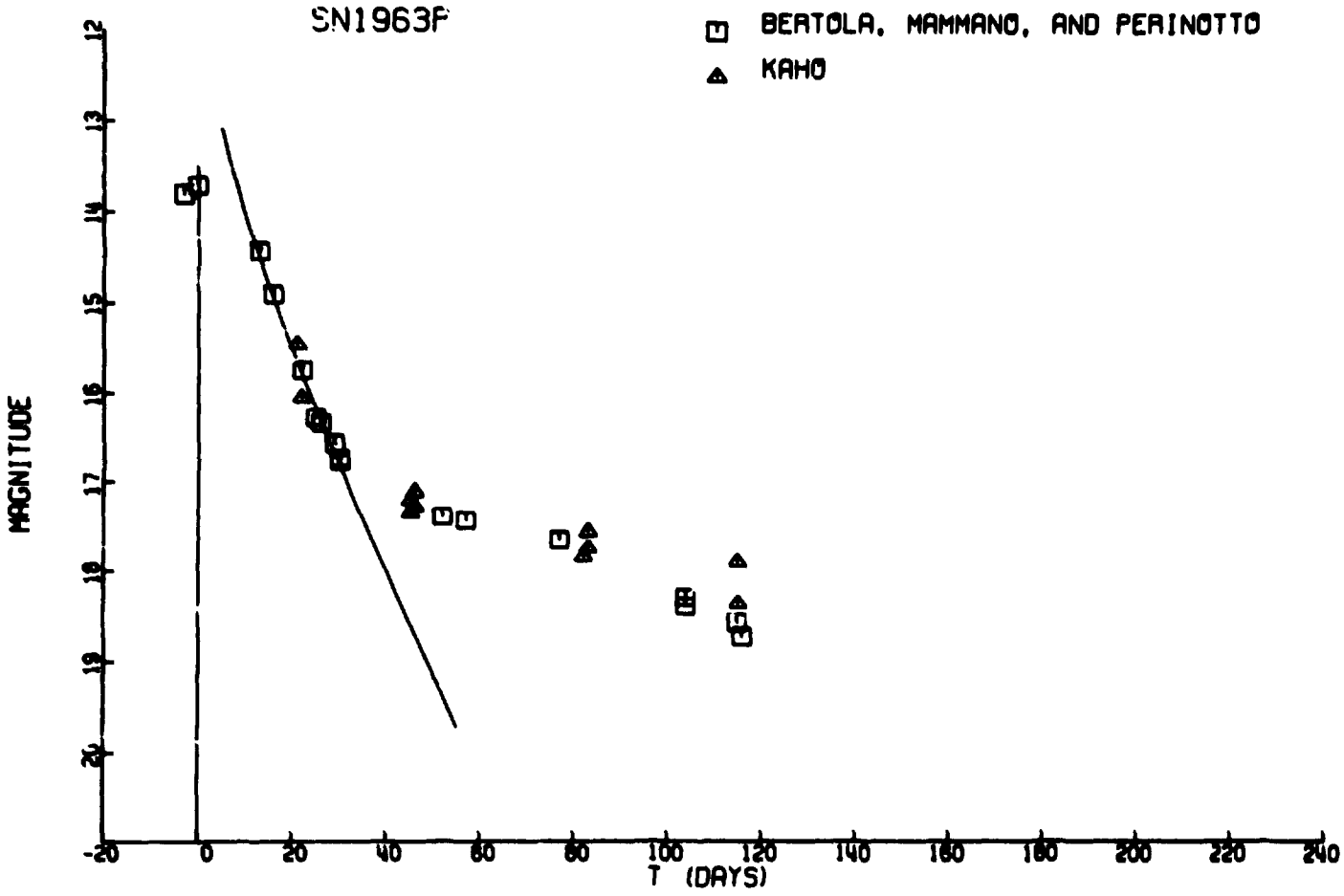

Figure A2-1.27

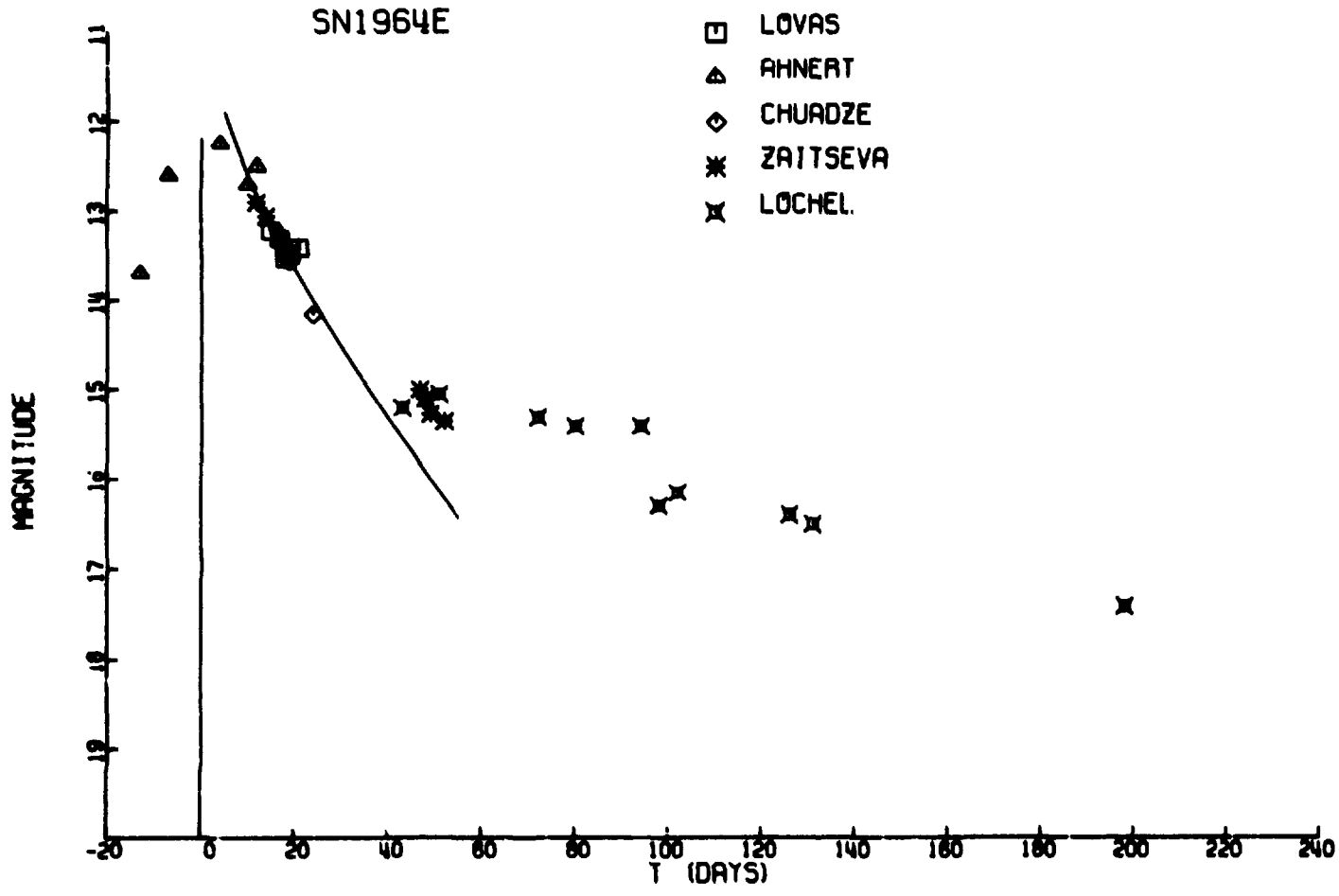

Figure A2-1.28

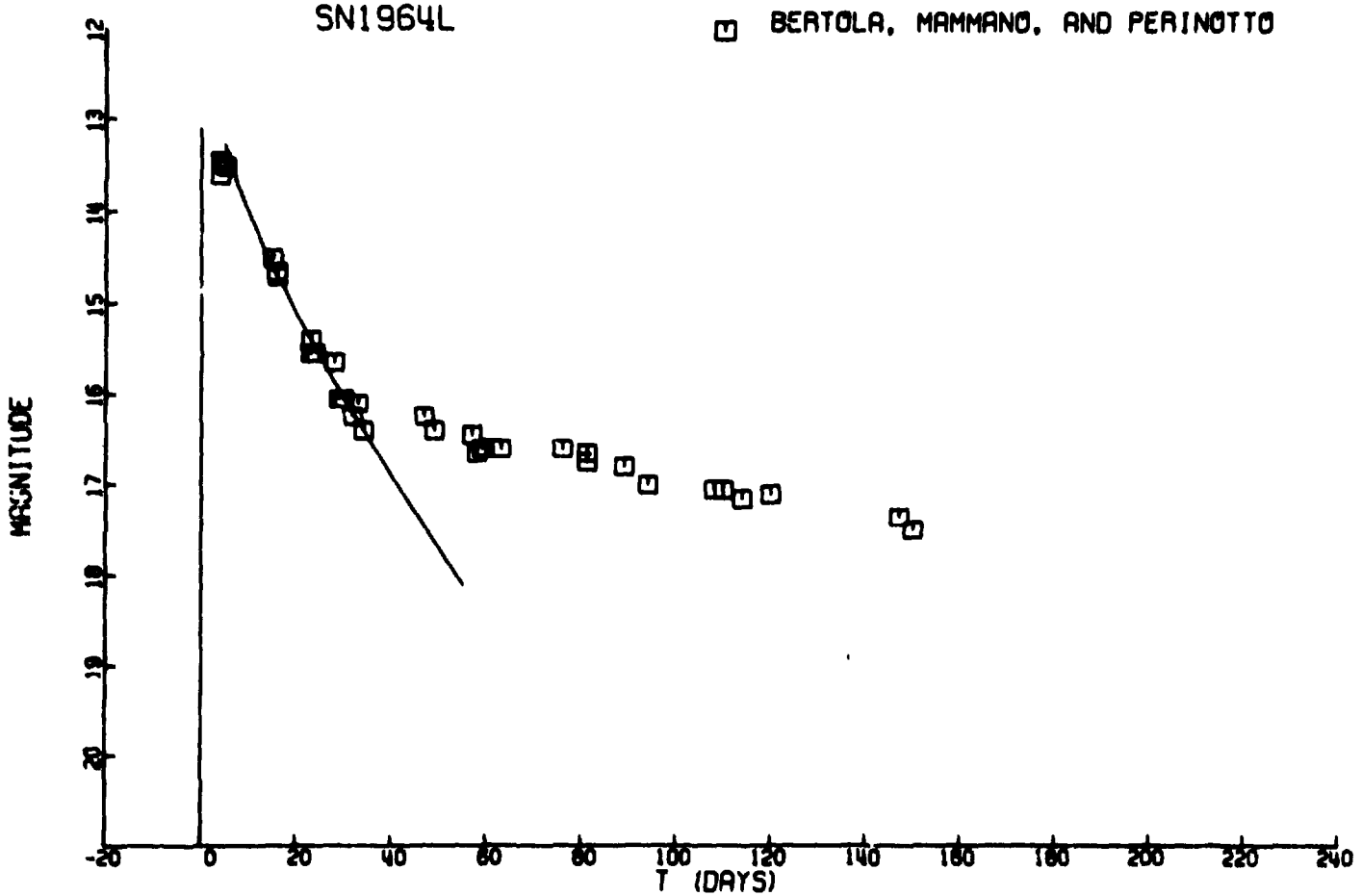

Figure A2-1.29

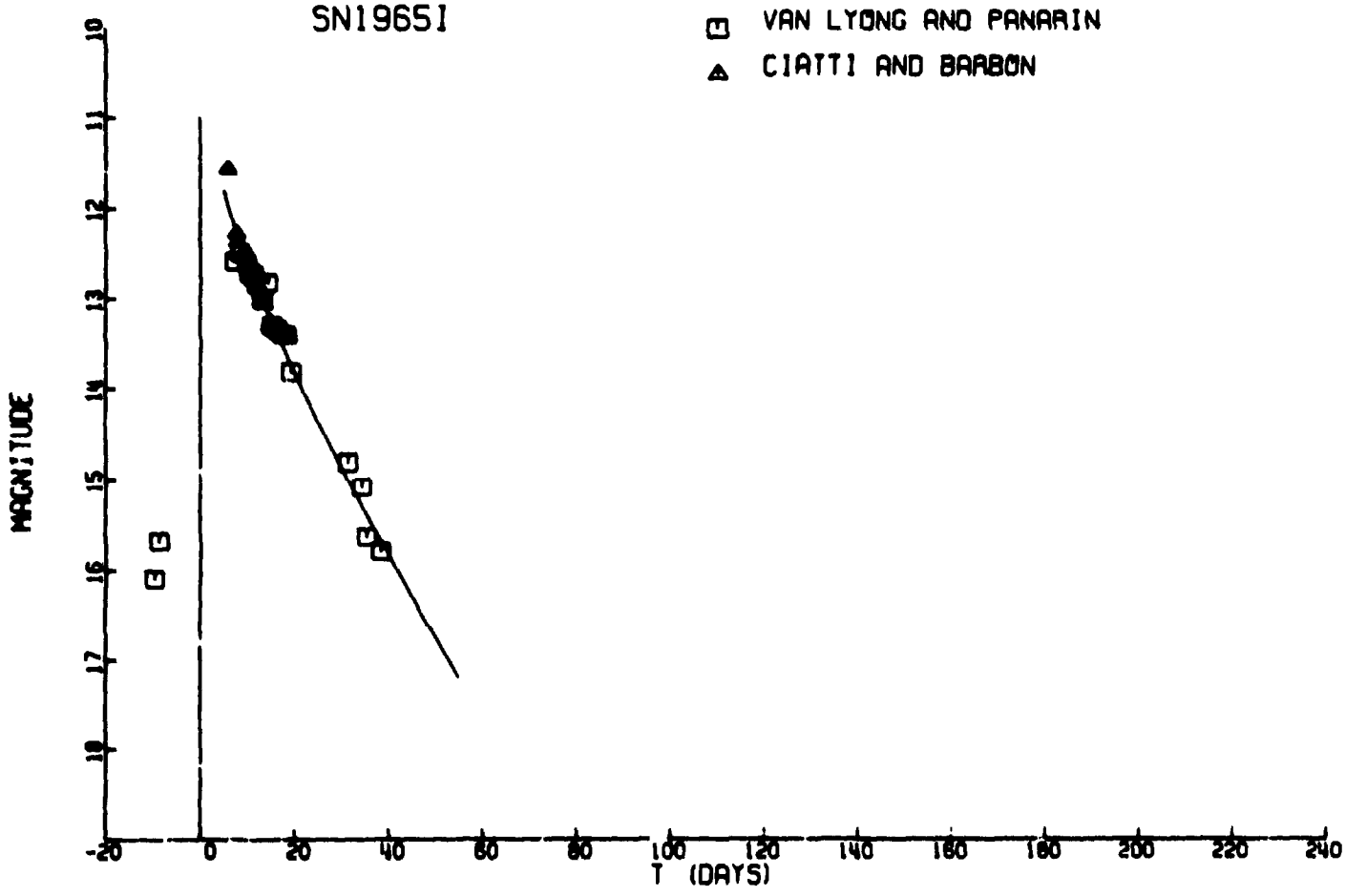

Figure A2-1.30

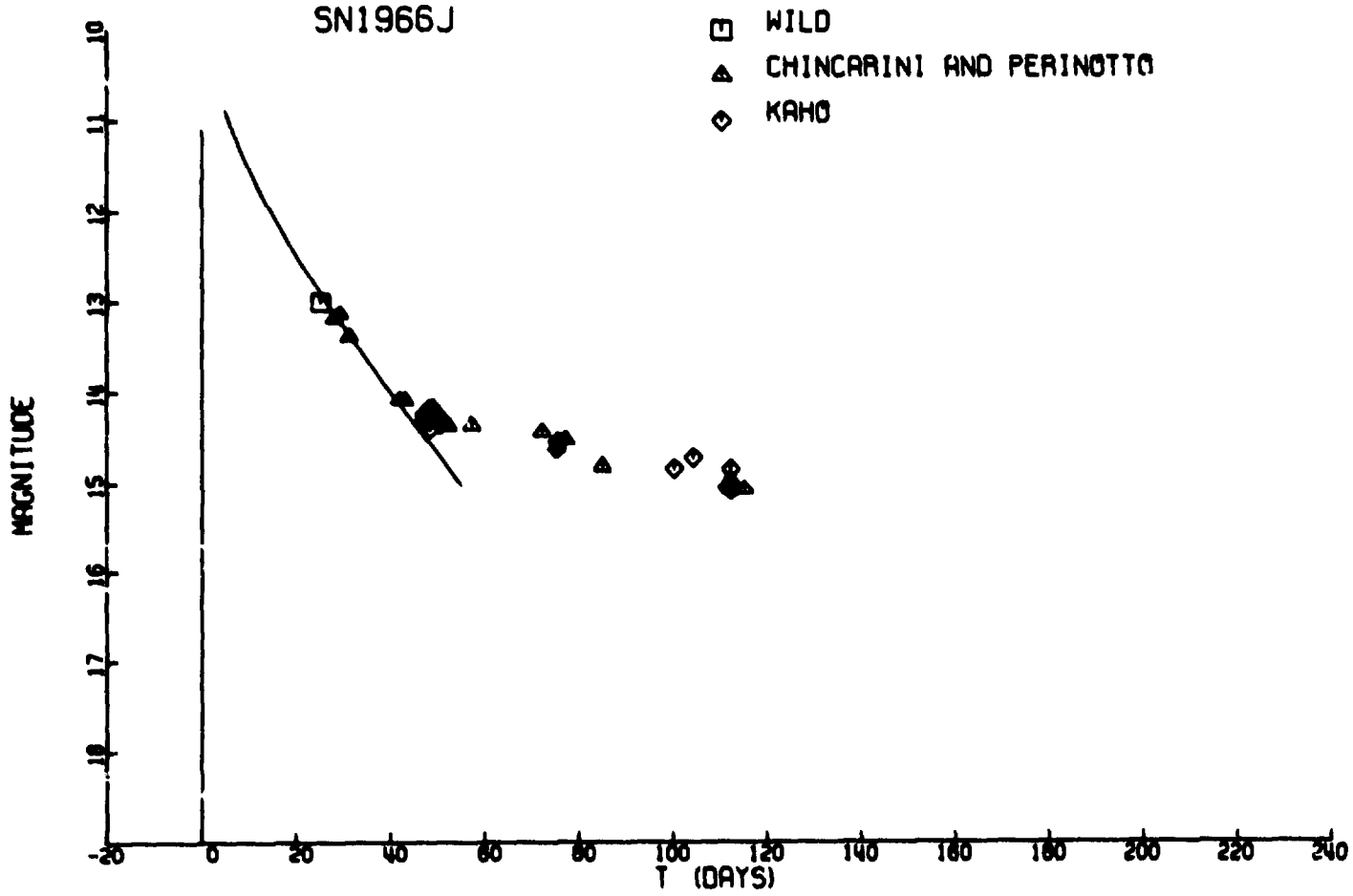

Figure A2-1.31

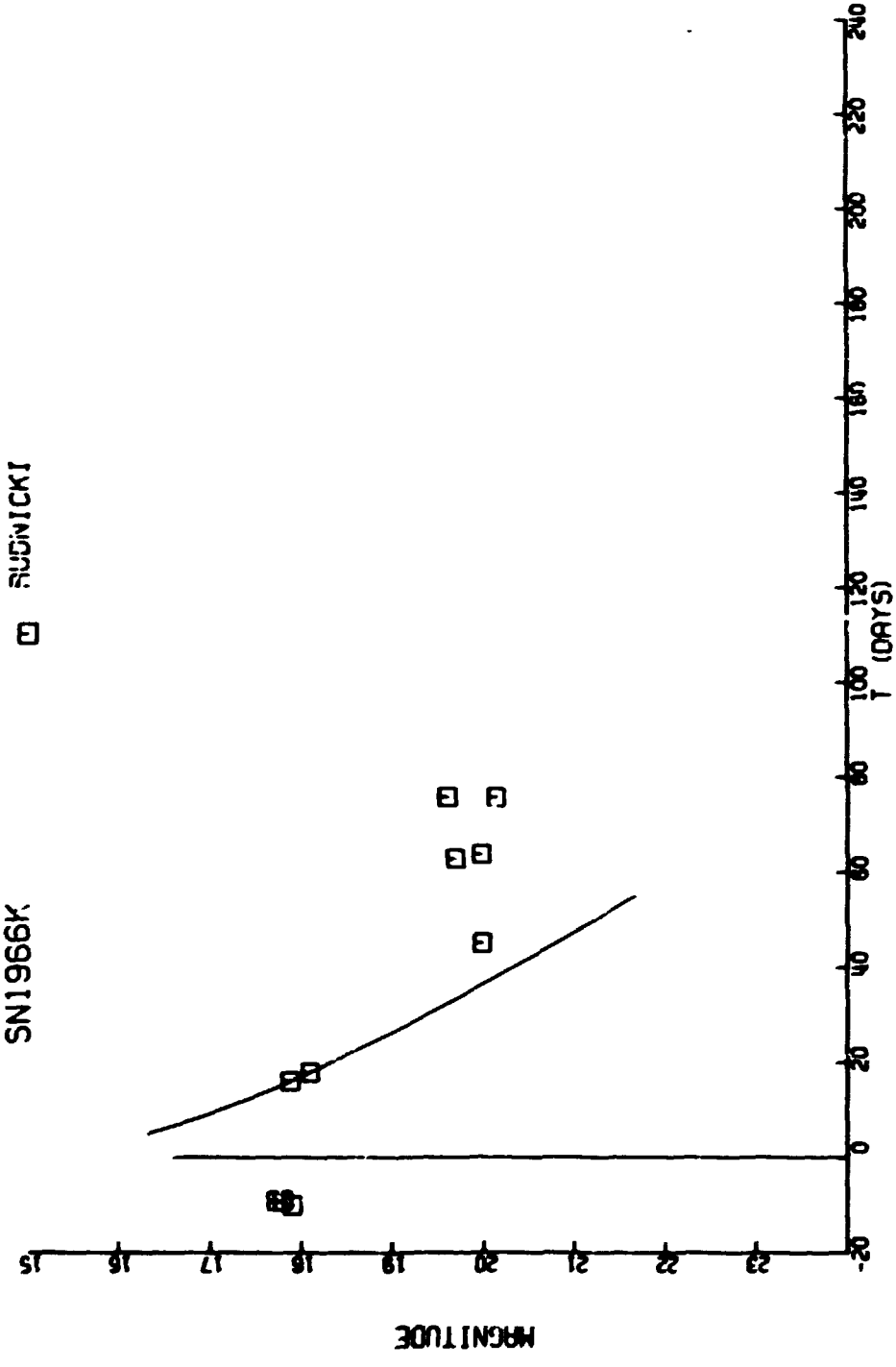

Figure A2-1.32

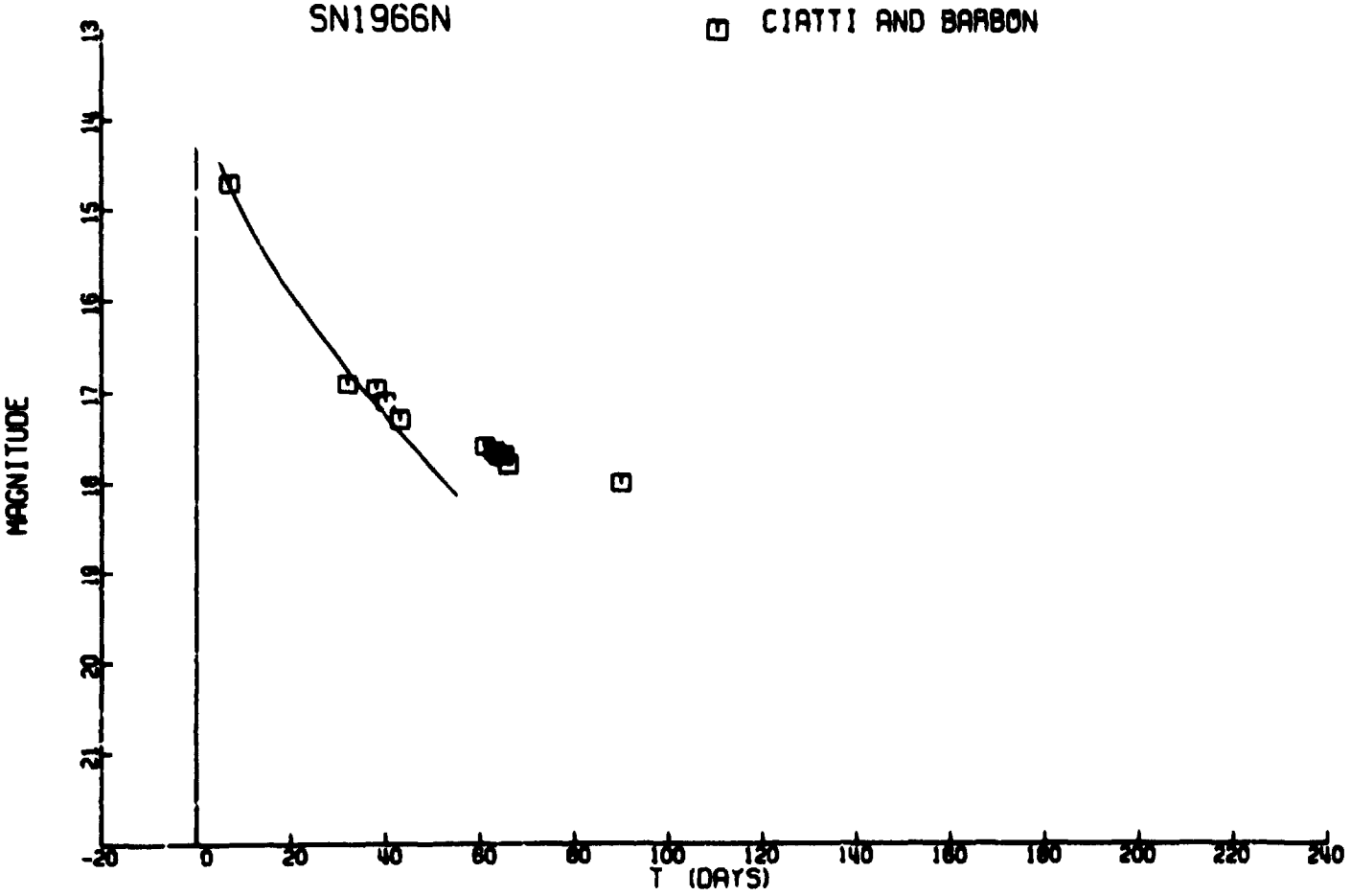

Figure A2-1.33

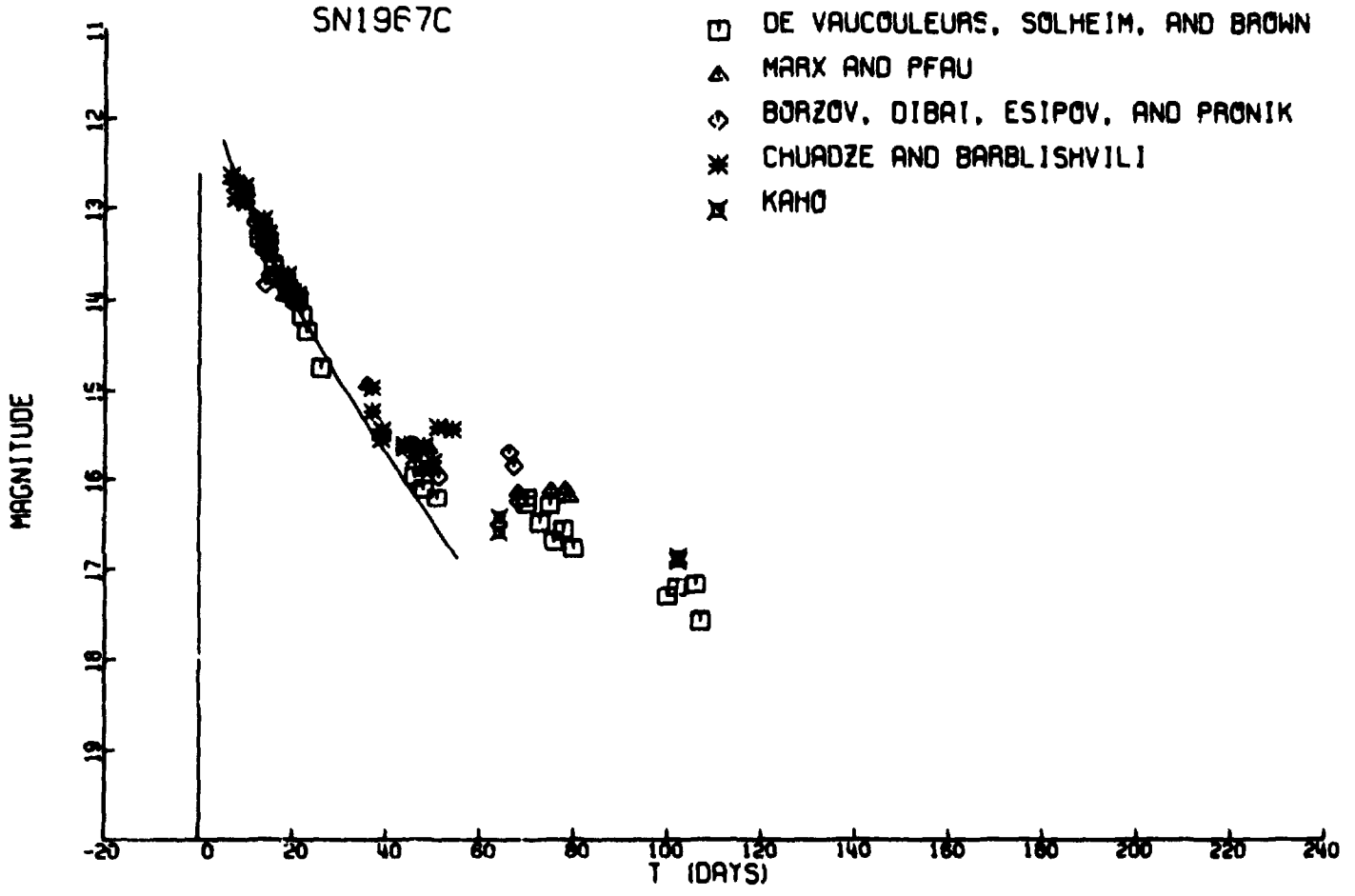
SN1967C
DE VAUCOULEURS, SOLHEIM, AND BROWN
MARX AND PFAU
BORZOV, DIBAI, ESIPOV, AND PRONIK
CHUADZE AND BARBLISHVILI
KAHO
MAGNITUDE
T (DAYS)
11
12
13
14
15
16
17
18
19
-20
0
20
40
60
80
100
120
140
160
180
200
220
240

Figure A?-1.54

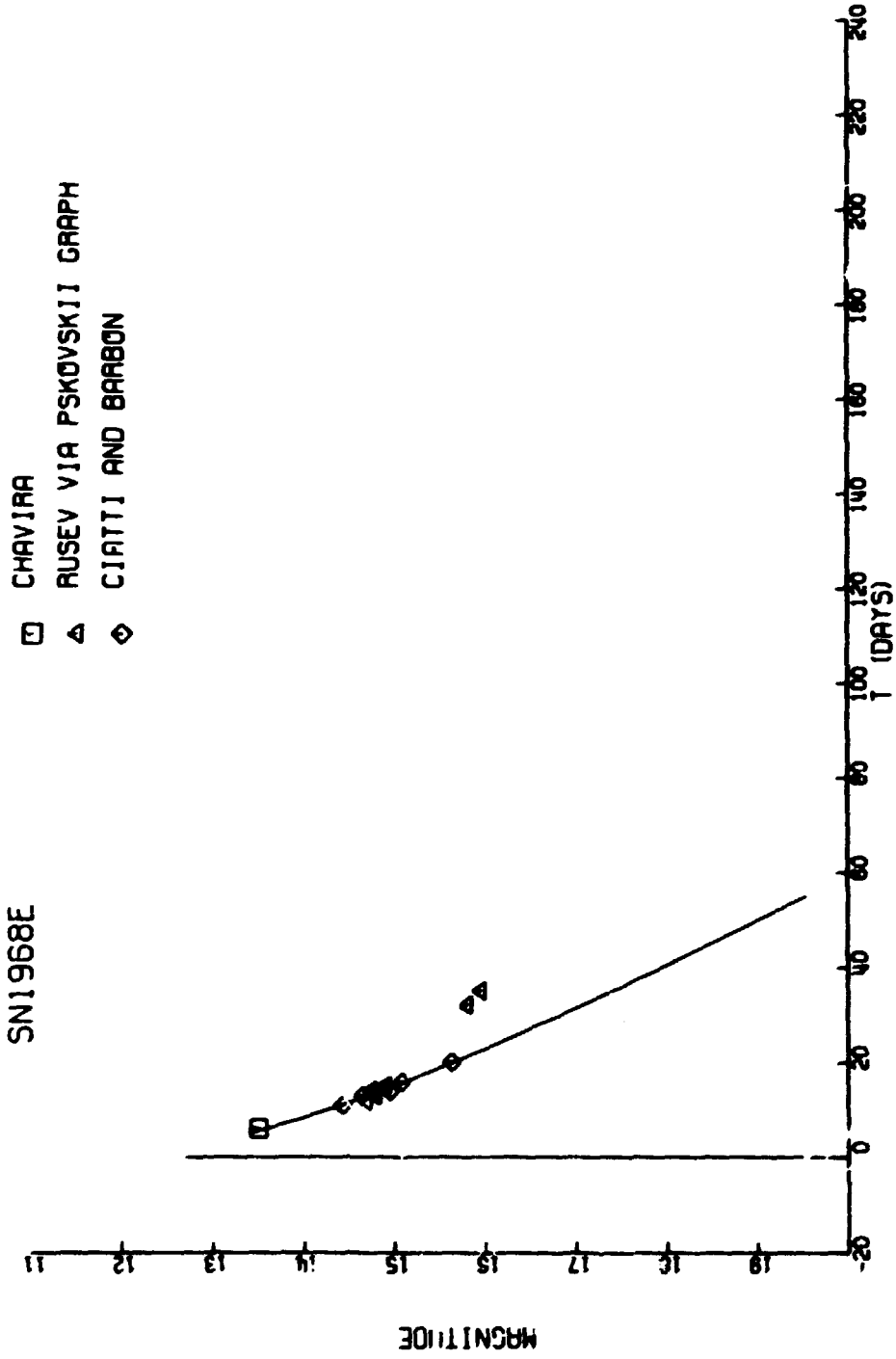

Figure A2-1.35

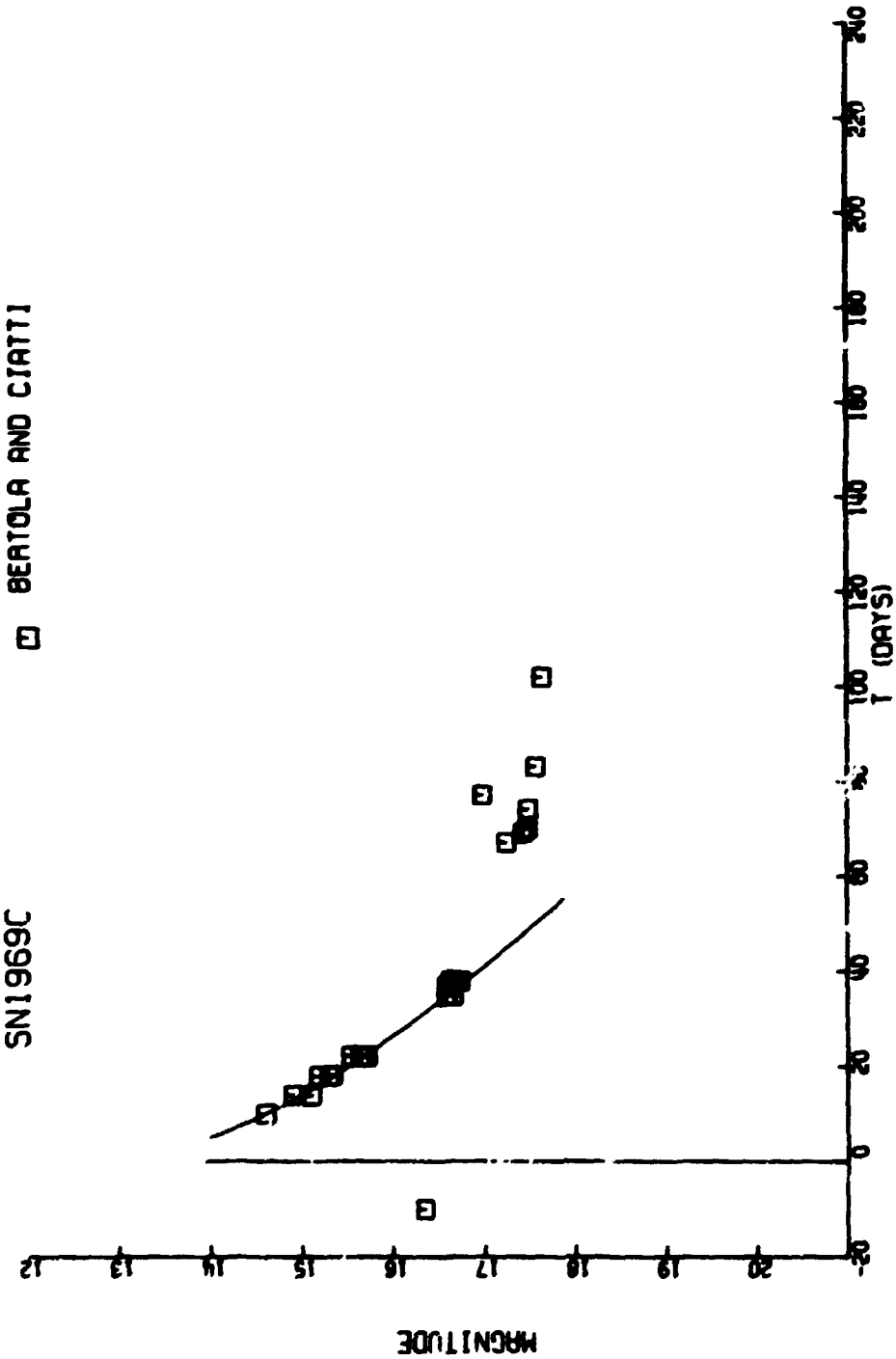

Figure AC-1.36

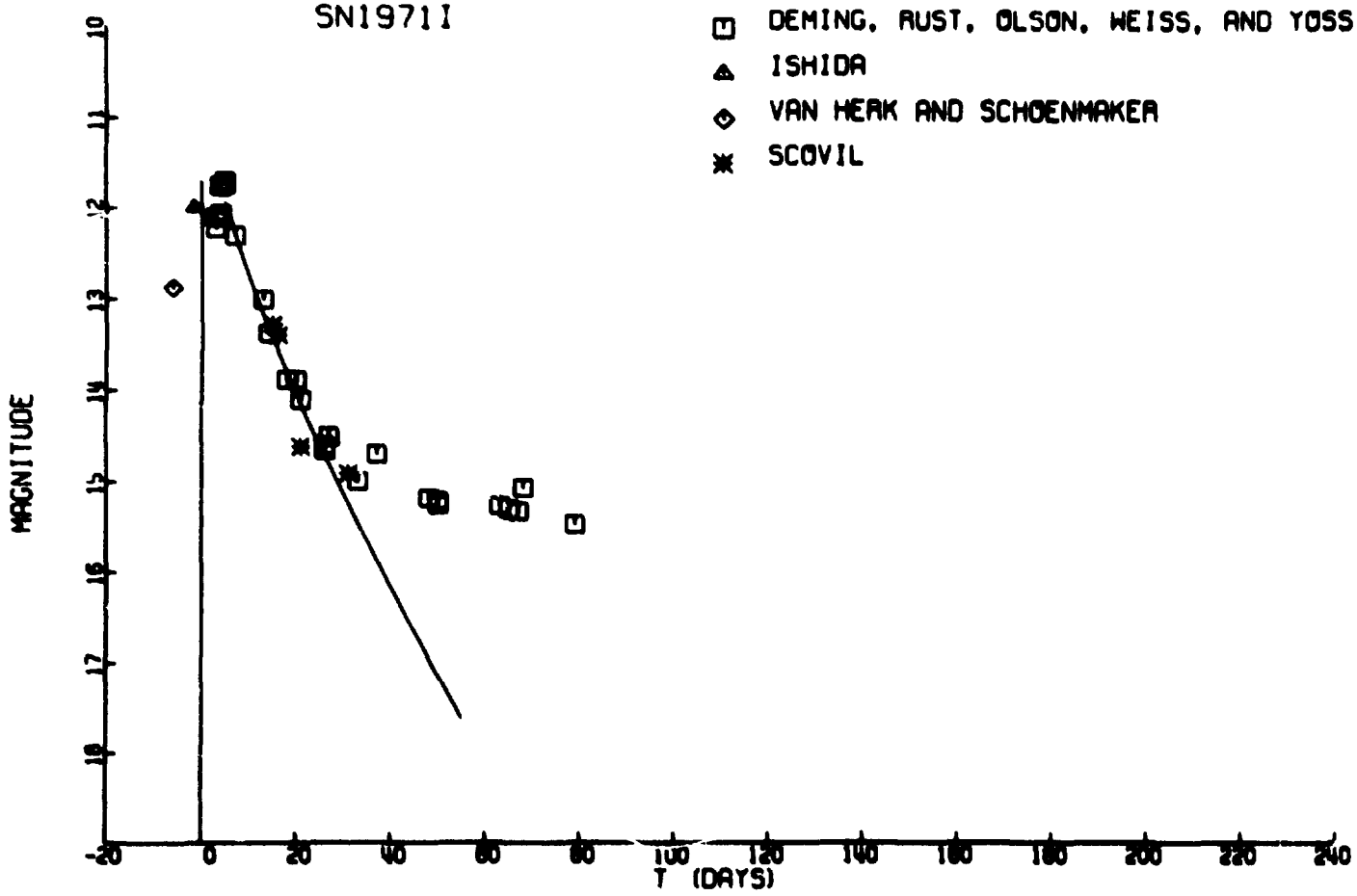
SN1971I
DEMING, RUST, OLSON, WEISS, AND YOSS
ISHIDA
VAN HERK AND SCHOENMAKER
SCOVIL
MAGNITUDE
T (DAYS)

Figure A2-1.2

APPENDIX F

COMPARISONS OF THE ESTIMATES OF M_o WITH THOSE OF PREVIOUS AUTHORS

Comparisons of the absolute magnitudes calculated in the present study with those of van den Bergh, Kowal, and Pskovskii are given in Table AF-1 and Figure AF-1. The table compares the averages, standard deviations and sample sizes. Column 5 was obtained by recalculating the absolute magnitudes in the present study with the peak apparent magnitudes, m_o, corrected only for absorption within our own galaxy. The magnitudes thus obtained should be comparable to those obtained by van den Bergh and Kowal. The table indicates an extremely good agreement on the average with those of van den Bergh and fairly good agreement with those of Kowal. The discrepancy between the average value of Rust and that of Kowal is

TABLE AF-1

Comparison of the Absolute Magnitudes with Those of Previous Studies

Sample / Statistic	(1) van den Bergh's M_o	(2) Kowal's M_o	(3) Rust's M_o corrected only for abs in our galaxy	(4) Pskovskii's M_o	(5) Rust's final M_o corrected for everything
Average	-19.7	-19.4	-19.37	-19.18	-19.41
Standard Deviation	$1^m.1$	$0^m.7$	$1^m.7$	$0^m.5$	$0^m.5$
Sample Size	23	19	27	45	42

$0^m.27$ with the Rust magnitudes being the brighter. There are 19 supernovae common to the two studies. Figure A3-1(a) is a plot of Kowal's estimates against the partially corrected estimates in this study for those 19 common supernovae. The straight line, which has a 45° slope, is the relation

$$M_o \text{ (Kowal)} = M_o \text{ (Rust)} + 0^m.27 \quad .$$

Although the scatter around the line is large, there are no obvious systematic deviations from it.

Column 5 of Table A3-1 gives the average and standard deviation of the absolute magnitudes given in column 8 of Table 9-3. The magnitudes have been corrected for absorption both in our own and in the parent galaxy. They should be comparable to the magnitudes calculated by Pskovskii. The average differs from that of Pskovskii by $0^m.33$ with the Rust estimates being the brighter. The discrepancy is less than half of either of the standard deviations, which differ by only $0^m.09$. Figure A3-1(b) gives a plot of Pskovskii's estimates against those of this study for the 21 supernovae common to the two samples. The straight line is the relation

$$M_o \text{ (Pskovskii)} = M_o \text{ (Rust)} + 0^m.33 \quad .$$

Clearly the scatter around the line is random and there are no systematic deviations from it.

The agreement between the final estimates of this study and those of Pskovskii is good when one considers that the methods for estimating the absorption in the parent galaxy were very different. Pskovskii took

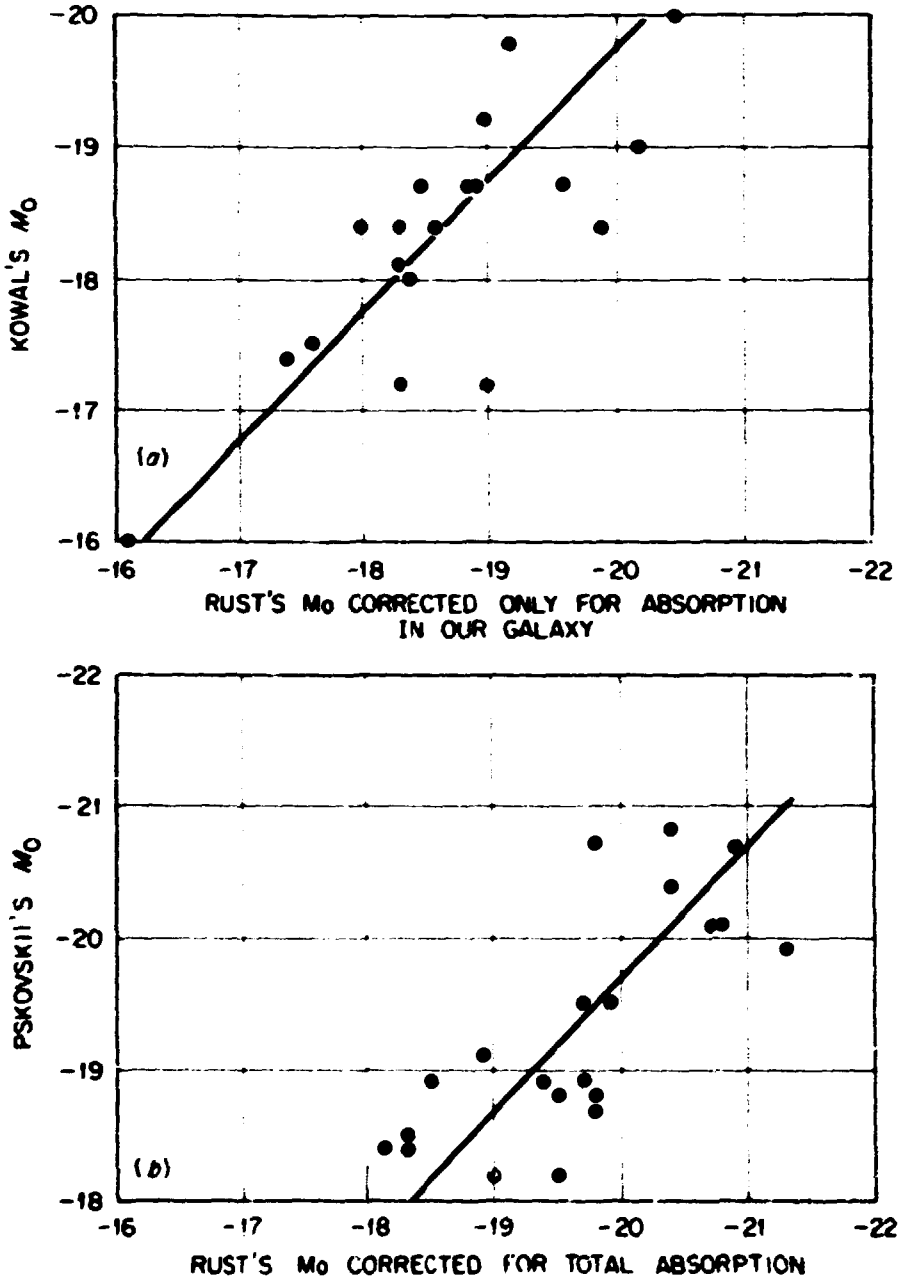

Figure A7-1. Comparison of the Absolute Magnitudes with Those Obtained by Previous Authors.

the internal absorption to be insignificant in elliptical and irregular galaxies. He based the estimates for the absorption in spiral galaxies on the inclination of the plane of the galaxy assuming a plane-parallel model for the absorbing material. Figure A3-2 gives the comparison of the total absorption corrections A_{pg} for the 21 supernovae common to the two samples. The solid line is the 45° line

$$A_{pg}(\text{Pskovskii}) = A_{pg}(\text{Rust}) ,$$

and the two dashed lines represent $\pm 0^{m}.5$ deviations. A closer examination of the 9 points lying outside the band described by the two dashed lines reveals that for 7 of them, the calculated A_{pg}(Rust) are based on observed color excesses, and only two of them (shown encircled) represent estimates. This implies that most of the corrections in the present study which deviate widely from the corresponding corrections of Pskovskii are among the more reliably determined corrections in this study. This conclusion is strengthened further by Figure A3-3, which is a plot of the total absorption correction against color excess for the 12 supernovae with measured color excesses which were common to the two studies. Pskovskii's corrections are shown as filled circles while the corrections for the present study are shown as open circles. It is not surprising that the latter lie along a straight line since they were computed by Eq. (9-5). Pskovskii's corrections, in contrast, do not exhibit any significant correlation with the color excess. Two extreme cases are SN1959c and 1962l which have observed color excesses of $0^{m}.10$ and $0^{m}.85$ respectively. Pskovskii's estimates for the absorption corrections are $1^{m}.7$ and $0^{m}.7$ respectively. These estimates are inconsistent with the

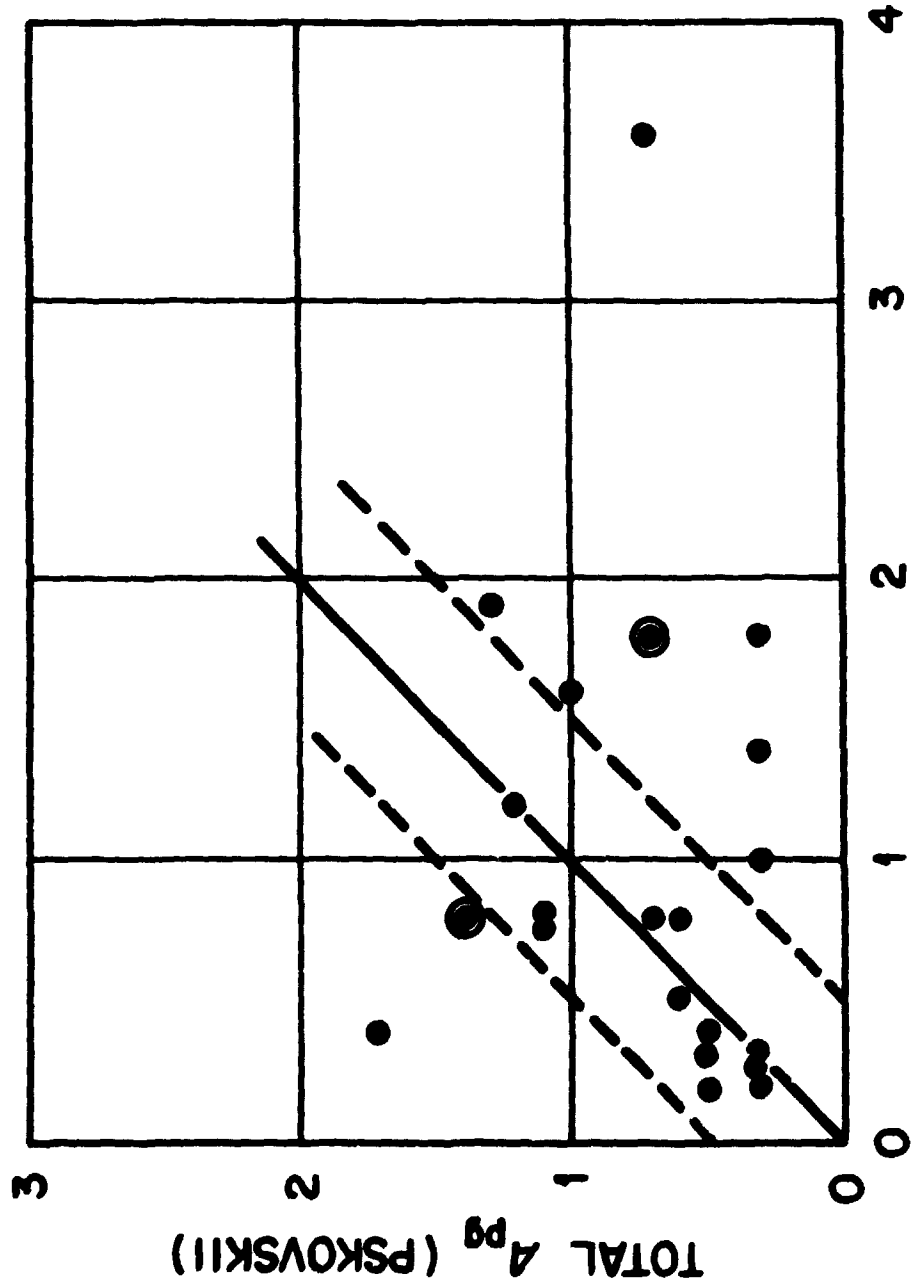

Figure A3-2. Comparison of the Total Absorption Corrections Calculated by Rust and by Pskovskii.

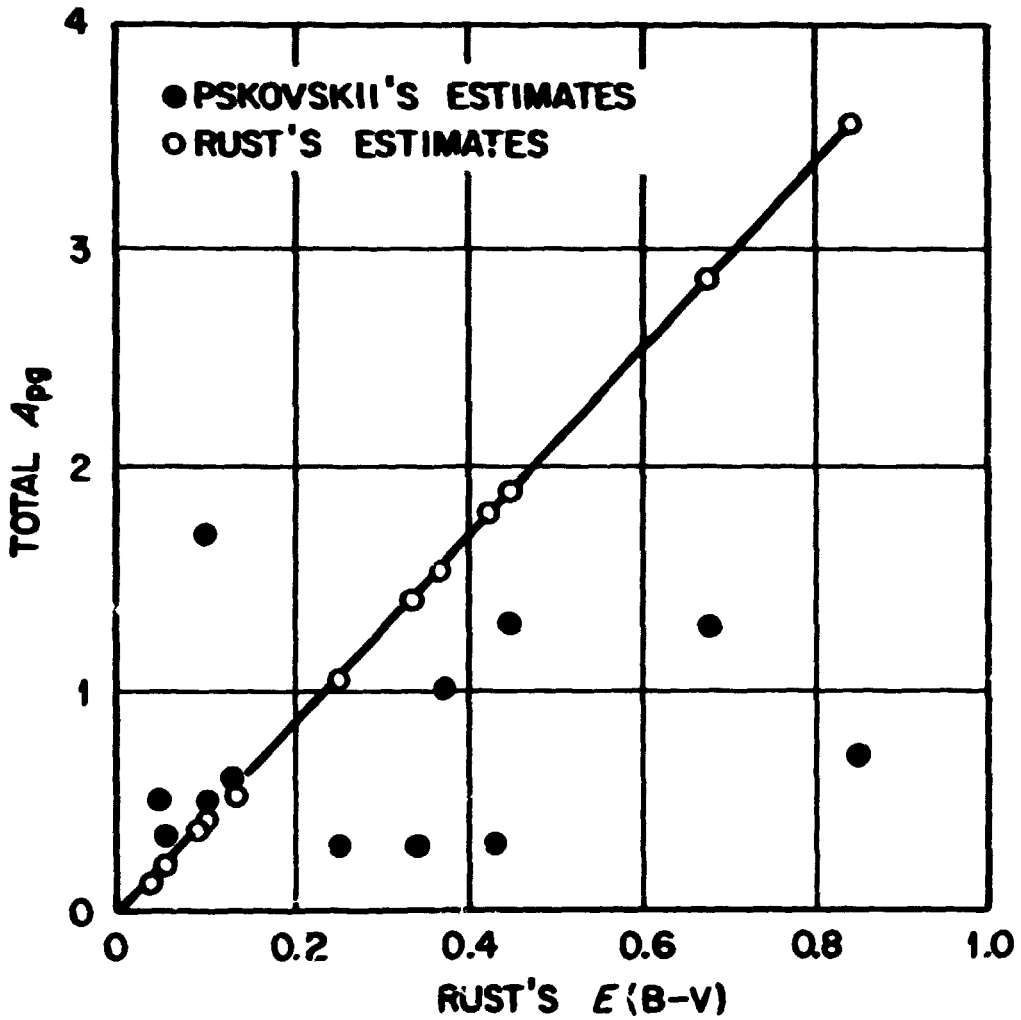

Figure A3-3. Total Absorption Correction as a Function of Color Excess.

observations since SN1962l could not possibly have suffered 8.5 times the reddening but at the same time less than half the absorption suffered by SN1959c. It would appear then that the color excess method is a more consistent method for calculating absorption corrections than the inclination method, and, since most of the deviations in Fig. A3-2 are in the direction A_{pg}(Rust) > A_{pg}(Pskovskii), that the inclination method may be on the average too conservative. This would certainly account for the $0^{m}.33$ excess in the average intrinsic luminosity estimates of the present study over those of Pskovskii.

APPENDIX 4

CORRELATIONS BETWEEN THE PEAK ABSOLUTE MAGNITUDES OF THE SUPERNOVAE AND PROPERTIES OF THE PARENT GALAXIES

In his 1967 paper (50), Pskovskii found a weak correlation between the peak absolute magnitudes of the supernovae and the Hubble types of the parent galaxies. Figure A4-1 gives a plot of the magnitudes versus the Hubble types both for Pskovskii's estimates, shown as solid circles, and for the estimates of the present study, shown as open circles. There does appear to be a slight correlation, with the brightness increasing as the type of the galaxy progresses through the Hubble sequence from elliptical to irregular. The correlation is perhaps more clearly indicated in the lower graph, which is a plot of the average magnitude for each type. These averages, together with the standard deviations are given in Table A4-1. In the plot, the average values are connected by straight line segments (Pskovskii's by solid lines and Rust's by broken lines) in order to emphasize the difference between the two sets of averages: (1) The averages of Rust increase more smoothly along the sequence of galaxies than do those of Pskovskii, and (2) The range of the increase is less for the estimates of Rust than for those of Pskovskii, the ranges being (-18.8, -19.8), respectively. Thus, the correlation appears to be more regular but less pronounced for the estimates of Rust than for those of Pskovskii. It is difficult to assess the significance of the correlation, considering the range of standard deviations of the estimates about the averages.

BLANK PAGE

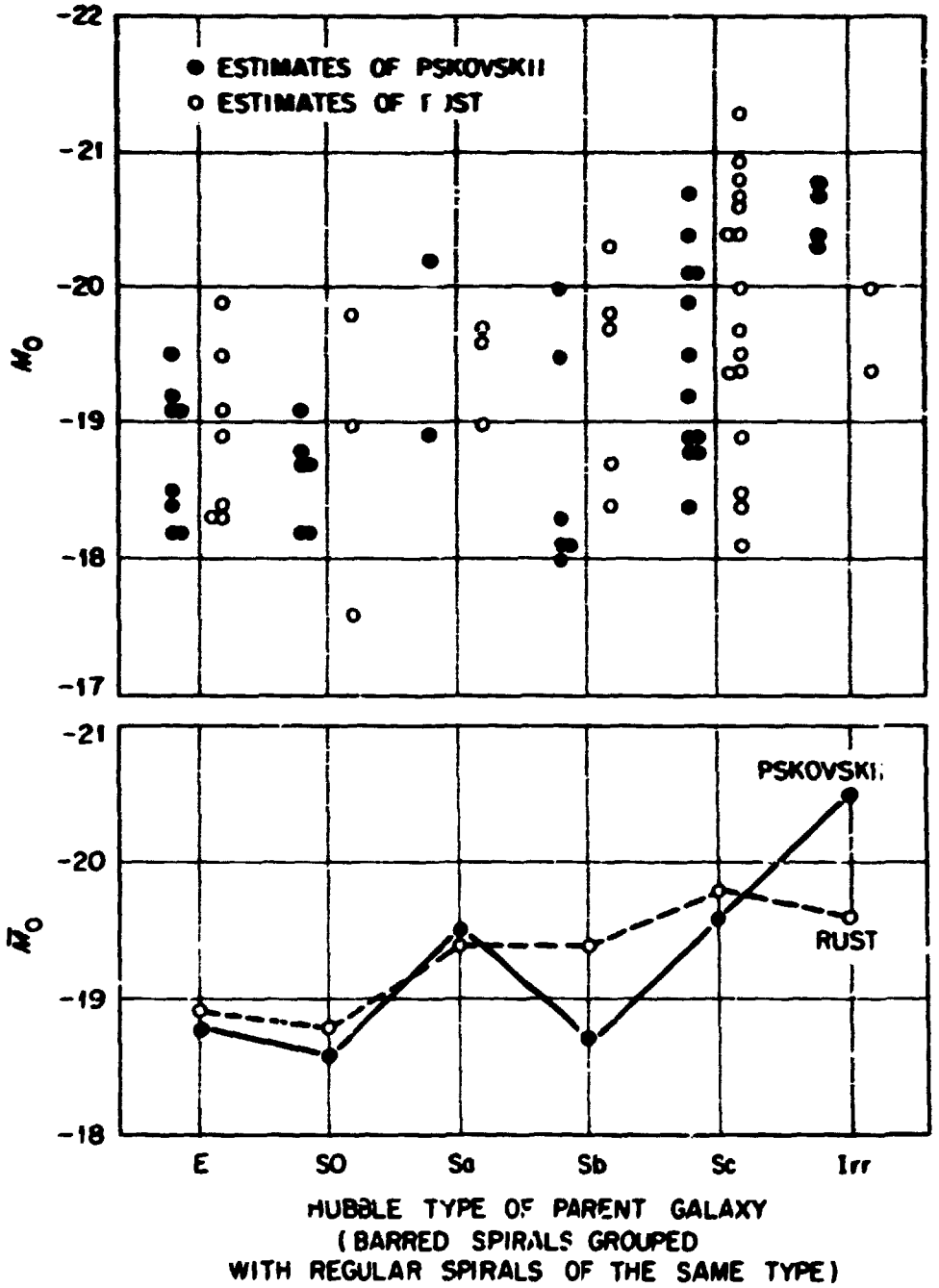

Figure A4-1. Peak Absolute Magnitude as a Function of the Hubble Type of the Parent Galaxy.

TABLE A4-1

Average Peak Absolute Magnitudes as a Function of Galaxy Type for the Estimates of Pskovskii and Rust

Type of Galaxy	Pskovskii's Estimates		Rust's Estimates	
	No.	$\bar{M}_o \pm \sigma(M_o)$	No.	$\bar{M}_o \pm \sigma(M_o)$
E	8	$-18.8 \pm 0.^{m}5$	7	$-18.91 \pm 0.^{m}63$
S0	6	-18.6 ± 0.4	3	-18.80 ± 1.11
Sa*	2	-19.5 ± 0.9	3	-19.43 ± 0.38
Sb*	6	-18.7 ± 0.9	5	-19.38 ± 0.80
Sc*	12	-19.5 ± 0.7	16	-19.81 ± 0.98
Irr	4	-20.5 ± 0.2	2	-19.60 ± 0.28

*Barred spirals are grouped with regular spirals of the same type.

In an earlier paper (145), Pskovskii reported a correlation between the peak absolute magnitudes of the supernovae and the integrated absolute magnitudes of the parent galaxies. In his 1967 paper (50) he said that the correlation is not reliably determined because of the large dispersion in M_o and the lack of data on supernovae in low luminosity galaxies. Figure A4-2 illustrates the regression of Pskovskii's estimates of M_o on his estimates of the integrated absolute magnitudes M_{galaxy} using all the supernovae in his 1967 sample for which he gave estimates of M_{galaxy}. The equation of the best fitting regression line, shown in the figure as a solid line, is

$$M_o = -(26.57 \pm 2.34) - (0.379 \pm 0.121)M_{galaxy} ,$$

and the correlation coefficient is $\rho = -0.532$. The t-statistic for testing the significance of the slope has the value $t = -3.14$ which gives, for the 27 points in the sample, significance at about the 99.9% level. The regression was performed both with and without the point at the upper left corner (SN1937c) in order to show that it did not have an inordinate influence in determining the slope. Without that point, the regression line is

$$M_o = -(26.16 \pm 3.16) - (0.539 \pm 0.162) M_{galaxy} ,$$

with the correlation coefficient $\rho = -0.[illegible]$ and $t = -2.2[illegible]$ which gives significance at the [illegible] level. Figure A-[illegible] illustrates the same regression using the estimates of the present study as the sample. The best fitting least squares line is

$$M_o = -([illegible] \pm [illegible]) - ([illegible] \pm [illegible]) M_{galaxy},$$

the correlation coefficient is $\rho = -0.2[illegible]$, the t-statistic has the value $t = -1.35$, and there are 37 points in the sample so the correlation is significant at the 9[illegible]% level. When the left hand extreme point, SN1937c, is omitted the results are

$$M_o = -(27.94 \pm 5.09) - (0.436 \pm 0.262) M_{galaxy} ,$$

$\rho = -0.275$, and $t = -1.67$ which gives significance at the 94.7% level. It would appear then that there is a significant correlation between the estimates of M_o and the estimates of M_{galaxy} in both studies, but there is a wide scatter in the M_o estimates. The two sets of estimates give similar values of the slope of the regression line but the correlation is not as pronounced in the present sample which contains 10 supernovae more than the sample of Pskovskii.

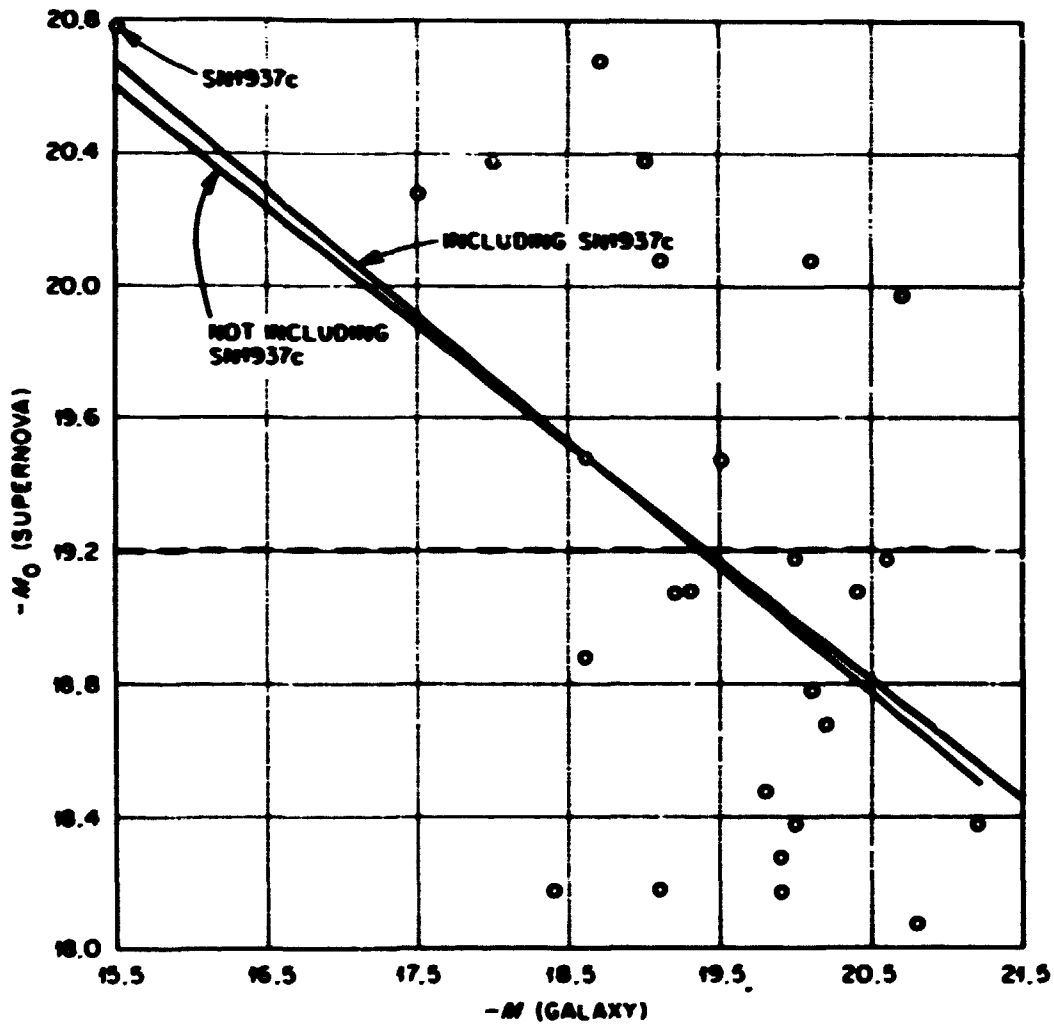

Figure A4-2. Regression of Peak Absolute Magnitude on the Integrated Absolute Magnitude of the Parent Galaxy for Pskovskii's Sample.

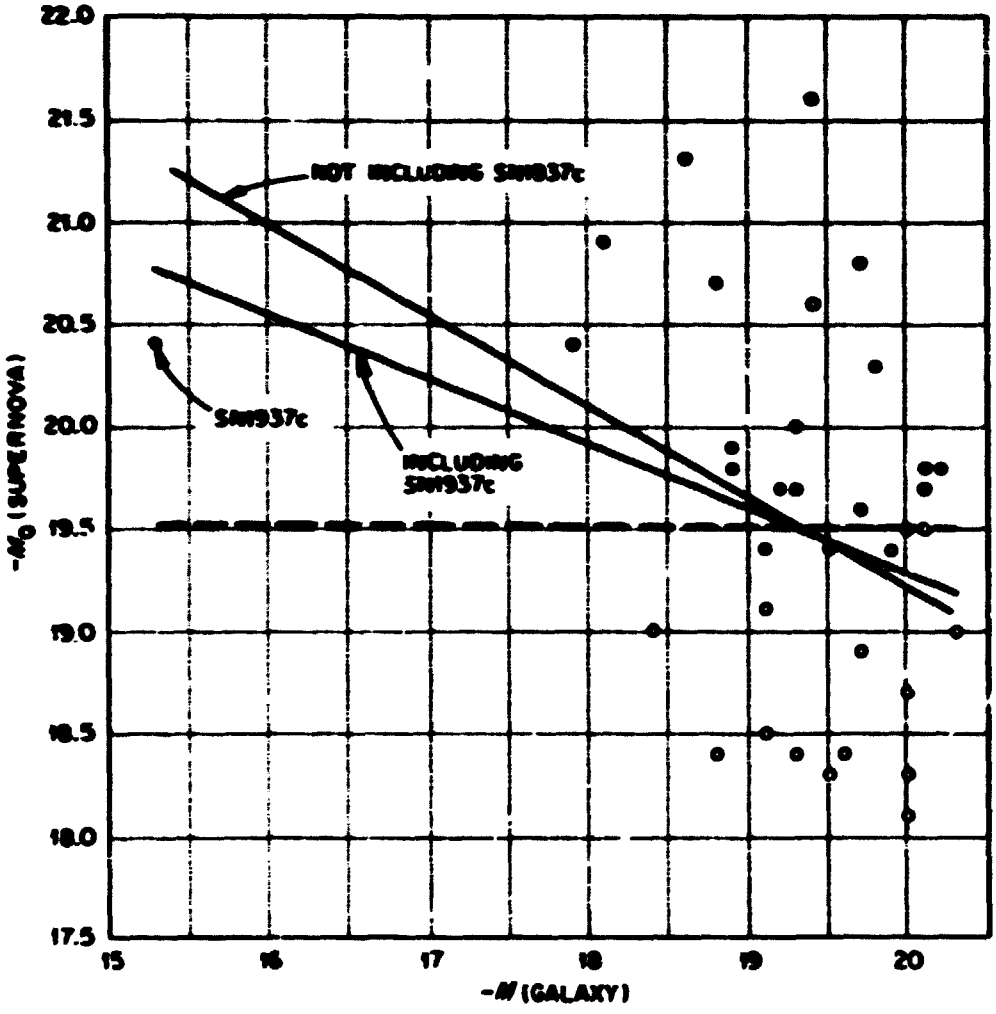

Figure A4-5. Regression of Peak Absolute Magnitude on the Integrated Absolute Magnitude of the Parent Galaxy for Rust's Sample.

APPENDIX 5

TESTS FOR SYSTEMATIC EFFECTS IN ESTIMATING THE M_o

Four different methods were used for estimating the original uncorrected m_o: (1) inspection of the observed light curve, (2) Pskovskii's estimates by his point k method, (3) Pskovskii's estimates by his average light curve method, and (4) Rust's estimates using Pskovskii's point k method. Table A5-1 gives a summary of the number of times each of these methods was used in the two luminosity groups.

TABLE A5-1

Summary of the Number of Times Each Method of Estimating m_o was Used for the Two Luminosity Groups

Method	Number in More Luminous Group	Number in Less Luminous Group	$M_o \pm \sigma(M_o)$
Observed light curve	8	4	-19.65 ± 0.65
Pskovskii's point k	3	2	-19.42 ± 0.76
Pskovskii's av. light curve	2	5	-18.94 ± 0.69
Rust's point k	6	6	-19.72 ± 1.31

Clearly there is no strongly exclusive association of either group with any of the methods. Furthermore the average values of M_o for the various methods are very similar except perhaps for Pskovskii's average light curve method which is lower because of the 5 to 2 ratio of the less luminous group to the more luminous group. This imbalance is

probably a small sample effect and certainly is not the cause of the gap. Thus, if a bias was built into the estimates of m_c, it must have occurred in correction process.

The corrections for absorption could easily have built in a bias if the corrections applied to part of the m_c were systematically and significantly greater than those applied to the others. But the average total correction applied to the more luminous group was $\overline{A_{pg}}$ = [illegible] and for the less luminous group was $\overline{A_{pg}}$ = [illegible]. The difference, [illegible], is less than one fourth the standard deviations. The t-statistic for testing the significance of the difference has the value t_M = [illegible], which even with [illegible] degrees of freedom is not significant at the [illegible] level. Clearly the gap was not caused by systematically correcting the more luminous group more than the less luminous one, and in fact if either group were systematically corrected further to make its magnitudes consistent with the other group, then a bias would be built in and the corrections for that group would be systematically different from those of the other. It is a coincidence that the 1[illegible] to 17 ratio of the two luminosity groups is identical to the ratio of the number of m_o corrected by the observed color excess method to the number for which the absorption within the parent galaxy was obtained by estimation. That it is no more than a coincidence is clearly shown by Table A-2 which gives the number of times each method of correcting for absorption was used in each luminosity group.

TABLE A-2

Summary of the Number of Times Each Method of Estimating the Absorption in the Parent Galaxy was Used in Each Luminosity Group

Method	Number in More Luminous Group	Number in Less Luminous Group	$M_c \pm \sigma(M_c)$
Observed Color Excess	1	[illegible]	[illegible]
Est. $\overline{T}$ (Elliptical)	1	[illegible]	
Est. $\overline{T}$ (Spiral)			[illegible]
Est. $1^{\overline{m}}$ (Spiral)	[illegible]	1	

Clearly there is no strong association of either group with any of the methods. Furthermore the average M_c for the observed color excess group does not differ significantly from the group for which the absorption correction was obtained by estimation.

APPENDIX 6

DISTRIBUTION OF THE SUPERNOVAE IN THIS STUDY ON THE CELESTIAL SPHERE

Figure A6-1 is a plot in equatorial coordinates of the positions in the sky of the 36 supernovae in the present sample. The pattern of occurrences reflects the areas patrolled in the regular surveys rather than real preferences for certain directions. The two different luminosity groups are distinguished by open and closed circles. Clearly the two groups coexist in the same parts of the sky. This fact indicates that they were not caused by an anisotropy in the Hubble law.

BLANK PAGE

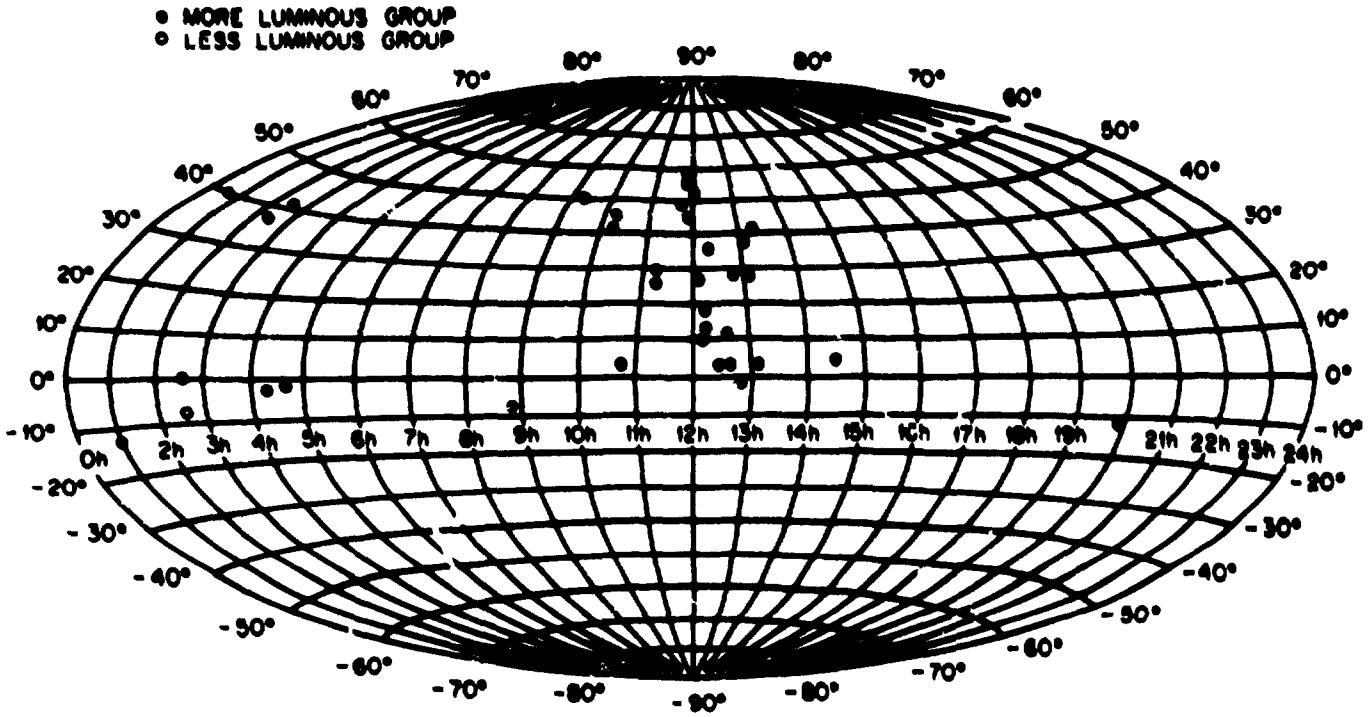

Figure A6-1. Distribution in Equatorial Coordinates of the Supernovae in This Study.

APPENDIX 7

FREQUENCIES OF OCCURRENCE IN VARIOUS TYPES OF GALAXIES

Bertola and Sussi (147) suggested that there are two kinds of Type I supernovae associated with Population I and Population II stars. Their only evidence was an analysis of the frequency of occurrence in different kinds of galaxies. Using as their sample 44 type I supernovae taken from various lists published by Zwicky (148,149) and from various other sources, they obtained a distribution having two frequency maxima corresponding to E and to S(B)c galaxies. Although the supernovae in the present study were selected using a different criterion, namely the availability of a more or less complete light curve, it is interesting to compare the frequency distribution with that of Bertola's and Sussi's sample. The frequency distribution with that of Bertola's and Sussi's sample. The two distributions are shown in Figure A7-1, plotted as number of occurrences versus Hubble type of the parent galaxy without any corrections for the frequency distribution of galaxies according to type. This latter correction would have the effect of enhancing the E-galaxy peak and lowering the Sc-galaxy peak. Even so, the correction would leave intact the double-peaked structure which is clearly evident in both distributions.

It is also interesting to consider the distribution of the two luminosity types in the present sample. This is indicated in the figure by the shaded and unshaded areas, and is given in detail in Table A7-1. Supernova 1966n was omitted because the exact type of its parent galaxy is not known with certainty though it is known to be a spiral. Note

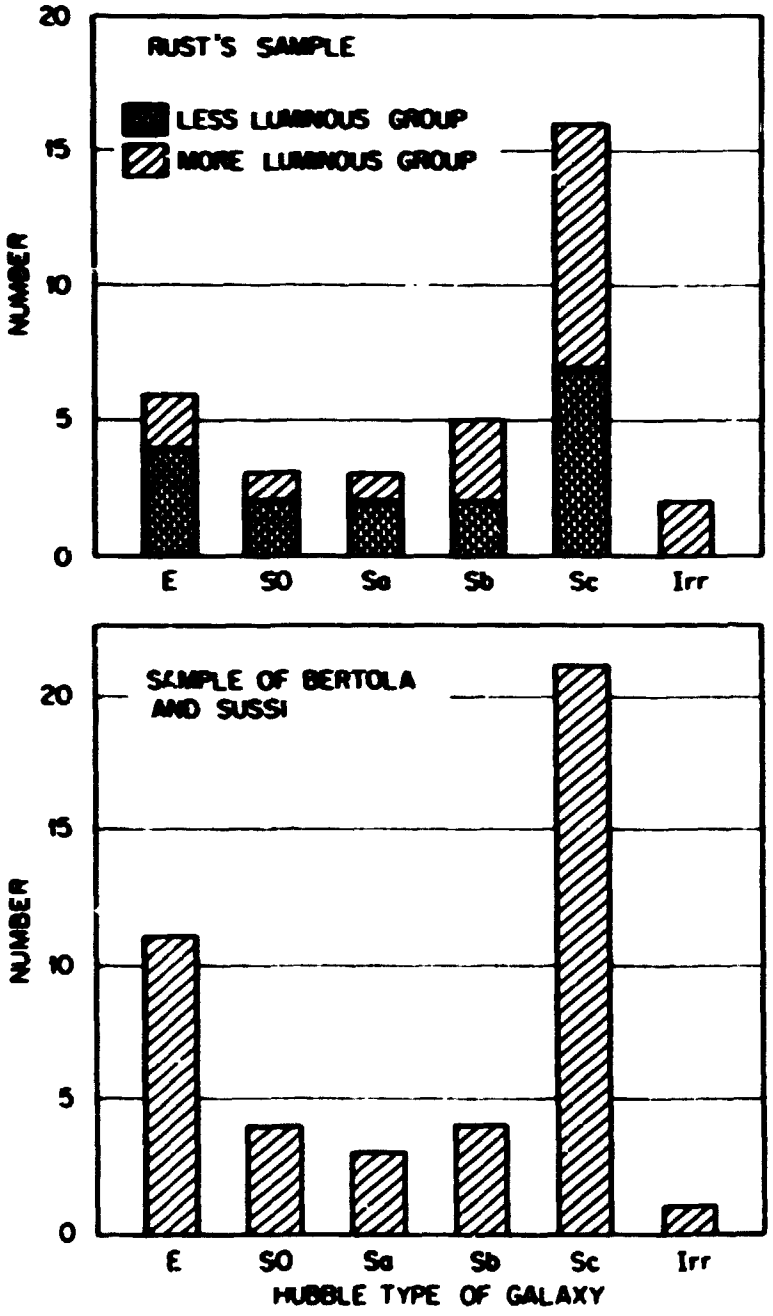

Figure A7-1. Distribution of Supernovae in the Various Types of Galaxies.

TABLE A7-1

Number of Supernovae in Different Types of Galaxies

Galaxy Type	More Luminous Group		Less Luminous Group		Both Groups Together	
	Number	%	Number	%	Number	%
E	2	11.1	4	23.5	6	17.1
S0	1	5.6	2	11.8	3	8.6
Sa	1	5.6	2	11.8	3	8.6
Sb	3	16.7	2	11.8	5	14.3
Sc	9	50.0	7	41.2	16	45.7
Irr	2	11.1	0	0	2	5.7

that both luminosity groups have occurred in all the galaxy types except Irr in which there were only two occurrences in the entire sample. In particular, both luminosity groups occur in elliptical galaxies, a fact which rules out an identification of them with Populations I and II stars. There appears to be a slight trend for the more luminous group to occur more often in galaxies of later type (Sb, Sc, Irr) and for the less luminous group to predominate in earlier types (E, S0, Sa). The numbers in the various types are too small to judge whether this trend is statistically significant, but such a tendency would explain the correlation of M_o with galaxy type shown in Figure A4-1 and perhaps the correlation of M_o with the absolute magnitude of the parent galaxy shown in Figure A4-3.

ORNL-4953
UC-34b
Physics — Cosmic and Terrestrial

INTERNAL DISTRIBUTION

1-3. Central Research Library
4. ORNL — Y-12 Technical Library Document Reference Section
5. K-25 Library
6-55. Laboratory Records Department
56. Laboratory Records, ORNL R.C.
57. ORNL Patent Office
58. K. T. Barry
59. A. A. Brooks
60-69. J. A. Carpenter
70. H. P. Carter
71. J. S. Crowell
72. F. L. Culler
73. D. L. DeAngelis
74. R. E. Funderlic
75. C. M. Haaland
76. R. F. Hibbs
77. J. B. Mankin
78. J. K. Munro
79. S. K. Penny
80. Herman Postma
81-110. Bert W. Rust
111. H. C. Schweinler
112. J. G. Sullivan
113. P. R. Vanstrum
114. G. W. Westley
115. G. E. Whitesides

EXTERNAL DISTRIBUTION

116. G. O. Abell, Department of Astronomy, University of California, Los Angeles, California 90024
117. B. Abramenko, AEG Rechenzentrum, Frankfurt (Main), Federal Republic of Germany
118. V. A. Ambartsumian, Academy of Sciences, Erevan, Armenia, U.S.S.R.
119. R. J. Angione, Astronomy Department, California State University, San Diego, California
120. H. C. Arp, Hale Observatories, 813 Santa Barbara Street, Pasadena, California 91106
121. J. N. Bahcall, Institute for Advanced Study, Princeton, New Jersey 08540
122. Neta A. Bahcall, Princeton University Observatory, Princeton, New Jersey
123. R. Barbon, Asiago Astrophysical Observatory, University of Padova, I-36012 Asiago, Italy
124. Ronnie C. Barnes, Physics Department, University of Missouri, Columbia, Missouri 65201
125. Jeno M. Barnothy, 833 Lincoln Street, Evanston, Illinois 60201
126. S. Bellert, Department of Electronics, Warsaw Technical University, Warsaw, Poland
127. S. van den Bergh, David Dunlap Observatory, University of Toronto, Richmond Hill, Ontario, Canada
128. Ch. Bertaud, Observatoire de Paris-Meudon, F-92190 Meudon, France
129. F. Bertola, Asiago Astrophysical Observatory, University of Padova, Asiago, Italy
130. S. Bonometto, Instituto di Fisica "Galileo Galilei", Padova, Italy

BLANK PAGE

131. E. M. Burbidge, Department of Physics, University of California, San Diego, La Jolla, California 92037
132. G. R. Burbidge, University of California, San Diego, Box 109, La Jolla, California 92037
133. W. R. Burrus, Tennecomp Systems, Inc., 795 Oak Ridge Turnpike, Oak Ridge, Tennessee 37830
134. J. H. Cahn, University of Illinois Observatory, Urbana, Illinois 61801
135. E. Chavira, Observatorio Astrofisico, Nacional, Aptdo Postal 216, Puebla Pue, Mexico
136. F. Ciatti, Asiago Astrophysical Observatory, University of Padova, I-36012 Asiago, Italy
137. S. A. Colgate, New Mexico Technical Institute, Socorro, New Mexico 87801
138. S. Collin-Souffrin, Observatoire de Meudon, F-92190 Meudon, France
139. N. Dallaporta, Instituto di Astronomia dell' Universita, Vicolo dell' Observatorio, 5, I-35100 Padova, Italy
140. D. Deming, Department of Astronomy, University of Illinois Observatory, Urbana, Illinois 61801
141. John R. Dickel, University of Illinois Observatory, Urbana, Illinois 61801
142. P. A. M. Dirac, Florida State University, Tallahassee, Florida
143. J. R. Dunlap, 1629 Stoll Drive, Las Cruces, New Mexico 88001
144. George B. Field, Department of Astronomy, University of California, Berkeley, California 94720
145. A. Finzi, Israeli Institute of Technology, Department of Mathematics, Haifa, Israel
146. W. K. Ford, Jr., 7400 Summit Avenue, Chevy Chase, Maryland 20015
147. Wayne L. Fullerton, Los Alamos Scientific Laboratory, Los Alamos, New Mexico 87544
148. B. J. Geldzahler, Department of Astronomy, University of Pennsylvania, Philadelphia, Pennsylvania 19104
149. T. Gold, Department of Astronomy, Cornell University, 410 Space Science Building, Ithaca, New York 14850
150. G. Golub, Eidgenossische, Technische Hochschule Zurich, Seminar fur Angewandte Mathematik, Clausiusstrasse 55, 8006 Zurich, Switzerland
151. J. E. Gunn, California Institute of Technology, Robinson Laboratory, Pasadena, California 91109
152. P. A. Y. Gunter, Department of Philosophy, North Texas State University, Denton, Texas
153. Michael J. Haggerty, Department of Physics, University of Texas, Austin, Texas 78712
154. E. R. Harrison, Department of Physics and Astronomy, University of Massachusetts, Amherst, Massachusetts
155. G. S. Hawkins, Dickinson College, Department of Physics and Astronomy, Carlisle, Pennsylvania 17013
156. M. T. Heath, Computer Science Department, Serra House, Stanford University, Stanford, California
157. P. W. Hodge, Astronomy Department, University of Washington, Seattle, Washington 98105

158. Sebastian von Hoerner, N.R.A.O., Greenbank, West Virginia
159. Alan Hoffman, Joseph Henry Laboratories, Physics Department, Princeton University, Princeton, New Jersey
160. E. Holmberg, Astronomical Observatory, Uppsala, Sweden
161. F. Hoyle, 1 Clarkson Close, Cambridge, England
162. M. L. Humason, P. O. Box 165, Mendocino, California
163. I. Iben, University of Illinois Observatory, Urbana, Illinois 61801
164. T. Jaakkola, Observatorio ja Astrofysiikan Laboratorio, Tahtitorninmaki, SF-00130 Helsinki 13, Finland
165. James Kaler, University of Illinois Observatory, Urbana, Illinois 61801
166. M. Karpowicz, Astronomical Observatory, Warsaw University, Warsaw, Poland
167. K. I. Kellermann, National Radio Astronomy Observatory, Green Bank, West Virginia
168. James Kercher, Lawrence Livermore Laboratory, Livermore, California
169. C. T. Kowal, Department of Astrophysics, California Institute of Technology, Pasadena, California 91106
170. J. Maslowski, Astronomical Observatory of the Jagiellonian University, Cracow, Poland
171. W. H. McCrea, University of Sussex, Astronomy Centre, Physics Building, Falmer, Frighton, BN 19 QH England
172. W. H. McCutcheon, Physics Department, University of British Columbia, Vancouver 8, Canada
173. G. C. McVittie, 74 Old Dover Road, Canterbury, Kent, England
174. T. L. May, 5034 Westminster Terrace, San Diego, California 92116
175. S. N. Milford, Department of Physics, University of Queensland, St. Lucia, Brisbane, Queensland 4067, Australia
176. R. Minkowski, Radio Astronomy Laboratory, University of California, Berkeley, California 94720
177. P. Morrison, Room 6-308, Massachusetts Institute of Technology, Cambridge, Massachusetts 02139
178. J. V. Narlikar, Tata Institute of Fundamental Research, Bombay 400 005, India
179. G. D. Nickas, 2040 York Street, 115, Vancouver, B.C., Canada V6J 1E7
180. J. Nicoll, Rm 13-3126, M.I.T., Cambridge, Massachusetts 02139
181. Thomas W. Noonan, Brockport State College, Brockport, New York
182. E. C. Olson, Department of Astronomy, University of Illinois Observatory, Urbana, Illinois 61801
183. T. L. Page, National Aeronautics and Space Administration, Manned Spacecraft Center, Houston, Texas 77058
184. J. C. Pecker, College de France, I. A. P., 98 bis Bld Arago, F-75014 Paris, France
185. P. J. E. Peebles, Princeton University, Department of Physics, Joseph Henry Laboratories, Princeton, New Jersey 08540
186. Yu. P. Pskovskii, Sternberg Astronomical Institute, Moscow W-234, 117234 U.S.S.R.
187. M. S. Roberts, National Radio Astronomy Observatory, Edgemont Road, Charlottesville, Virginia 22901

188. G. Romano, Viale S. Antonio 7, 31100 Treviso, Italy
189. Herbert J. Rood, Astronomy Department, Michigan State University, East Lansing, Michigan 48823
190. L. Rosino, Asiago Astrophysical Observatory, University of Padova, I-36012 Asiago, Italy
191. V. C. Rubin, Department of Terrestrial Magnetism, 5241 Broad Branch Road, Washington, D.C. 20015
192. K. Rudnicki, Observatorium Astronomiczne U.W., Aleje Ujazdowskie 4, Warsaw, Poland
193. A. R. Sandage, Hale Observatories, 813 Santa Barbara, Pasadena, California 91106
194. W. L. W. Sargent, Astronomy Department, California Institute of Technology, Pasadena, California 91109
195. M. Schmidt, California Institute of Technology, Hale Observatories, 1201 East California Blvd., Pasadena, California 91109
196. I. E. Segal, Room 2-244, Massachusetts Institute of Technology, Cambridge, Massachusetts 02139
197. Harlan J. Smith, Astronomy Department, University of Texas, Austin, Texas 78712
198. P. A. Strittmatter, University of California at San Diego, Physics Department, Box 109, La Jolla, California
199. G. W. Swenson, Jr., Electrical Engineering Department, University of Illinois, Urbana, Illinois 61801
200. G. A. Tammann, Hale Observatories, 813 Santa Barbara Street, Pasadena, California 91106
201. William G. Tifft, Steward Observatory, University of Arizona, Tucson, Arizona 85721
202. H. M. Tovmassian, Byurakan Observatory, Armenian Academy of Science, Byurakan, U.S.S.R.
203. Thomas C. Van Flandern, U.S. Naval Observatory, Washington, D.C. 20390
204. G. de Vaucouleurs, Department of Astronomy, University of Texas, Austin, Texas 78712
205. G. L. Verschuur, National Radio Astronomy Observatory, Green Bank, West Virginia
206. E. T. Wampler, Lick Observatory, University of California, Santa Cruz, California 95060
207. J. Webber, University of Illinois Observatory, Urbana, Illinois 61801
208. S. Weinberg, Physics Department 6-320, Massachusetts Institute of Technology, Cambridge, Massachusetts 02139
209. D. H. Weinstein, The Superior Oil Company, Houston, Texas 77004
210. Raymond E. White, Math and Physical Sciences Division, National Sciences Foundation, 1800 G Street, N.W., Washington, D.C. 20550
211. E. P. Wigner, 8 Ober Road, Princeton, New Jersey
212. A. G. Willis, Sterrewacht, Leiden, The Netherlands
213. O. C. Wilson, Hale Observatories, 813 Santa Barbara Street, Pasadena, California 91106
214. K. G. Witz, Mathematics Department, University of Illinois, Altgeld Hall, Urbana, Illinois 61801
215. S. Woosley, Kellogg Radiation Laboratory, California Institute of Technology, Pasadena, California 91109

216. S. P. Wyatt, University of Illinois Observatory, Urbana, Illinois 61801
217. K. M. Yoss, University of Illinois Observatory, Urbana, Illinois 61801
218. Aarne Karjalainen Observatorio, 90101 Oulu, Finland
219. Air Force Cambridge Research Laboratories, L. G. Hanscom Field, Bedford, Massachusetts 01730
220. Air Force Office of Scientific Research, 1400 Wilson Blvd., Arlington, Virginia 22209
221. Allegheny Observatory Library, University of Pittsburgh, Riverview Park, Pittsburgh, Pennsylvania 15214
222. All-Union Society of Astronomy and Geodesy, Leninsky Prospekt 14, Moscow V-71, U.S.S.R.
223. The American Museum of Natural History, Central Park West at 79th Street, New York, New York 10024
224. Armagh Observatory, Armagh, Northern Ireland
225. Astronomical Council, Ulitsa Vavilova 34, Moscow, U.S.S.R.
226. Astronomical Institute, Konkoly Thege M. útca 13-17, Budapest XII, Hungary
227. Astronomy Institute Library, 38 Astronomicheskaya, Tashkent, U.S.S.R.
228. Astronomy Library, Princeton University Observatory, Peyton Hall, Princeton, New Jersey 08540
229. Astronomy Library, Yale University, Box 2023, Yale Station, New Haven, Connecticut 06520
230. Astronomy-Mathematics-Statistics Library, University of California, 113 Campbell Hall, Berkeley, California 94720
231. Astronomy-Physics-Mathematics Library, Swain Hall, Indiana University, Bloomington, Indiana 47401
232. Astrophysical Observatory, Smithsonian Institution, 60 Garden Street, Cambridge, Massachusetts 02138
233. Astrophysical Observatory Library, Zelenchuk, Stavropol Region, U.S.S.R.
234. Astrophysical Observatory of Abastumani, Kayubili Mount, Abastumani, Georgian SSR, U.S.S.R.
235. Astrophysical Observatory of Byurakan, Byurakan, Ashtarak Region, Armenian SSR, U.S.S.R.
236. Astrophysical Observatory of the Crimea, P/B Nauchny, Crimea, Ukranian SSR, U.S.S.R.
237. Astrophysical Observatory of Padua University, Asiago, Italy
238. Astrophysical Observatory of Shemakha, 71 Narimanov Prospekt, Baku, U.S.S.R.
239. Astrophysics Institute, Alma-Ata 68, U.S.S.R.
240. Astrophysics Institute, Ulitsa Sviridenko 22, Dushanbe 42, Tadzhik SSR, U.S.S.R.
241. Bosscha Observatory, Lembang, Indonesia
242. Ceskoslovenska Akademie Ved, Astronomical Institute, Budecska 6, Vinohrady, Prague 2, Czechoslovakia
243. Chemistry-Physics Library, University of Kentucky, Lexington, Kentucky 40506
244. Dearborn Observatory Library, Lindheimer Astronomical Research Center, Northwestern University, Evanston, Illinois 60201

245. Department of Astronomy and Observatory, Boston University, 725 Commonwealth Avenue, Boston, Massachusetts
246. Cole Memorial Library of Physics, Ohio State University, 174 West 18th Avenue, Columbus, Ohio 43210
247. Division of the Physical Sciences, University of Chicago, 1118 East 58th Street, Chicago, Illinois 60637
248. Dudley Observatory, 100 Fuller Road, Albany, New York
249. Engineering and Physics Library, 410 Weil Hall, University of Florida, Gainesville, Florida 32601
250. European Southern Observatory, Bergedorfer Strasse 131, 205 Hamburg, West Germany
251. The Franklin Institute Library, Benjamin Franklin Parkway at 20th Street, Philadelphia, Pennsylvania 19103
252. Frank P. Brackett Observatory, Pomona College, Claremont, California 91711
253. George C. Marshall Space Flight Center Technical Library, Marshall Space Flight Center, Alabama 35812
254. Gerstenzang Science Library, Brandeis University, 415 South Street, Waltham, Massachusetts 02154
255. Hamburg Observatory, Gojenbergsweg 112, 2050 Hamburg 80, Germany FR
256. High Altitude Observatory Library, National Center for Atmospheric Research, P. O. Box 1558, Boulder, Colorado
257. Institut National D'Astronomie et de Geophysique, 5 place Jules Janssen, 92 Meudon, France
258. Kapteyn Astronomical Laboratory, Broerstraat 7, Groningen, The Netherlands
259. Kapteyn Observatory, Mensingeweg 20, Roden, The Netherlands
260. Kiev Astronomical Observatory Library, Goloseevo, Kiev 127, Ukrainian SSR, U.S.S.R.
261. Kitt Peak National Observatory Library, P. O. Box 4130, Tucson, Arizona 85717
262. Konkoly Observatory, Budapest, Hungary
269. Leander McCormick Observatory, Box 3818, University Station, Charlottesville, Virginia 22903
270. Leningrad Central Astronomical Observatory Library, Pulkovo, Leningrad, U.S.S.R.
271. Mathematics-Physics Library, University of Pennsylvania, 209 South 33d Street, Philadelphia, Pennsylvania 19104
272. Max Planck Institute for Astronomy, 69 Heidelberg-Konigstuhl, Germany FR
273. Max Planck Institut fur Physik und Astrophysik, Fohringer Ring 6, 8 Munich 23, Germany FR
274. Melton Memorial Observatory, Department of Physics and Astronomy, University of South Carolina, Columbia, South Carolina 29208
275. Mount Cuba Astronomical Observatory Library, P. O. Box 3915, Greenville, Delaware 19807
276. Mount Stromlo Observatory, Canberra, Australia
277. National Observatory of Athens, Lophos Nymphon, Athens 306, Greece
278. National Radio Astronomy Observatory Library, Edgemont Road, Charlottesville, Virginia 22901

279. Naval Observatory Library, Massachusetts Avenue and 34th Street, N.W., Washington, D.C. 20390
280. Observatoire de Paris, 61 Avenue de l'Observatoire, 75 Paris-14e, France
281. Observatoire Royal de Belgique, Avenue Circulaire 3, 1180 Brussels, Belgium
282. Observatoriet, Oster Voldgade 3, DK-1350 Copenhagen K, Denmark
283. Observatory Library Georgetown University, 37th and O Streets, N.W., Washington, D.C. 20007
284. Observatory Library, University of Illinois, Urbana, Illinois 61801
285. Perkins Observatory Library, P. O. Box 449, Delaware, Ohio 43015
286. Phillips Library, Harvard College Observatory, 60 Garden Street, Cambridge, Massachusetts 02138
287. Physical Sciences Library, Brown University, Providence, Rhode Island 02912
288. Physical Sciences Library, Clark Hall, Cornell University, Ithaca, New York 14850
289. Physics and Astronomy Institute Library, Tiakhetoru, Tartu, U.S.S.R.
290. 290 Physics Astronomy Library, University of Michigan, Ann Arbor, Michigan 48104
291. Physics Library, 801 Pupin Building, Columbia University, New York, New York 10027
292. Physics Library, The University of Texas, Austin, Texas 78712
293. Redstone Scientific Information Center, U.S. Army Missile Command, Redstone Arsenal, Alabama 35809
294. Royal Observatory, Blackford Hill, Edinburgh EH9 3HJ, United Kingdom
295. Royal University Observatory, Lund, Sweden
296. Science and Engineering Library, University of California, San Diego, P. O. Box 109, La Jolla, California 92037
297. Sciences and Engineering Library, San Diego State College, 5402 College Avenue, San Diego, California 92115
298. Science and Technology Library, University of Colorado Libraries, Boulder, Colorado 80302
299. Science Division, University of Oregon Library, Eugene, Oregon 97403
300. Science/Technology Information Center, University of Virginia Library, Charlottesville, Virginia 22901
301. Steward Observatory, University of Arizona, Tucson, Arizona 85717
302. Strawbridge Observatory Library, Haverford College, Haverford, Pennsylvania 19041
303. University Astronomical Observatory, Uppsala, Sweden
304. University Library, University of Hawaii, Honolulu, Hawaii 96822
305. University Observatory, Bologna, Italy
306. University of Washington Libraries, Seattle, Washington 98105
307. Van Vleck Observatory Library, Wesleyan University, Middletown, Connecticut 06457

308. Warner and Swasey Observatory, Taylor and Brunswick Road, East Cleveland, Ohio 44112
309. Woodman Astronomical Library, Washburn Observatory, University of Wisconsin, Madison, Wisconsin 53706
310. Yerkes Observatory Library, Yerkes Observatory, Williams Bay, Wisconsin 53191
311. V. A. Kamath, Scientific Advisor, Attention: P. K. Patwardhan, Bhabha Atomic Research Centre, Trombay, Bombay, India
312. J. W. Rogers, Division 8321, Sandia Laboratories, P. O. Box 969, Livermore, California 94550
313. Milton E. Rose, Mathematical and Computer Sciences Program, Molecular Sciences and Energy Research, Division of Physical Research, U.S. Atomic Energy Commission, Washington, D.C. 20545
314. R. D. McCulloch, IAEA, Kaerntner Ring 11, P. O. Box 645, A-1010, Vienna, Austria
315. Research and Technical Support Division, AEC, ORO
316-399. Given distribution as shown in TID-4500 under Physics — Cosmic and Terrestrial category (25 copies — NTIS)

☆U. S. GOVERNMENT PRINTING OFFICE: 1974-748-189/94